AN INVESTIGATION INTO THE ROLE OF THE CXCR7 CHEMOKINE RECEPTOR IN ACUTE MYOCARDIAL INFARCTION AND ANGIOGENESIS

Report submitted by Staša Taferner

BSc (First class with Honours)

For upgrade to the degree of Doctor of Philosophy

University College London, UK

The Hatter Cardiovascular Institute,

Institute of Cardiovascular Science,

University College London,

67 Chenies Mews, London, WC1E 6HX

Declaration

I, Staša Taferner confirm that the work presented in this thesis is my own. Where information has been derived from other sources, I confirm that this has been indicated in the thesis. All technical assistance relevant to the results presented herein is duly acknowledged.

Abstract

Introduction: SDF-1α is a chemoattractant cytokine that can deliver both acute and chronic cardioprotective benefits to the heart. Although CXCR4 has been viewed as a main receptor for SDF-1α, a secondary receptor, CXCR7, has emerged as an important mediator of SDF-1α signalling. Interestingly, endothelial CXCR7 has been found to promote regeneration and ameliorate fibrosis in various tissues and organs; however, its exact role in ischaemic disease has yet to be determined. Therefore, we sought to examine the expression and function of CXCR7 in cardiovascular tissues, focusing on its potential as a novel cardioprotective strategy.

Methods: RNAscope in situ hybridization, western blotting and flow cytometry were used to investigate expression and function of CXCR7 on endothelial cell lines, isolated mouse endothelial cells, and in the whole mouse heart. We examined CXCR7 downstream signalling pathways in presence and absence of CXCR7 agonists TC14012 and VUF11207 fumarate, as well as the effects of the CXCR7 agonists on endothelial cell migration and acute ischaemia-reperfusion injury.

Results: CXCR7 is expressed in the adult mouse heart and in the endothelial cell lines MCEC and HUVEC. Most CXCR7 protein in the endothelial cells was observed to be intracellular under basal conditions. In line with this expression profile, exposure to CXCR7 agonists failed to activate cardioprotective protein kinases ERK1/2 and PI3K/Akt. Moreover, VUF11207 did not ameliorate acute ischaemia-reperfusion injury, whereas the role of both CXCR7 agonists in migration and angiogenesis is less clear.

Conclusions: CXCR7 is expressed in the mouse vascular endothelium, but its role in activating cardioprotective signalling pathways, as well as its overall contribution to cardioprotection is unclear. Activation of the CXCR7 receptor does not appear to be a viable acute cardioprotective strategy in mice.

Impact statement

Acute myocardial infarction (MI) affects over 180,000 people per year in the UK alone. Despite advances in emergency medicine, which significantly reduced the morbidity and mortality of cardiovascular diseases in the last 60 years, there is still scope to limit the damage levered by MI, via novel cardioprotective or pro-regenerative interventions.

This work presents the results of an investigation into the role of CXCR7 receptor in MI and whether its modulation can afford cardioprotection or stimulate angiogenesis in *ex vivo* and *in vitro* models. It suggests a pro-angiogenic role of endothelial CXCR7, specifically pertaining to cell migration, which could affect future approaches to either limit or initiate angiogenesis in a physiological or a pathological setting. There was no direct cardioprotective effect of CXCR7 observed in our experiments and further work is needed to elucidate its role in cardioprotection after MI. The results presented in this thesis will mostly benefit the research community within academia who could draw on its work to design experiments to further test the hypotheses set in this thesis. Furthermore, this work could also benefit research organizations outside academia to build upon the data presented in this work and to design pro- or anti-angiogenic therapies based on CXCR7 receptor modulation.

Most of all, the work in this thesis contributes to a body of research on a relatively novel CXCR7 receptor and its role in cardioprotection and cell migration aspect of angiogenesis. Combined with research that will be performed over the following years or decades this thesis could help to bring advances in cardioprotective and pro-regenerative therapies, which could positively impact patient morbidity and mortality after MI.

Acknowledgements

My sincerest thanks to my supervisors Dr Sean Davidson and Prof Derek Yellon for all their help, encouragement and excellent guidance over the past couple of years. I would also like to thank all staff and students at the Hatter Cardiovascular Institute for all their help, and for making my time at the Hatter Institute such a wonderful experience. It has been a pleasure working with you all.

I would also like to specifically acknowledge Dr Catherine Wilder for her help with the *ex vivo* isolated heart perfusion and Kaloyan Takov for his contribution to the cell migration chapter of this thesis. Their help with this thesis was invaluable, and their humour and friendly demeanour made my days at the Hatter all the more enjoyable.

Finally, my warmest thanks to my amazing family and friends who have always been there to support me and who believed in me no matter what.

Publications

- Rossello X, Riquelme JA, He Z, Taferner S, Vanhaesebroeck B, Davidson SM and Yellon DM. The role of PI3K alpha isoform in cardioprotection. *Basic Research in Cardiology* 2017; **112(6)**:66

- Bromage DI, Taferner S, Pillar M, Yellon DM and Davidson SM. A novel recombinant antibody specific to full-length stromal derived factor-1 for potential application in biomarker studies. *Plos One* 2017; **12(4)**: e0174447

- Malik A, Bromage DI, He Z, Candilio L, Hamarneh A, Taferner S, Davidson SM and Yellon DM. Exogenous SDF-1 alpha Protects Human Myocardium from Hypoxia-Reoxygenation Injury via CXCR4. *Cardiovascular Drugs and Therapy* 2015; **29(6)**: 589–592.

Contents

Declaration 2

Abstract 3

Impact statement 4

Acknowledgements 5

Publications 6

Contents 7

Tables 13

Figures 14

Abbreviations 18

1 Introduction 22

1.1 Myocardial infarction 23

1.1.1 Ischaemic injury 24

1.1.2 Reperfusion injury 25

1.2 The role of endothelial cells and angiogenesis in MI 27

1.2.1 Endothelial cell development 27

1.2.2 Angiogenesis 28

1.3 The role of ligand SDF-1α and chemokine receptors CXCR4 and CXCR7 in cardiovascular health 31

1.3.1 SDF-1α 31

1.3.2 CXCR4 33
1.3.3 CXCR7 34
1.4 Cardioprotective and pro-regenerative interventions 41
1.4.1 Current cardioprotective interventions 41
1.4.2 The role of CXCR4 and CXCR7 44
1.5 Hypothesis and Aims 57
1.5.1 Original hypothesis 57
1.5.2 Aims 57
2 Materials and methods 59
2.1 Experimental use of animals 59
2.2 Transgenic mouse lines 59
2.2.1 Generation of transgenic mice 59
2.2.2 Endothelial-specific gene ablation 61
2.2.3 Colony maintenance 61
2.2.4 Mouse genotyping 64
2.2.5 Tamoxifen administration 71
2.3 Cell cultures 72
2.4 Mouse cardiac endothelial cell isolation 73
2.4.1 Preparation of anti-CD31 coated Dynabeads 73
2.4.2 Cardiac endothelial cell isolation 73
2.5 Western blotting 74

2.5.1 Tissue collection 74
2.5.2 BCA protein quantification 74
2.5.3 Experimental protocol 75
2.5.4 WES western blotting 76
2.6 Ac-LDL uptake assay 77
2.7 Flow cytometry 77
2.8 RNAscope in situ hybridization 78
2.9 Langendorff perfusion 80
2.9.1 Experimental protocol 81
2.9.2 Exclusion criteria 82
2.9.3 Endpoint 1: Infarct size assessment 83
2.9.4 Endpoint 2: LDH release 85
2.10 Cell migration 86
2.11 RNA isolation and quantitative real-time PCR 88
2.11.1 RNA extraction 88
2.11.2 Reverse transcriptase polymerase chain reaction protocol (RT-qPCR) 89
2.12 Statistical analysis and power calculations 96
3 Investigation of CXCR7 expression in cardiovascular cell types 97
3.1 Background 97
3.2 Research aims and objectives 97

3.3 Methods 98

3.3.1 Flow cytometry 98

3.3.2 Western blotting antibodies 99

3.4 Results 99

3.5 Discussion 109

3.5.1 Summary 113

4 The effect of CXCR7 agonist VUF11207 fumarate in the Langendorff *ex vivo* heart perfusion model 114

4.1 Background 114

4.2 Research aims and objectives 114

4.3 Methods 115

4.4 Results 116

4.5 Discussion 123

4.5.1 Summary 134

5 The effect of CXCR7 agonists VUF11207 and TC14012 on the RISK pathway 135

5.1 Background 135

5.2 Research aims and objectives 135

5.3 Methods 136

5.3.1 Western blotting antibodies 136

5.3.2 Cell treatments 136

5.3.3 Normalization of western blotting results 137
5.4 Results 137
5.5 Discussion 145
5.5.1 Summary 152
6 Unsuccessful endothelial-specific inducible Cxcr7 gene deletion with Pdgfb-CreER^{T2} in adult mice 153
6.1 Background 153
6.2 Research aims and objectives 154
6.3 Methods 154
6.3.1 Transgenic animals 154
6.3.2 Western blotting 154
6.3.3 WES western blotting 155
6.3.4 RNAscope in situ hybridization 155
6.3.5 Quantitative real-time PCR 155
6.4 Results 155
6.5 Discussion 163
6.5.1 Summary 170
7 Examining the effect of VUF11207 and TC14012 on endothelial cell migration 171
7.1 Background 171
7.2 Research aims and objectives 171

7.3 Methods 172
7.3.1 Cell culture 172
7.3.2 Cell treatments with VUF11207 and TC14012 172
7.3.3 Cell migration analysis 172
7.4 Results 173
7.5 Discussion 180
7.5.1 Summary 186
8 General conclusions 187
9 References 191

Tables

Table 2-1: PCR reaction mix components for CXCR4 and CRE genotyping. ... 65

Table 2-2: PCR reaction mix components for CXCR7 genotyping. 66

Table 2-3: PCR primer sequences and their melting temperatures. 67

Table 2-4: CXCR4 and CRE PCR thermocycling protocol. 68

Table 2-5: CXCR7 PCR thermocycling protocol. 71

Table 2-6: Pre-set exclusion criteria for ex vivo Langendorff experiments. 83

Table 2-7: RNA extraction was performed using RNeasy kit (Qiagen), as per the manufacturer's suggestion. 89

Table 2-8: Reagents and volumes used to perform reverse transcription step, to obtain cDNA from RNA. 90

Table 2-9: RNA reverse transcription thermocycling protocol used for obtaining cDNA from RNA. 91

Table 2-10: Quantitative PCR reaction reagents and volumes. 92

Table 2-11: Quantitative PCR thermocycling protocol. 92

Table 2-12: RT-qPCR primer sequences 93

Figures

Figure 1-1: Hypoxia acts as a powerful angiogenesis stimulus. 30

Figure 1-2: Signalling crosstalk between CXCR4 and CXCR7. 33

Figure 1-3: RISK and SAFE signalling pathways 34

Figure 1-4: Chemical structure of VUF11207 fumarate...... 40

Figure 1-5: Signalling through RISK and SAFE cardioprotective pathways... 46

Figure 1-6: SDF-1α/CXCR4 signalling through the RISK cardioprotective pathway. 49

Figure 1-7: SDF-1α/CXCR7 signalling through the RISK cardioprotective pathway. 51

Figure 1-8: RISK and SAFE signalling pathways 57

Figure 2-1: Cre/Lox mechanism for transgenic mouse generation.. 60

Figure 2-2: Transgenic mouse breeding scheme...... 64

Figure 2-3: Detection of wildtype (WT) and floxed (FL) gene sequences. . 69

Figure 2-4: Representative mouse PCR genotyping images. 70

Figure 2-5: RNAscope in situ hybridization workflow. 79

Figure 2-6: Cannulated heart on the Langendorff perfusion apparatus...... 81

Figure 2-7: Langendorff perfusion experimental protocol. 82

Figure 2-8: Quantifying AAR via planimetry...... 84

Figure 2-9: Quantifying IS via planimetry. 85

Figure 2-10: Technical diagram of a representative chemotaxis chamber.. 87

Figure 2-11: Representative plot of fluorescence during qPCR amplification. 94

Figure 2-12: Representative melt curve. 95

Figure 3-1: CXCR7 mRNA expression in murine vascular endothelium.. 101

Figure 3-2: Positive and negative control mRNA probe RNAscope experiment..... 101

Figure 3-3: Ac-LDL uptake assay on cardiac endothelial cell culture..... 102

Figure 3-4: Flow cytometry gating for a viable cell population on cardiac EC culture.. 103

Figure 3-5: Flow cytometry IB4 endothelial labelling of cardiac EC culture. 104

Figure 3-6: CXCR7 western blotting of murine cardiovascular tissues, cardiac EC and commercially available cells. 105

Figure 3-7: Membrane-bound and intracellular expression of CXCR4 and CXCR7 in MCEC. 106

Figure 3-8: Membrane-bound and intracellular expression of CXCR4 and CXCR7 in HUVEC.. 107

Figure 3-9: Intracellular and membrane-bound expression of CXCR4/CXCR7 in MCEC and HUVEC. 108

Figure 4-1: Area at risk and infarct size assessment in isolated rat hearts. 116

Figure 4-2: LDH release during ex vivo isolated heart perfusion. 117

Figure 4-3: Flow rate and heart rate measured during the ex vivo isolated heart perfusion...... 119

Figure 4-4: Left ventricular developed pressure during the *ex vivo* isolated heart perfusion..... 120

Figure 4-5: Perfusion pressure and heart temperature during the ex vivo isolated heart perfusion. 121

Figure 4-6: Experimental exclusions during ex vivo isolated rat heart perfusion experiments. 123

Figure 5-1: The effect of VUF11207 (100 nM) on phosphorylation of AKT in HUVEC. 138

Figure 5-2: The effect of VUF11207 (100 nM) on phosphorylation of ERK1/2 in HUVEC.. 139

Figure 5-3: The effect of VUF11207 (250 nM) on phosphorylation of ERK1/2 in HUVEC. 140

Figure 5-4: The effect of TC14012 on phosphorylation of AKT in HUVEC. 141

Figure 5-5: Effect of TC14012 on phosphorylation of ERK1/2 in HUVEC. 142

Figure 5-6: Effect of insulin and SDF-1α on AKT phosphorylation in HUVEC – pooled data...... 143

Figure 5-7: Effect of insulin and SDF-1α on ERK1/2 phosphorylation in HUVEC – pooled data.. 144

Figure 6-1: CXCR7 western blotting on Cxcr7^{WT} and Cxcr7$^{i\Delta EC}$ whole mouse hearts. 156

Figure 6-2: CXCR7 western blotting on Cxcr7^{WT} and Cxcr7$^{i\Delta EC}$ whole mouse hearts. 157

Figure 6-3: CXCR7 western blotting on Cxcr7^{WT} and **Cxcr7$^{i\Delta EC}$ whole mouse hearts.** 158

Figure 6-4: WES western blotting for CXCR7 on isolated mouse cardiac endothelial cells. 160

Figure 6-5: Quantitative real-time PCR for CXCR7 in mouse aortic tissue. 161

Figure 6-6: CXCR7 mRNA expression in Cxcr7^{WT} and Cxcr7$^{i\Delta EC}$ mouse whole heart slices. 162

Figure 7-1: The effect of VUF11207 on 6 h cell migration in HUVEC. 174

Figure 7-2: The effect of VUF11207 on 3 h cell migration in HUVEC. 175

Figure 7-3: The effect of TC14012 on cell migration in HUVEC. 176

Figure 7-4: The effect of TC14012 + SDF-1α on cell migration in HUVEC. 178

Figure 7-5: The effect of TC14012 and SDF-1α on cell migration in HUVEC - pooled data. 179

Abbreviations

AAR	Area At Risk
ACKR3	Atypical Chemokine Receptor 3
AcLDL	Acetylated Low Density Lipoprotein
ATP	Adenosine Triphosphate
BHF	British Heart Foundation
BP	Base Pair
BSA	Bovine Serum Albumin
BSU	Biological Services Unit
CABG	Coronary Artery Bypass Surgery
CAD	Coronary Artery Disease
DMEM	Dulbecco's Modified Eagle Medium
EC	Endothelial Cells
EC_{50}	Half maximal effective concentration
ECG	Electrocardiography
EGM-2	Endothelial Growth Medium-2
EPC	Endothelial Progenitor Cells
FBS	Foetal Bovine Serum
FGFR	Fibroblast Growth Factor Receptor

GLP-1	Glucagon-Like Peptide 1
GWAS	Genome Wide Association Study
HMEC-1	Human Microvascular Endothelial Cells
HR	Heart Rate
HSC	Haematopoietic Stem Cells
HUVEC	Human Umbilical Vein Endothelial Cells
IB4	Isolectin B4
Id1	Inhibitor of DNA biding 1
IPC	Ischaemic Preconditioning
I/R	Ischaemia/Reperfusion
I-TAC	Interferon-inducible T-cell alpha chemoattractant
JAK	Janus Kinase
kDa	Kilo Daltons
KO	Knockout
LAD	Left Anterior Descending Aorta
LDH	Lactate Dehydrogenase
LV	Left Ventricle
MAPK	Mitogen Activated Protein Kinases
MCEC	Murine Cardiac Endothelial Cells

MI	Myocardial Infarction
MMP	Matrix Metalloprotease
mPTP	Mitochondrial Permeability Transition Pore
MSC	Mesenchymal Stem Cells
P	Postnatal Day
PBS	Phosphate Buffered Saline
PCI	Primary Percutaneous Coronary Intervention
PDGFB	Platelet Derived Growth Factor Subunit B
PI3K	Phosphoinositide-3-kinase
PKA	Protein Kinase A
PLC	Phospholipase C
RDC1	Receptor Dog cDNA 1
RIC	Remote Ischaemic Conditioning
RISK	Reperfusion Injury Salvage Kinase
ROS	Reactive Oxygen Species
RT	Room Temperature
SAFE	Survivor Activator Factor Enhancement
SDF-1α	Stromal Derived Factor 1 Alpha
SEM	Standard Error Of The Mean

STAT	Signal Transducer and Activator of Transcription proteins
STEMI	ST-segment Elevation Myocardial Infarction
TNF	Tumour Necrosis Factor
VIP	Vasoactive Intestinal Peptide
WT	Wild Type

1 Introduction

The term cardiovascular disease encompasses a multitude of conditions, where narrowing or blockage of blood vessels leads to detrimental effects on the heart. One of the most prevalent causes of morbidity and mortality in the western world is a group of conditions that belong under an umbrella term of coronary artery disease (CAD). Characterized by formation of an atherosclerotic plaque that forms inside one or more coronary arteries, via the process known as atherosclerosis; CAD is an inflammatory and fibrotic process that occurs in stages [2]. It begins with an accumulation of white blood cells and fatty lipids inside the coronary arteries, followed by formation of one or more lipid cores that can be surrounded by a fibrous cap [3,4]. There is progressive stenosis and a gradual stiffening of the vessels, which impedes coronary blood flow. Due to decreased lumen and haemodynamic changes present in the vessels, the thin fibrous cap overlying the plaque can rupture or erode, which causes accumulation of red blood cells and formation of a blood clot that can either fully occlude the artery in question or form a thrombus [3, 5]. Subsequently, if the narrowing of the vessel is severe enough, the lack of oxygen flowing to the heart will cause myocardial ischemia and can even lead to myocardial infarction. The formation of an atherosclerotic plaque is not an immediate process and it can take decades for the vessel to be occluded enough to become clinically significant. Patients with atherosclerosis are often not aware of the severity of their condition. That is, until they experience an ischaemic episode, characterized by a transient chest pain, known as angina [6].

Hyperlipidaemia, diabetes, hypertension, as well as unhealthy lifestyle choices, including obesity, poor diet and smoking can severely affect the rate of atherosclerosis, and lead to coronary artery disease development [7, 8].

Due to high prevalence of CAD and atherosclerosis in the increasingly aging population it is important to promote prevention, especially regarding the risk factors and lifestyle choices, which can play an important role in the development

of coronary artery disease [9, 10]. Overall, cardiovascular disease is a widespread problem with approximately 7 million people affected by it in the UK alone (BHF statistic, 2016). Thus, it is important to develop strategies and promote new research to tackle the growing problem of cardiovascular disease not only in the UK, but globally.

1.1 Myocardial infarction

Although the rate of deaths attributable to cardiovascular disease has declined by more than three quarters since 1961, there are still a high proportion of patients with CAD that will go on and suffer a myocardial infarction (BHF statistic 2016). Acute myocardial infarction (MI) affects around 188,000 people in the UK every year and despite constant advances in emergency medicine it is still responsible for significant morbidity and mortality (BHF statistics, 2016) [11]. In terms of pathophysiology, acute myocardial infarction can be defined as a loss of cardiomyocytes as a consequence of an ischaemic insult [12]. However, myocardial infarction is a complex process with many metabolic and structural changes providing additional detrimental effects to the heart. During MI the coronary arteries become blocked, cutting off oxygen supply to the heart and generating an ischaemic environment that results in necrosis of the affected part of the heart muscle [13]. There are several recognized clinical interventions, such as intravenous thrombolytic therapy and primary percutaneous coronary intervention (PCI) that aim to re-establish blood flow. However, these treatments focus primarily on early reperfusion, which, although beneficial overall, is known to cause additional reperfusion-related injury [14]. Further to the more common mechanical interventions, there are also pharmacological interventions capable of affording cardioprotection and salvaging the still-viable myocardium. Kubler and Haass defined the term cardioprotection (also known as acute cardioprotection) as any intervention, either mechanical or pharmacological, that is capable of preserving the integrity of the heart by reducing or preventing myocardial damage [15].

The field of cardioprotection has come a long way since then, with several interventions emerging as potentially suitable clinical therapies. For example, a member of the β-blocker family metoprolol and glucagon-like peptide-1 drug exenatide, which have shown promise in clinical trials, are currently undergoing further evaluations as to their cardioprotective potential [16-18].

Nevertheless, the extent of damage suffered by the myocardium is still dependent on timely reperfusion; therefore, research into minimizing reperfusion injury and promoting regeneration of damaged myocardium is one of the most important areas of cardiovascular research [19].

The damage seen after MI occurs in two stages, first during ischaemia and then again during reperfusion. As the blood vessel is blocked and the blood supply to the myocardium is affected, a series of biochemical and metabolic changes take place in the now ischaemic heart muscle [20, 21]. After MI, reperfusion is crucial to begin myocardial salvage, while itself being a detrimental phenomenon [14]. The reestablishment of coronary blood flow during reperfusion can cause further cardiomyocyte necrosis, myocardial stunning and microvascular dysfunction, where the damage to the endothelium prevents normal blood flow and causes a potentially deadly no-reflow phenomenon [20, 22]. Therefore, when devising approaches to protect the viability of heart muscle, either ischemic injury, reperfusion injury, or both can be targeted. To describe these actions, the term cardioprotection is commonly used.

1.1.1 *Ischaemic injury*

Myocardial ischaemia occurs as a result of a mismatch between the supply and the demand of oxygen, with the extent of the damage to the myocardium dependent on the duration and magnitude of tissue ischaemia [23]. Consequentially, timely reperfusion strategy remains a foremost priority when it comes to MI interventions. During ischaemia, there is a series of metabolic changes that underpin the diminished oxygen supply to the heart muscle.

Obstruction or blockage of a coronary blood vessel impedes blood flow and causes a reduction in available glucose in myocardial tissues. This leads to reduced availability of ATP, and with it a switch to anaerobic metabolism, namely anaerobic glycolysis [12]. However, the myocardium is not equipped with sufficient anaerobic metabolic pathways to supply the high provisions of ATP needed for normal function, and available ATP is quickly used up [24, 25].

Therefore, when exposed to ischemia, there is a dilatation of coronary vessels to try and increase the blood flow and keep the myocardium sufficiently supplied with oxygen and glucose to satisfy the metabolic needs. Despite these efforts, ATP is quickly depleted, leaving the heart vulnerable to the effects of ischaemia. Meanwhile, the switch from aerobic to anaerobic metabolism lowers the pH, and activates a buffering mechanism [12]. Hydrogen ions are excreted via the $Na^{+/}H^{+}$ exchanger followed by a large influx of sodium ions to balance the loss of intracellular hydrogen [26]. Furthermore, activation of various ATPases brought on by a lowered pH causes an efflux of potassium ions accompanied by an accumulation of cytosolic calcium, which provides an arrhythmogenic environment [27,12]. The metabolic changes outlined above also trigger the release of intracellular proteases, such as the calcium-dependent protease calpain [28]. Calpain then exerts a disruptive effect on the cell structure, and its activation leads to hypercontractility and subsequent activation of apoptotic pathways. It also paves the way for the opening of the mitochondrial permeability transition pore (MPTP) during reperfusion [26, 28].

1.1.2 *Reperfusion injury*

The existence of lethal reperfusion injury separate from the ischaemic damage has been something of a controversy over the past couple of decades, with its existence having sometimes being called into question [29-31]. Some authors have contested the evidence in favour of reperfusion injury, citing the lack of available human data and failure to translate the beneficial effects of ameliorating reperfusion injury from bench to bedside. However, since then, lethal reperfusion

injury has garnered support and has become generally accepted as an insult to the myocardium that occurs separate from the ischaemic damage [14]. As with ischaemic injury, reperfusion injury is also associated with damage and death of cardiomyocytes, although via different pathologies than those outlined above.

Microvascular dysfunction in the form of activated leukocytes and platelets, generation of reactive oxygen species (ROS), increased extravasation of fluid and proteins all converge to deal a harmful blow to the endothelium [22, 32]. A detrimental process known as the no-reflow phenomenon can also occur during reperfusion period of myocardial infarction [33]. The term refers to damage sustained by the endothelium by all major pathogenic mechanisms, namely injury due to ischaemia/reperfusion (IR), thrombus formation and increased endothelial susceptibility to injury [34]. It is also associated with adverse post-infarct complications, as well as a higher mortality rate and can occur in as many as a third of cases of MI [35, 36]. A less harmful process that can occur during reperfusion is myocardial stunning, which unlike the no-reflow phenomenon is deemed less injurious and is usually followed by a complete functional recovery [37]. It can arise after as little as 15 minutes of ischaemic injury and is largely facilitated by release of free radicals and excessive calcium [38]. Even though the myocytes are injured in this process, they ultimately recover their function without a prolonged detriment to the heart muscle [19]. Altogether, reperfusion injury prompts a second wave of cardiomyocyte death, however, if it is established early enough (between 2 to 3 hours) the benefits greatly exceed the harm and aid in salvaging the at-risk myocardium [19].

1.2 The role of endothelial cells and angiogenesis in MI

1.2.1 *Endothelial cell development*

The term endothelium refers to the innermost layer of vessels found in the cardiovascular and lymphatic system. Therefore, it is broadly divided into vascular and lymphatic endothelium. This thesis primarily focuses on the vascular endothelium, which is further divided into arterial and venous endothelium, and comprised of specialized cells called endothelial cells. In mice, as well as humans, endothelial cells develop from hemangioblasts derived from the mesoderm, which give rise to both, multipotent haematopoietic stem cells (HSC) and angioblasts [39]. To generate both cell types, hemangioblasts form clusters, also called blood islets, and positioning of the cells within those clusters provides the distinction between the two cell types [40]. Cells, which will become haematopoietic cells become clustered in the middle, while the angioblasts arrange themselves along the periphery [39, 41]. Angioblasts give rise to endothelial cells, which further differentiate into either arterial or venous endothelial cells. The entire process of endothelial cell development is highly regulated and involves a multitude of transcription and growth factors in order to achieve formation of vascular plexuses present in the adult organism [42].

Pinto *et al*. suggest that 55% of all nuclei in the murine heart belong to the endothelial cells, 32% to cardiomyocytes and 13% to fibroblasts [43]. Moreover, endothelial cells are reported to make up only 3.2 – 5.3% of the volume fraction of the rat heart [44]. Disparities in numerical representation of different cell types that appear in the published literature can be partially attributed to different research methods employed to investigate the cellular composition of the heart, with results obtained by Pinto *et al*. considered to be the most reliable [45]. However, the percentages of cells that comprise the heart are also proposed to vary between species and regions of the heart [46]. Furthermore, despite the endothelial cells not comprising a large proportion of the heart volume, they play an important role in cardiac physiology and pathology. For example they play a pivotal role in

maintaining vasomotor tone, modulating cardiac growth and development, and are known to modulate cardiac rhythmicity [47]. Additionally, endothelial dysfunction contributes to the development of congestive heart failure through impaired systemic perfusion and diminished exercise capacity [48].

Along with the aforementioned cell types, there is another type of cell postulated as capable of differentiating into mature endothelial cells. Endothelial progenitor cells (EPC) are bone marrow-derived cells, first identified by Asahara *et al*. in 1997 [49]. They were described by Urbich and Dimmeler as non-endothelial progenitor cells, which possess clonal ability to multiply and are capable of differentiating into mature endothelial cells [50]. The existence of EPC has been widely debated, as it is unclear how exactly they develop and give rise to mature endothelial cells [51, 52]. Furthermore, to investigate EPC researchers have employed numerous different methods of cell isolation and characterization, which makes it difficult to surmise if the investigated populations of cells were comparable across different studies [53]. Additionally, there is a lack of *in vivo* evidence of EPC existence and only a few studies so far have attempted to examine the clinical relevance of these cells [51]. So far, research points towards EPC being comprised of HSC in various stages of differentiation, and which display certain pro-angiogenic functions (e.g. vascular repair), but with little evidence of potential for vascular differentiation [54, 55]. Due to the increasing presence of EPC in the literature, research regarding these cells cannot be ignored, but the use of term “EPC” should be further defined to include a specific type of cell and its precise function so their contribution to vascular processes in health and disease can be properly characterized [56].

1.2.2 *Angiogenesis*

Angiogenesis is an important physiological process, whereby new vessels develop from pre-existing vessels through migration, growth and differentiation of endothelial cells and their progenitors, as mentioned above [57].

This requires cooperation of a range of cell types and signalling pathways, as well as numerous pro-angiogenic factors such as vascular endothelial growth factor (VEGF), basic fibroblast growth factor (bFGF) and others [58, 59]. As in other crucial physiological processes angiogenesis is tightly regulated; however, it becomes dysregulated during many pathological conditions, such as inflammation, cancer and ischaemic heart disease [59, 60]. One of the mechanisms through which angiogenesis occurs is sprouting, which proceeds in several key stages: i.) endothelial cell activation by various growth factors (e.g.:VEGF, bFGF) and subsequent degradation of extracellular matrix (ECM) components by MMPs and (MMP1 and MMP2) ii.) migration of endothelial cells into ECM and towards a pro-angiogenic stimulus (e.g. hypoxia) forming new endothelial sprouts as they proceed, iv.) after which the sprouts extend towards the pro-angiogenic stimulus, creating a vessel lumen and ultimately forming a new blood vessel [61]. This thesis will focus on one aspect of angiogenesis, namely endothelial cell migration. It consists of three distinct processes: i.) directional migration of cells toward a gradient set by soluble chemoattractants (e.g. VEGF) - chemotaxis, ii.) directional migration produced by mechanical forces (e.g. fluid shear stress) - mechanotaxis and iii.) directional migration, which is generated by a gradient of immobilized ligands (e.g. integrins) - haptotaxis [62-67].

The role of angiogenesis in many pathological conditions, including cardiovascular diseases, has been well documented. Current therapies aimed at treating myocardial infarction mainly deal with restoration of blood flow to the ischaemic area, be it mechanical or pharmacological. This brings with it its own problems and its efficacy is largely dependent on the time of initiation of the treatment [68]. As the understanding of neovascularization after myocardial infarction has grown, so has the notion to harness angiogenesis as a potential tool to restore blood flow to ischaemic myocardium [69].

One of the strongest stimuli for the induction of angiogenesis is hypoxia, whilst also being a defining feature of ischaemic heart disease. VEGF represents a crucial element in the angiogenic process, since it can stimulate quiescent endothelial cells and activate them to commence the process of new vessel growth. During a period of hypoxia, there is activation of hypoxia inducible factor 1 (HIF-1), a heterodimeric transcription factor that induces VEGF gene expression and subsequently secretion of VEGF, leading to new sprout formation (Fig. 1-1) [70].

Hypoxia is also one of the main characteristics of MI. As described in section 1.1.1 the blockage of coronary vessels leads to impaired oxygen delivery to the area of infarcted myocardium, resulting in localized tissue ischaemia [12]. This causes oxygen sensing mechanisms in the heart to detect low levels of oxygen in the tissue and initiate the pro-angiogenic response, which forms a part of the tissue regeneration process in infarcted myocardium [71]. Early reperfusion of the infarcted myocardium was shown to be an effective strategy in improving outcome after MI [14].

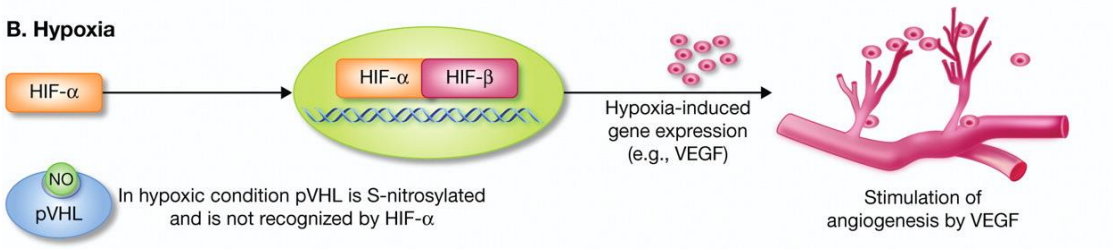

Figure 1-1: Hypoxia acts as a powerful angiogenesis stimulus. Hypoxia activated HIF-1α, which couples to ubiquitously expressed HIF-1β subunit to form initiate gene expression of several hypoxia-induced genes, such as VEGF. Pro-angiogenic properties of VEGF then stimulate activation, migration and differentiation of endothelial cells into new blood vessels. Image adapted from Rahimi *et al*.[72]

The idea to use angiogenesis to aid heart regeneration after MI is not new, and such treatments are defined as pro-regenerative. PCI, thrombolysis and other pharmacological interventions are already being used to minimize damage seen from MI and can be very effective when applied quickly. However, these procedures will not benefit all patients equally. Patients presenting with microvascular dysfunction, who lack a well-developed collateral circulation exhibit prolonged ischaemia, and perfusion of the ischaemic myocardium via PCI does little to improve the clinical outcome [73]. In such cases, stimulating angiogenesis and restoring microvascular integrity can be an effective way to overcome the hurdle posed by dysfunctional microvasculature and aid in successfully reperfusing the ischaemic myocardium. Similarly, use of pro-angiogenic growth factors has been hypothesized to have beneficial effects on the ischaemic myocardium, although this area of research is still in its infancy and needs to be explored further [74].

1.3 The role of ligand SDF-1α and chemokine receptors CXCR4 and CXCR7 in cardiovascular health

1.3.1 *SDF-1α*

SDF-1 (stromal derived factor 1); also termed CXCL12 is an 8 kDa peptide belonging to a group of peptides known as chemokines. Chemokines are made of four conserved cysteines with two disulphide bonds and function primarily as chemoattractants [75]. They are involved in various cell processes, including cell trafficking, activation, and differentiation. In order to achieve this, they bind to G-protein coupled receptors (GPCRs) that signal via G-proteins or less commonly, through β-arrestins [76, 77]. SDF-1 is a ligand for two such G-protein coupled receptors, CXCR4 and CXCR7, where CXCR4 signals through G-proteins and CXCR7 through the β-arrestin pathway (Fig 1-2)[78]. There are multiple splice variants of SDF-1, with SDF-1α, which is made up of three exons being the most common [75].

The remaining splice variants all contain the same three exons as SDF-1α, with an additional fourth exon that is unique to each of the alternative splice variants [75]. Due to SDF-1α being expressed in most body tissues and organs, its degradation is an important and well-regulated process and consists of N-terminus proteolysis and C-terminus degradation. The latter is mediated by carboxypeptidase N and is specific to SDF-1α, which is the most widespread and arguably most crucial variant [75, 79, 80]. Other SDF-1 isoforms include SDF-1β that exhibits functions relating to the embryonic development and the vascular system, and SDF-1γ, which is a predominant variant of SDF-1 expressed in the rat adult brain, whilst also being expressed in the hearts of humans and mice [80-83]. Little is known about the rest of the SDF-1 splice variants, namely the δ, ε and φ isoforms [75]. Considering they have only recently been identified in human tissues, their prospective roles in the human body have not yet been defined.

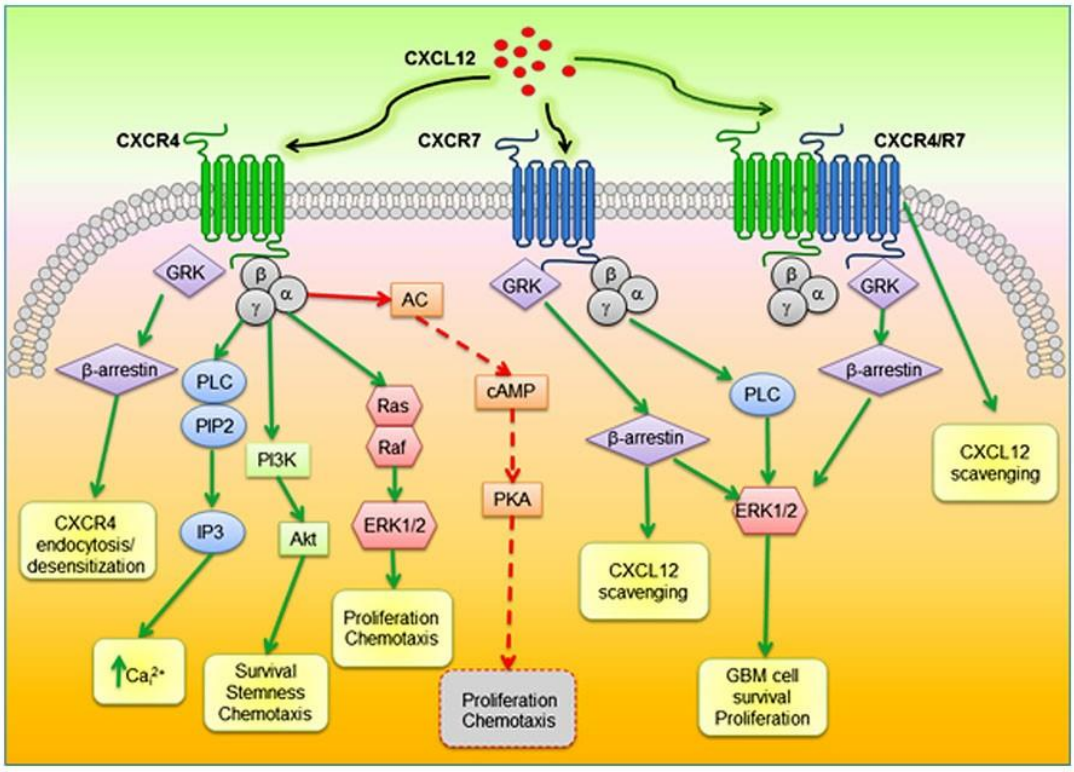

Figure 1-2: Signalling crosstalk between CXCR4 and CXCR7. Binding of SDF-1α to CXCR4, CXCR7 or the CXCR4/CXCR7 heterodimer activates several downstream signalling pathways and induces phosphorylation of various kinases, including, MAPK, PKA and PI3K. Image from Wuerth *et al*.[84].

1.3.2 *CXCR4*

SDF-1α/CXCR4 axis is important in numerous physiological processes, including cell migration, homing, survival, organogenesis and angiogenesis [1, 85]. CXCR4 receptor belongs to the C-X-C family of chemokine receptors, where two N-terminal cysteine (C) residues are separated by a different amino acid (X) [86]. Originally identified as a human immunodeficiency virus co-receptor, CXCR4 is expressed in a variety of cells including cells of the immune and central nervous system, endothelial cells, cardiomyocytes, and fibroblasts [87-91]. Due to the wide range of actions it encompasses it can be exploited for clinical applications, such as mobilization of hematopoietic stem cells in certain types of cancer, via blockage of the CXCR4 receptor [92, 93]. It therefore comes as no surprise that this axis has been widely studied in the context of cancer and autoimmune diseases, as well as being identified as a possible cardioprotective effector [76, 94, 95].

Deregulation of the SDF-1α/CXCR4 axis is crucial to many pathological states and has also been found to be an important player in myocardial infarction and other hypoxic conditions, such as ischaemic cardiomyopathy [96, 97]. Exploiting its cell homing properties, SDF-1α/CXCR4 axis has also been used to home cells to the ischaemic myocardium to increase myocardial salvage and improve left ventricular (LV) function [98-100]. Supporting the role of SDF-1α/CXCR4 in cardiovascular disease are also numerous genome-wide association studies (GWAS) that link it with increased risk for myocardial infarction and death, but leave us in the dark as to the exact nature of this link [101-103]. Despite the fact that there is still much to be discovered about the CXCR4 receptor, it is the lesser known CXCR7 receptor that will be the main focus of this thesis.

1.3.3 *CXCR7*

While the SDF-1α/CXCR4 axis might be well studied, CXCR4 receptor is not the only receptor capable of binding SDF-1α. CXCR7, also known by its alternative names, ACKR3 (atypical chemokine receptor 3) and RDC1 (receptor dog cDNA 1) is an atypical chemokine receptor that binds two known ligands, I-TAC (Interferon-inducible T-cell alpha chemo-attractant or CXCL11) and SDF-1α. Interestingly, recent studies have shown that CXCR7 can bind SDF-1α with approximately ten to twenty times greater affinity than CXCR4 [78, 104]. CXCR7 was first cloned from the canine cDNA library in 1990 by Libert *et al*., and attracted interest due to greater than 90% similarity between its dog and human homologs [105]. It was initially thought to be a VIP (vasoactive intestinal peptide) or calcitonin-gene related receptor; however, this notion was later dismissed due to lack of evidence [106-108]. Thus, it was not until 2005, when its now-confirmed ligands I-TAC and SDF-1α were identified, that the interest in the CXCR7 receptor began to grow [78, 106, 109].

Expression and signalling

CXCR7 is expressed in a variety of mammalian cells and tissues, including in the heart, lung, liver, brain and the immune system, however, its exact expression profile, as well as its function remain disputed [109]. Recent studies have shown CXCR7 expression by several different types of endothelial cells, including endothelial progenitor cells, human pulmonary microvascular endothelial cells, human umbilical vein endothelial cells (HUVEC), and human lymphatic endothelial cells [110-113]. Meanwhile the expression profile of CXCR7 in the cardiac endothelial cells has not yet been thoroughly examined, with most CXCR7 expression data postulated from effects seen in transgenic mice with endothelial-specific inducible CXCR7 deletion [114, 115]. Cardiac origin of endothelial cells might be an important factor when investigating the role of endothelial CXCR7 in the heart, due to high degree of heterogeneity and a different transcriptional profile that can be attributed to endothelial cells in a tissue-specific manner [116, 117].

Similarly, the expression level of CXCR7 in cardiomyocytes is not well established.

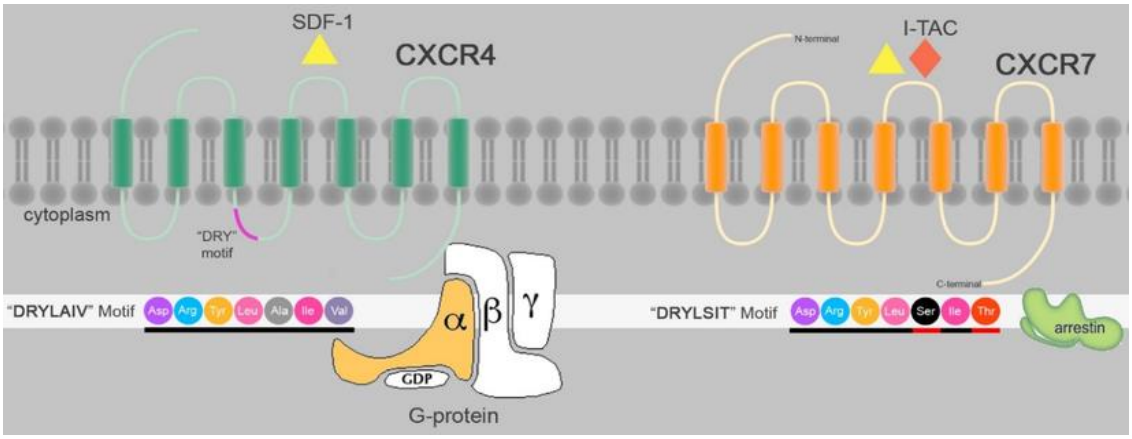

Figure 1-3: Comparison of DRYLAIV and DRYLSIT motifs in CXCR4 and CXCR7. Classical chemokine receptors, such as CXCR4 exhibit a DRYLAIV motif that is necessary for G protein signalling. On the other hand, atypical chemokine receptors (e.g. CXCR7) possess a DRYLSIT motif that replaces the DRYLAIV motif (differences between motifs are underlined in red) and allows them to preferentially bind and signal through β-arrestins. Substituted amino acids are underlined red on the graphic. Image adapted from Asri *et al*. [1].

CXCR7 has been shown to induce SDF-1α ligand internalization and degradation, along with providing cells with a growth and survival advantage and increased adhesion properties [113, 118]. Upon further examination it was discovered that the DRYLAIV motif (Asp-Arg-Tyr-Leu-Ala-Ile-Val) present in the majority of chemokine receptors is replaced by the DRYLSIT (Asp-Arg-Tyr-Leu-Ser-Ile-Thr) motif in CXCR7 (Figure 1-3) [109]. Since, DRYLAIV motif is considered vital for G protein coupling and calcium signalling, it is proposed that CXCR7 cannot signal through G-proteins, as it is common with GPCRs, and is also insensitive to pertussis toxin in most tissues [113, 119, 120].

Calcium plays an important role in many cellular processes, such as cell survival, cell death, as well as setting the cellular membrane potential [121]. Since Ca^{2+} signalling typically occurs through G protein signalling, CXCR7 signalling on its own cannot elicit Ca^{2+} mobilization. In order to initiate the rise in intracellular calcium, phospholipase C (PLC) cleaves phosphatidylinositol bisphosphate (PIP2) into secondary messengers inositol trisphosphate (IP3) and diacylglycerol (DAG). IP3 then goes on to stimulate the opening of the IP3-mediated Ca^{2+} channels and subsequently triggers a rise in intracellular calcium, as seen in Figure 1-6 [76, 122].

Since CXCR4 and CXCR7 both possess the same ligand, SDF-1α, it can be a challenge determining precisely which receptor is responsible for the observed actions. One of the hallmarks of CXCR7 signalling is its inability to signal through G proteins and its reliance, instead, on signalling via β-arrestins [123]. β-arrestins are scaffolding proteins more commonly associated with receptor desensitization and were long believed to lack meaningful signalling capacity, acting instead as cellular response dampeners [124]. Rather than signal through a G-protein signalling pathway, CXCR7 recruits β-arrestin in a ligand-dependent fashion [123]. Cells featuring transfected CXCR7 were shown to recruit β-arrestin to the plasma membrane following the incubation with either, SDF-1α or I-TAC ligand [125, 126]. One of the most prominent differences of β-arrestins and G-protein signalling is the inability of β-arrestins to induce calcium mobilization, a hallmark of GPCR signalling [113, 120]. However, active signalling of the SDF-1α/CXCR7 axis that is capable of activating effectors downstream of β-arrestins, has since been shown in various cell types, such as haematopoietic stem cells [127, 128].

One exception where CXCR7 seems to utilize G proteins for signalling is in astrocytes, where there is evidence of a G-protein dependent mechanism resulting from SDF-1α binding to CXCR7 [129-132]. However, due to its inability to signal thorough G proteins in other tissues, CXCR7 was initially thought incapable of independent signalling and viewed solely as a decoy receptor for SDF-1α [119].

It is true that upon binding of SDF-1α or I-TAC, CXCR7 aids in internalizing and degrading the ligand, functioning as a scavenger receptor [133, 134]. However, recent evidence points to it also being capable of independent signalling through β-arrestins. This appears to be the case with CXCR7, where evidence points to activation of mitogen activated protein kinases (MAPK), PI3K and AKT after binding by SDF-1α and I-TAC [84, 123, 127, 135, 136].

CXCR7 receptor also heterodimerizes with its fellow chemokine receptor CXCR4, in response to binding of the SDF-1α ligand. Before the discovery of CXCR7, CXCR4 was considered a unique receptor for SDF-1α and this ligand –receptor couple was widely studied due to its importance in a variety of cellular processes [137]. CXCR4/CXCR7 heterodimers form quickly and efficiently and can signal through G proteins and β-arrestins, with the argument being made for preferential activation of the latter [120, 135]. Formation of CXCR4/CXCR7 heterodimers also modifies some of the properties of CXCR4 when not bonded in a dimer, namely calcium signalling [120]. Interestingly, CXCR7/CXCR4 heterodimers on the other hand are able to elicit a greater Ca^{2+} response than CXCR4 receptor signalling on its own [135, 138]. Furthermore, SDF-1α is also capable of forming homodimers under physiological conditions, but CXCR7 receptor preferentially binds the monomeric form [109, 139, 140]. Despite abundant evidence of heterodimerization *in vitro*, in recent years questions were posed whether CXCR4/CXCR7 can form heterodimers *in vivo,* since there is not a lot of evidence to support this claim [109, 133, 141, 142].

It has been previously reported that CXCR7 is scarcely expressed on the surface of most cells, including endothelial cells, with a substantial intracellular pool of the receptor present in the cytosol of various types of cells [143, 144]. SDF-1α-CXCR4/CXCXR7 ligand-receptor pair is internalized following SDF-1α binding, which might explain the intracellular reservoir of the receptor [141]. It is also a possibility that internally located CXCR7 recycles back to the cell membrane, where it regains functional activity [78, 109].

Hartmann *et al.* showed that in T-cells a portion of intracellular CXCR7 is located in endosomes, as evidenced by the co-staining of CXCR7 with endosomal markers [144]. Therefore, they propose that only a small fraction of CXCR7 that constantly shuttles between the intracellular stores and the surface membrane is available under a steady-state level. As such, CXCR7 is capable of scavenging and internalizing its chemokine ligands, which are then degraded to prevent their release back into the circulation [134]. Nevertheless, in the presence of increasing evidence the prospect of CXCR7 possessing a signalling role independent of its scavenging function cannot be ignored.

CXCR7 in cardiac development and transgenic knockout models

CXCR7 is also important in embryogenesis and early cardiac development as evidenced by cardiovascular defects present in transgenic mice with germline deletion of the receptor. In the heart, CXCR7 expression has been detected at embryonic day (E) 10.5, followed by a change in the expression pattern at E14.5. Thereby, it is postulated that CXCR7 is abundantly expressed during periods of critical cardiac growth and vascularization [109]. This is supported by the fact that CXCR7 expression also corresponds to the period of coronary vascular development, including vascular plexus formation and vascular remodelling between E11.5 and E16.5, after which the receptor expression steadily decreases [145]. Interestingly, just as the expression of CXCR7 decreases, there is a rise in CXCR4 receptor expression, which also coincides with the period of development when CXCR4 and SDF-1α germline knockout mice die [88, 109, 113, 146, 147].

There have been several papers published on the effects of CXCR7 germline deletion. Gerrits *et al*. reported that mice with a germline $CXCR7^{-/-}$ genotype exhibited a 30% survival rate 1 week after birth, with adult mice of the same genotype displaying signs of myocardial degeneration and fibrosis [148]. They also noted that some $CXCR7^{-/-}$ mice presented with an enlarged heart, as well as hyperplasia of the ventricles and the septum [148].

Yu *et al*. published observations of semilunar valve thickening and ventricular septal defects, while Sierro *et al*. observed thickening of the pulmonary valve, the aorta and the bicuspid arterial valves; a phenotype, which was also reiterated in mice with endothelial-specific deletion of CXCR7 [114, 119]. There are slight but noticeable differences in phenotypes of CXCR7$^{-/-}$ mice produced by different groups, which can be attributed to distinct genetic manipulations used to generate these mice. Some of these characteristics are shared with the CXCR4$^{-/-}$ mice, but most are unique to the CXCR7 $^{-/-}$ mice [149].

CXCR4 and CXCR7 receptor agonists

As the interest in CXCR7 increased, so did the demand for a highly selective CXCR7 agonist, which does not activate CXCR4. There are currently three agonists of CXCR7 available for commercial use, the small molecule agonists VUF11207 and VUF11403, and the peptidomimetic TC14012 agonist. TC14012 started out as TC140, a CXCR4 inverse agonist, derived from the horseshoe crab peptide polyphemusin [150]. It was later modified to TC14012, a serum-stable CXCR4 compound. Introduction of C-terminal amidation on TC14012 removed conformational constrains present on T140, which allowed it to bind to CXCR7 and recruit β-arrestins, with a binding strength comparable to the natural ligand SDF-1α [151, 152]. VUF11207 was among 24 derivates that were synthesized by Wijtmans *et al*. from a styrene-amide scaffold and pharmacologically evaluated to determine their structure-activity relationship and functional activity. Structural-activity relationship was determined by competition binding experiments and assessed the impact of different chemical groups “attached” to the styrene-amide scaffold on CXCR7 affinity. The compounds that displayed favourable affinity to CXCR7 were then subjected to further functional evaluation. VUF11207 along with another compounds VUF11403 emerged as the compounds that performed best in the functional pharmacological tests.

The β-arrestin2 recruitment assay on CXCR7-expressing HEK293 cells revealed VUF11403 as a high-affinity ligand of CXCR7 with an EC_{50} of 1.0 nM and VUF11207 with an EC_{50} of 1.6 nM, surpassing the affinity displayed by SDF-1α in this assay (EC_{50}= 2.6 nM) [153]. Additionally, both compounds also performed well in an ELISA internalization assay, with both reducing CXCR7 surface availability, although VUF11207 (EC_{50} = 14.1 nM) displayed higher efficacy than VUF11403 (EC_{50} = 23.7 nM). Based on these results, VUF11207 was selected as the best CXCR7 agonist to use in the study. Moreover, VUF11207 is also one of the few commercially available CXCR7 agonists and antagonists with a fully disclosed chemical structure (Figure 1-4) [153].

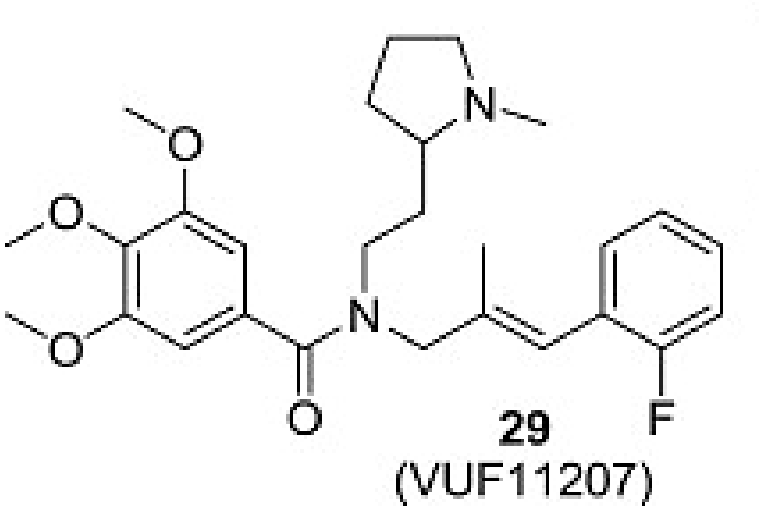

Figure 1-4: Chemical structure of VUF11207 fumarate. Image courtesy of Wijtmans *et al*. [153]

1.4 Cardioprotective and pro-regenerative interventions

1.4.1 *Current cardioprotective interventions*

Cardioprotective agents – ischaemic injury

There are a considerable number of cardioprotective strategies that have been shown to be effective in experimental models, with most of them focusing on reperfusion, but there are some, such as β-blocker drugs, that are aimed solely at ameliorating ischaemic injury. β-blockers are believed to be able to reduce the progression of ischaemic damage and therefore reduce the final infarct size [154]. However, clinical trials have failed to conclusively demonstrate this effect when administered to the patients [155-158]. As such, they might not be the universal cardioprotective agents they were once believed to be.

Nevertheless, β-blockers are still considered an important part of post-myocardial infarction management, and represent one of the most prescribed cardiovascular drug groups [154]. Another approach in targeting ischaemia associated with myocardial infarction makes use of hypothermia (30 - 35°C), which is thought to arrest the progression of ischaemic damage and improve outcomes after MI [159, 160]. Still, this therapeutic approach is not without its limitations. There is a lack of safe cooling techniques available, and since target temperature should be reached well before the reperfusion stage to ensure maximum benefit, it might not be very advantageous for patients suffering with out-of-hospital MI. However, It could bring additional benefits to patients if administered as an adjunct therapy together with PCI [161]. Moreover, sodium-hydrogen exchange inhibitors (e.g. Cariporide), capable of ameliorating the rise in intracellular calcium have been shown to afford cardioprotection when administered prior to the index ischaemia [162, 163]. However, that makes them useful agents in circumstances such as coronary artery bypass surgery (CABG) where ischaemic insult is expected, and less so in acute myocardial infarction where the onset of ischaemia cannot be predicted. Furthermore, sodium-hydrogen inhibitors exhibit adverse off-target

effects, increasing mortality and the rate of cardiovascular events, which further limits their prospective use as safe and effective cardioprotective agents [164, 165]

Cardioprotective agents – reperfusion injury

As opposed to dealing with ischaemic injury, the bulk of interventions and drugs show a cardioprotective effect on the heart by exhibiting their effects at the reperfusion stage of the I/R injury. To date, rapid restoration of blood flow to the affected area of the heart muscle remains the most effective cardioprotective strategy. This is mostly achieved via primary percutaneous coronary intervention (PCI) or thrombolytic therapy (e.g. tissue plasminogen activator, streptokinase) that breaks down the obstructing blood clot [166-168].

In recent years, a lot of effort has been put into shortening the time between the onset of symptoms and the start of reperfusion [169]. However, it is not always possible to bring the patients to the cardiology unit in sufficient time to allow for maximum benefit that can be gained from mechanical reperfusion [166]. Therefore, pharmacological therapies that have shown promise in protecting the heart against the onslaught of damage seen after myocardial infarction could help provide additional benefit in situations where timely PCI cannot be achieved.

Volatile anaesthetic agents have been shown to exert beneficial effects during CABG surgery, where transient ischemia due to surgery is known to occur. There is also evidence of a more direct cardioprotective involvement of volatile anaesthetics, such as isoflurane and other fluranes, in various *in vitro* and *in vivo* models of I/R injury [170-173]. Exenatide, an antidiabetic drug is another agent that has been shown to reduce the final infarct size when administered as a continued infusion, just before the start of PCI. Exenatide is an analogue of hormone glucagon-like peptide 1 (GLP-1), linked with activation of pro-survival kinase pathways when administered prior to reperfusion [174, 175]. Despite these actions, it is not yet known if its effects lead to improved clinical outcomes, with more clinical trials needed to assess its cardioprotective ability [17, 176].

In contrast, Cyclosporine-A displays its cardioprotective capacity by preventing the opening of the MPTP at reperfusion stage, which reduced the final infarct size in experimental studies [177]. Therefore, it comes as a surprise that a recent large randomized clinical trial Cyclosporine and Prognosis in Acute Myocardial Infarction Patients (CIRCUS), which included patients with ST-segment elevation myocardial infarction (STEMI), did not show a beneficial effect for Cyclosporine-A with all-cause mortality as primary endpoint of the trial [176, 178] . This goes to show how hard it is to achieve a successful translation of a cardioprotective approach from experimental models *in vitro* and *in vivo* to the efficacious therapy that can be used in the clinic.

Pre-conditioning

One of the most promising non-pharmacological cardioprotective interventions is ischaemic pre-conditioning. A technique, that delays cell death by subjecting the myocardium to brief episodes of ischaemia before a sustained episode of infarction has been first described by Murry *et al*. who showed that it reduces infarct size in dogs [179].

Pre-conditioning is not dependent on the existence of collateral coronary circulation or the size of the animal model and the beneficial effects afforded by pre-conditioning have been since observed in many different species, including humans [180-183]. Despite the breakthrough pre-conditioning provided, it was hard to apply it to the clinical setting, since the pre-conditioning treatment would have to be applied in the patient before the MI has even occurred. It was not until the discovery of ischaemic post-conditioning by Zhao *et al.* that the clinical application became a possibility [184]. Post-conditioning works on a similar basis to pre-conditioning with the only exception being that the brief ischaemic cycles are applied prior to reperfusion instead of prior to ischaemia. The discovery of post-conditioning also cemented the case for lethal reperfusion injury, since the treatment was applied after ischaemia and could therefore not reduce its impact [185].

To test how well the treatments that were so successful in animal models performed in humans, STEMI patients were subjected to post-conditioning cycles of ischaemia shortly after initiating reflow in the proof of concept trial by Staat *et al*. [186]. The clinical trial was a success and showed a reduced creatine kinase (surrogate marker for infarct size) in the pre-conditioned group of patients. However, many clinical trials that came thereafter showed only a small benefit of pre- and post-conditioning or failed to replicate this feat entirely [187, 188]. This might be due to the latter trials making use of a less regulated patient environment, with a more real-life scenario where potential confounders and variables cannot be controlled for accurately.

Overall, pre-conditioning technique and its variations (remote ischaemic conditioning, post-conditioning) are seen as beneficial for the heart, however finding the right setting for their utilization, so they can exert the most impact, has proven challenging.

1.4.2 *The role of CXCR4 and CXCR7*

RISK cardioprotective pathway

The Reperfusion Injury Salvage Kinase (RISK) signalling pathway was first described by Yellon's group in 2002 to define the cardioprotective effects of urocortin [189]. It consists of two parallel signalling cascades PI3K/AKT and MEK1/ERK1/2, which underlie the cardioprotective effects of several known interventions (e.g. preconditioning, adenosine) [190-192]. In order for the pro-survival kinases of the RISK pathway to be able to afford cardioprotection, they must be activated at the time of early reperfusion [190]. For example, IPC-mediated cardioprotection through the RISK pathway occurs in two phases: i.) the trigger phase, which occurs during the preconditioning cycles and ii.) the early reperfusion phase, when activation of pro-survival kinases is postulated to prevent the opening of the mPTP and consequently mitigates the I/R injury [193, 194].

However, the cardioprotective effects exhibited by RISK pathway activation are not limited to IPC and can also be observed with administration of pharmacological agents, such as adenosine, insulin, opioids and others [190, 194-196]. Thus, the current consensus is that the RISK signalling pathway is shared by most cardioprotective therapies [191].

The RISK pathway is activated by G protein signalling, which phosphorylates Phosphoinositide-3-kinase (PI3K) and MEK1/2, triggering a signalling cascade involving phosphorylation of AKT also known as protein kinase B and ERK1/2 also known as mitogen protein kinase (MAPK3/1), respectively. It is important to note that PI3K/AKT and ERK1/2 are not restricted to the RISK pathway. In fact they are involved in many pathological and physiological signalling pathways and represent some of the most ubiquitous signalling molecules present in nearly every cell in the human and murine organism [197, 198]. However, in the context of cardioprotection, where AKT and/or ERK1/2 signalling is posited to culminate in beneficial effects on the myocardium, the term RISK signalling pathway is used to describe their involvement. Similarly, the so-called Survivor Activating Factor Enhancement (SAFE) pathway, which signals through JAK-STAT has also been shown to confer cardioprotection, independently of the RISK pathway [199]. Both, RISK and SAFE signalling pathway activation was shown to reduce final infarct size at reperfusion, with the pathways often described as a molecular basis of cardioprotection [200-202]. Additionally, Huang *et al*. suggested that the SDF-1α/CXCR4 axis affords cardioprotection directly by working through STAT3, which forms a part of the SAFE signalling pathway [203]. The cardioprotective stimulus is thought to work twofold, indirectly through the ability of CXCR4 to mobilize stem cells and directly via activation of the RISK and SAFE pathways (Fig. 1-5) [203, 204]. However, this thesis will focus on the role of RISK signalling pathway in SDF-1α signalling.

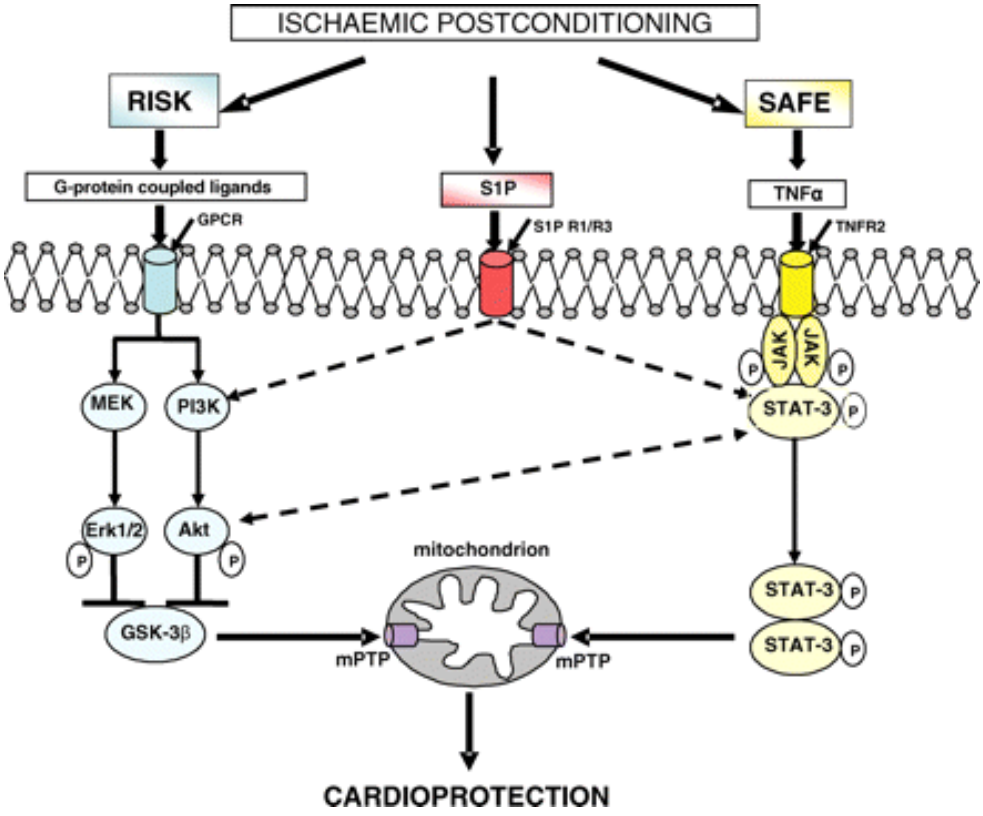

Figure 1-5: Signalling through RISK and SAFE cardioprotective pathways. RISK pathway signalling involves activation of a GPCR, which in turn phosphorylates either MAPK or PI3K, leading to ERK1/2 and AKT activation, respectively. This in turn blocks the mPTP opening and prevents cell death from reperfusion injury. On the other hand, SAFE cardioprotective pathways signals through TNF-α binding to a TNF receptor, which induces activation of the JAK/STAT complex. This again leads to blockage of the mPTP and cell survival. Image adapted from Lacerda et al [199].

The role of CXCR4 in cardioprotection

Due to known effects of SDF-1α on stem cell homing, retention, repair, as well as ventricular remodelling it comes as no surprise that investigation of cardioprotective properties of SDF-1α/CXCR4 axis has garnered a lot of interest [100, 205, 206]. The sustained release of engineered SDF-1α analogue from a hydrogel injected into the myocardium peri-MI, has proven an effective cardioprotective measure in a rat model of myocardial infarction [207]. The procedure was performed *in vivo* with permanent ligation of the LAD and analysis of rat hearts 4 weeks post-MI showed reduction of LV fibrosis in hearts injected with a hydrogel containing the engineered SDF-1α analogue versus hearts injected with hydrogel alone. The administration of SDF-1α has also proven cardioprotective when delivered directly via an intracardiac injection post-MI in an *in vivo* permanent ligation model. Mice injected with SDF-1α displayed significantly better cardiac function than the controls, immediately post infarction and in the longer term, along with decreased scar formation, which was observed several weeks after the initial ischaemic insult [100]. Furthermore, pre-conditioning increases the levels of SDF-1α, and it is hypothesized that the cardioprotective effects exhibited by this intervention are due to SDF-1α/CXCR4 signalling through RISK cardioprotective pathway (Figure 1-6) [91, 190].

Additionally, injection of skeletal myoblasts overexpressing SDF-1α post-MI in an *in vivo* rat model of MI with permanent LAD ligation, improved LV contractile function and promoted myocardial regeneration in the long term [208]. Interestingly, administration of skeletal myoblasts overexpressing SDF-1α into the peri-infarct zone 8 weeks post-MI still managed to improve contractility of the LV 8 weeks post-treatment, specifically fractional shortening, compared to the LV contractility observed prior to cell therapy. Meanwhile, administration of skeletal myoblasts without SDF-1α overexpression, did not afford such cardioprotection [209]. Furthermore, SDF-1α administration prior to MI improved myocardial functional recovery immediately post-MI in a mouse Langendorff I/R model.

These beneficial effects have largely been attributed to the SDF-1α/CXCR4 signalling axis, with fewer studies focusing on the role of the CXCR7 receptor [203].

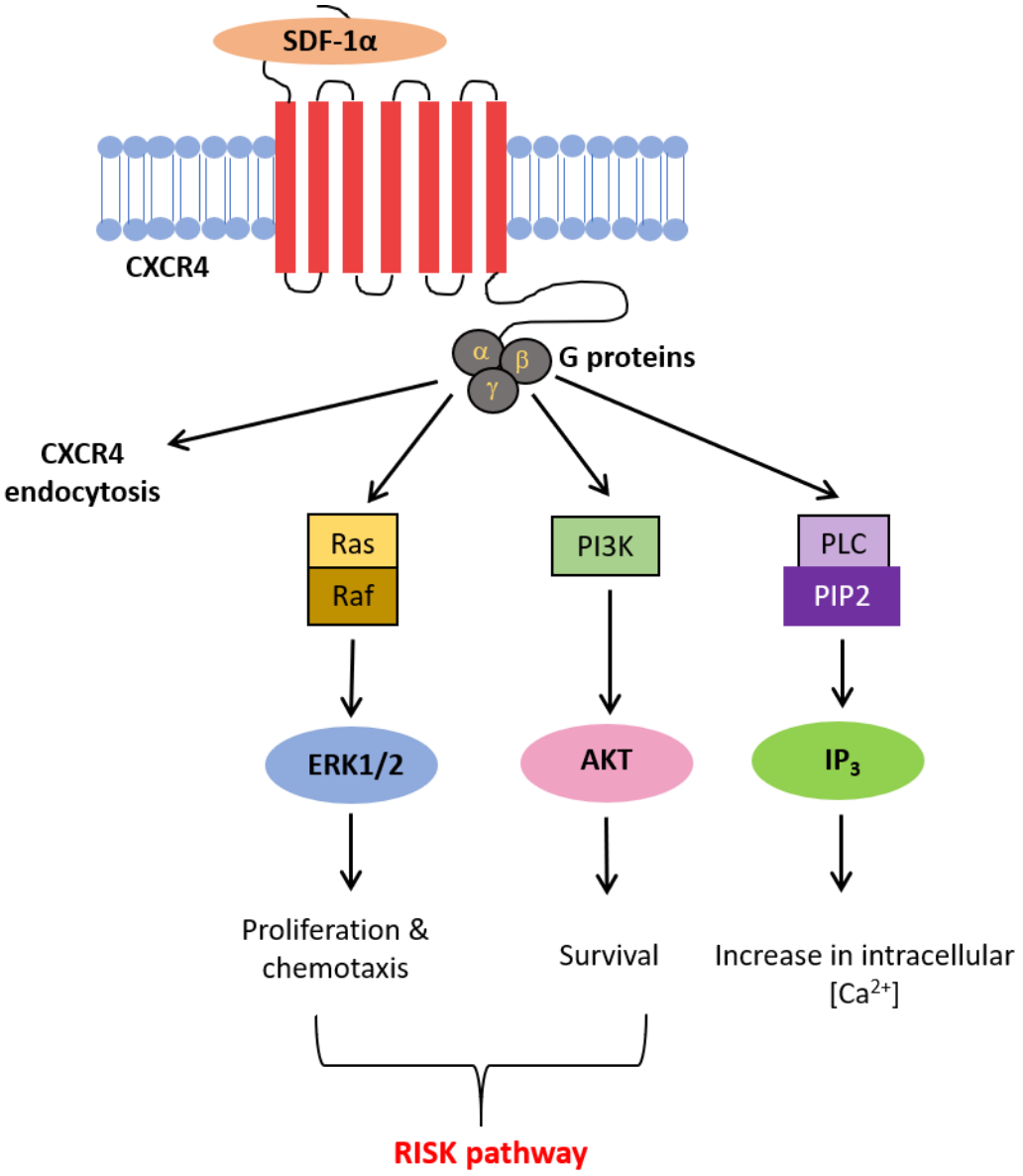

Figure 1-6: SDF-1α/CXCR4 signalling through the RISK cardioprotective pathway. RISK pathway signalling involves activation of a GPCR, which in turn phosphorylates either MAPK or PI3K arm of the signalling pathway, leading to ERK1/2 and AKT activation, respectively. This in turn blocks the opening of the mPTP and prevents cell death. At the same time SDF-1α/CXCR4 signalling also triggers Ca^{2+} mobilization, involved in many cellular processes, through PIP2/IP3 signalling.

On the other hand, there is also evidence that CXCR4 can act in a detrimental fashion, worsening the outcome after MI. In a study by Liehn *et al*. CXCR4 heterozygous knockout mice exhibited reduced infarct size when measured 4 weeks after myocardial infarction [210]. This could be due to CXCR4-dependent alteration of adverse remodelling and involvement of reparative pathways, however there were no additional effects on cardiovascular function [210]. Transgenic rats, in which CXCR4 overexpression in the heart has been achieved with administration of an adenoviral vector, showed an increase in infarct size and worsening cardiac function, when compared to wild type rats. CXCR4 overexpression was also associated with increased inflammatory cell infiltration and cardiomyocyte apoptosis in the ischaemic heart [211].

Similarly, induced overexpression of SDF-1α in rat cardiomyocytes led to worse outcomes when rats were subjected to I/R injury compared to controls. Although, supra-physiological levels of the ligand could be responsible for part of the effect [211, 212]. The case remains that there is evidence for both, protective and detrimental effects of CXCR4 receptor in the cardiovascular setting. Previous studies also suggested that the timescale of CXCR4 increase in the heart after MI does not correspond to the peak of SDF-1α activity [213]. It looks as though the way SDF-1α/CXCR4 axis behaves, depends at least partially upon the temporal alignment and/or the timing of SDF-1α and CXCR4 expression, which then dictates whether the subsequent downstream signalling events prove to the beneficial or detrimental to the ischaemic heart [206].

The role of CXCR7 in cardioprotection

Compared to CXCR4, less is known about the signalling through CXCR7 in cardioprotection, be it through the RISK pathway, or other signalling pathways. There is mounting evidence of RISK and SAFE pathway involvement through ERK1/2, AKT, JAK/STAT and MAPK pro-survival signalling downstream of CXCR7 receptor in tumour progression and metastasis, but less is known about CXCR7 signalling in cardiovascular cell types [214-218]. One of the hallmarks of RISK pathway activation is phosphorylation of ERK1/2 and AKT, which can be easily determined in an experimental setting, for example via western blotting. Past research shows that CXCR7 activation, using either SDF-1α or TC14012, can induce ERK1/2 and/or AKT phosphorylation on various cell types, including cardiac stem cells, HUVEC, and T cells of the immune system [115, 219, 220]. CXCR7 has been shown to signal via recruitment of β-arrestins to the plasma membrane, as described in section 1.3. However, less is known about signalling downstream of CXCR7, and what further signalling pathways this might activate. Current knowledge of SDF-1α/CXCR7 signalling via RISK pathway in different cell types is summarized in Figure 1-7.

Chen *et al*. showed by western blotting that SDF-1α induced phosphorylation of AKT on c-kit^{+} rat cardiac stem cells 15 min after administration [219]. On the other hand, the administration of CXCR7 small interfering RNA (siRNA), in the presence of SDF-1α, inhibited AKT phosphorylation and restricted cell migration in response to SDF-1α [219]. Kumar *et al*. showed that pre-treatment of Jurkat T cells with CXCR4-blocking antibody and subsequent administration of SDF-1α, induced maximal phosphorylation of AKT 15 min after administration [220]. This was interpreted as an indication of PI3K/AKT signalling by SDF-1α via CXCR7.

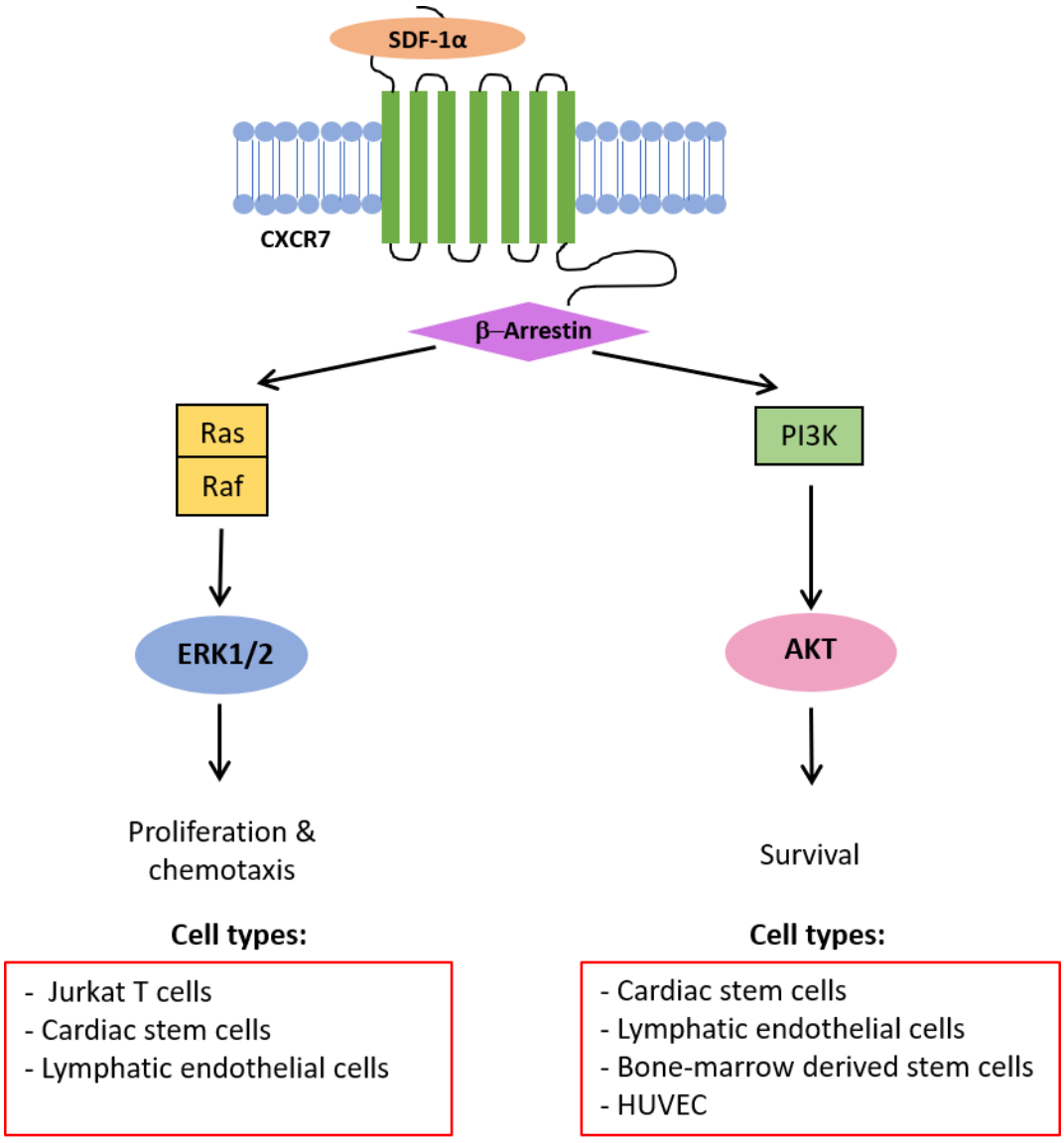

Figure 1-7: SDF-1α/CXCR7 signalling through the RISK cardioprotective pathway. The binding of SDF-1α to CXCR7 triggers β-arrestin recruitment, which in turn activates either the MAPK (ERK1/2) or the AKT arm of the RISK signalling pathway, leading to cell proliferation and chemotaxis or cell survival, respectively.

Phosphorylation of AKT was abrogated in the presence of wortmannin, an irreversible PI3K inhibitor. Pre-treatment of Jurkat T cells with wortmannin before stimulation with SDF-1α also inhibited cell survival, suggesting the importance of CXCR7-AKT signalling pathway for T cell survival [220].

Similarly, SDF-1α incubation in the presence of CXCR4-blocking antibody elicited maximal phosphorylation of ERK1/2 10 min post-administration, and was found to play an important role in the chemotactic response of Jurkat T cells [220]. Moreover, Rajagopal *et al.* showed that HEK293 cells transfected with CXCR7 have the ability to recruit β-arrestins after stimulation with SDF-1α, leading to sustained ERK1/2 activation [135]. Moreover, phosphorylation of AKT and ERK1/2 as a result of CXCR7 stimulation has been reported in rat cardiac stem cells [219]. Similarly, Zhao *et al.* showed that SDF-1β signalling through CXCR7 protects from palmitate-induced apoptosis via AMPK and p38 MAPK in H9C2 (rat cardiac myoblast) cells [221]. Thus, various evidence suggests that CXCR7 activation is able to couple to PI3K/AKT and ERK1/2 kinases.

Only a few papers focus specifically on CXCR7 in endothelial cells. Zhang *et al*. showed that activation of CXCR7 via administration of TC14012 in HUVEC induces phosphorylation of PI3K, which stimulates endothelial tube formation. This change in phosphorylation status was abrogated by administration of PI3K inhibitor, LY294002, which also inhibited tube formation [222]. Further information about the importance of AKT and ERK1/2 activation in endothelial cells comes also from experiments performed on isolated mouse aorta endothelial cells by Hao *et al*. [115]. In this study, pre-treatment of cells with IL-1β induced cell proliferation, while the administration of CXCR7 antagonist or CXCR7 siRNA, decreased phosphorylation of AKT and ERK1/2 and consequently reduced cell proliferation. Therefore, it seems that in endothelial cells CXCR7-dependent activation of ERK1/2 and/or AKT plays a role in angiogenesis and cell proliferation, processes through which CXCR7 could exert its cardioprotective effects. Nevertheless, the exact signalling components downstream of SDF-1α/CXCR7 have not yet been elucidated, and they might differ in various cell types and tissues

Hao *et al*. have shown that intraperitoneal administration of CXCR7 agonist, TC14012 (10 mg/kg), immediately post-MI and then every 6 days for 24 days, in an *in vivo* mouse model of MI with permanent ligation, significantly decreased final infarct size 4 weeks post-MI. However, the role of CXCR7 and its agonists in an acute myocardial infarction setting has not yet been defined [115]. Hao *et al*. reported that mice with inducible, endothelial-specific CXCR7 deletion exhibit increased neointima formation after endothelial denudation injury in the femoral artery [115]. Furthermore, Hao's group also showed that endothelial deletion of CXCR7 in mice impaired cardiac function, reduced survival rate and increased infarction size after permanent ligation myocardial infarction. Therefore, evidence exists of endothelial CXCR7 being important for not only cardiac development, but also cardiac function and warrants further investigation in terms of its cardioprotective capacity.

The study by Hao *et al*. has been published during my PhD, and unfortunately explored many of the same ideas that I was also interested in, especially the role of CXCR7 agonists on long-term cardioprotection and the role of CXCR7 in myocardial infarction in CXCR7 knockout mice [115]. That prompted me to focus more on the acute side of cardioprotection, as well as the pro-angiogenic aspects of CXCR7 so as to explore more novel concepts, rather than just repeat what has already been published before.

The role of CXCR4 and CXCR7 in myocardial regeneration

As already discussed in section 1.4.1 there are a variety of clinical interventions, either mechanical of pharmacological, that can be utilized in the setting of myocardial infarction. Most of those interventions are based on re-establishing blood flow, providing so-called reperfusion therapy. However, not all patients will benefit from reperfusion therapy equally; for example those with microvascular dysfunction will experience less benefit from reperfusion therapy than those without [223]. For those patients, increasing the rate of vessel regeneration in the infarcted myocardium can offer an alternative, long-term approach to cardioprotection afforded by timely reperfusion. Most current therapies focus on acute cardioprotective interventions, usually administered during or immediately after MI. However, many MI patients then go on to develop heart failure and designing therapies aimed at long-term pro-regenerative solutions that go past the scope of acute cardioprotection, could also improve patient prognosis and decrease the rate of heart failure occurrence. Native pro-angiogenic response after MI is present in the adult heart to some extent although the mechanism of vessel regeneration in the ischaemic heart in general is not well understood [224, 225] . Furthermore, this response is likely insufficient to cope with the damage caused by coronary vessel occlusion [225, 226].

Pro-angiogenic therapies administered after MI have shown therapeutic potential in preclinical studies in the past. Most pro-angiogenic therapies investigated so far have focused on delivery of angiogenic growth factors or stem and progenitor cells that are believed to have pro-angiogenic potential, with limited success [63, 227, 228]. However, there are many different stages involved in the mechanism of angiogenesis, offering numerous therapeutic targets that researchers can explore, with the hopes that SDF-1α can become one of them.

SDF-1α is a major contributor to the process of angiogenesis. It plays a crucial role in endothelial cell migration, retention, proliferation, as well as recruitment and survival of EPCs to sites of ischaemia-induced injury [229,112, 230]. Therefore, SDF-1α/CXCR4 signalling in the infarcted myocardium is thought to promote recruitment and survival of adipose-derived regenerative cells, c-kit+ endogenous cardiac stem cells and bone marrow stem cells [96, 98, 206]. Stem cells that have been externally delivered to the ischaemic heart (e.g. intramyocardial, intracoronary injection) have been shown to improve cardiac function and limit damage to the left ventricle, despite poor retention and engraftment at the site of injection [99, 100]. The beneficial effects of injected stem cells are hypothesized to be a result of paracrine effects of stem cells on their surrounding cells, such as release of cytokine growth factors and stimulation of angiogenesis and are largely believed to rely on SDF-1α/CXCR4 signalling. Preliminary animal studies on rodents showed good regeneration of cardiac function after injection of stem cells into ischaemic myocardium [231]. However, despite several clinical trials showing improvement in clinical outcomes after stem cell administration in patients with ischaemic heart disease, no study has yet shown myocardial regeneration on a scale of that seen in animal studies [232, 233]. This further highlights the widening chasm between bench and bedside and is emblematic of what is occurring in the areas of myocardial regeneration, cardioprotection and beyond.

The role of CXCR7, however, is even less understood. There is a lack of knowledge regarding the role of CXCR7 in cardiac injury and subsequent revascularization and regeneration efforts that take place in the damaged tissues. Most of the data so far comes from groups studying CXCR7 in regeneration and fibrosis of various tissues, with little research focusing specifically on the heart [234, 235]. A great deal of studies on CXCR7 have focused on its role in angiogenesis in the context of cancer biology, but less so in other processes [236, 237]. Increased levels of CXCR7 have been shown in tumour vasculature, where CXCR7 plays an important role in tumour formation, metastasis, and tumour angiogenesis [238, 239].

Research conducted by Yan *et al.* suggests that CXCR7 is not involved in EPC migration and proliferation, whereas EPC survival depends solely on CXCR7 [112]. Formation of SDF-1α-induced EPC tube formation on the other hand, is heavily dependent on both receptors working in unison to guarantee a maximum response [112]. This highlights a complementary rather than redundant role of both receptors regarding the EPC, which could also extend to other cell types (e.g. differentiated endothelial cells). CXCR7 was also found to mediate matrix metalloprotease- 2 (MMP-2) release, which could represent another mechanism responsible for CXCR7-triggered revascularization after ischaemic injury [112, 118]. Additionally, Hao *et al*. showed that inhibition of CXCR7 negatively affects angiogenesis, while Zhang *et al.* showed that SDF-1α promotes tube formation, proliferation and migration of HUVEC, although they do not distinguish whether these actions are mediated through CXCR4 or CXCR7 receptors [115, 222]. Furthermore, Ding *et al*. reported that CXCR7-Id1 signalling mediates liver regeneration and limits fibrosis, while CXCR4-FGFR1 signalling in the same setting promoted fibrogenesis [234]. CXCR7 was also found to promote lung alveolar repair and to abrogate fibrosis after acute lung injury, by signalling through the Wnt signalling pathway [240]. Additionally, SDF-1α/CXCR7 signalling after pneumonectomy prompted AKT-dependent MMP-14 release from activated platelets, which stimulated alveolar regeneration [235].

All in all, there is mounting evidence of CXCR7 involvement in angiogenesis and through that a potential to help re-establish sufficient vascular supply to the myocardial tissue damaged by ischaemia/reperfusion (I/R) injury. This pro-angiogenic approach through CXCR7 could potentially provide long term benefits to the heart.

1.5 Hypothesis and Aims

1.5.1 *Original hypothesis*

The original hypotheses to be investigated in this thesis are:

1. CXCR7 is expressed on cardiovascular cell types.
2. Activation of endothelial CXCR7 stimulates components of cardioprotective and regenerative signalling pathways.
3. Activation of CXCR7 induces acute cardioprotection after myocardial infarction
4. Activation of CXCR7 promotes long-term regeneration by stimulating angiogenesis

1.5.2 *Aims*

The specific aims and objectives of the study are to:

1. Investigate expression of CXCR7 in cardiovascular cell types.

- Confirm expression of CXCR7 in mouse cardiovascular tissues.
- Confirm expression of CXCR7 in endothelial cells of cardiac origin.
- Investigate localization of CXCR7 and CXCR4 receptors in endothelial cells and identify an appropriate cell line for use in *in vitro* experiments.

2. Investigate whether CXCR7 agonist VUF11207 exhibits cardioprotective effects in a rat *ex vivo* perfusion model.

- Investigate if the administration of VUF11207 prior to reperfusion has an effect on the final infarct size in MI.
- Investigate if the administration of VUF11207 prior to reperfusion has an effect on the LDH release during MI.

- Examine whether the administration of VUF11207 prior to reperfusion has an effect on the functional parameters of the heart.

3. Investigate whether administration of CXCR7 agonists is able to induce AKT and/or ERK1/2 phosphorylation, in order to examine RISK pathway signalling.

- Examine the effect of VUF11207 and SDF-1α on AKT, ERK1/2 phosphorylation status in HUVEC.
- Examine the effect of TC14012 and SDF-1α on AKT, ERK1/2 phosphorylation status in HUVEC.

4. Generate mice with inducible, endothelial-specific CXCR7 deletion.

- Characterize the mouse model by investigating endothelial CXCR7 RNA and protein content.
- Examine whether the mice exhibit the loss of endothelial CXCR7 protein.

5. Investigate the effects of CXCR7 agonists on HUVEC migration.

- Examine the effects of CXCR7 agonists, VUF11207 and TC14012 on HUVEC migration via Boyden chemotaxis chamber.

2 Materials and methods

This chapter describes the general methods and materials used throughout this thesis. All reagents used were from Sigma-Aldrich (Dorset, UK), unless stated otherwise. All perfusion solutions were made using water from a MiliQ dispenser with a resistance of >18.0 MΩ and filtered (1 µm pore size) before use.

2.1 Experimental use of animals

All animals were housed in individually ventilated cages with 12h light/dark cycles under pathogen-free conditions. Standard chow and water for the animals was provided *ad libitum*, with the temperature of the housing unit maintained at 21°C. Animals were regularly inspected for signs of ill health (reduced weight gain, piloerection, hunching etc.) and routine care was administered by the University College London (UCL, UK) Biological Services Unit (BSU). Experiments were performed in line with best practice as described by the Home Office License Training Course Modules 1-4. All animal work was carried out in accordance with the Guidelines on the operation of Animals (Scientific Procedures) Act, as published by the UK home office in 1986 and Amendment Regulations 2012. All procedures contained within the application have been reviewed by the institutional veterinary surgeon Olga Woolmer (2017). The experiments are conducted within the terms of the Animals (Scientific Procedures) Act 1986, under Project License number PPL 70/8556, ("Protection of the Ischaemic and Reperfused Myocardium") issued to Prof. Derek Yellon in 2015.

2.2 Transgenic mouse lines

2.2.1 *Generation of transgenic mice*

Ackr3$^{tm1Twb\ flox/+}$ mice were originally generated by Timothy W. Behrens, M.D. (University of Minnesota, MN, USA) [114]. Mice were obtained from Mutant Mouse Resource and Research Centre (MMRRC) from a cryopreserved embryo stock.

Briefly, mice were generated with the help of a targeting vector designed to insert *loxP* sites, which are 34 base pair (bp) sequences that allow DNA to be modified in the presence of Cre recombinase, from either side of exon 2 of the *Cxcr7 (Ackr3)* locus (Figure 2-1). The targeting vector used for the generation of this transgenic line was created from PCR cloned 129/SvEv genomic DNA that has been inserted into the pK11-2xLox-MCS12.

The linearized targeting vector was then electroporated into 129/SvEv embryonic stem (ES) cells. Correctly targeted, ES cells were injected into C57BL/6 mouse blastocysts. Chimeric offspring were crossed with C57BL/6J mice, and agouti offspring were screened for presence of the targeted allele, Cxcr7 flox.

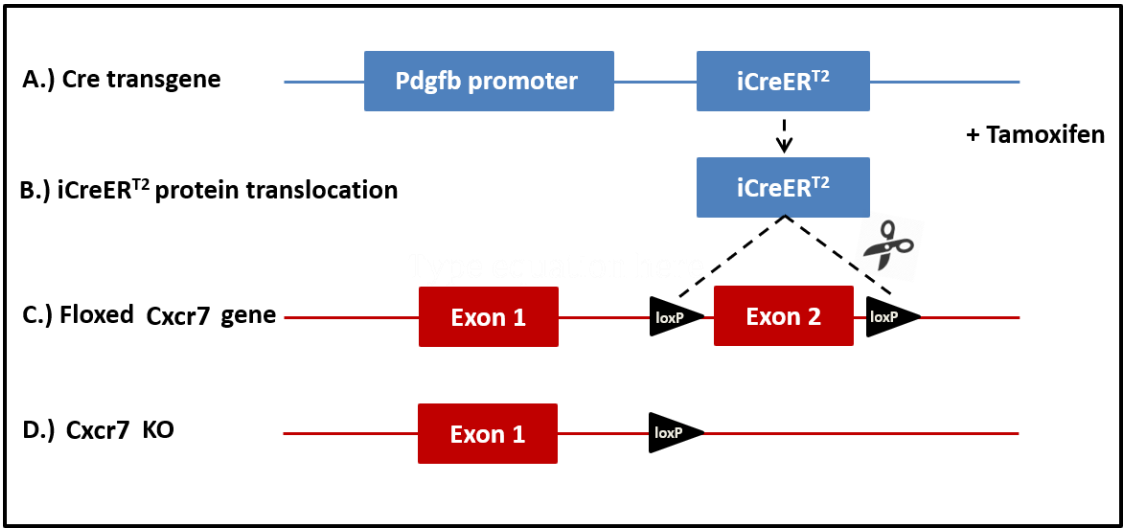

Figure 2-1: Cre/Lox mechanism for transgenic mouse generation. A.) iCreER^{T2} (inducible Cre) transgene product expression is spatially regulated by the Pdgfb promoter. B.) Administration of tamoxifen causes a translocation of iCreER^{T2} protein into the nucleus. C.) In the nucleus, Cre induces recombination at loxP sites flanking exon 2, D.) resulting in excision of exon 2 and generation of endothelial-specific Cxcr7$^{i\Delta EC}$ mice. KO = Cxcr7$^{i\Delta EC}$.

2.2.2 *Endothelial-specific gene ablation*

In order to examine the tissue-specific effects of Cxcr7 in adult mice, inducible iCreER^{T2} recombinase driven by the endothelial-specific *platelet- derived growth factor B promoter* (Pdgfb), referred to as Pdgfb-iCreER^{T2} was used.

Since this form of Cre recombinase first needs to be induced by tamoxifen injection, it allowed us to not only spatially, but also temporally regulate the induction of Cre recombinase, and with it, Cxcr7 gene deletion. Temporal regulation of Cxcr7 deletion in vascular tissues is particularly important due to severe cardiovascular defects exhibited by embryos lacking Cxcr7 in the vasculature [119, 148]. The iCreER^{T2} form of the Cre gene encodes a Cre sequence adjoined to a single human mutated ER (oestrogen receptor) binding domain, to which tamoxifen (oestrogen receptor modulator) binds to initiate nuclear translocation of iCreER^{T2} protein. Importantly, mutated ER receptor domain is not activated by endogenous ligand 17β-oestradiol to prevent unwarranted translocation of Cre protein [241].

iCreER^{T2} has been previously reported as having lower background activity and higher efficacy than other Cre systems [242]. C57BL/6J$^{Cre/+}$ mice expressing tamoxifen-inducible improved Cre recombinase driven by the platelet derived growth factor subunit B promoter (Pdgfb-iCreER^{T2}), were obtained from Dr Marcus Fruttiger (UCL, London) and generated as described elsewhere [243]. Pdgfb-iCreER^{T2} colony founders used to set up our colony also contained floxed Cxcr4 alleles. Cxcr4$^{fl/fl}$ animals were obtained from Dr Dan R. Littman (Columbia University, NY, USA) and generated using methods published elsewhere [244].

2.2.3 *Colony maintenance*

Mice were bred as outlined in Figure 2-2 below. The iCreER^{T2} (henceforth called “Cre”) transgene was maintained as heterozygous for several reasons. Firstly, the exact insertion site of the Cre transgene is unknown due to random integration of the transgene construct and therefore it is difficult to distinguish homozygous and

heterozygous genotype, with heterozygous expression of Cre sufficient to induce recombination at the loxP sites [243, 245]. Additionally, the very insertion of the Cre construct can cause disruption of the gene into which it inserts [246]. Certain versions of Cre also have the ability to produce unanticipated effects when in homozygous form, such as myocardial dysfunction observed in myocyte-Cre overexpressing mice [247]. Therefore, it is preferable to maintain mice as heterozygotes.

Breeding pairs were made up of animals between 8 and 16 weeks of age, with females being allowed a maximum of 6 litters. Litters were weaned at 3 weeks of age after which ear biopsies were collected and genotypes determined by PCR.

To describe the genetic status of transgenic animals, certain abbreviations are used throughout the text: wild type (WT, $Cxcr7^{fl/fl}$ Cre^{-}, $Cxcr7^{WT}$), floxed (FL, fl/fl, $Cxcr7^{fl/fl}$ Cre^{+} injected with Tamoxifen, $Cxcr7^{i\Delta EC}$).

A.)

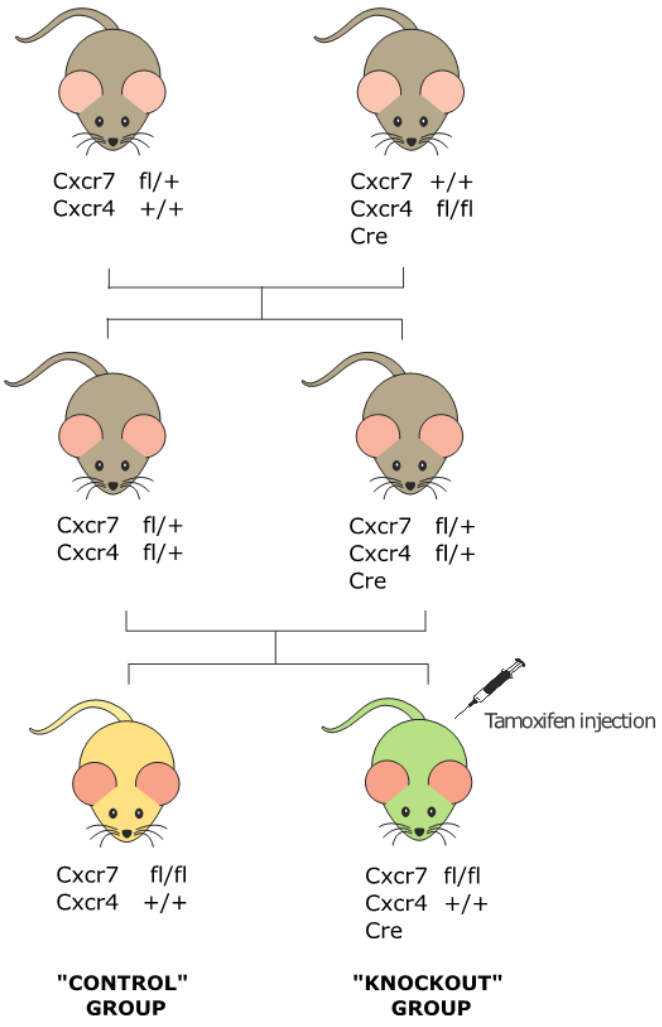

Generated mice:

B.)

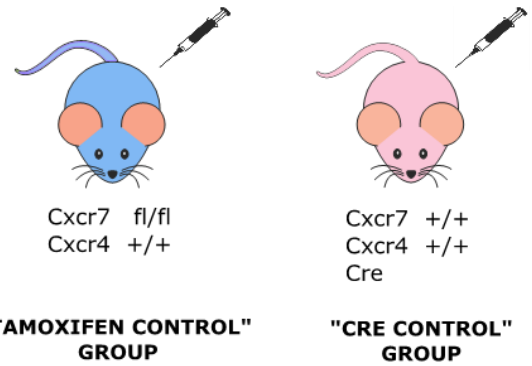

Additional control mice:

Figure 2-2: Transgenic mouse breeding scheme. A) Depicted are mouse breeding pairs used to breed experimental transgenic animals in our experiments. B.) Additional control mice that would need to be generated in order to investigate any potential effects of tamoxifen or Cre, since tamoxifen can exhibit various degrees of toxicity and certain Cre strains display detrimental effects on mouse tissues.

2.2.4 *Mouse genotyping*

Mouse biopsies were collected by BSU staff shortly after weaning at 3 weeks of age. Total DNA was isolated from mouse ear biopsies, using Direct PCR lysis reagent (Viagen Biotech, CA, USA) and Proteinase K (Qiagen, Norway) in a ratio of 10:1 overnight at 55°C. Afterwards, samples were heated to 90°C for 45 min to terminate the lysis process and were subsequently stored at -20°C before analysis.

PCR reactions were run using Taq PCR Master Mix Kit (Qiagen, 201443) with reagents outlined in Table 2-1 and 2-2 below. Sequences of PCR primers used are listed in Table 2-3.

Reagent	Volume per sample (µl)	Final concentration
10mM dNTPs	2.0	250µM of each dNTP
10x PCR buffer	0.4	2x
Forward primer	0.5	0.2 pmol/µL
Reverse primer	0.5	0.2 pmol/µL
Distilled water	15.4	-
Taq DNA polymerase	0.2	-
Template DNA	1.0	-
Total volume per sample (µl)	20	

Table 2-1: PCR reaction mix components for Cxcr4 and Cre genotyping.

Reagent	Volume per sample (µl)	Final concentration
10mM dNTPs	2.5	250µM of each dNTP
10x PCR buffer	0.5	2x
WT forward primer	0.5	0.2 pmol/µL
FL forward primer	0.5	0.2 pmol/µL
Common reverse primer	0.5	0.2 pmol/µL
Distilled water	13.3	-
DMSO	0.5	-
Taq DNA polymerase	0.2	-
Template DNA	1.5	-
Total volume per sample (µl)	20	

Table 2-2: PCR reaction mix components for Cxcr7 genotyping.

Primer name	Primer sequence (5'-3')	T_m (°C)
Cxcr7 WT forward primer	GCTGCAAACCCGTGAACAAGG	61.7
Cxcr7 FL forward primer	TCTATCGCCTTCTTGACGAGTTCTTC	60.1
Cxcr7 Common reverse primer	GGGCTCTCTGGCCGTTCTCTC	65.2
Cxcr4 forward primer	CCACCCAGGACAGTGTGACTCTAA	64.4
Cxcr4 reverse primer	GATGGGATTTCTGTATGAGGATTAGC	61.6
Pdgfb-Cre forward primer	CCAGCCGCCGTCGCAACT	62.8
Pdgfb-Cre reverse primer	GCCGCCGGGATCACTCTCG	65.3

Table 2-3: PCR primer sequences and their melting temperatures.

All PCR primers were purchased from Eurofins Genomics (Germany) and were dissolved in distilled MiliQ water at 100 pmol/µL, with the final working concentration of 10 pmol/µL.

The PCR-cycling protocol outlined in Table 2-4 was used for Cxcr4 and Cre PCR reactions on a PTC-200 Peltier Thermal Cycler (MJ Research, Canada), including a heated lid setting. Samples were run using a "touch-down" cycling technique, where the annealing temperature is reduced from 65°C to 60°C by 1°C per cycle prior to standard cycling at 60°C annealing temperature. This allows for primers to achieve a highly specific binding at the first available temperature with further cycles utilizing incrementally lower annealing temperatures to achieve maximum efficiency of reaction. Subsequently, this also allows for reduction of non-specific binding at lower annealing temperatures providing a specific, sensitive and high-yield reaction [248].

PCR stage	Temperature and duration	Description
5 cycles of:		
1.	94°C – 30 s	DNA denaturing
2.	65°C – 30 s, decreasing 1°C per cycle until it reaches 60°C	Primer annealing
3.	72°C – 30 s	DNA synthesis
Then 40 cycles of:		
16.	94°C – 30 s	DNA denaturing
17.	60°C – 30 s	Primer annealing
18.	72°C – 1 min	DNA synthesis
Then 4°C until collection.		

Table 2-4: Cxcr4 and Cre PCR thermocycling protocol.

Loading buffer was added to the samples and they were subsequently run on an agarose gel consisting of 2% agarose powder dissolved in 1x TAE buffer (Tris 40 mM, acetic acid 20 mM and EDTA 1mM) at 118V in an Owl Easycast B2 Mini Gel Electrophoresis System (Thermo Fisher, MA, USA) electrophoresis chamber filled with TAE buffer. Migration distance was determined using the marker dyes added to the PCR loading buffer and electrophoresis of the gel was stopped once the leading front of the dye reached approximately 75% of the available gel distance, which occurred around the 40-minute time mark. The Cxcr4 WT band presented at 481 bp and FLOXED band at 550 bp, whereas Pdgfb-Cre had a single band with a molecular weight of 440 bp. Primers utilized for detection of WT and FL bands are outlined in Figure 2-3 below.

Syto® 60 Red Fluorescent Nucleic Acid Stain (Thermo Fisher) was added to the gel before it solidified to allow for fluorescent detection of DNA bands. Images were obtained using a 700 nm laser via Odyssey® LI-COR imagining platform and software.

To determine the sizes of DNA bands, each experiment was run alongside a BenchTop 1 Kb DNA Ladder (Promega, WI, USA). To detect any possible contamination each experiment was also run with an additional lane containing PCR master mix where DNA template was substituted with distilled water.

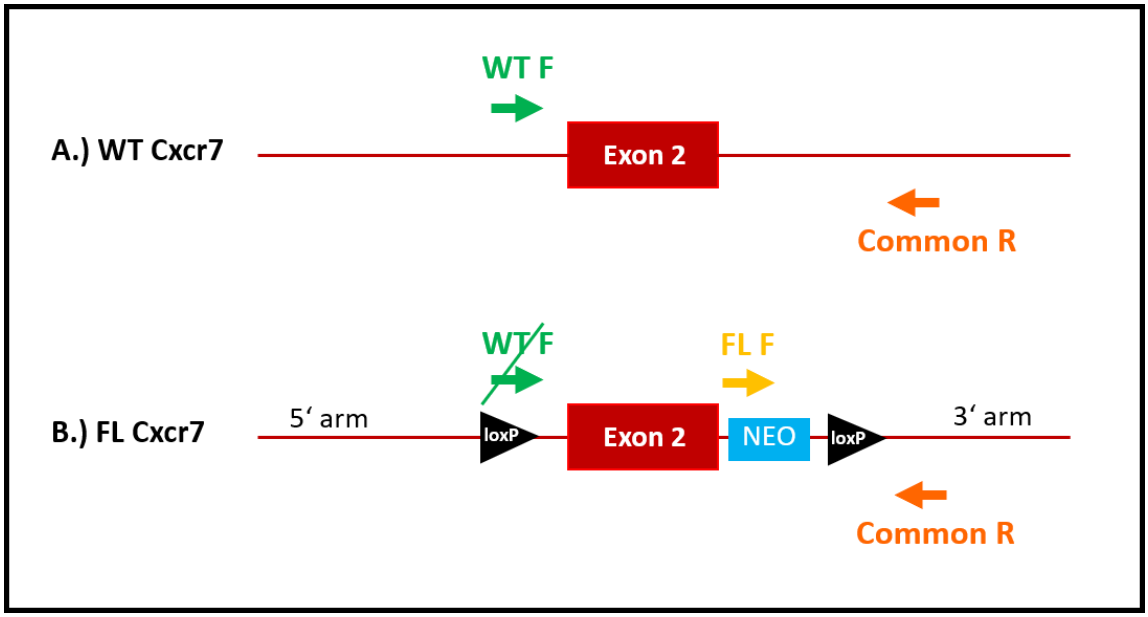

Figure 2-3: Detection of wildtype (WT) and floxed (FL) gene sequences. A.) Combination of the WT forward primer (green arrow) and common reverse primer (orange arrow) produces a 212 bp gene product, indicative of a WT genotype. B.) In mice with floxed Cxcr7 (FL) the sequence utilized by the WT forward primer is largely separated or obstructed, which renders the WT forward primer ineffective. Instead, floxed mice possess a neomycin resistance gene (neo) cassette insert, to which the FL forward primer (yellow arrow) binds and together with the common reverse primer forms a 709 bp gene product indicative of a FL genotype. F = forward, R = reverse.

Representative images of expected PCR results are shown in Figure 2-4 below.

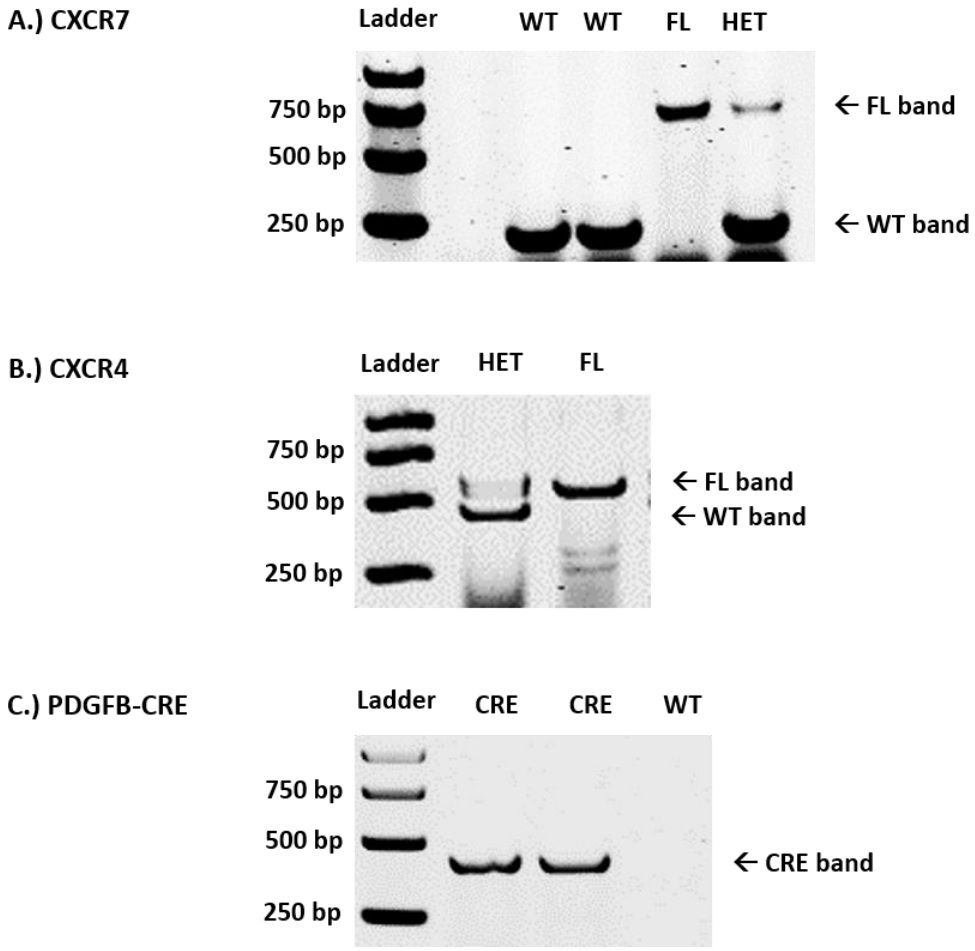

Figure 2-4: Representative mouse PCR genotyping images. A.) Cxcr7 had a floxed (FL) band at 709 bp and wild type (WT) band at 212 bp, with B.) Cxcr4 presenting with a WT band at 481 bp and FL at 550 bp and finally, C.) the presence of Pdgfb-Cre was confirmed by a single 440 bp band, whereas WT animals displayed no visible bands.

Cxcr7 genotyping was performed using the thermocycling protocol outlined in Table 2-5.

PCR stage	Temperature and duration	Description
1.	94°C – 5 min	Initiation/melting
Then 40 cycles of:		
2.	94°C – 15 s	DNA denaturing
3.	65°C – 30 s, decreasing 1°C per cycle until it reaches 55°C	Primer annealing
4.	72°C – 40 s	DNA elongation
Followed by		
5.	72°C – 5 min	Amplification
Then 4°C until collection.		

Table 2-5: Cxcr7 PCR thermocycling protocol.

Once the thermocycling protocol has ended, the samples were run on a 1.5% agarose gel at 90 V for 90 min in 1 x TAE buffer, before visualisation on the Odyssey LI-COR system as described above. WT band (primer 1 and 2) was visible on the gel as 212 bp and FLOXED band (primer 2 and 3) at 709 bp.

2.2.5 *Tamoxifen administration*

Since mice were generated using the inducible version of Cre recombinase, administration of tamoxifen or its active metabolite 4-hydroxytamoxifen was necessary to induce translocation of Cre product from the cytoplasm into the nucleus. In the absence of tamoxifen the iCreER^{T2} protein remains in the cytoplasm, where it is sequestered by heat shock protein 90 (HSP90) [243]. Tamoxifen (T5648, Sigma-Aldrich) was adminstered via intraperitoneal (i.p.) injection, daily for three consecutive days with 100 µL of 15 mg/mL.

Tamoxifen was dissolved in 1:10 ratio of 100% ethanol to groundnut oil, by first introducing tamoxifen powder into 100% ethanol and agitating for ~20 min or until dissolution occurred, before adding the correct volume of groundnut oil and further agitating the mixture at 37°C until adequately mixed. Mice were injected between the ages of 6 – 14 weeks and left for 3 weeks after the date of the last injection to ensure the loss of protein, then used between the ages of 9 – 17 weeks. The age of experimental mice used did not surpass 16 weeks old due to susceptibility of the C57BL/6 strain to develop various age-related conditions (obesity, type 2 diabetes, atherosclerosis) [249]. Generated transgenic mouse lines produced litters with predicted robust expression of the recombinant enzyme throughout the microvascular endothelium of adult mice approximately 48 hours after administration of tamoxifen, as previously reported [243]. After administration of tamoxifen, mice were monitored daily for any adverse effects. Tamoxifen-associated mortality was <10%.

2.3 Cell cultures

Human umbilical vein endothelial cells (HUVEC, C2519A, Lonza, Switzerland) and immortalized mouse cardiac endothelial cells (MCEC, Cellutions Biosystems, Ontario, Canada), were both cultured as monolayers. HUVEC were cultured using Endothelial cell growth medium 2 kit (CC22111, PromoCell, Germany) or EGM-2 bullet kit medium (CC-3162, Lonza) at 37°C and 5% CO_2, while MCEC cells were cultured using DMEM media (11965092, Gibco, MA, USA) supplemented with 5% foetal bovine serum (FBS) and penicillin/streptomycin also at 37°C and 5% CO_2. Both cell types were passaged when they reached 70- 80% confluence.

Accutase solution or TrypLE Express Enzyme (12605028, Gibco) were used for the passaging of HUVEC and 0.25% Trypsin-EDTA (Thermo-Fisher Scientific) was used for passaging of MCEC cells. The media was changed every 2-3 days.

2.4 Mouse cardiac endothelial cell isolation

2.4.1 *Preparation of anti-CD31 coated Dynabeads*

Dynabeads Sheep Anti-Rat IgG (11035, Invitrogen, MA, USA) were prepared by using 25 µl of Dynabeads solution (1 x 10^7 beads) in 1500 µl of wash buffer (0.1% bovine serum albumin/phosphate buffered saline), and subsequently washed four times with the wash buffer using the DynaMag^{TM} magnetic separator (Thermo Fisher), before resuspending in wash buffer and addition of anti-mouse CD31 antibody (1:100, 553370, BD Biosciences, NJ, USA). Dynabeads were left to incubate on the rotator, overnight in the fridge at 4°C, before being washed and resuspended in the wash buffer, and stored at 4°C, for a maximum of 2 days, before use.

2.4.2 *Cardiac endothelial cell isolation*

Two to four C57BL/6 mice were anesthetized via i.p. injection of pentobarbitone sodium (30mg/kg; Animalcare, UK) and heparin (30IU). Once the mice were under deep anaesthesia and no longer possessed a pedal reflex, hearts were rapidly excised and placed in cold DMEM media (Gibco). The hearts were then transferred to the sterile laminar flow hood, where they were washed with phosphate buffered saline (PBS, Oxoid, UK) twice to remove blood and minced into small pieces to increase cell yield. Afterwards, hearts were digested by 1 mg/mL collagenase II (Worthington, NJ, USA) dissolved in DPBS with calcium and magnesium (Dulbecco's Phosphate Buffered Saline, sterile, Gibco) and filtered using 0.2 µm cellulose acetate membrane filter, then placed on the shaker at 37°C, 150 revs/min for 1 hour, with occasional swirling to prevent sedimentation.

After, the solution was triturated and passed through a 70 µm strainer (Falcon, Fisher Scientific, NH, USA), followed by the addition of 10 mL EGM-2 medium (CC-3162, Lonza). The suspension was centrifuged for 5 min at 2300 rpm, after which the pellet was resuspended in anti-CD31-enriched Dynabeads and

incubated for 40 min on the rotator at 30 revs/min and 4°C to reduce phagocytic activity. After incubation, the cell suspension was repeatedly washed with the wash buffer on the DynaMag™ magnetic separator and finally resuspended in EGM-2 medium (Lonza) and plated in a 12-well plate. Cells were incubated in the incubator at 37°C, 5%CO_2 and media was changed every 3 days. After 10-12 days in culture, when cells reached approximately 70% confluence, cells were harvested for experiments.

2.5 Western blotting

2.5.1 *Tissue collection*

Mice were anaesthetized as described in section 2.4.2. Tissues were harvested and immediately homogenized using cold lysis buffer (Tris 100 mM pH 6.8, NaCl 300 Mm, NP40 0.5%) with the volume topped up to 100 mL with distilled water and pH adjusted to 7.4. Whole mouse hearts were first mounted on the 21G cannula via the aorta and flushed with cold PBS buffer, before undergoing homogenization. Lysis buffer was further supplemented with Halt™ Phosphatase Inhibitor Cocktail 100X (final conc. 1X, Thermo Fisher) and Halt™ Protease Inhibitor Cocktail 100X (final conc. 1X, Thermo Fisher) before use. A total of 100 µL of lysis buffer was used per 10 mg of tissue to achieve satisfactory protein extraction. For cell samples, a confluent T75 flask was scrapped using a Corning® cell scraper, with 150 µL of supplemented lysis buffer used per flask. After manual homogenization or cell scrapping, samples were left for 10 min on ice, before centrifugation at 10,000 rpm for 10 min. Subsequently, the supernatant was placed in a fresh Eppendorf tube and stored at -80°C until use.

2.5.2 *BCA protein quantification*

Total protein content of samples was calculated using bicinchoninic acid (BCA)-copper (II) sulphate ($CuSO_4$) colorimetric assay as described below. Protein content is measured by reduction of Cu^{2+} to Cu^{+} by protein present in the sample and subsequent chelation of two BCA molecules to each Cu^{+} ion.

This reaction causes the solution to change from green to purple colour, with the intensity of the colour proportional to the concentration of protein in the sample.

After protein extraction samples were further diluted 1:5 in lysis buffer and a total of 5 µL of the mix was placed into a 96-well plate in duplicates, along with pre-diluted bovine serum albumin (BSA) standards from Pierce (Thermo Fisher, 23208). This was topped up to 200 µL with a 1:50 mix of copper sulphate (Thermo Fisher) and BCA (Pierce). The plate was placed in the 37°C incubator for 30 mins and then absorbance at 562 nm measured on a FLUOstar Omega plate reader (BMG Labtech). The protein concentrations were calculated by interpolation from the standard curve obtained from the abovementioned BSA standards.

Once the total protein concentration was known, samples were diluted to the same volume and concentration needed to load 20 µg of protein. Finally, loading buffer consisting of Laemmli buffer (Bio-Rad, CA, USA) and β-mercaptoethanol in ratio 20:1 were added to the samples, before they were boiled for 10 min at 100°C in order to ensure denaturation of proteins. Samples were then used straight away or stored at -20°C until needed.

2.5.3 *Experimental protocol*

A total of 20 µg of protein was loaded on to a 10% Invitrogen Nuvex NuPAGE MOPS SDS gel (Invitrogen) or TGX Tris-Glycine 10% gel (Bio-Rad), subjected to electrophoresis in an XCell Sure Lock Mini Cell chamber (Invitrogen) or Mini Trans-Blot® Electrophoretic Transfer Cell (Bio-Rad), respectively. NuPAGE™ MOPS SDS Running Buffer (20X, Invitrogen) was used for Invitrogen gels and 10x Tris/Glycine Buffer (Bio-Rad) was used for Bio-Rad gels.

Voltage and duration were set as suggested by the manufacturer for a given gel. After electrophoresis, proteins were transferred onto an Amersham Protran nitrocellulose membrane (GE Healthcare, IL, USA) in a Bio-Rad Mini Protean chamber (Bio-Rad) using freshly-made transfer buffer (Tris-base 25 mM, glycine 200 mM, 20% methanol, pH 8.3) at 100 V, 0.3 mA for 1 h on ice.

Successful transfer was confirmed with 0.1% Ponceau S staining of the membrane. Once the transfer was complete the membranes were blocked with 5% bovine serum albumin (BSA) in PBS for 1 hour at RT and subsequently incubated with relevant antibodies in 5% BSA in 0.1% PBS-Tween. Following incubation with primary antibodies, membranes were washed three times in PBS-Tween (PBS-T), and subsequently incubated with goat anti-rabbit or goat anti-mouse secondary fluorescent antibodies (both 1:10,000, LICOR) in Odyssey® blocking buffer (LI-COR, Bad Homburg, Germany) and PBS 1:1, for 1 h at room temperature, before being washed six times for 10 min in PBS. Precision Plus Protein™ Dual Color Standard (Bio-Rad) was used to determine protein band size. Blots were visualized and quantified using Odyssey Infrared Imaging System (LI-COR).

2.5.4 *WES western blotting*

Murine cardiac endothelial cells were isolated as described in section 2.4. Following 10-12 days of incubation in PromoCell endothelial growth medium (CC22111, PromoCell) supplemented with 10% penicillin/streptomycin (Gibco), cells were lysed using a total of 60 µL of lysis buffer (Tris 100 mM pH 6.8, NaCl 300 Mm, NP40 0.5%). A total of 1 µg of protein sample was loaded into the 13 – 230 kDa protein cartridge (ProteinSimple, CA, USA) with each capillary already containing protein standards, and run according to the manufacturer's instructions. All reagents were purchased from ProteinSimple. WES western blotting (ProteinSimple) is system with automated protein separation and detection using capillary-based cartridges.

It allows for use of very small protein quantities and is gel-free, since the entire western blotting process for an individual sample takes place within a single capillary. Western blotting analysis was performed using Compass software for Simple Western (ProteinSimple).

2.6 Ac-LDL uptake assay

The identity of endothelial cells can be confirmed via an acetylated low-density lipoprotein (Ac-LDL) uptake assay. Scavenger pathway present in endothelial cells and macrophages allows for 7-15 times higher uptake of fluorescently-labelled Ac-LDL, when compared to fibroblasts and smooth muscle cells, and provides a simple, yet effective way to confirm endothelial cell identity [250]. Isolated murine cardiac EC were obtained as described in section 2.4. They were plated on Nunc™ Glass Bottom Dishes (Thermo Fisher) and cultured in EGM™-2 Endothelial Cell Growth Medium-2 BulletKit™ (Lonza, Switzerland) for 10 days. Afterwards, cells were incubated with 10 µg/mL Alexa Fluor™ 488 AcLDL (L23380, Thermo Fisher) for 2 hours at 37°C and the nuclei stained with Hoechst 33342 Solution (1:200, 62249, Thermo Fisher). After staining cells were washed with DPBS and images obtained using a 40x objective on a Leica confocal microscope, with excitation wavelength at 488 nm, and collecting the 500-550 nm emitted light.

2.7 Flow cytometry

MCEC, HUVEC or isolated murine endothelial cells were detached using either 0.25% Trypsin (Thermo Fisher) for MCEC or Accutase for HUVEC and isolated mouse endothelial cells. All cells were counted using a haemocytometer (Marienfeld, Germany) and centrifuged at 1,200 rpm for 5 min. Cells were then resuspended in 1 mL DBPS (Thermo Fisher) and fixed using 1% paraformaldehyde for 10 min on ice. Afterwards, cells were washed with 0.1% BSA/PBS (isolation buffer) and centrifuged at 5,000 rpm for 5 min.

Cell samples that underwent permeabilization were resuspended in 0.1% Triton X-100 for 3 min at room temperature prior to washing with the isolation buffer. Cells were then re-suspended in isolation buffer and incubated with either anti-CXCR7 rabbit monoclonal primary antibody (1:100, ab138509, Abcam, UK), anti-CXCR4-PE mouse antibody (1:20, FAB21651P, R&D systems, MN, USA), rat IgG2B PE-conjugated isotype control (R&D Systems, IC013P, 1:50) or Isolectin GS-IB4 Alexa 647 (IB4, 1:50, I32450, Thermo Fisher). Goat anti-rabbit Alexa-488 conjugated antibody (1:1000, A11008, Thermo Fisher) was used as a CXCR7 secondary antibody in flow cytometry experiments.

Samples were then analysed using a BD Accuri™ C6 flow cytometer (BD Biosciences) with 10,000 live cells (as determined by forward scatter/side scatter gating) counted for each sample. Positive Alexa-488 fluorescence (CXCR7) was determined on the FL-1H channel (488 nm laser, 585/30 nm filter; H-height). Positive CXCR4-PE and IgG2B PE-conjugated isotype fluorescence was measured on the FL-2H channel (488 nm laser, 585/40 nm filter) and positive GS-IB4 Alexa 647 fluorescence was measured using the FL-4H channel (640 nm laser, 675/25 nm filter). The number of positively labelled (+ve) cells was determined using FlowJo (Tree Star, OR, USA) analysis software via a gating method described in section 3.3.1.

2.8 RNAscope in situ hybridization

Mice were anaesthetized as previously described in section 2.4.2 and hearts quickly excised. The aorta was cannulated using a 21G cannula and the heart was manually flushed through with ~5 mL PBS to remove the remaining blood, then flushed with 10% formalin solution for fixation. Hearts were left immersed in 10% formalin overnight before being sent to UCL IQPath histology services (UCL, UK), where they were paraffin-embedded and cut longitudinally into equally thick slices (<7 µm), ready for staining. RNAscope® technology (Advanced Cell Diagnostics, CA, USA), was used to detect mRNA expression, according to the instructions published on the manufacturer's website (Figure 2-5).

Briefly, Cxcr7-specific probe manufactured by Advanced Cell Diagnostics was used to probe for mRNA expression and amplified by TSA® Plus fluorophore Cyanin 3 (1:500, Perkin Elmer, MS, USA). Following this, slices were also stained with Isolectin GS-B4 - Alexa 647 (1:50, I32450, Thermo Fisher) for 2 h, before washing with PBS, counter-staining the nuclei with DAPI (Advanced Cell Diagnostics) for 30 s and finally mounting on to a glass slide with Prolong Gold Antifade Mountant (P36930, Life Technologies). After leaving the slides to dry overnight, the fluorescent signal was scanned using a Leica confocal microscope. Confocal images were obtained using a 40x objective and at 1024 x 1024 pixel resolution. Cxcr7 probe was detected using excitation wavelength 488 ± 20 nm and emission wavelength 510 ± 20 nm. For Isolectin GS-B4 Alexa 647 an excitation wavelength of 650 ± 10 nm and emission wavelength of 670 ± 10 nm was used.

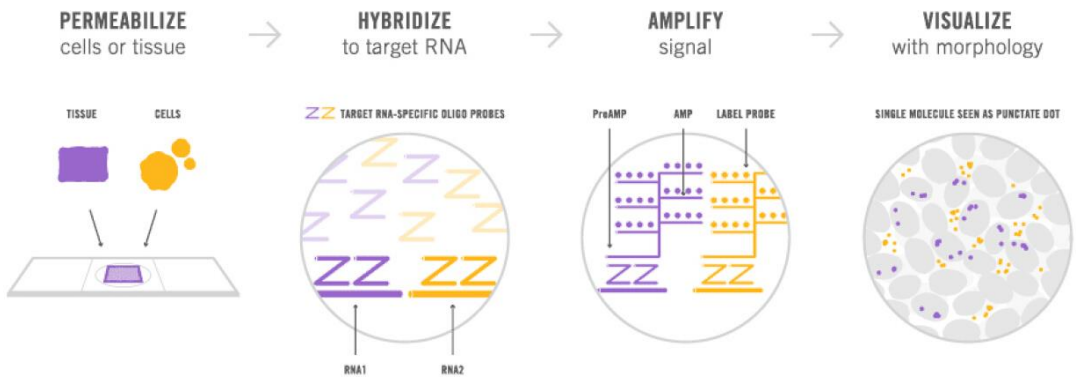

Figure 2-5: RNAscope in situ hybridization workflow. Cells or tissue are first permeabilized before undergoing hybridization of target-specific oligo probes to target RNA. After, signal generated by the hybridized probes is amplified and subsequently detected

2.9 Langendorff perfusion

Sprague Dawley rats were provided from a colony established and maintained by the BSU facility (UCL, UK). Male rats weighing 250-350 g were anaesthetized by i.p. injection of pentobarbitone (170 mg/kg) and heparin (160 IU/kg). The onset of surgical level of anaesthesia was determined by the absence of pedal and corneal reflexes prior to cardiac excision and exsanguination. Following this, hearts were excised and immediately arrested in ice-cold Krebs control solution, containing: NaCl 118 mM, $CaCl_2$ 1.84 mM, glucose 11 mM, $NaHCO_3$ 25 mM, $MgSO_4$ 1.22 mM, KH_2PO_4 1.21 mM and KCl 4.7 mM. The aorta was cannulated, and the hearts were mounted on a Langendorff apparatus, with continuous perfusion performed through the aorta with gassed Krebs control solution (95% O2: 5% CO2, pH 7.3-7.4). Solutions were circulated through the perfusion apparatus at 37°C and at a constant pressure of approximately 80 mmHg (generated by the height of the perfusion columns). Special care was taken to avoid any bubbles in the perfusion apparatus that might impede the flow of solution. A silk suture (3-0, Ethicon, UK) was placed under the left anterior descending artery, mid-distance to the apex and subsequently tightened during the period of ischaemia, to produce regional ischaemia distal to the placement of the suture. The left atrium was removed, and an intraventricular balloon made of polyvinyl chloride cling film and connected to the pressure transducer was passed through the left atrium into the left ventricle and filled with distilled water to provide the systolic and diastolic pressure measurements. A unipolar electrocardiogram (ECG) recording was used to assess cardiac rhythm: two ECG leads were attached to the cannula (earth and negative electrodes), and a wire electrode was inserted into the left ventricular wall at the apex of the heart. A representative image of rat heart mounted on the Langendorff apparatus can be seen in Figure 2-6.

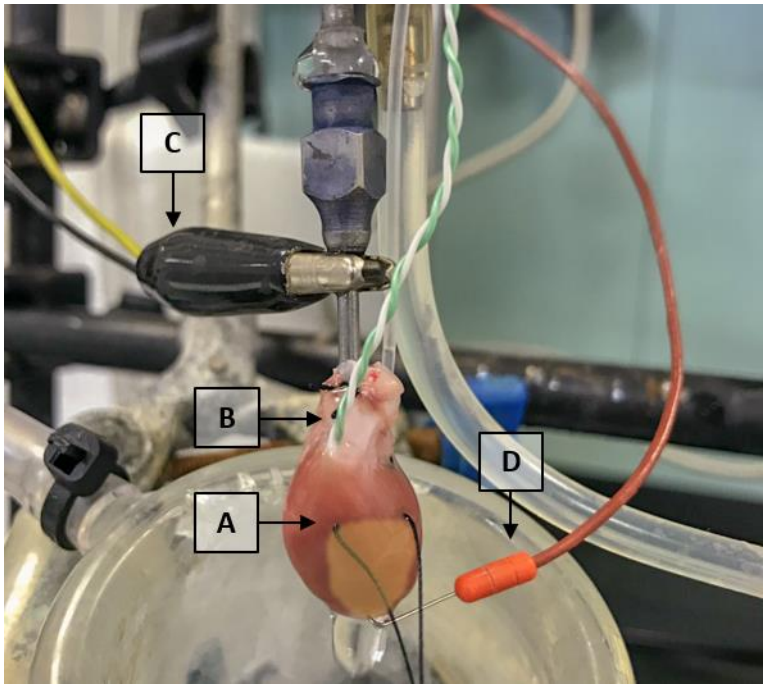

Figure 2-6: Cannulated heart on the Langendorff perfusion apparatus. A.) Silk suture underlying the LAD that when tightened results in an area of regional ischaemia downstream of LAD (added yellow shading), B.) Temperature probe in the right atrium, C.) ECG earth and negative leads, D.) ECG positive lead.

2.9.1 *Experimental protocol*

The term “ischaemic preconditioning (IPC)” describes several short cycles of global ischaemia and reperfusion that are applied to the heart before the onset of index ischaemia, and induce a potent cardioprotection in all mammalian species tested [251]. Therefore, IPC was used as a positive control for cardioprotection in a Langendorff perfusion model. The drug to be tested, CXCR7 agonist VUF11207 fumarate (Tocris, UK) was administered via the perfusate beginning 5 min before reperfusion until the end of reperfusion. Rats were randomized to one of three groups, with researchers blind to the treatment, however due to the nature of IPC, the blinding for that group was not possible (Figure 2-7).

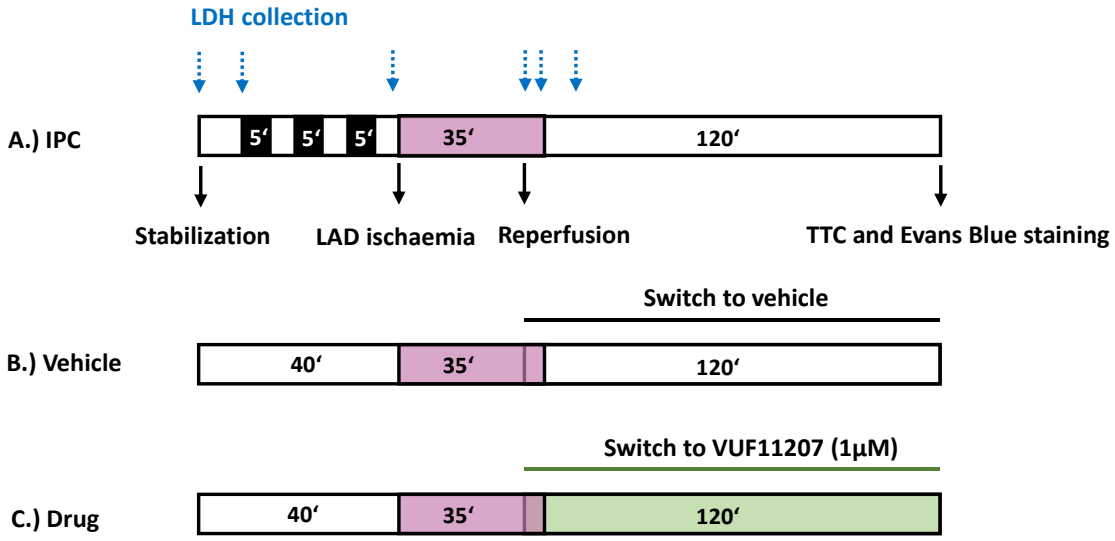

Figure 2-7: Langendorff perfusion experimental protocol. Rats were randomly allocated to three different groups. A.) 10 min stabilization period, three 5 min cycles of IPC, 35 min LAD ischaemia, 2 h reperfusion; B.) 40 min stabilization, 35 min LAD ischaemia, 2 h reperfusion with a perfusion switch from Krebs to vehicle (Krebs) 5 min before onset of reperfusion; C.) 40 min stabilization, 35 min LAD ischaemia, 2 h reperfusion with a perfusion switch from Krebs to VUF11207 (1µM) 5 min before onset of reperfusion. LDH samples were collected at times as indicted by blue arrows. Figure not to scale.

2.9.2 *Exclusion criteria*

Pre-defined exclusion criteria were set according to recommendations of Botker *et al*. before the experiment to ensure consistency as seen in Table 2-6 below [252]. Heart rate, coronary flow, temperature, perfusion pressure (mmHg), systolic, diastolic and developed pressure (mmHg) were collected every 5 min to ensure optimal heart function and adherence to exclusion criteria.

Baseline exclusion criteria (prior to any intervention, e.g. IPC)	
Parameter	**Rat Heart**
Time to perfusion	> 3 min
Coronary flow	< 10 or > 28 mL/min
Arrhythmias	> 10 ectopic beats Ventricular tachycardia or fibrillation should not occur
HR	< 200 or > 400 bpm
LV diastolic pressure	< 5 or > 10 mmHg
LV developed pressure	< 70 or > 130 mmHg
Temperature	37 ± 0.5°C (< 36 or > 38°C for > 1 min)
Reperfusion exclusion criteria	
Parameter	**Rat Heart**
Coronary flow	≤ ischaemic flow
Arrhythmia duration (VT or VF)	> 2 min (intervene immediately – flicking, KCl or cold buffer)
HR	< 150 bpm
Infarct criteria	
Parameter	**Rat Heart**
AAR	< 35 or > 70% of ventricular tissue

Table 2-6: Pre-set exclusion criteria for ex vivo Langendorff experiments.

2.9.3 *Endpoint 1: Infarct size assessment*

The primary endpoint of *ex vivo* experiment was infarct size (IS) after IR. This was expressed as a percentage of area at risk (IS/AAR), which is the area of myocardial tissue, that was susceptible to ischaemic damage during the period of LAD occlusion.

After the conclusion of the experimental protocol, the heart was taken off the perfusion rig, the silk-suture underlying the LAD was re-tightened and the heart was injected with approx. 0.5 mL of 0.25% Evans Blue dye to delineate the AAR, which was set as percentage of whole heart area (AAR/whole heart area) as seen in Figure 2-8 below.

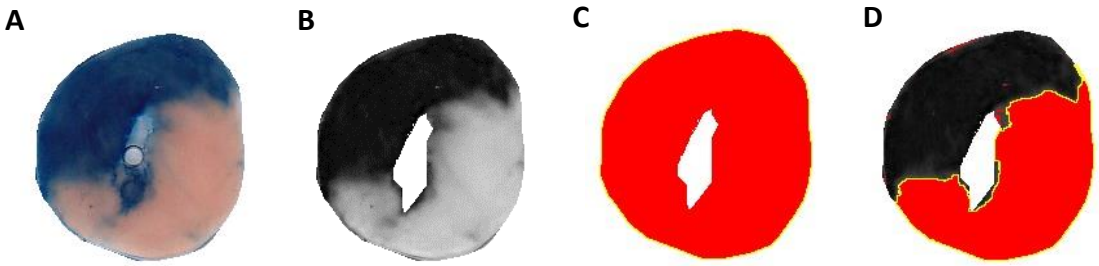

Figure 2-8: Quantifying AAR via planimetry. A.) Scanned transverse section of the heart showing staining with Evans blue; B.) The background was removed, and the colour channels separated to obtain only the red channel image; C.) The pixel intensity threshold was set to encompass the entire heart slice to obtain whole heart area for AAR calculation; D.) The threshold was set to encompass only the portion of the heart slice not stained by Evans blue (white area) to delineate AAR. AAR was calculated as percentage of whole heart area by measuring threshold area (pixels) in ImageJ.

At the end of perfusion, the heart was removed from the cannula, weighed and placed into the -20°C freezer for 1 hour. Subsequently, the heart distal to the site of LAD occlusion was sliced into 5-8 sections and stained with 1% 2,3,5-Triphenyltetrazolium chloride (TTC) dissolved in 5 mL of phosphate buffer (2 parts 100 mM monobasic sodium phosphate and 8 parts 100 mM dibasic sodium phosphate). TTC staining was used to differentiate metabolically active versus inactive tissue. It is a white compound that is enzymatically reduced to red 1,3,5-triphenylformazan (TPF) in metabolically active tissues due to activity of various dehydrogenases. However, in metabolically inactive (dead) tissues the enzymes are washed out and white [253].

Following incubation in TTC for 20 min in the dark at 37°C, heart slices were fixed in 10% formalin at RT and incubated in formalin for further 15 min before scanning with a Canon scanner (LiDE 210, Canon, Japan) and analysed with Image J (version 1.52a, National Institute of Health, MD, USA), using planimetry as depicted in Figure 2-9. Analysis was performed blinded to the treatment group by both researchers separately, after which the results were averaged between the two observers. If the obtained values differed more than 10% between the observers, the heart slices were re-analysed by both.

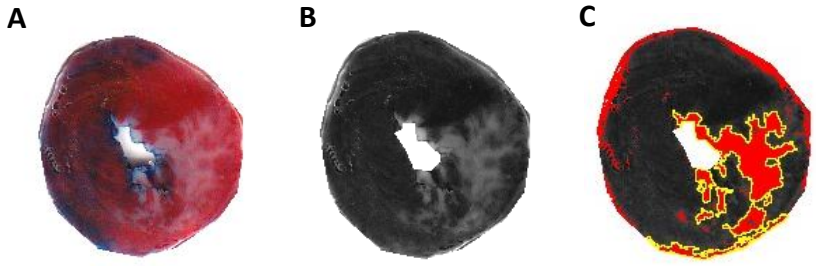

Figure 2-9: Quantifying IS via planimetry. A.) Scanned transverse section of the heart; B.) The background section was removed, and channels separated to obtain only green channel image; C.) The threshold was set to encompass only the portion of the heart that was metabolically inactive as determined by TTC (red area). IS was calculated as percentage of AAR by measuring threshold area (pixels) in ImageJ.

2.9.4 *Endpoint 2: LDH release*

To provide an alternate endpoint to IS assessment, coronary effluent samples were collected for lactate dehydrogenase (LDH) measurement at defined timepoints in the protocol as outlined in Figure 2-7 above. LDH is an intracellular enzyme present throughout most cells and normally located in the cytosol. Following damage to the sarcolemma it is released into the circulation, where it has historically served as a surrogate marker of cardiac injury in clinical practice and cardiovascular research [253-255] .

The first sample for LDH measurement was collected immediately after heart was mounted on the cannula, followed by collection at 9 min into stabilization/prior IPC intervention, then 39 min into stabilization just prior to ischaemia, then at 31 and 34 min into ischaemia, before and after switching to vehicle/drug, respectively. Finally, the last and most important LDH sample was collected 15 min into reperfusion, which was the point of maximum LDH release, as determined from previous experiments in our laboratory [255].

LDH content was measured with a commercially available LDH kit, Pierce™ LDH Cytotoxicity Assay Kit (88953, Thermo Fisher) in a 96-well plate according to the manufacturer's instructions. The prepared plate was subsequently measured using a FLUOstar Omega microplate reader (BMG Labtech, UK) at 490 nm and 680 nm wavelengths, whereby subtracting the 680 nm from the 490 nm wavelength ensured the elimination of background signal from the samples. The LDH measurements were adjusted to the flow rate (mL/min) and weight (g) of each individual rat heart to ensure consistency. The final LDH measurement was therefore calculated as amount of LDH product in a coronary effluent concentration (pg x mL^{-1}) x coronary flow divided by the weight of the rat heart (mL x min^{-1} x g^{-1}), and finally expressed as pg x g^{-1} x min^{-1}.

2.10 Cell migration

HUVEC were cultured as described in section 2.3. At passage 4-8 they were detached from the surface of the flask using TrypLE Express (Gibco) reagent and counted using a haemocytometer (Marienfeld,). 450,000 cells were centrifuged at 1,300 rpm for 5 min and resuspended in Endothelial Cell Serum-free Defined Medium (Cell Applications Inc., CA, USA), supplemented with 5% penicillin/streptomycin (Gibco). Drug treatments were prepared in DPBS and included FBS, SDF-1α (Miltenyi Biotec, Germany), TC14012 (Tocris, UK), VUF11207 fumarate (Cayman Chemical, MI, USA).

Before the start of the experiment, a 12-well chemotaxis chamber (Neuro Probe, MD, USA) was disassembled (see Figure 2-10 for chamber diagram) and 150 µL DPBS containing drug treatments was pipetted into the wells in the lower portion of the chamber. A polycarbonate filter membrane with 8 µm pores was placed on top of the lower chamber (PFB8, Neuro Probe), followed by a rubber gasket and the top portion of the chamber. Finally, a cell mixture containing 150,000 HUVEC suspended in 100 µL of Endothelial Cell Serum-free Defined Medium was carefully pipetted into the top wells of each chemotaxis chamber. The cellular migration was allowed to proceed for 3 hours in a cell incubator at 37°C and 5% CO_2. Afterwards, the membrane was carefully removed from the chamber, dipped in PBS and the bottom-part of the membrane was wiped free of residual non-migrated cells three times before being placed in ice-cold methanol for 5 mins. After fixation, the membrane was air dried and stained with 0.5% crystal violet dye in PBS for 5 min, before air-drying and scanning with a Canon scanner (LiDE 210, Canon, Japan).

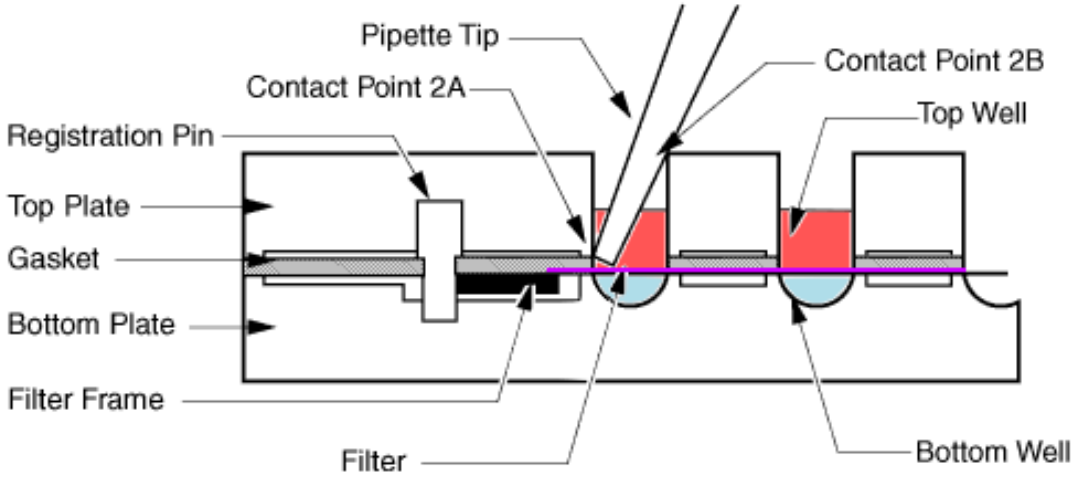

Figure 2-10: Technical diagram of a representative chemotaxis chamber. DBPS containing drug treatments is shaded blue and HUVEC cell mixture is coloured red, with the filter membrane (purple line) placed in between. Cellular migration proceeds in a downward direction (from red to blue), and cells remain attached to the underside of the filter membrane, after migrating through membrane filter pores. Adapted image courtesy of Neuro Probe.

2.11 RNA isolation and quantitative real-time PCR

2.11.1 *RNA extraction*

Mice were anaesthetized as described in section 2.4.2. An incision made just below the sternum of the mouse was extended diagonally and distally, and a section of ribcage was removed to expose the heart. Lungs and oesophagus were removed and distal end of thoracic aorta exposed. The aortas was blunt dissected along their length and separated from the underlying spinal tissue. The aortas were cut at the distal thoracic end and at the level of descending aorta and fatty tissue removed. Harvested aortas were stored in 300 µL of RNAlater® solution until needed. Total RNA was isolated using a RNeasy kit (Qiagen, Germany) at RT with RNase-free DNase I (Qiagen) used for removal of trace amounts of DNA, as per the manufacturer's instruction, as briefly outlined in Table 2-7 below. Prior to RNA extraction, aortas (30 mg total) were homogenized using 23G needle, vortexing and sonication (10 s, 130W, 20 kHz, Vibra-Cell, CT, USA) in 600 µL of RLT buffer (RNeasy kit, Qiagen) with 1% β-mercaptoethanol (β-ME), which reduced RNases and disrupted protein sulphide bonds, respectively. Lysate was then centrifuged at 20,000 g and 1 volume of 70% of ethanol was added to the supernatant before transferring the solution to a RNeasy spin column containing a silica-based membrane, which bound the RNA, before elution with RNA-free water. RNA was quantified using an LVIS plate in a FLUOstar Omega plate reader (BMG Labtech, Germany), with 1 unit of absorbance (260 nm) corresponding to 44 µg/mL of RNA. Extracted RNA was either stored at -20°C or used immediately in a reverse transcriptase polymerase chain reaction.

Step	Buffer	Centrifugation (speed, duration)
1.	RLT + 1% β-ME/ethanol 700 µL	10,000 rpm for 15 s, discard flow-through
2.	RW1 500 µL	10,000 rpm for 15 s, discard flow-through
3.	10 µL DNase I solution + 70 µL RDD	Incubate for 15 min at RT
4.	RW1 500 µL	10,000 rpm for 15 s, discard flow-through
5.	RPE 500 µL	10,000 rpm for 15 s, discard flow-through
6.	RPE 500 µL	10,000 rpm for 2 min, discard flow-through
	Change collection tube	
7.	RNase-free water 50 µL	10,000 rpm for 1 min, keep flow-through (RNA-rich)

Table 2-7: RNA extraction was performed using RNeasy kit (Qiagen), as per the manufacturer's suggestion.

Initially, RLT buffer supplemented with 1% β-ME was added to the homogenized tissue sample in the supplied RNeasy spin column (step 1), centrifuged and flow-through from the collection tube discarded. Subsequently, different buffers were added to the sample and either incubated or immediately centrifuged (steps 2-6). Finally, a fresh collection tube was used to elute the RNA-rich flow-through (step 7) with RNase-free water.

2.11.2 *Reverse transcriptase polymerase chain reaction protocol (RT-qPCR)*

A two-step RT-qPCR reaction was used, firstly reverse transcribing extracted RNA to cDNA and secondly, utilizing a qPCR step to obtain quantifiable levels of RNA in our samples.

cDNA was generated using 100 ng of RNA with the AffinityScript cDNA Synthesis Kit (Agilent, CA, USA), using 20 µL RNase-free distilled H_2O, 10 µL first strand master mix, 3 µL Oligo(uT) primer, 1µL Affinity Script reverse transcriptase and 100ng of RNA per reaction, as described in Table 2-8.

Reagent	**Volume per sample (µL)**
RNase-free water	20
cDNA master mix (2X)	10
Oligo(dT) primers	3
AffinityScript reverse transcriptase	1
Template RNA	Variable
Total volume per sample (µL)	34 + template RNA volume

Table 2-8: Reagents and volumes used to perform reverse transcription step, to obtain cDNA from RNA.

The thermocycling protocol (Table 2-9) was used to reverse transcribe extracted RNA into cDNA, using PTC 200 Thermal Cycler, MJ Research).

PCR stage	Temperature and duration	Description
1.	25°C for 5 minutes	Primer annealing
2.	42°C for 25 minutes	cDNA synthesis
3.	95°C for 5 minutes	Termination of reaction

Table 2-9: RNA reverse transcription thermocycling protocol used for obtaining cDNA from RNA.

The cDNA was then used immediately in a quantitative polymerase chain reaction (qPCR) or stored at 4°C for a maximum period of 5 days.

By utilizing a dye that fluoresces when bound specifically to the minor groove of double stranded DNA (dsDNA), qPCR allows for real-time quantification of DNA in the sample. During the annealing phase, PCR primers bind to the target sequence and elongate to produce complementary dsDNA, to which SYBR ® green dye binds and fluoresces. As the amount of PCR product increases over the successive cycles, so does the signal intensity of the fluorescent tag, providing a way to detect and quantify the amount of RNA in the sample.

The qPCR step was performed using 2X Brilliant SYBR® green (Agilent), according to the manufacturer's instructions, with the full list of reagents and quantities used set out in the Table 2-10 and the qPCR thermocycling protocol outlined in Table 2-11.

Reagent	Volume (µL)
2X Brilliant SYBR® green	12.5
Nuclease-free water	5.5
Forward primer (2 pmol/L)	1
Reverse primer (2 pmol/L)	1
Template cDNA	5
Total volume (µL)	**25**

Table 2-10: Quantitative PCR reaction reagents and volumes.

PCR stage	Temperature and duration	Description
1.	95°C for 5 min	Hot start
2.	95°C for 30 s	DNA denaturing
3.	60°C for 30 s	Primer annealing
4.	72°C for 30 s	DNA synthesis
Repeat steps 2-4 for 39 cycles		
5.	65°C to 95°C, increment 1°C for 5 s	Melt curve generation

Table 2-11: Quantitative PCR thermocycling protocol.

All primers were maintained in a stock solution of 100 pmol/µL in autoclaved distilled water with a working concentration of 2 pmol/µL.

Gapdh and Hprt are constitutively expressed genes that were used as controls in the qPCR experiments. Primers for qPCR were purchased from Sigma-Aldrich (Cxcr7) or Eurofins (Gapdh, Hprt). Primer sequences are described in Table 2-12.

Primer name	Primer sequence (5'-3')
Gapdh forward	AGGTCGGTGTGAACGGATTTG
Gapdh reverse	TGTAGACCATGTAGTTGAGGTCA
Hprt forward	TCAGTCAACGGGGGACATAAA
Hprt reverse	GGGGCTGTACTGCTTAACCAG
Cxcr7 forward	AAAAACATTTGAGTTCAGGGG
Cxcr7 reverse	TACAGCAAGTTTCACTCAAC

Table 2-12: RT-qPCR primer sequences

After loading the samples into a 96-well PCR plate (Thermo Fisher), the plate was placed on a shaker for 30 s and briefly centrifuged, before being placed in a CFX Connect™ Real time PCR Detection System (Bio-Rad) and run as outlined in Table 2-11 above.

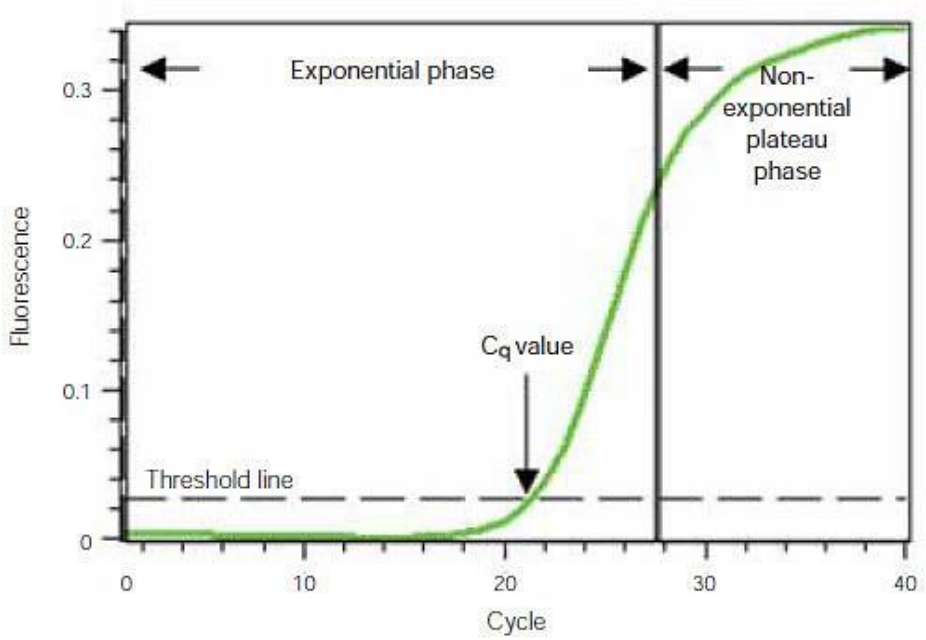

Figure 2-11: Representative plot of fluorescence during qPCR amplification. Fluorescence intensity (arbitrary units) is shown on y-axis and cycle number on x-axis. The representative amplification curve crosses the detection threshold line (Cq value) at approx. cycle 21, whereas a curve for a sample without template cDNA would not rise above the threshold line, unless contaminated. Image courtesy of Bio-Rad.

Typical data obtained from a qPCR is shown in Figure 2-11. The fluorescence intensity (y-axis) is detected by the spectrofluorometric thermal cycler and it increases proportionately with the amount of detected PCR product. There are two distinct amplification phases, the exponential phase, where the amount of PCR product doubles with each subsequent cycle (x-axis) and the non-exponential phase in which the reaction gradually uses up the reaction components and eventually plateaus. The most important point during the amplification reaction is the quantification cycle (Cq/Ct) value, which signifies the cycle number at which intensity of fluorescence rises above background levels and can be successfully detected. A lower Cq value represents a higher level of target template present in the sample and can therefore be detected sooner. Higher Cq values represent lower amount of target template, with higher number of cycles needed for successful fluorescent detection.

Double Delta Ct analysis ($2^{-\Delta\Delta Ct}$) was used to calculate the relative differences between our chosen samples and expressed as a fold-difference, with target gene values (Cxcr7 ΔCt) averaged to Gapdh and Hprt housekeeping genes in representative graphs. Ct values for all genes were obtained in triplicates. Cxcr7 ΔCt = Ct (average of Cxcr7) – (average of Ct Gapdh + Ct Hprt), $\Delta\Delta$Ct = ΔCt ($Cxcr7^{WT}$) – ΔCt ($Cxcr7^{i\Delta EC}$), fold gene expression = $2^{-\Delta\Delta Ct}$.

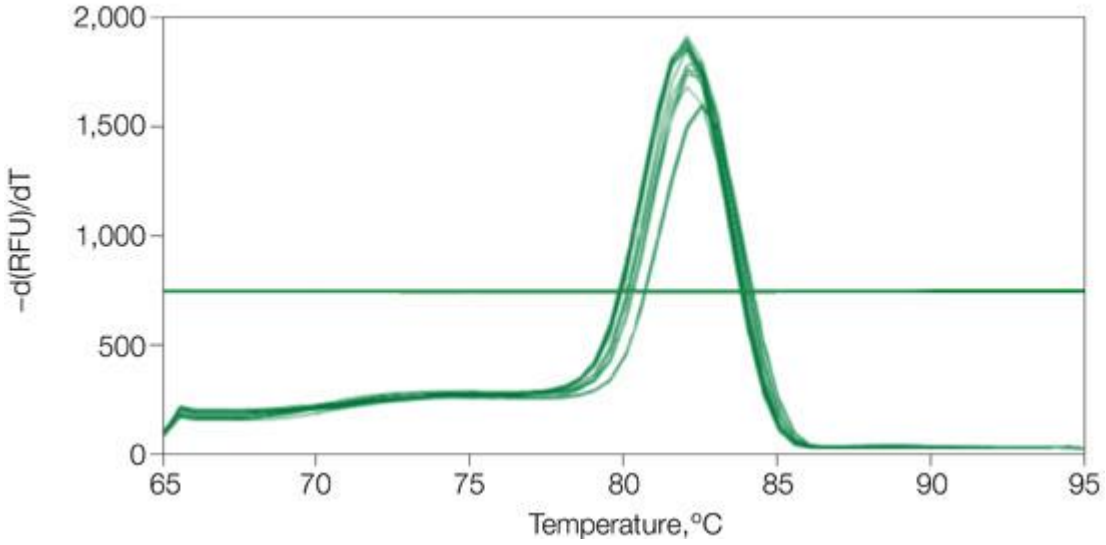

Figure 2-12: Representative melt curve. The melt curves of several samples. All curves in this example are single-peak curves, denoting a homogenous melting point and therefore a relatively pure sample. Reaction temperature is plotted on the x-axis, with y-axis showing the rate of change of the relative fluorescence units (RFU) versus time (T), with the peak at the melting temperature (Tm). Image courtesy of Bio-Rad.

In addition to amplification plots, a melt (dissociation) curve was also generated for each sample with representative image (Figure 2-12). The premise of a melt curve is the detection of dissociation of cDNA, which should provide a single, defined peak for pure samples and allows us to detect the signal produced by template cDNA accumulation, as opposed to non-specific dsDNA presence.

2.12 Statistical analysis and power calculations

In estimating the total number of repeats required per experiment, calculations of statistical power were made using an online tool from the powerandsamplesize.com website. Statistical analysis was performed using GraphPad PRISM version 5.0 for Windows (GraphPad Software, Inc., CA, USA). Data is expressed as mean ± SEM, and $p < 0.05$ was accepted as statistically significant with the specific statistical test reported with each result.

Sample size: Sample size calculations were used to estimate the minimum number of repeats for each experiment, based on pilot data. For all power calculations Gaussian distribution was assumed with a significance level of 5% ($\alpha=0.05$) and 80% power ($\beta=0.2$). Sample size is reported with each result separately.

Normality: Sample-size permitting, a normality test was performed to determine whether the data come from a Gaussian (parametric test) or non-Gaussian (non-parametric test) population. Due to small sample sizes the most relevant test used was the Shapiro-Wilk normality test. If a sample size was too low to run a normality test, a Gaussian distribution was assumed. Since non-parametric tests exhibit lower power and require substantially higher sample sizes, if sample size was too low to run a normality test, a Gaussian distribution was assumed.

3 Investigation of CXCR7 expression in cardiovascular cell types

3.1 Background

Since the discovery of CXCR7 receptor ligands, SDF-1α and I-TAC, over a decade ago, the presence of CXCR7 has been confirmed in many tissues, including in endocardial cells where it aids early cardiac development, and germline deletion of the receptor results in perinatal lethality [114]. Less is known about the presence of the receptor in adult cardiovascular tissues, (e.g. endothelial cells), and its expression and function in various cell types has yet to be elucidated. Previously published literature also suggests that CXCR7 is expressed in juvenile mouse cardiomyocytes up to at least P5, but additional evidence of expression in cardiomyocytes from adult mice is not available. therefore, we also wanted to observe whether CXCR7 expression can also be detected in the adult cardiomyocytes [148].

Therefore, we aimed to determine the expression profile of endothelial CXCR7 in the mouse heart, while we also wanted to observe whether CXCR7 expression can be detected in the adult cardiomyocytes [148, 115]. CXCR7 expression in mouse vascular endothelium was visualized by using in situ hybridization while in cardiac endothelial cells western blot analysis was used [115, 119]. Moreover, since successful isolation of endothelial cells can present a challenge, HUVEC, as well as the immortalized mouse cardiac endothelial MCEC cell line were utilized to examine the expression of CXCR7 and CXCR4 .

3.2 Research aims and objectives

Investigate expression of CXCR7 in cardiovascular cell types:

- Confirm expression of CXCR7 in mouse cardiovascular tissues.
- Confirm expression of CXCR7 in endothelial cells of cardiac origin.

- Investigate localization of CXCR7 receptor in endothelial cells and identify an appropriate cell line for use in *in vitro* experiments.

3.3 Methods

In addition to the general methods described in Chapter 2, the following specific methods were used in the experiments described in this chapter.

3.3.1 *Flow cytometry*

First, cultured cells were trypsinized and fixed as described in section 2.7, before being run through the Accuri C6 flow cytometer. To identify the live population of cells in fixed-cell samples, a gating protocol was established based on forward (FSC) and side scatter (SSC) parameters, as well as propidium iodide (PI) staining. Forward scatter plotted against side scatter in a density plot reveals the size of cells and their granularity, respectively, which allows for exclusion of very small and granular cells, likely to be cell debris [256, 257].

However, this method only enriches for live cells but does not have the power to completely eliminate non-viable cells from the analysis. Therefore, PI, a fluorescent nucleic acid stain able to discern viable cells from non-viable ones, was used. PI intercalates into the nuclear DNA of dead cells which have a disrupted plasma membrane, without any sequence preference, binding to every fourth or fifth base pair in the sequence.

This allows detection of dead cells by the emission of red fluorescence, when excited with a laser of an appropriate wavelength [258]. Experiments in which <5% of cells were positive for PI staining, were accepted. To determine the percentage of PI-labelled cells, manual gating was used with gates placed at the intersection of peaks from negative control sample and target sample in a histogram overlay. A total of 10,000 cells were counted per sample.

3.3.2 *Western blotting antibodies*

Western blotting was performed according to the protocol described in section 2.5 with anti-CXCR7 (RDC1) rabbit monoclonal antibody (1:1000, ab138509, Abcam). Anti-GAPDH mouse monoclonal antibody (1:2000, ab8245, Abcam) or anti-α-Tubulin mouse monoclonal antibody (1:2000, ab7291, Abcam) were used to quantify loading controls. IRDye® 800CW goat anti-rabbit IgG (1:10,000, Li-COR), or IRDye® 680RD Goat anti-mouse IgG (1:10,000, LI-COR) secondary fluorescent antibodies were used for detection.

3.4 Results

To confirm the presence of CXCR7 mRNA in mouse cardiac tissue, RNAscope in situ-hybridization was performed on paraffin-embedded whole-heart mouse slices. Initially, the tissue samples underwent antigen retrieval and protease treatment to ensure target mRNA availability. After, an RNA-specific oligonucleotide probe was added and allowed to bind to the target mRNA and was subsequently hybridized to a series of signal amplification molecules. Finally, the addition of TSA® Plus Cyanine 5 fluorophore enabled visualization of the target mRNA using a confocal microscope. Since the main objective was to identify the presence of CXCR7 in endothelial cells, the tissues were also co-stained with isolectin B4-Alexa 647 conjugate (IB4) to delineate the endothelial cells present in the myocardium (Figure 3-1).

Co-staining with IB4 allowed confirmation of CXCR7 mRNA detection in endothelial cells and autofluorescence emitted by myocardial tissues confirmed the presence of CXCR7 mRNA in cardiomyocytes. Autofluorescence emitted by cardiac tissues, specifically cardiomyocytes, is thought to arise from mitochondrial dehydrogenases, containing flavin adenine dinucleotide (FAD) undergoing oxidation and detectable with a green laser (488 nm) excitation used in confocal microscopy [259]. This enabled the typical morphology of cardiomyocytes to be observed even in the absence of cardiomyocyte-specific markers.

To confirm that the CXCR7 mRNA signal was not caused due to autofluorescence or non-specific signals, positive and negative species-specific RNAscope control mRNA probes, obtained as part of the RNAscope kit were used. The positive control probe targeted the gene Ppib, which gives rise to Peptidyl-prolyl cis-trans isomerase B enzyme, otherwise known as Cyclophilin B, a cyclosporine-binding protein involved in protein folding and variety of immune responses, and which is known to be present in the heart [260-263]. The Ppib positive control probe gave rise to easily identifiable, specific Ppib mRNA dots that were present in moderate numbers throughout mouse myocardium, as expected (Figure 3-2, B). The negative control probe is specific to the *Escherichia coli* dihydrodipicolinate reductase (DapB), involved in bacterial lysine synthesis pathway [264].

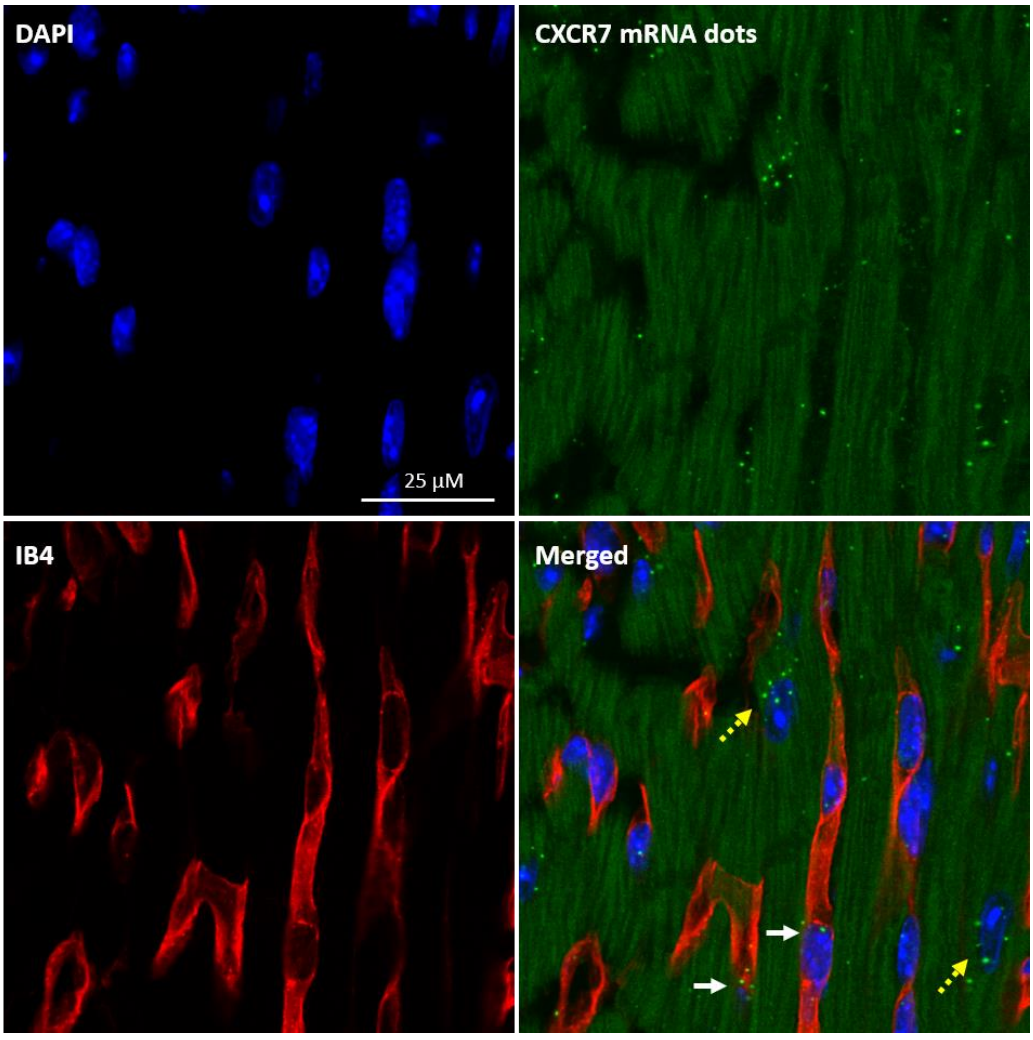

Figure 3-1: CXCR7 mRNA expression in murine vascular endothelium. CXCR7 mRNA (green dots) is present in endothelial cells (white arrows) and cardiomyocytes (yellow arrows) of adult mouse hearts as detected by RNAscope in situ hybridization. IB4 (red) was used to label endothelial cells and DAPI (blue) depicts cellular nuclei. Autofluorescence on the green (488 nm) channel allows visualization of cardiomyocytes.

Since DapB is not known to be present in animal or human tissues, no specific signal was expected. The probe only produced a few faint dots, lacking the intensity of dots produced by application of the positive control probe, as would be expected from a successful RNAscope experiment (Figure 3-2, A).

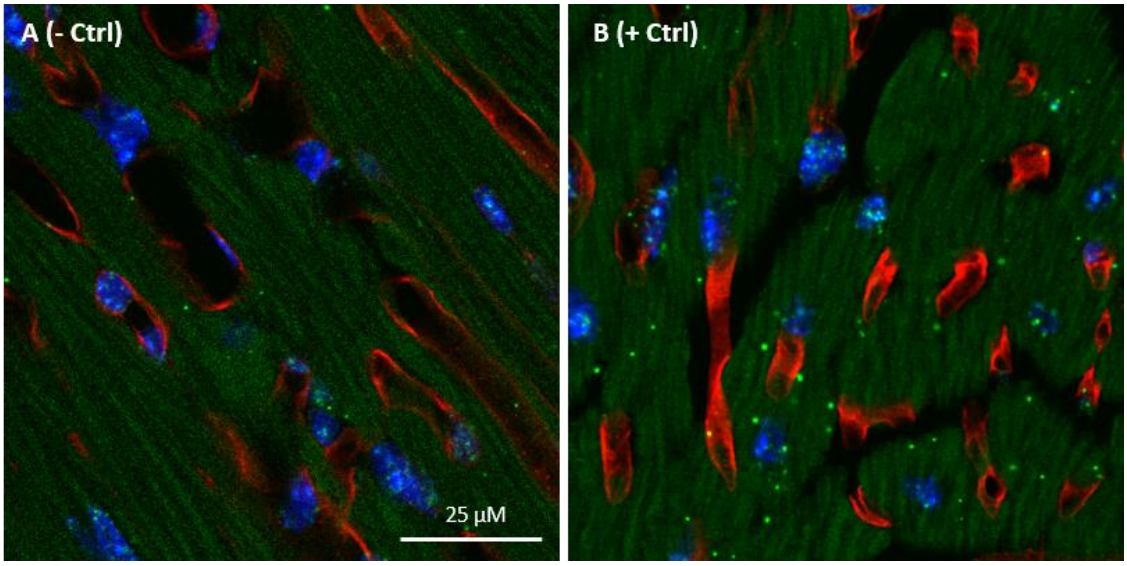

Figure 3-2: Positive and negative control mRNA probe RNAscope experiment. A.) The negative control probe targeted to bacterial DapB (green dots) shows only a faint signal, while B.) positive control probe against Ppib mRNA (green dots) gives rise to strong fluorescent signals on the green (488 nm) channel. Nuclei are stained with DAPI (blue) and endothelial cells are labelled with IB4 (red).

Expression of mRNA in the tissue does not always correlate with protein expression, therefore CXCR7 protein expression was investigated using a western blot analysis. CXCR7 protein expression was examined in whole mouse heart and mouse aorta tissue homogenates, as well as cell homogenates obtained from MCEC and HUVEC cell cultures. Further, cardiac endothelial cells (EC) were isolated from wild type mouse hearts using a CD31-Dynabeads

complex and were also included in the western blot analysis. Isolation of EC is known to be challenging due to their fragility, and cell cultures often contain cells of non-endothelial origin. Hence, several assays were deployed to validate the population of cells obtained as endothelial cells.

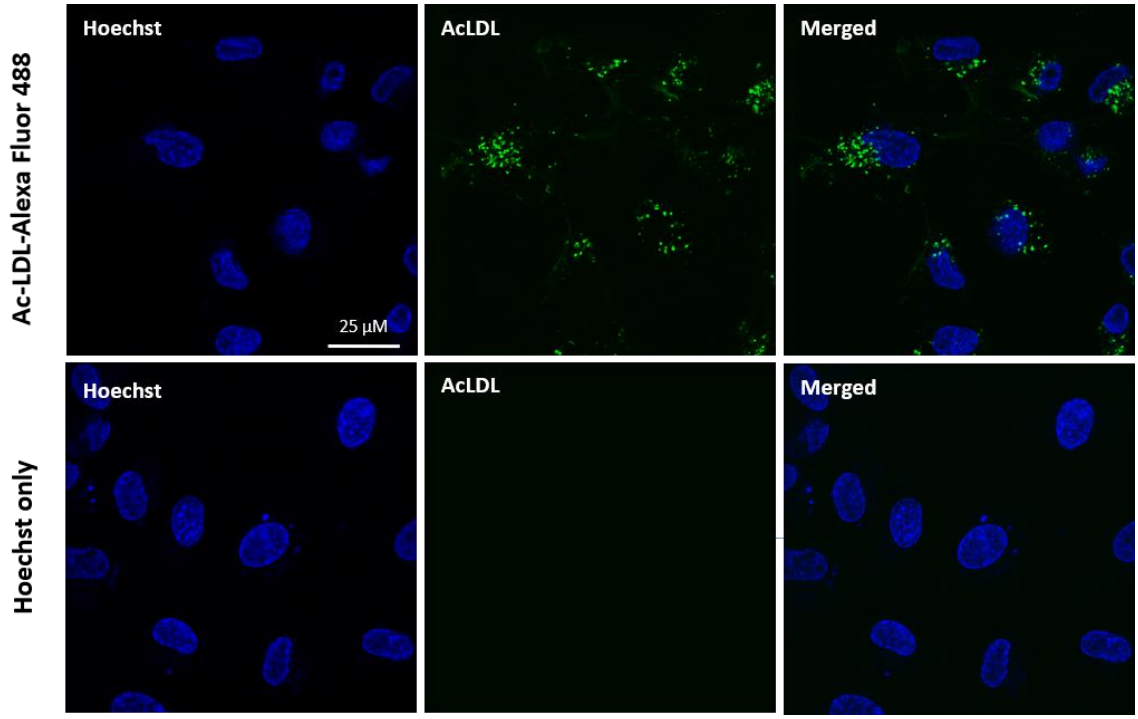

Figure 3-3: Ac-LDL uptake assay on cardiac endothelial cell culture. Cardiac endothelial cells were isolated using CD31-Dynabeads complex. Addition of ac-LDL-Alexa Fluor 488 to a live endothelial cell culture results in the uptake of ac-LDL by endothelial cells, and detection of a strong signal when excited with the green (488 nm) confocal laser (top panel). Addition of Hoechst nuclear stain (blue) on its own, does not produce a detectable signal on the 488 nm channel (bottom panel).

One method of identifying endothelial cells is to incubate them with a fluorescent modified acetylated LDL (ac-LDL), which they readily take up. When submitted to an ac-LDL uptake assay EC displayed positive uptake, with >90% EC becoming fluorescent after 2 h (Figure 3-3, top row). There was little background fluorescence present after the addition of ac-LDL, nor was there any observable fluorescent signal on the 488 nm channel when Hoechst nuclear stain was

added to the cell culture in the absence of ac-LDL; indicating the validity of detected signal (Figure 3-3, bottom row).

To further determine the percentage of endothelial cells in the isolated cell culture, EC were fixed, labelled with IB4 and analysed by flow cytometry.

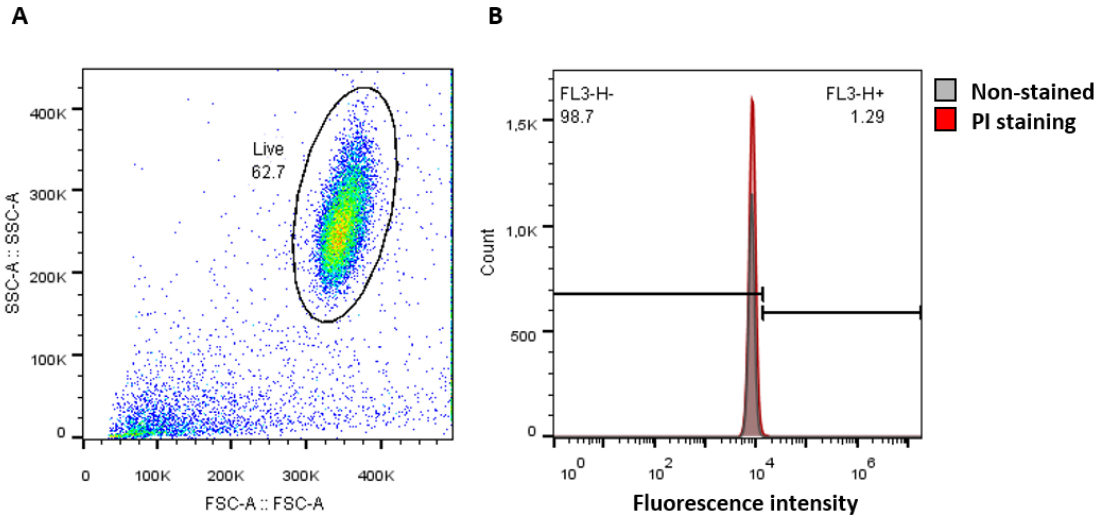

Figure 3-4: Flow cytometry gating for a viable cell population on cardiac EC culture. A.) A representative density plot depicting a gated "live" subpopulation of cells based on forward and side scatter parameters, with 62.7% of counted cells determined as viable. B.) Histogram overlay with non-stained (grey) and PI stained (red) cells already gated for live population (as shown in A) on the FL-3H channel (>670 nm emission), depicting only a single defined peak, which overlays the non-stained sample almost completely with only 1.29% of cells identified as positively labelled with PI, and therefore determined to be non-viable.

Flow cytometry samples were first gated to separate intact cells from debris. This was achieved by displaying the cells population on a FSC and SSC density plot, with a gate placed manually around the region containing the cells (Figure 3-4, A). The percentage of non-viable cells in the population was then determined by counting the percentage of PI^{+ve} cells in the FL-3H fluorescent channel (Figure 3-4, B; 1.29%).

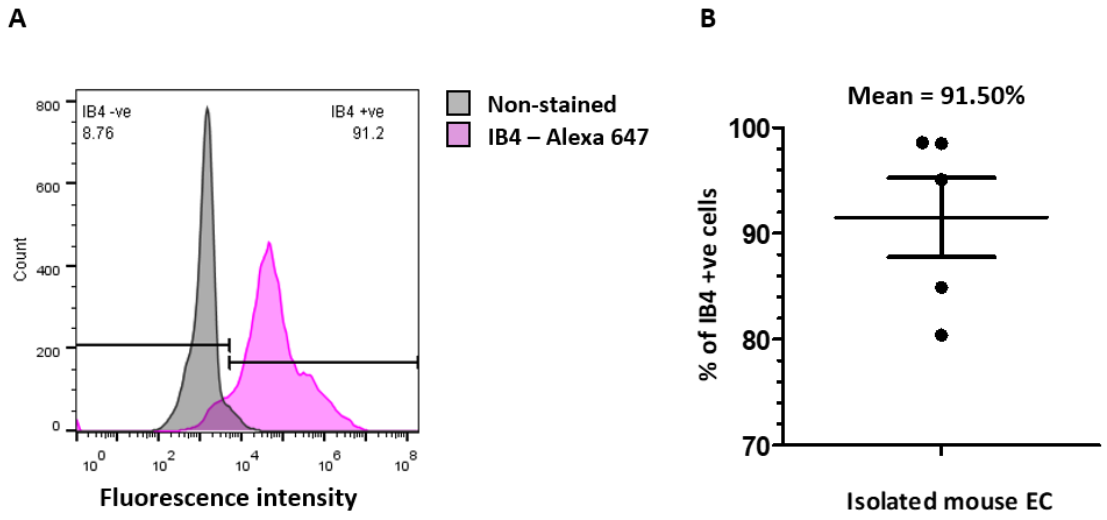

Figure 3-5: Flow cytometry IB4 endothelial labelling of cardiac EC culture. A.) Representative histogram overlay of IB4 labelling, with IB4-Alexa 647 (pink) and unlabelled cells (grey) on the FL-4H channel (675/25 nm emission), with 91.2% of cells $IB4^{+ve}$. B.) The percentage of isolated EC that were determined to be $IB4^{+ve}$ in 5 individual isolations.

When labelled with endothelial cell marker IB4, the major peak of endothelial cells is shifted to the right, denoting greater fluorescence on the FL-4H channel, and confirming the majority of cells to be endothelial (Figure 3-5, A). These preliminary experiments revealed that ~90% of the cells isolated from mouse heart using this procedure were endothelial cells, as they were positively identified using the endothelial marker IB4 (Figure 3-5, B).

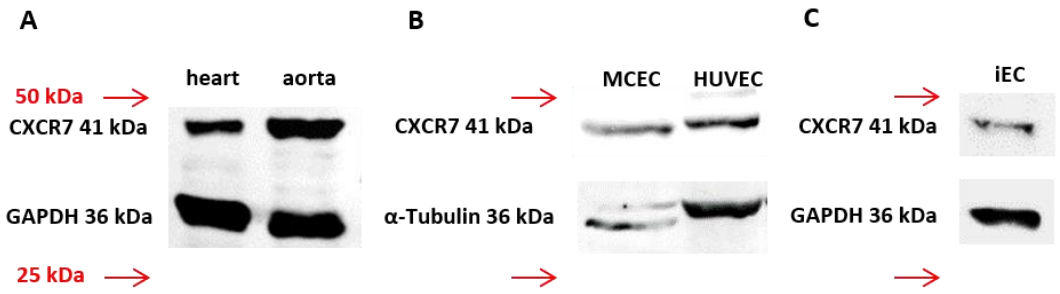

Figure 3-6: CXCR7 western blotting of murine cardiovascular tissues, cardiac EC and commercially available cells. Western blot analysis of murine heart and aortic tissues A.), MCECs and HUVEC B.), as well as murine isolated cardiac endothelial cells C.). All tissues and cell types display CXCR7 protein band at approximately 41 kDa. GAPDH and α-Tubulin were used as loading controls, both displayed bands approx. 36 kDa in size. Red arrows signify the molecular weight markers.

Once satisfied that the isolated cardiac cultures contained mainly cells of endothelial origin, the focus was shifted to the investigation of CXCR7 protein expression in various tissues. CXCR7 expression was examined by western blot analysis in whole mouse heart and aorta tissue homogenates (Figure 3-5, A), commercially available human umbilical vein endothelial cells (HUVEC) and immortalized mouse cardiac endothelial cells (MCEC, Figure 3-5, B), as well as EC (Figure 3-5, C). A 41 kDa band was detected in all tissues and cell types tested, which is the size expected for CXCR7. This suggests that CXCR7 is expressed in the adult mouse heart, aorta and likely in cardiac endothelial cells. Since CXCR7 is readily internalized and yet must be present on the plasma membrane in order to be capable of binding its ligand and activating signalling pathways, the intracellular localization of CXCR7 in EC was determined [265].

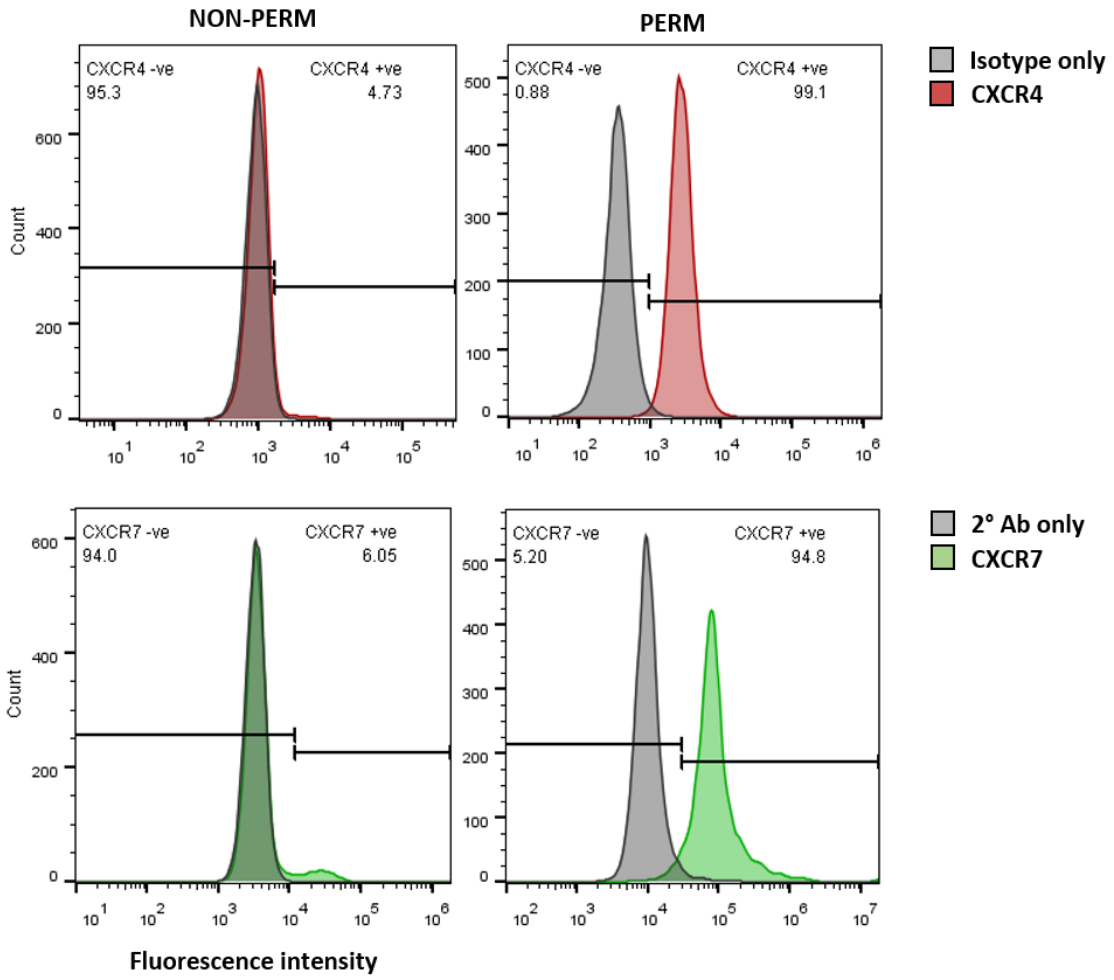

Figure 3-7: Membrane-bound and intracellular expression of CXCR4 and CXCR7 in MCEC. Representative flow cytometry histograms of cells labelled with CXCR4 (red), CXCR7 (green) and isotype-labelled or labelled with the secondary antibody alone (grey). Cell count is represented on the y-axis, plotted against fluorescence intensity on the x-axis. Left panels depict membrane-bound (i.e.: non-permeabilized) CXCR4/CXCR7 labelling, and right panels depict intracellular (i.e.: after permeabilization) signal. The percentage of labelled cells is indicated. NON-PERM = non-permeabilized, PERM = permeabilized.

Due to the low number of endothelial cells that could be isolated from the mouse heart, it was not feasible to evaluate CXCR4 and CXCR7 expression in these cells. Instead, intracellular and cell-surface expression of CXCR4 in the MCEC and HUVEC cell lines was examined.

However, since the utilized CXCR7 antibody recognized the C-terminus of the protein it cannot be used to determine intracellular vs cell-surface expression profile of CXCR7. Instead, this experiment can be used as a gauge of antibody specificity where non-permeabilized or “membrane-bound” labelling corresponds to non-specific binding and permeabilized or “intracellular” labelling to specific binding of the monoclonal CXCR7 antibody (ab138509).

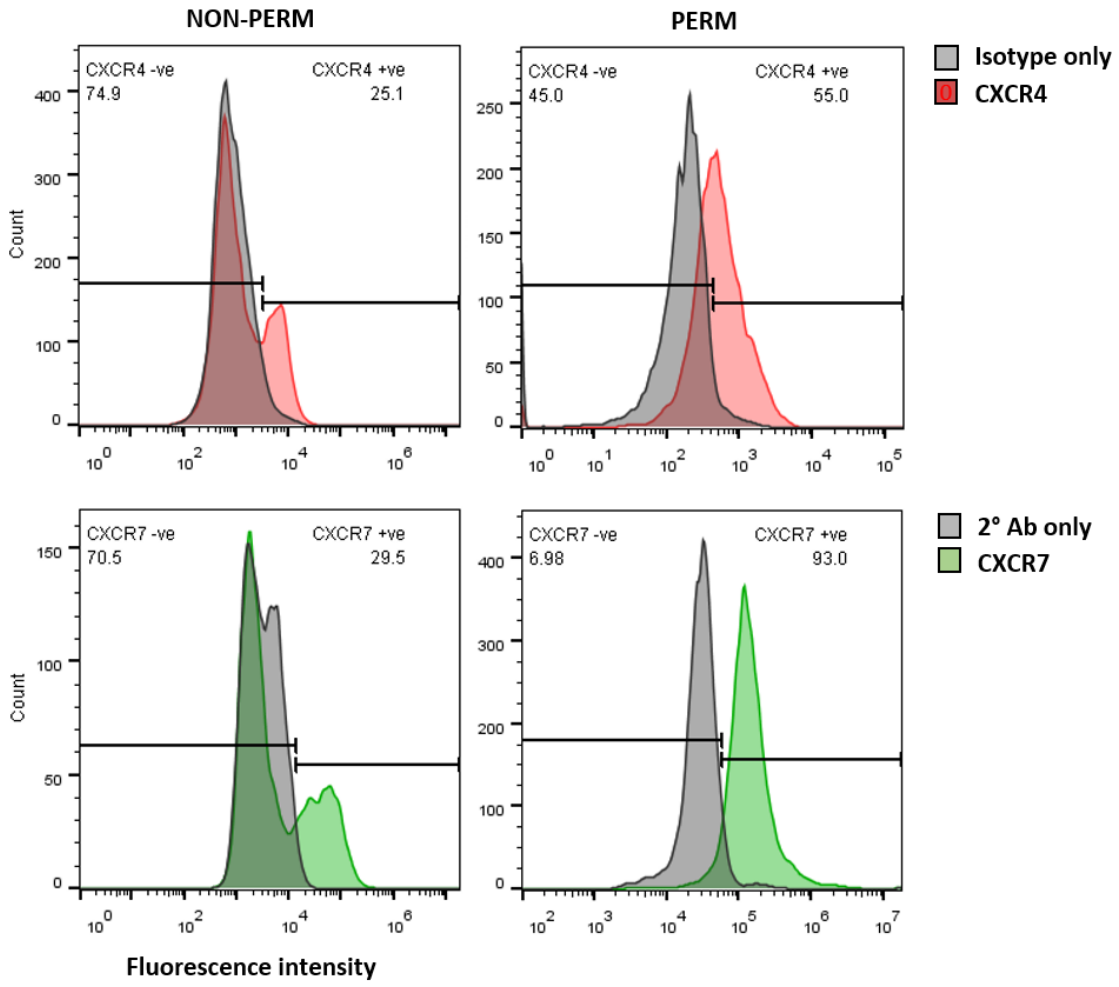

Figure 3-8: Membrane-bound and intracellular expression of CXCR4 and CXCR7 in HUVEC. Representative flow cytometry histograms of cells labelled with CXCR4 (red), CXCR7 (green) and isotype-labelled or labelled with the secondary antibody alone (grey). Cell count is represented on the y-axis, plotted against fluorescence intensity on the x-axis. Left panels depict membrane-bound (i.e.: non-permeabilized) CXCR4/CXCR7 labelling, and right panels depict intracellular (i.e.:

after permeabilization) signal. The percentage of labelled cells is indicated. NON-PERM = non-permeabilized, PERM = permeabilized.

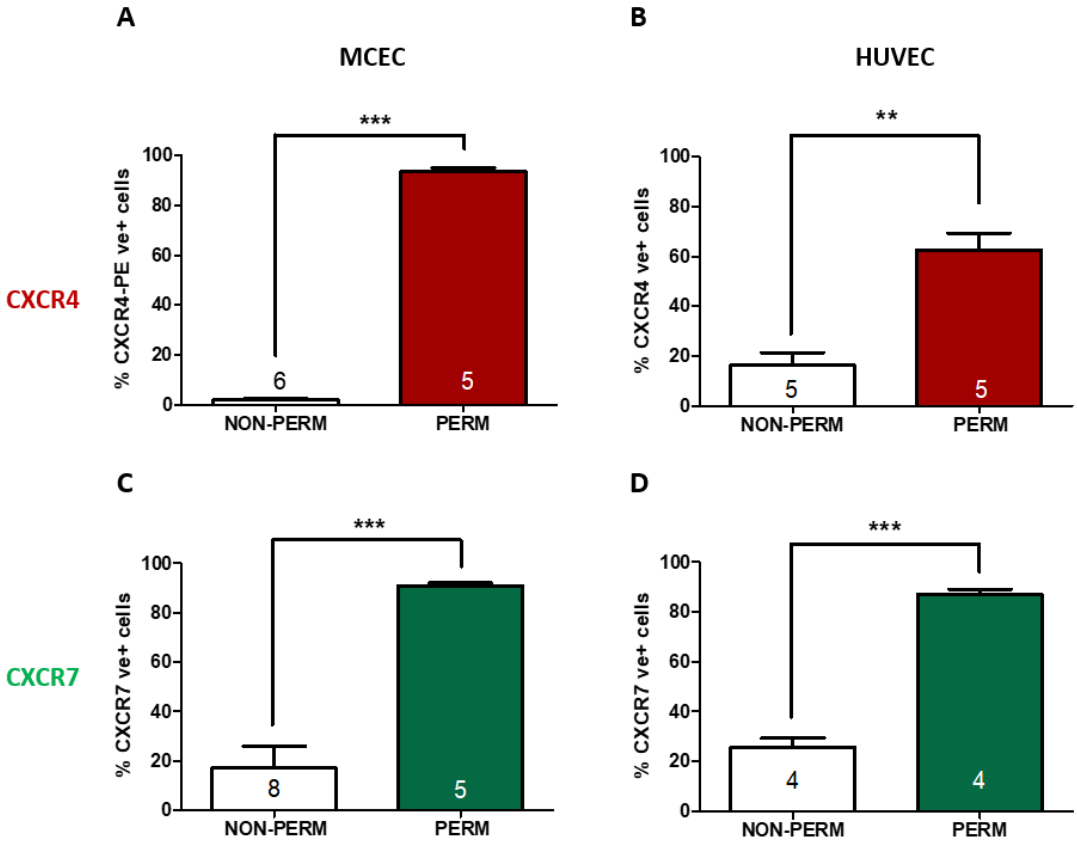

Figure 3-9: Intracellular and membrane-bound expression of CXCR4/CXCR7 in MCEC and HUVEC. The percentage of cells exhibiting cell-surface (NON-PERM) and internal (PERM) CXCR4/CXCR7 labelling in MCEC and HUVEC cell lines. Green bars depict CXCR7 labelling and red bars indicate CXCR4. Permeabilized (intracellular, PERM) samples displayed significantly increased percentages compared to their non-permeabilized (membrane-bound, NON-PERM) counterparts for both receptors, CXCR4/7 and both cell lines, MCEC and HUVEC, indicating that the majority cells express receptor intracellularly. ** $p < 0.01$, *** $p < 0.001$, Student's t-test, n = an individual flow cytometry experiment.

Cells were either permeabilized, to allow the antibody to reach the intracellular, internalized population of CXCR4 receptor, or non-permeabilized to investigate surface, membrane-bound expression, with representative histogram overlays for MCEC and HUVEC shown in Figure 3-7 and 3-8, respectively.

Only a small proportion of MCEC were found to possess detectable surface CXCR4 labelling (Figure 3-9, A; non-perm vs perm = 2.1 ± 0.3% vs 93.5 ± 1.7%, n=6; $p < 0.001$). In HUVEC, the proportion of cells with surface CXCR4 labelling was slightly higher (Figure 3-9, B; non-perm vs perm = 16.2 ± 5.0% vs 62.8 ± 6.6%; $p < 0.01$). When either cell type was permeabilized, the majority of cells displayed CXCR4 labelling, indicative of intracellular pool of receptors capable of binding the utilized anti-CXCR4 antibody. Overall, the percentage of cells with membrane-bound CXCR4 was quite low, which denotes that only a small proportion of MCEC and HUVEC express detectable levels of active receptors on the cell surface.

Interestingly, when non-permeabilized MCEC or HUVEC were labelled with CXCR7 antibody there were detectable levels of staining on both cell types (Figure 3-9, bottom row; MCEC vs HUVEC = 17.1 ± 8.8% vs 25.7% ± 3.5%), suggesting that the specificity of this particular antibody was lower than expected.

3.5 Discussion

Despite being revealed as an SDF-1α receptor over a decade ago, the expression of CXCR7 in the heart, and specifically in the heart endothelium has not received as much attention as in other tissue types. Additionally, some published results have been obtained using antibodies with questionable specificity for CXCR7 and are therefore not particularly informative [266]. Therefore, the expression of CXCR7 mRNA and protein in the heart endothelium needed to be confirmed.

RNAscope in situ hybridization confirmed the presence of CXCR7 mRNA in endothelial and cardiomyocyte cells found in the adult mouse myocardium. Furthermore, using western blot analysis CXCR7 protein was detected in whole mouse heart and aortic tissue, as well as commercially available endothelial cell lines and freshly isolated cardiac EC.

These results are consistent with published data reporting CXCR7 expression in cells of endothelial origins as described in detail in section 1.3.3 [110-113]. Most previous studies focused on non-cardiac tissues and none have shown the expression of CXCR7 on isolated cardiac endothelial cells specifically. Due to the limited numbers of cells that could be isolated from the mouse heart, in this study western blot analysis was only performed on a single EC sample. However, western blot analysis coupled with RNAscope in situ hybridization is enough to confirm the presence of CXCR7 in endothelial cells of cardiac origin.

Additionally, RNAscope in situ hybridization revealed positive CXCR7 mRNA staining on cardiomyocytes, which were identified based on their observed morphological features. In general, not much is known about expression of CXCR7 in non-endothelial cardiovascular cell types, including cardiomyocytes, with only a handful of papers addressing the expression of CXCR7 receptors in those cells [123, 265, 267]. This is perhaps not surprising given the fact that recent studies point specifically to endothelial CXCR7 as capable of pro-regenerative and anti-fibrotic effects in multiple tissue types [234, 235]. Furthermore, the presence of CXCR7 mRNA might not correlate with actual tissue protein expression and further experiments are needed to confirm CXCR7 expression in adult mouse cardiomyocytes. Cardiac EC served as a valuable tool to show the expression of CXCR7 protein, however, isolation and culture of cells has proven challenging. Using a Dynabeads-CD31 complex, a semi-pure population of EC was obtained, but at a cost of reduced cell numbers. This meant that using EC for experiments where a high volume of cells is needed to achieve valid results was not deemed feasible. Therefore, commercially available cell lines were utilized to provide cells of endothelial origin capable of expressing endogenous CXCR7.

When probed with anti-CXCR7 antibodies MCEC and HUVEC cell lines displayed a strong CXCR7 band using a western blot method. However, western blotting analysis does not distinguish between membrane-bound and intracellular (and therefore inactive) CXCR7. Therefore, further examination of the intracellular vs membrane-bound expression profile of CXCR7 was needed.

Flow cytometry revealed that for both cell types studied, only a small proportion of cells contain detectable membrane-bound CXCR4 receptor. A higher proportion of cells with of CXCR4 membrane-bound labelling was detected in HUVEC compared to MCEC. Despite being of cardiac origin, MCECs are an immortalized cell-line, and therefore resemble their endogenous counterparts less. Primary cells, like HUVEC, more closely resemble healthy cells found in their tissue of origin, especially during early passages, as they have not yet accumulated mutations due to tumorigenesis or continuous cell culture [268]. Immortalized cell lines are produced by overcoming the replicative senescence, which occurs in non-immortalized cells and is characterized by biochemical, morphological and functional changes, such as gradual shortening of telomeres [269, 270]. This can affect cell signalling and as a result, some immortalized cell lines display altered cell signalling pathways compared to non-immortalized cells [268, 271]. However, the published literature suggests that immortalized EC can retain their angiogenic potential *in vivo* and are deemed a valuable *in vitro* model, despite being less comparable to cells that one might find *in vivo*. [272, 273].

Interestingly, permeabilization of MCEC and HUVEC revealed intracellular CXCR4 labelling of a much greater proportion of cells. There are multiple published studies noting the presence of intracellular pools of CXCR4 and CXCR7 receptors in various cell types. Intracellular expression of CXCR4 receptor has been confirmed in hematopoietic progenitor cells, foetal mesenchymal cells and HUVEC [274, 275 276]. The function of the intracellular pool of receptors remains disputed.

Early research suggests that after binding to SDF-1α, CXCR4 is rapidly endocytosed to regulate CXCR4 plasma membrane expression, playing a vital role in modulation of migratory clues [274].

Meanwhile, intracellular pools of CXCR7 receptors have been detected in several cells of the immune system, including B and T cells, as well as tumour cells [143, 144, 214, 277]. Intracellular pool of CXCR7 receptor is thought to aid the scavenger function of CXCR7, by providing a way to quickly clear excess SDF-1α from circulation [133]. However, the solely scavenging function of CXCR7 has been questioned by studies suggesting an active signalling role of CXCR7 through β-arrestins [123]. One theory would be that an intracellular pool of CXCR7 can recycle back to the membrane as either a scavenger of SDF-1α or as a receptor capable of active signalling, a capacity that will be discussed further in section 5.5. However, since we did not examine the intracellular vs membrane-bound labelling of CXCR7 receptor in our experiments, we cannot compare the percentage of cells expressing membrane-bound vs intracellular CXCR7 labelling in HUVEC and MCEC. Nevertheless, the existence of intracellular pool of not only CXCR4 but also CXCR7 in endothelial cells is highly likely, although future research with a reliable and flow cytometry-compatible antibody is needed to confirm it.

However, we have observed that the CXCR7 antibody utilized for flow cytometry (ab138509) might have lower specificity than desired. As it recognizes an intracellular epitope on the C-terminus section of the CXCR7 protein, non-permeabilized cells should not display labelling with this particular antibody. However, ~17% MCEC and ~26% HUVEC displayed labelling with CXCR7 antibody in their non-permeabilized state. Despite the antibody not being advertised as flow cytometry-compatible it raises questions regarding it's specificity. Antibodies advertised as specific, which also recognize additional epitopes, can be hugely detrimental to scientific research, since the results obtained with such antibodies are not reliable.

Research into CXCR7 has garnered a lot of interest in the past years and specificity, or lack thereof, of antibodies represents a major hurdle for the scientific community, a topic previously addressed by Berahovich *et al*. [266]

3.5.1 *Summary*

The expression of CXCR7 was demonstrated in mouse cardiovascular tissues, endothelial cell lines and endothelial cells of cardiac origin. CXCR7 mRNA was also detected in cardiovascular cells of non-endothelial origin, namely cardiomyocytes. Additionally, CXCR7 receptor was detected in both, MCEC and HUVEC cells, however due to its primary cell origins HUVEC were chosen as the most suitable cell type for further *in vitro* experiments.

4 The effect of CXCR7 agonist VUF11207 fumarate in the Langendorff *ex vivo* heart perfusion model

This chapter contains a project that was carried out in collaboration with Dr Catherine Wilder, who provided technical expertise necessary for the use of this experimental model.

4.1 Background

Previous studies have shown that administration of SDF-1α in various forms acts in a cardioprotective fashion, improving the state of myocardial tissue after I/R (e.g. infarct size reduction). Since CXCR7, an SDF-1α receptor has been shown to activate CXCR4-independent, β-arrestins-biased signalling it was postulated that it could exhibit cardioprotective effects in a wider range of cardiovascular disorders, including MI. More specifically, past research highlighted a cardioprotective role for β-arrestins signalling in mice with exaggerated catecholamine stimulation, such as heart failure [278, 279].

In order to investigate the role of CXCR7 in acute MI setting, a rat *ex vivo* Langendorff I/R perfusion model was utilized. To allow for distinction between the effects of CXCR4 and CXCR7 receptor, VUF11207 a CXCR7-specific receptor agonist, was used immediately prior to reperfusion, as outlined in Figure 2-7.

4.2 Research aims and objectives

Investigate whether CXCR7 agonist VUF11207 exhibits cardioprotective effects in a rat *ex vivo* perfusion model:

- Investigate if the administration of VUF11207 prior to reperfusion has an effect on the final infarct size in MI.
- Investigate if the administration of VUF11207 prior to reperfusion has an effect on the LDH release during MI.

4.3 Methods

The methods used are described in section 2.9. Rat isolated perfused hearts were randomized to one of three experimental groups: 1.) vehicle perfused group, where 5 min prior to reperfusion the perfusion solution was switched from Krebs to vehicle; 2.) IPC group, which received 3 x 5 min cycles of regional ischaemia prior to index ischaemia and 3.) VUF11207 perfused group, where Krebs perfusion was switched to 1 µM VUF11207 5 min before the onset of reperfusion. Experimental protocol is further described in section 2.9.1.

During each experiment, LDH samples were collected and analysed as described in section 2.9.4. Following the conclusion of each experiment, hearts were stained with Evans blue dye and TTC, and analysed as described in section 2.9.3.

4.4 Results

When using the Langendorff *ex vivo* perfusion model it is important to maintain the consistency of LAD suture placement between experimental groups. To ensure that, AAR was measured independently by two observers, with the average results reported in Figure 4-1, A. There was no significant difference observed between AAR of different groups, therefore the experimental consistency was deemed satisfactory.

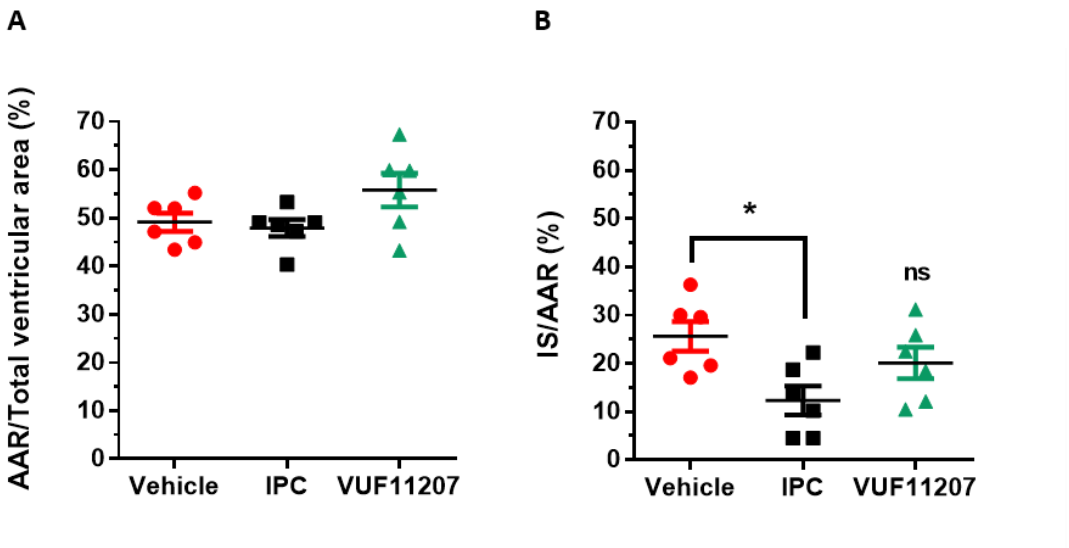

Figure 4-1: Area at risk and infarct size assessment in isolated rat hearts. A.) Area at risk as a percentage of total ventricular area did not differ between groups. B.) Infarct size as a percentage of area at risk was found to be significantly lower in the IPC group compared to the vehicle group. The VUF11207 group was found not to be significantly different from the vehicle group. Normality was confirmed with a Shapiro - Wilk test. n = 6 hearts per group, * $p < 0.05$, One-way ANOVA with Dunnett's post-hoc test with all groups compared to vehicle. AAR = area at risk, IS = infarct size, ns = non-significant.

Infarct size was also independently determined by two observers, with the average values for each heart reported as a percentage of area at risk, in Figure 4-1, B. The infarct size analysis showed that the positive control group, which received IPC prior to index ischaemia, exhibited significantly lower average infarct size than the vehicle group (vehicle vs IPC = 25.6 ± 3.1 vs 12.3 ± 3.0; $p < 0.05$). The VUF11207 group was not significantly different than the vehicle group.

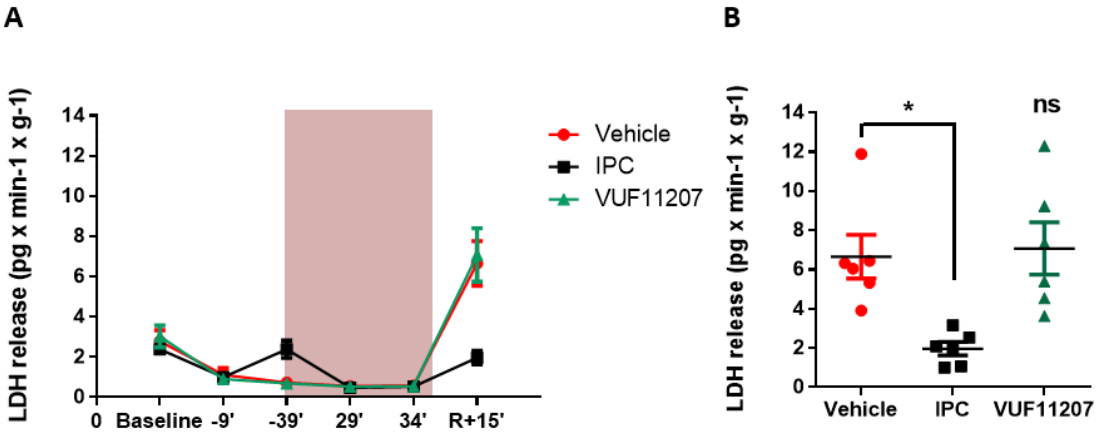

Figure 4-2: LDH release during ex vivo isolated heart perfusion. A.) Graphical representation of time-dependent release of LDH (the amount of LDH in pg released per min per gram of ventricular weight). B.) Dot plot representing release of LDH 15 min after onset of reperfusion (R+15'). IPC group displayed a significantly lower LDH release than the vehicle group, * $p < 0.05$, One-way ANOVA with Dunnett's post-hoc test with all groups compared to vehicle. The period of index ischaemia is shaded pink on the graph; n = 6 hearts per group.

In order to confirm the infarct size measurements using a different analysis, some of the perfusate was collected for LDH analysis at various timepoints during the experiment, as shown in section 2.9.1. Timepoints for collection of LDH samples were derived from previously published literature [255]. The time-course of LDH release from the perfused heart is shown in Figure 4-2, A.

Due to potentially confounding effect of IPC treatment at timepoint -39' the area under the curve for this experiment was not examined and overall statistical analysis was not performed for all timepoints together. Instead, samples collected 15 min after the onset of reperfusion were of special interest, since peak LDH release was previously shown to occur during the first 10-15 min of the reperfusion stage Figure 4-3, B [255]. Corroborating the infarct size measurements, the IPC group exhibited significantly lower "peak" LDH release than the vehicle group (vehicle vs IPC = 6.7 ± 1.1 vs 2.0 ± 0.3; $p < 0.05$), but the VUF11207 group was unchanged from vehicle.

Along with the infarct size and LDH release measurements, several functional parameters were also observed during the course of the experiment. Flow rate was measured in mL of perfusate per minute and was not significantly different between any of the groups (Figure 4-3, A). Flow rate gradually decreased as the experiment progressed, for all three groups. The lowest flow rate in the IPC group prior to index ischaemia occurred during the 3 x 5 min IPC cycles as expected. During the three IPC cycles, total flow was manually turned off and those timepoints were, therefore, not included in the statistical analysis. Heart rate was not significantly different between the vehicle and the IPC group for all observed timepoints (Figure 4-3, B). VUF11207 group displayed a gradual lowering of the heart rate, especially in the last couple of timepoints; however, this was not statistically significant when compared to the vehicle group.

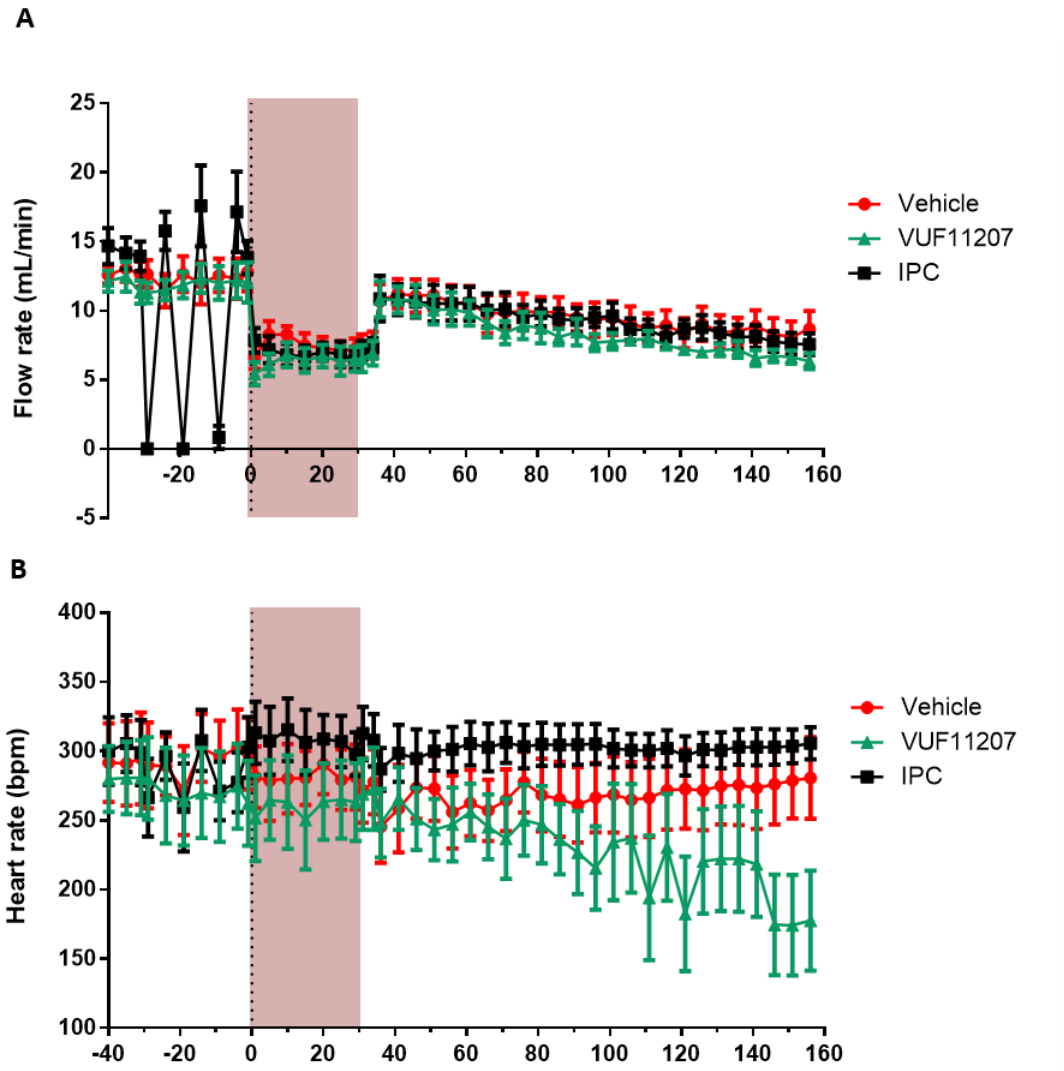

Figure 4-3: Flow rate and heart rate measured during the ex vivo isolated heart perfusion. A.) Time-course of flow rate measurements showed no significant differences between different experimental groups. B.) The time-course of heart rate measurements showed that for the last three timepoints at the end of the reperfusion stage, VUF11207 group displayed a significantly lower heart rate than the IPC group. The period of index ischaemia is shaded pink on the graph. One-way ANOVA with Dunnett's post-hoc test with all groups compared to vehicle, all comparisons were non-significant; n = 6 hearts per group.

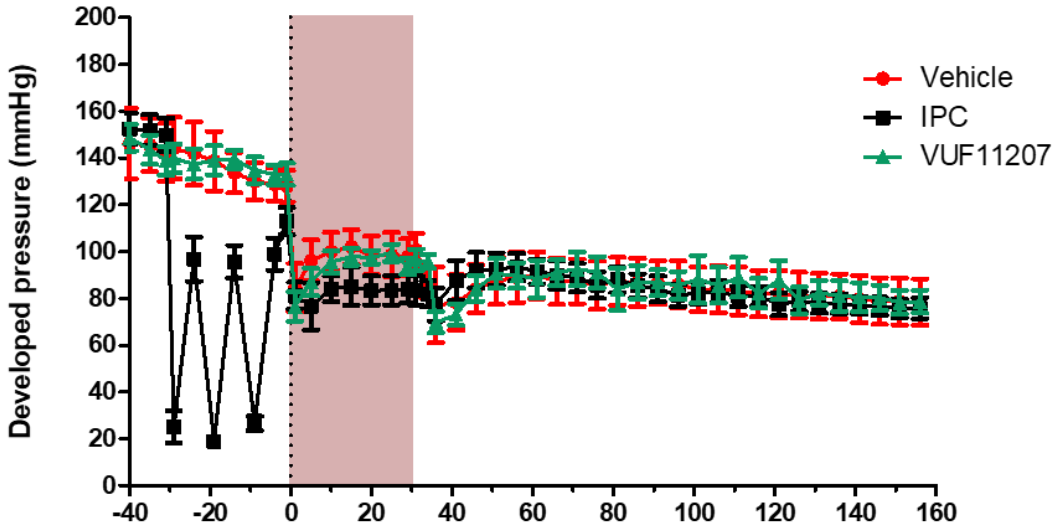

Figure 4-4: Left ventricular developed pressure during the *ex vivo* isolated heart perfusion. Left ventricular developed pressure was obtained by subtracting the end-diastolic pressure from the systolic pressure, both obtained via the intraventricular balloon. The time-course of developed pressure measurements showed no significant differences between the groups. One-way ANOVA with Dunnett's post-hoc test with all groups compared to vehicle, all comparisons were non-significant; n = 6 hearts per group.

Another functional parameter that was observed during the course of the experiment was left ventricular developed pressure. The left ventricular developed pressure was obtained by subtracting the end diastolic pressure from the systolic pressure, which was measured via a balloon positioned inside of the left ventricle. The plotted time-course of the developed pressure showed no significant differences between the groups for the entire duration of the experiment (Figure 4-4). Due to the lack of perfusion during the 3 x 5 min IPC cycles, the contractility of the heart was reduced. As a result, the developed pressure was lower in the IPC group than in other groups for the same timepoints. Therefore, those timepoints were not included in the statistical analysis.

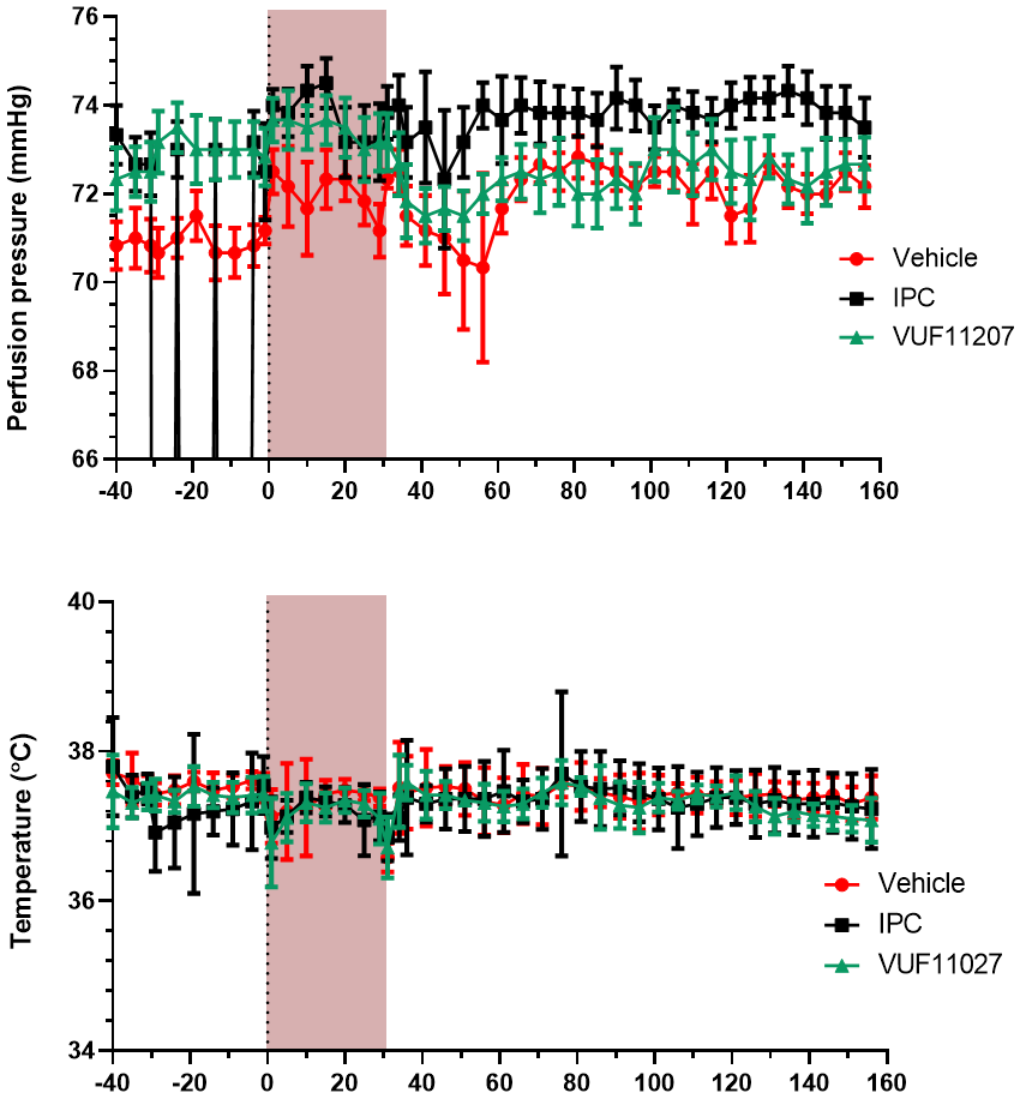

Figure 4-5: Perfusion pressure and heart temperature during the ex vivo isolated heart perfusion. Perfusion pressure was maintained at 70mmHg or above, during the experiment. There were no significant differences observed between the three groups. During the 3 x 5 min IPC cycles, perfusion was switched off, hence the pressure reading was 0 (below the y-axis limit). Temperature was maintained at 37 ± 0.5°C with some fluctuations observed between when switching between different stages of the experiment (stabilization, ischaemia, reperfusion). Statistical analysis showed no significant differences between the three experimental groups. One-way ANOVA with Dunnett's post-hoc test with all groups compared to vehicle, all comparisons were non-significant; n = 6 hearts per group.

Further functional parameters that were observed during the course of the experiment were perfusion pressure and internal heart temperature. Perfusion pressure was maintained around 70mmHg and there were no significant differences in the perfusion pressure between the vehicle, IPC and VUF11207 groups for the entire duration of the experiment (Figure 4-5, A). The slight dip in the perfusion pressure following the change from the regional ischaemia to the reperfusion stage of the experiment was mostly related to the switch between the perfusion columns on the Langendorff apparatus. Heart temperature was maintained at 37 ± 0.5°C and remained stable throughout the duration of the experiment, with no significant differences present, when either the IPC group or the VUF11207 were compared to vehicle (Figure 4-5, B).

There were a total of 29 rats used in the *ex vivo* isolated heart experiment with 18 included in the final analysis (Figure 4-6). Exclusions were made based on the exclusion criteria described in section 2.9.2. Most hearts (8) were excluded due to AAR being <35%, after staining with Evans blue dye. One heart was excluded due to tearing of the aorta mid-way through the experiment, which made further retrograde perfusion through the aorta impossible. A single heart was excluded due to a period of ventricular fibrillation, which lasted for more than 2 min and did not respond to ice-cold KCl treatment. Lastly, another heart was excluded for presenting with a heart rate that did not consistently stay above 200 bpm during the stabilization period. The total number of exclusions per group was very similar across the three groups. Three hearts were excluded from the VUF11207 group and 4 hearts excluded from each of the IPC and vehicle groups. There was no significant difference in the numbers excluded from each group.

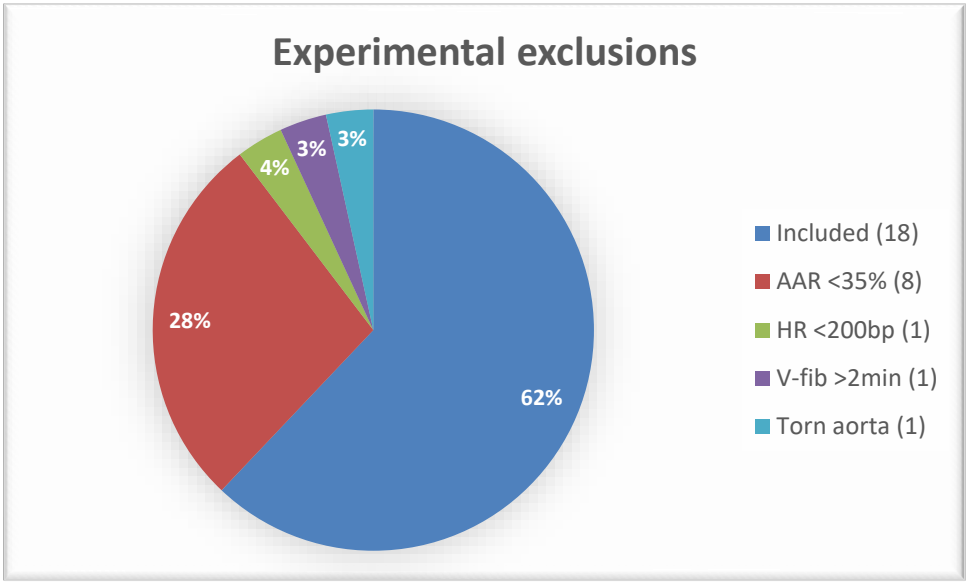

Figure 4-6: Experimental exclusions during ex vivo isolated rat heart perfusion experiments. 29 animals were used with 18 included in the analysis. Most animals (62%) were excluded due to their AAR falling outside of the inclusion criteria. Further exclusions occurred either because of low heart rate (3%, HR) and being too low or long duration of ventricular fibrillation (3%, v-fib). A single heart (4%) was also excluded due to a torn aorta.

4.5 Discussion

The Langendorff *ex vivo* perfusion model is a well-described model used to investigate cardiac function independently of other organ systems and can offer important insights into the ability of drugs to protect the heart from I/R injury. One of the most common endpoints of *ex vivo* isolated heart perfusion is infarct size assessment, normally performed using a combination of Evans blue dye and TTC staining. In vivo, larger infarct size has been shown to correlate with adverse cardiac remodelling and haemodynamic dysfunction; therefore, interventions that can limit the initial infarct size are expected to confer long-term cardioprotective benefit [280-282]. Many cardioprotective interventions that are applied immediately prior to reperfusion aim to inhibit the opening of the mPTP, as this is associated with attenuation of reperfusion injury [283, 284].

Such interventions that target myocardial reperfusion are considered as having potential clinical relevance, since they can be delivered after the onset of the ischaemic insult and prior to the reperfusion intervention, such as PCI, in the clinic.

In the Langendorff model, the position of the suture with regard to the LAD determines the volume of myocardium subjected to regional ischaemia. The most common way to analyse the size of the ischaemic area at risk (AAR), and thereby ensure experimental consistency, is by re-tightening the suture at the end of the experiment and perfusing the heart with Evans blue dye, staining the perfused (i.e. non-ischaemic) tissue blue [285]. In this experiment, the size of the AAR was not found to be significantly different between the experimental groups; therefore, the consistency of suture placement was deemed acceptable. The functional parameters measured during the course of the study were also found to be consistent between the experimental groups.

Coronary flow rate was unchanged between the experimental groups, with the values consistent with previously published results [286]. During the period of ischaemia, coronary flow rate exhibited a marked decline, which is expected due to perfusion of a smaller region of the heart. After the period of ischaemia, coronary flow rate briefly recovered, but then continued to gradually decline due to the “dying preparation” nature of the experimental model [286]. Heart rate was maintained consistently up until the reperfusion stage of the experiment, when the VUF11207 group exhibit lowered heart rate in the last three timepoints of the experiments. Nevertheless the reduction in heart rate was not statistically significant when compared to the vehicle.

Left ventricular developed pressure (LVDP) was also monitored during the experiment. Developed pressure is used as a measure of cardiac function and exhibited a reduction for all three experimental groups (vehicle, IPC, VUF11207), during the period of ischaemia. The recorded fall in LVDP is a well-established consequence of regional ischaemia, and agrees with previously published values of ~30% reduction, across all experimental groups [285].

Additionally, the combined effect of the delivered ischaemic insult and the dying preparation nature of the isolated heart model caused a gradual decline in the LVDP until the conclusion of the experiment [286]. Perfusion pressure, which was maintained at approx. 70 mmHg, remained stable throughout the experiment for all experimental groups, as it should in a so-called “constant pressure” model. This type of model is a preferred model in a setting of regional myocardial ischaemia as it enables autoregulation of coronary tone [252].

Heart temperature is another important parameter that was closely monitored, since it can greatly affect the overall function of the heart [285]. Failure to maintain the heart at a physiological temperature (37 ± 0.5°C) can affect the susceptibility of the heart to I/R injury, haemodynamic performance, and response to drugs [287]. Since temperature remained within specified parameters for the entire duration of the experiment for all three experimental groups, there is no reason to assume that it modified the susceptibility of the rat heart to VUF11207 administration in any way.

From 11 rat hearts that were excluded due to pre-defined exclusion criteria, small size of AAR (<35%) was the most common reason for exclusion (n=8). This likely occurred due to improper placement of the ligature or insufficient tightening prior to the ischaemic insult, and is undesirable, since it is associated with smaller infarct sizes and hinders testing of potential cardioprotective interventions in an *ex vivo* isolated heart perfusion model [288]. Other exclusions were also unremarkable, with no significant differences in the number of exclusions between the groups. They included a low baseline heart rate (<200 bpm, n=1) and an episode of ventricular fibrillation (n=1), which lasted longer than 2 min. Low baseline heart rate is not desirable since it suggests an impaired cardiac function, while after the episode of ventricular fibrillation normal sinus rhythm was not restored, which prevented the conclusion of the experiment. A single heart also displayed a torn aorta, which occurred due to operator error.

Final infarct-size assessment and LDH measurements at various timepoints during the *ex vivo* heart perfusion were used as experimental endpoints. Rat hearts that received 3 x 5 min cycles of IPC administered prior to index ischaemia, exhibited significantly reduced infarct size compared to the vehicle-perfused group, which did not receive IPC (Figure 4-1). There has been extensive research into the mechanism IPC. It has been shown to exert cardioprotective effects through Protein kinase C (PKC) signalling, which is also a common target of various cardioprotective pharmacological agents (e.g. opioids, bradykinin) [289, 290]. Controversy exists surrounding the particular isoenzyme of PKC responsible for conferring cardioprotection in the IPC setting, with PKC-δ (delta) and PKC-ε (epsilon) emerging as the most likely contenders [291-293]. Furthermore, IPC has been shown to require activation of PI3K/AKT and ERK1/2 signalling within IPC in the first few minutes of reperfusion. This discovery provided a paradigm shift from early thinking, which postulated that IPC exerts most of its beneficial effect during the period of ischaemia [191, 289]. The IPC stimulus was also shown to be responsible for the inhibition of the opening of the mPTP during the reperfusion period [294]. This is believed to be mediated by the PI3K/AKT pathway, thought the precise target of the kinase that decreases mPTP opening is not known. In the present study, IPC was used solely as a positive control, due to its well-documented and highly reproducible cardioprotective effect when used in this setting [183, 295, 296]. In contrast to IPC, administration of CXCR7 agonist VUF11207 (1 µM), commencing 5 min prior to and continuing throughout reperfusion, did not reduce infarct size. Possible reasons for this are discussed below.

To date, the only publication that directly addresses the role of CXCR7 in MI and its cardioprotective effects has been published by Hao *et al*. [115]. They showed that using an adenovirus to induce over-expression of CXCR7 prior to inducing *in vivo* MI in mice significantly reduced the average infarct size by ~13%, when measured 28 days after induction of MI; compared to hearts injected with a control adenovirus. Furthermore, Hao *et al*. administered a CXCR7-specific agonist TC14012 i.p., immediately post-MI and every 6 days thereafter for 24 days.

Final infarct size analysis 28 days post-MI showed a significant ~16% reduction in the average infarct size between the group that received TC14012 injection and the group that received saline [115]. Additionally, Hao *et al*. utilized a conditional, endothelial CXCR7-knockout model, which exhibited higher infarct sizes than the wild type group, when measured 28 days post-MI [115]. These mice also exhibited reduced survival, greater cumulative death and worse cardiac function within 28 days post-MI. However, the deleterious effects of endothelial CXCR7 deletion only became obvious after the induction of MI, showing that the absence of endothelial CXCR7 is detrimental after the occurrence of MI, but not before. These data suggest that endothelial CXCR7 plays an important protective role after MI and ameliorates the damage sustained by the heart from the ischaemic insult in the longer term. On the other hand, Hao *et al*. did not examine the acute role of CXCR7 activation or deletion on MI. Furthermore, all of the infarct size measurements were made 28 days post *in vivo* MI, and after the use of permanent ligation, a model which differs substantially from one of ischaemia and reperfusion.

In the permanent ligation experiment the coronary vessel, usually LAD, is permanently ligated, which does not allow for reperfusion to the ischaemic area to occur directly through the LAD but is achieved through any collateral circulation present in the area. This normally results in a larger infarct size, because the entire area at risk becomes infarcted [297]. It is a model predominantly used to investigate longer-term effects, such as ventricular remodelling and cardiac contractility. *Ex vivo* isolated heart experiments on the other hand are more commonly used to investigate short-term consequences of MI. They are the preferred model when investigating the effects of pharmacological agents, especially those administered before or early during the reperfusion period. In summary, a permanent ligation model is performed *in vivo* and focuses on longer term ischaemic damage, while the isolated heart perfusion is an *ex vivo* model investigating the effects of acute I/R injury.

Both models have their strengths and weaknesses but are ultimately designed to examine different aspects of ischaemic damage on the heart post-MI, which might be the reason why Hao's study showed a cardioprotective role of CXCR7, while in our experiments VUF11207 did not exhibit such cardioprotective effects.

Another difference between our study and that of Hao *et al*. is that they used Masson trichrome staining instead of the TTC method for determination of the final infarct size, which could also contribute to contrasting results. TTC in combination with Evan's blue dye is frequently used to assess final infarct size after an acute MI, since it has the ability to distinguish between metabolically active and inactive tissues in the first few hours after the ischaemic insult has occurred; as described in section 2.9.3 [253]. However, TTC staining also relies on adequate reperfusion occurring in the ischaemic area, to achieve a clear delineation of the infarcted zone. This is a crucial step prior to TTC staining, since washout of dehydrogenases upon which TTC acts and haem-containing proteins present in the heart is needed to avoid a mottled appearance of the infarcted area and underestimation of the infarct size [298]. Measuring flow rate can help determine whether sufficient washout has occurred for TTC staining to be effective. In this study, flow rate was adequate for all experimental groups throughout the duration of the experiment. Additionally, flow recovery after the period of index ischaemia was satisfactory for all experimental groups and it is unlikely that insufficient washout prevented accurate assessment of infarct size

There are additional factors that could have affected the response to VUF11207, among them the existence and extent of collateral coronary vasculature. For various mammalian species the extent of coronary collaterals that exist in the heart can be drastically different. For example, guinea pigs, dogs and cats exhibit much higher rates of collateral flow than rats and mice, which are more similar to young and/or healthy humans and display lower rates of collateralization in the heart [299-301]. However, formation of collaterals in the human heart varies greatly between individuals and can be affected by age and disease [302].

Past studies also show that in mice, the strain of mice can influence the extent of collateral vasculature formation in different vascular beds [303-306]. This is important because collaterals present in the heart can help ameliorate ischaemic injury by supplying blood flow to the ischaemic area, independent of the ligated coronary vessel [301]. Ultimately, the extent of collateral circulation in the heart could also affect the extent of delivery of a pharmacological agent, such as VUF11207, to the ischaemic region. Since VUF11207 was administered shortly before reperfusion this might not be as relevant as if it were administered prior to, or during ischaemia. However, it is still important to note that the varying extent of coronary collateralization could also represents a differing number of CXCR7 receptors present in endothelial cells, which can in turn have an impact on the strength of the response to a CXCR7 agonist. There is limited information on the presence and importance of coronary collaterals in murine species, it is difficult to determine whether collateralization played a significant part in the differences observed in results obtained by Hao's study and ours.

The time between the administration of CXCR7 agonist and the onset of MI might also be an important factor in determining the cardioprotective effects of said agonist. In the study performed by Hao *et al.* the time between the MI and final infarct size analysis was 4 weeks, which might mean that CXCR7 or its agonists need a longer period or several administrations before exerting beneficial effects on the heart. Studies performed on other tissue types by Ding and colleagues [234, 235, 240] and described earlier in section 1.3.3 would support the theory that CXCR7 might act in the longer term, with a more regenerative, anti-fibrotic mode of action, which could be the reason why VUF11207 did not exhibit cardioprotective effects in our study.

A further explanation for the lack of cardioprotection seen in our study might also be the choice of CXCR7 agonist, VUF11207. Most studies examining the effects of CXCR7 signalling use the agonist TC14012.

However, due to the long duration of the experiment, and consequently large volumes (litres) of perfusion buffer needed, the use of TC14012 was not deemed financially feasible. T140 compounds, precursor compounds to TC14012, were first synthesized and published two decades ago [150, 152, 307]. Consequently, TC14012 has been commercially available for longer than VUF11207. TC14012 has also been used in more published articles than VUF11207, and its mode of activation and binding properties have been fairly well described, which might also explain why this agonist is more popular than others [151, 308]. In contrast, VUF11207 was only synthesized in 2012, and there is only a single published paper using VUF11207 [153, 309]. Additionally, the two agonists have a different chemical structure; T14012 is a peptidomimetic agonist and VUF11207 is a small molecule agonist. A peptidomimetic compound mimics the properties of a natural peptide or protein (in this case SDF-1α) and is able to interact with the same biological target and elicit the same biological effect. Often, peptidomimetics also display improved bioavailability and duration of activity, compared to natural peptides, which makes them an attractive investigative tool for many researchers [310].

On the contrary, small molecule drugs are low molecular weight compounds, with relatively short half-lives that can typically pass through cell membranes with ease, due to their small size [311]. There are advantages and disadvantages to using either small molecule drugs, such as VUF11207 or peptidomimetic compounds, like TC14012 with both displaying markedly different pharmacokinetics and pharmacodynamics. Perhaps the preferential use of TC14012 to VUF11207 is simply due to the fact that it has been around longer and is therefore considered a tried and tested approach.

Based on the reported EC_{50} of 1.6 nM for VUF11207 in the β-arrestin2 recruitment assay in CXCR7-expressing HEK293 cell, it was expected that the concentration of 1 μM would be sufficient to exert any beneficial effects [153]. Nevertheless, it is possible that a greater or smaller concentration might yield different results, and time permitting, a concentration-response curve would be the next sensible step.

Furthermore, it would be preferable to have a biological readout confirming stimulation of CXCR7 receptor, such as a measure of β-arrestin activity, which is currently not feasible in an *ex vivo* model. Another measure that could have been taken to ensure that the utilized VUF11207 compound displays functional activity, especially after aliquoting and freezing, would be to test its functionality. Such a test would be best performed on a cell type where CXCR7-dependent SDF-1α signalling has already been shown, e.g. ERK1/2 signalling in Jurkat T cells, and with the same drug concentration as intended for isolated rat heart perfusion experiments [220]. This would help to confirm whether our chosen, commercially available CXCR7 agonist VUF11207 has the ability to elicit the same response in Jurkat T cells and inform us whether it would make an effective CXCR7 agonist.

The second endpoint of the *ex vivo* perfusion experiment was the analysis of LDH release at set timepoints throughout the experiment. LDH has been used as a surrogate marker of myocardial injury in the clinic, since high circulating values are associated with greater myocardial damage and subsequently worse prognosis after MI [312, 313]. Nowadays, it is still used as a marker of myocardial injury in basic research, although it is slowly being replaced by highly sensitive and specific cardiac troponin assays, as they become more cost efficient [314].

The timepoint selected for LDH analysis was 15 min (R+15') after the start of the reperfusion period, since Rossello *et al*. showed a pronounced peak of LDH release between 10 - 15 min of reperfusion and a steady decline thereafter [255]. IPC significantly reduced LDH release at R+15' compared to vehicle, whereas VUF11207 did not have an effect on LDH release at the same timepoint.

In general, previously published research has found LDH release to be a relatively inconsistent measure of the cardioprotective potential of IPC compared to TTC staining [254, 255, 315, 316]. Furthermore, peak LDH release does not appear to directly correlate to infarct size, whereas it does show correlation with the ischaemia length [255]. For these reasons, we considered LDH levels as being of secondary importance to TTC measurement.

It is possible that VUF11207 might have been found to alter LDH levels at timepoints other than R+15 min, but to determine this, a prolonged time-course of LDH measurements would be needed. Interestingly, Povlsen *et al*. showed two peaks of LDH release following ischaemia instead of one. The first peak occurred at 2 - 20 min and the second at 30 - 120 min, after the start of the reperfusion period, which is in contrast to the single peak reported by Rossello *et al*. [254, 255].

Povlsen *et al*. also make an interesting observation regarding the correlation between the second peak of the LDH release and cardioprotective interventions applied past the period of ischaemia [254]. They postulate that the first LDH peak in the rat heart occurs as a result of ischaemic and early reperfusion damage and the second LDH peak as a result of late reperfusion damage, with both peaks being amenable to cardioprotective interventions. This would fall in line with IPC, which is known to attenuate ischaemic and reperfusion damage, having the ability to reduce the level of LDH release during the first peak (R+15'). It is important to note that Rossello *et al*. performed the study on mice, whereas Povlsen *et al*. used rats, which could explain the inconsistent reporting of the existence of the second peak. Since our study only collected perfusate for LDH analysis up to R+15', neither the existence of the second peak, nor the effect of VUF11207 on said peak could be determined.

In brief, Hao *et al.* showed that increased expression of CXCR7 or administration of its agonist TC14012 is cardioprotective, while the lack of CXCR7 is deleterious. However, they investigated the impact of MI on the heart several weeks thereafter, when cardiac remodelling, angiogenesis, fibrosis and scar formation has already occurred. Consequently, all of these processes represent possible targets of CXCR7 and its agonist TC14012, with prior research already pointing to the importance of CXCR7 in ameliorating fibrosis in various tissues; as described in section 1.3.3. However, their choice of experimental model and staining preclude from investigating the effects of CXCR7 on the initial infarct formation, which according to our study are unremarkable.

Overall, in our hands the administration of VUF11207 just prior to reperfusion in an ischaemia/reperfusion model of a rat heart did not reduce either final infarct size or LDH release at our chosen investigated timepoint R+15'. As already discussed above, there are several limitations to this study which could preclude us from observing the hypothesized effects of VUF11207.

However, it could be that VUF11207, or potentially any CXCR7 agonist, lacks the ability to exert beneficial effects in an acute setting of MI. As previously published by Ding and colleagues, as well as others, most beneficial actions of CXCR7 were seen in a chronic setting, either as an anti-fibrotic or a pro-angiogenic effector [234, 235, 240]. This could mean that 2 h for which the VUF11207 is active during the reperfusion period is not long enough either to exert its beneficial effects or for the ischaemic myocardium to benefit from those effects in a way that we could observe in our experiment (i.e. infarct size, LDH release). Additionally, the study published by Hao *et al.,* where administration of another CXCR7 agonist, TC14012, did demonstrate cardioprotective effects in a chronic MI setting, the lack of acute (within hours of the ischaemic insult) cardioprotective response further indicates this as the most likely scenario [115]. Therefore, it would be prudent to direct further investigation into the beneficial effects of CXCR7 agonist administration in an ischaemia/reperfusion setting towards the more chronic anti-fibrotic and pro-regenerative actions of CXCR7 agonist, rather than into its acute cardioprotective actions.

4.5.1 *Summary*

IPC decreased final infarct size and reduced LDH release at R+15’. This positive control demonstrates that the experiment was successful, and detection of significant cardioprotection was technically feasible. However, CXCR7 agonist VUF11207 (1 μM) did not affect either the final infarct size, or the LDH release at set timepoints throughout the experiment. This suggests that this dose of VUF11207 administered at reperfusion does not exhibit cardioprotective effects in our *ex vivo* isolated heart perfusion model.

5 The effect of CXCR7 agonists VUF11207 and TC14012 on the RISK pathway

5.1 Background

As discussed previously in section 1.4.2. there is compelling evidence that activation of effectors downstream of CXCR7 is cell type-specific and encompasses processes such as, chemotaxis, cell migration and cell survival [123, 219, 220]. However, since our research focuses on the role of CXCR7 in endothelial cells, we wanted to investigate the effects of CXCR7 activation on the RISK pathway specifically in cells of endothelial origin and its possible links to cardioprotection. There is currently little evidence linking RISK pathway activation through CXCR7 signalling with a cardioprotective benefit to the heart. However, identifying whether CXCR7 is capable of signalling through the RISK pathway is an important step towards determining whether there is a role for CXCR7-dependent acute cardioprotection.

To investigate RISK pathway activation, CXCR7 agonists VUF11207 and TC14102 were used to examine phosphorylation of ERK1/2 and AKT downstream of CXCR7 receptor activation. The CXCR7 agonists used in below experiments are described in detail in section 1.3.3.

5.2 Research aims and objectives

Investigate whether administration of CXCR7 agonists is able to induce AKT and/or ERK1/2 phosphorylation, in order to examine RISK pathway signalling:

- Examine the effect of VUF11207 and SDF-1α on AKT, ERK1/2 phosphorylation status in HUVEC.

- Examine the effect of TC14012 and SDF-1α on AKT, ERK1/2 phosphorylation status in HUVEC.

5.3 Methods

In addition to the general methods described in Chapter 2, the following specific methods were used in the experiments described in this chapter.

5.3.1 *Western blotting antibodies*

RISK pathway signalling was investigated in HUVEC, using western blotting methods described in section 2.5. Membranes were incubated with anti-phospho AKT rabbit monoclonal (1:1000, #9271, Cell signalling), anti-pan AKT mouse monoclonal (1:1000, #2920, Cell Signalling), anti-p44/42 MAPK mouse monoclonal (1:1000, #9107, Cell Signalling) or anti-phospho p44/42 MAPK rabbit polyclonal (1:1000, #4370, Cell Signalling) primary antibodies.

IRDye® 800CW goat anti-rabbit IgG (1:10,000, Li-COR), or IRDye® 680RD Goat anti-mouse IgG (1:10,000, LI-COR) secondary fluorescent antibodies were used for detection.

5.3.2 *Cell treatments*

Prior to western blotting, HUVEC were cultured as described in section 2.3. HUVEC were serum-starved for 3 h with DMEM medium (Gibco) supplemented with penicillin/streptomycin (Gibco), prior to the administration of the following cell treatments prepared in 200 µL of PBS: insulin (100 nM, Sigma-Aldrich), SDF-1α (250 nM, Miltenyi Biotec), VUF11207 (100 nM/250 nM, Tocris), Bradykinin (1 µM, Sigma-Aldrich) or TC14012 (30 µM, Cayman Chemical). In western blotting experiments involving VUF11207, the control cell sample only received 200 µL of PBS. For experimental sets containing TC14012, vehicle contained DMSO (final conc. <0.05%).

5.3.3 *Normalization of western blotting results*

In order to be able to directly compare western blotting results obtained from different experimental repeats, individual blots were normalized using an additional sample (internal control sample). The internal control sample was used solely to ensure a correct analysis of western blots and is therefore not shown in the results section.

5.4 Results

In order to investigate the effects of CXCR7 agonists VUF11207 and TC14012 on phosphorylation of ERK1/2 and AKT, western blotting was used. The selected times for HUVEC cell incubation with the relevant drugs were based on previously published research described in section 1.4.2, which suggests that incubation of 5 - 15 min is needed to elicit maximal ERK1/2 and AKT phosphorylation. Insulin was used as a positive control for AKT phosphorylation, since its ability to induce AKT phosphorylation status in various cell types is well established [317, 318]. Similarly, SDF-1α has previously been shown to be able to induce phosphorylation of ERK1/2 in endothelial cells and was, therefore used as a positive control in ERK1/2 phosphorylation experiments [319, 320].

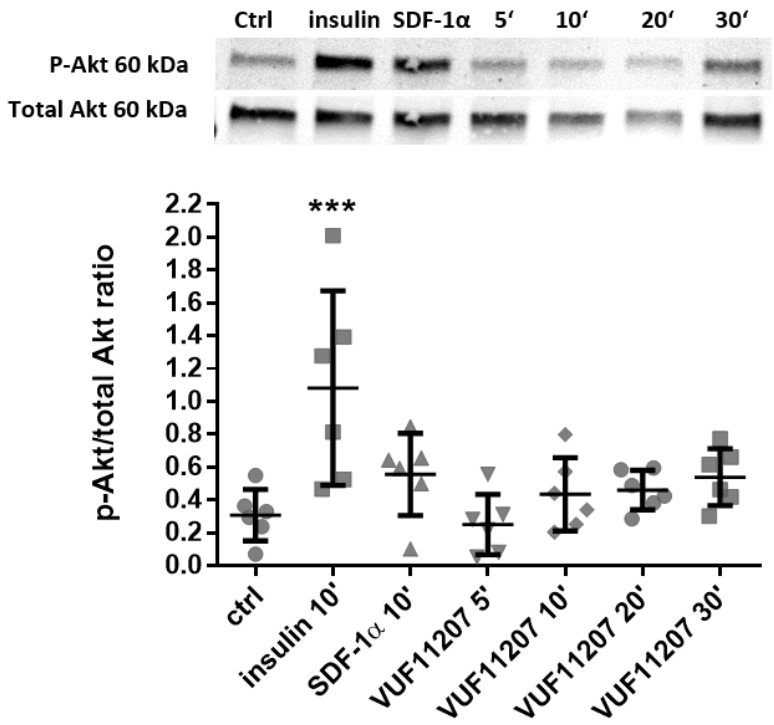

Figure 5-1: The effect of VUF11207 (100 nM) on phosphorylation of AKT in HUVEC. Administration of insulin (100 nM) 10 min prior to cell lysis induced a significant increase in AKT phosphorylation. Administration of SDF-1α (250 nM) for 10 min or VUF11207 (100 nM) for 5 – 30 min before cell lysis did not significantly affect AKT phosphorylation. Total AKT was used as a loading control. *** $p < 0.001$ insulin vs control, Repeated Measures ANOVA with Bonferroni post-hoc test comparing all groups to control; n = 6 independent experiments per group.

Western blotting for phospho-AKT in HUVEC revealed that 10 min treatment with insulin (100 nM), induced significant phosphorylation of AKT, with an approx. 4-fold increase, compared to control (Figure 5-1). The administration of SDF-1α for 10 min or VUF11207 for various lengths of time as indicated, did not significantly affect the phosphorylation status of AKT.

When western blotting for ERK1/2, SDF-1α administered 10 min prior to cell lysis induced significant ERK1/2 phosphorylation, which was increased approx. 5-fold, when compared to control (Figure 5-2). Again, administration of VUF11207 for various lengths of time did not induce phosphorylation of ERK1/2 at any timepoint.

Additionally, insulin administration for 10 min did not induce phosphorylation of ERK1/2.

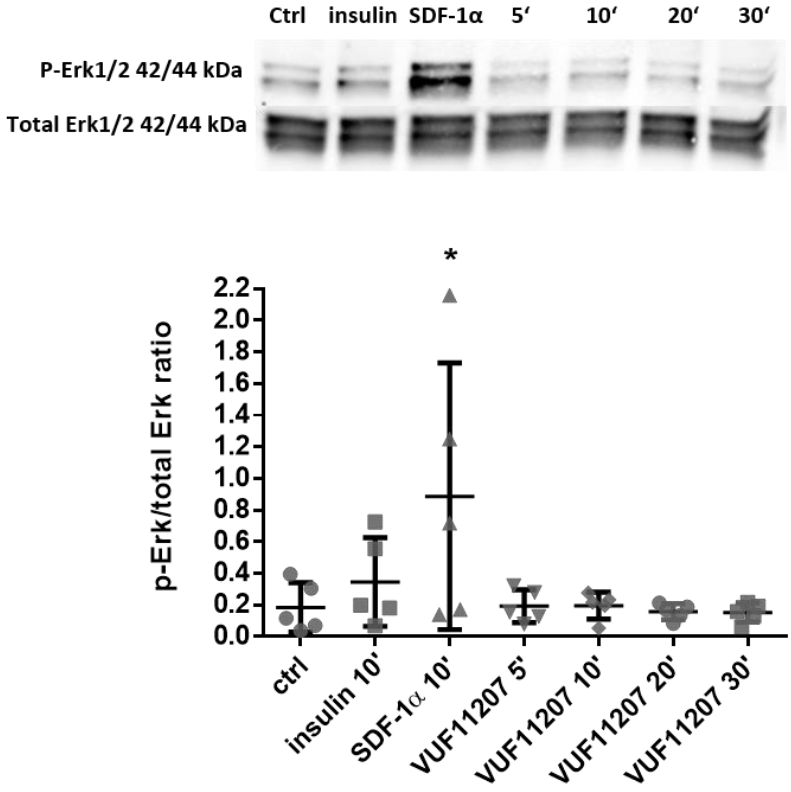

Figure 5-2: The effect of VUF11207 (100 nM) on phosphorylation of ERK1/2 in HUVEC. The administration of SDF-1α (250 nM) 10 min prior to cell lysis induced significant phosphorylation of ERK1/2. Administration of insulin (100 nM) for 10 min or VUF11207 (100 nM) for 5 – 30 min did not induce changes in ERK1/2 phosphorylation status. Total ERK1/2 was used as a loading control. * $p < 0.05$ SDF-1α vs control, Repeated Measures ANOVA with Bonferroni post-hoc test comparing all groups to control; n = 5 independent experiments per group.

Since the concentration of VUF11207 (100 nM) used in the western blotting experiments was lower than that of SDF-1α (250 nM), the concentration of VUF11207 was increased to 250 nM in the subsequent experiment (Figure 5-3). In this experiment, bradykinin (1 µM) was used as an alternative positive control for ERK1/2 activation [321]. A single incubation timepoint of 10 min was chosen for all experimental groups, on the basis of previously published research, where a 10 min incubation was sufficient to successfully induce phosphorylation of ERK1/2 [220, 320].

Bradykinin administration 10 min prior to cell lysis successfully induced phosphorylation of ERK1/2 in HUVEC cell, whereas VUF11207 (250 nM), administered for the same amount of time, did not induce phosphorylation.

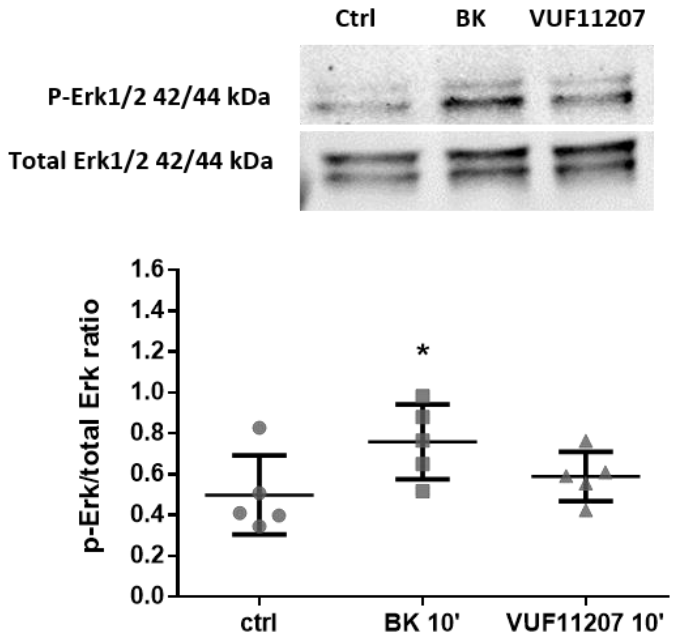

Figure 5-3: The effect of VUF11207 (250 nM) on phosphorylation of ERK1/2 in HUVEC. The administration of bradykinin (1 µM) 10 min prior to cell lysis significantly increased induction of ERK1/2 phosphorylation. Administration of VUF11207 (250 nM) 10 min prior to cell lysis did not have an effect on ERK1/2 phosphorylation levels. Total ERK1/2 was used as a loading control. * $p < 0.05$ bradykinin vs control, Repeated Measures ANOVA with Bonferroni post-hoc test comparing all groups to control; n = 4 independent experiments per group. BK = bradykinin.

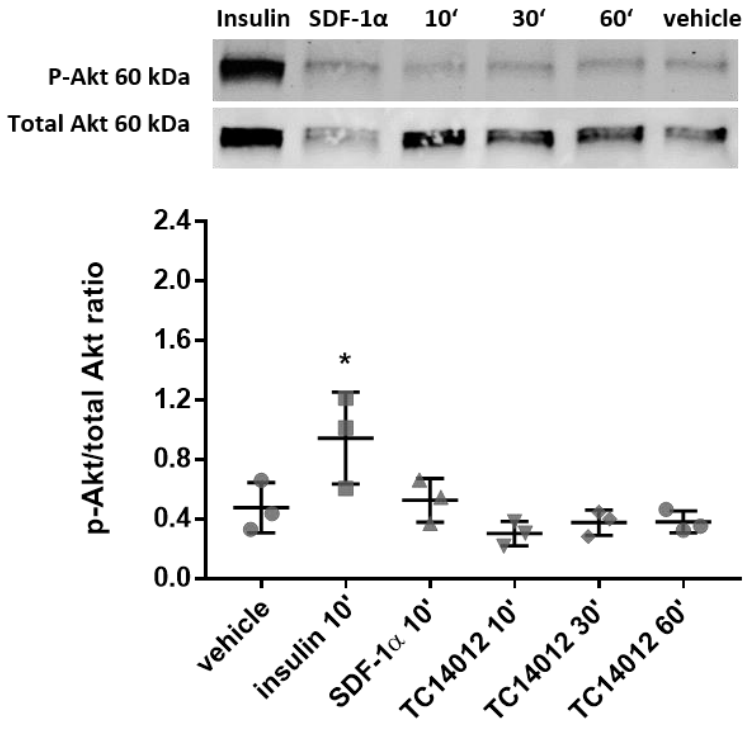

Figure 5-4: The effect of TC14012 on phosphorylation of AKT in HUVEC. The administration of insulin (100 nM) 10 min prior to cell lysis induced significant phosphorylation of AKT. Administration of SDF-1α (250 nM) for 10 min or TC14012 (30 µM) for 10 – 60 min did not induce changes in the AKT phosphorylation status. Total AKT was used as a loading control. * $p < 0.05$ insulin vs control, Repeated Measures ANOVA with Bonferroni post-hoc test comparing all groups to control; n = 3 independent experiments per group.

Since VUF11207 did not induce phosphorylation using western blotting, an alternative CXCR7 agonist, TC14012 was also investigated. In these experiments, administration of insulin (100 nM) 10 min prior to cell lysis induced AKT phosphorylation, which was approx. 2-fold greater than the vehicle control (Figure 5-4). Administration of TC14012 (30 µM) for 10, 30 or 60 min, or incubation with SDF-1α 10 min prior to cell lysis did not affect the phosphorylation status of AKT (Figure 5-4). When western blotting for phospho-ERK1/2, administration of neither TC14012, SDF-1α or insulin induced statistically significant phosphorylation (Figure 5-5).

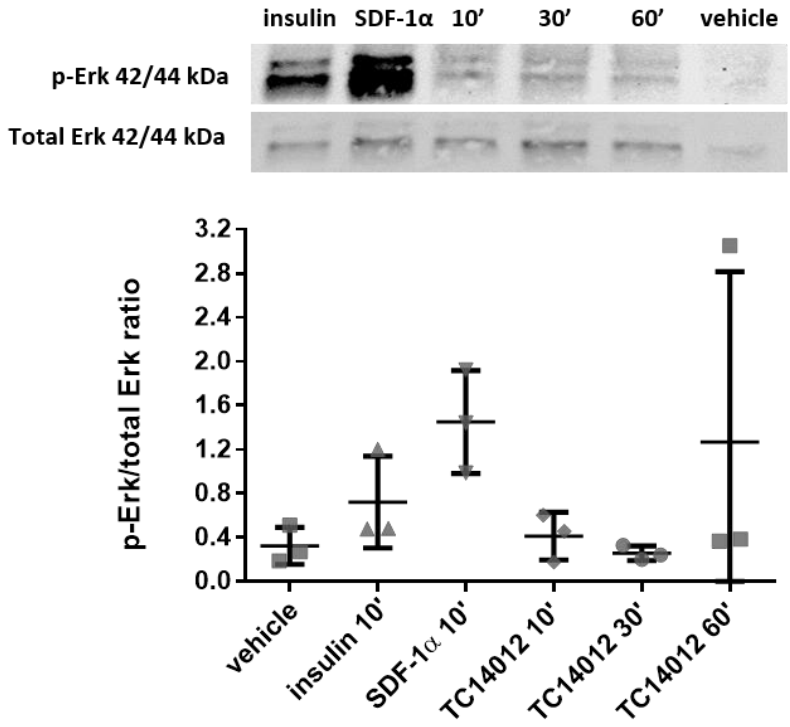

Figure 5-5: Effect of TC14012 on phosphorylation of ERK1/2 in HUVEC. There was no change in ERK1/2 phosphorylation levels with administration of either insulin (100 nM), SDF-α (250 nM) or TC14012 (30 μM) in HUVEC. n = 3 independent experiments per group. Total AKT was used as a loading control. * $p < 0.05$ insulin vs control, Repeated Measures ANOVA with Bonferroni post-hoc test comparing all groups to control; n = 3 independent experiments per group.

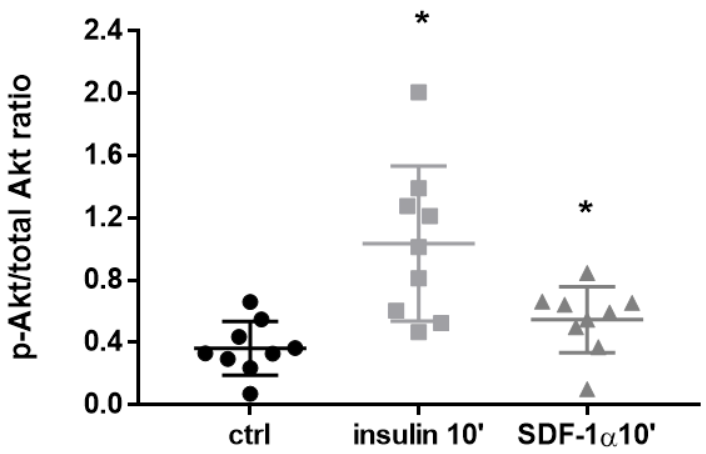

Figure 5-6: Effect of insulin and SDF-1α on AKT phosphorylation in HUVEC – pooled data. Administration of either SDF-1α (250 nM) or insulin (100 nM) significantly increased AKT phosphorylation response compared to control in HUVEC. Data were pooled from experiments in Figure 5-1 and Figure 5-4. Total AKT was used as a loading control. * $p < 0.05$ insulin vs control and SDF-1α vs control, Repeated Measures ANOVA with Dunnett's post-hoc test comparing all groups to control; n = 9 independent experiments per group.

In order to gain a clearer picture of the effects of insulin and SDF-1α on AKT phosphorylation, data concerning control, insulin and SDF-1α from western blotting experiments with VUF11207 and TC14012 from Figure 5-1 and Figure 5-4 were pooled together and presented in Figure 5-6. Statistical analysis revealed that administration of either insulin (100 nM) or SDF-1α (250 nM) 10 min before cell lysis significantly increased AKT phosphorylation compared to control. There was an approx. 3-fold increase in mean AKT phosphorylation response after administration of insulin and 1.5-fold increase after administration of SDF-1α, compared to control.

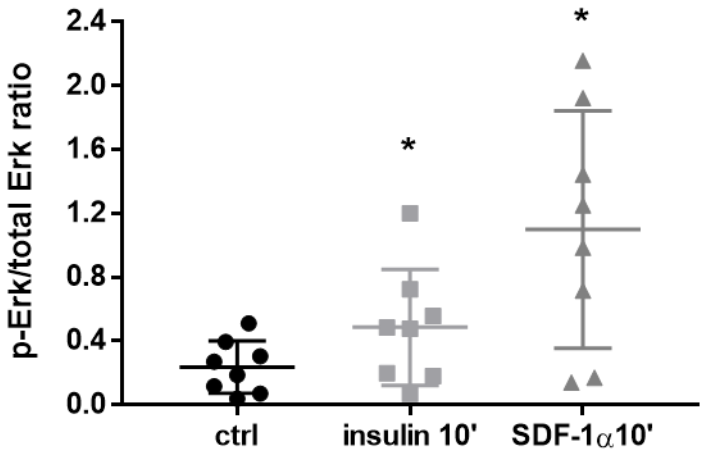

Figure 5-7: Effect of insulin and SDF-1α on ERK1/2 phosphorylation in HUVEC – pooled data. Administration of either SDF-1α (250 nM) or insulin (100 nM) significantly increased the ERK1/2 phosphorylation response compared to control in HUVEC. Data were pooled from experiments in Figure 5-2 and Figure 5-5. Total ERK1/2 was used as a loading control. * $p < 0.05$ insulin vs control and SDF-1α vs control, Repeated Measures ANOVA with Dunnett's post-hoc test comparing all groups to control; n = 8 independent experiments per group.

As in Figure 5-6, data in Figure 5-7 were also pooled from previous experiments already outlined in Figure 5-2 and Figure 5-5. Administration of insulin (100 nM) for 10 min prior to cell lysis significantly increased ERK1/2 phosphorylation response, which translated into a 2-fold increase compared to control. Similarly, administration of SDF-1α 10 min prior to cell lysis also induced a statistically significant increase in mean phosphorylation response of ERK1/2, which was approx. 4-fold greater when compared to control, although it exhibited a wide spread of data points and consequently a large standard error of the mean. Both, insulin and SDF-1α were able to induce a statistically significant induction of either AKT or ERK1/2 phosphorylation when values from all relevant experiments were collated.

5.5 Discussion

The RISK pathway is an important pro-survival pathway, utilized by many mechanical and pharmacological cardioprotective interventions [190, 194-196]. The parallel signalling cascades of PI3K/AKT and MEK1/ERK1/2 form the cornerstone of RISK pathway signalling. Consequently, measurement of the phosphorylation of these kinases can offer insight into whether or not a drug is able to induce RISK pathway signalling. To investigate the CXCR7-dependent activation of the RISK signalling pathway, CXCR7 agonists, VUF11207 and TC14012 were used in western blotting experiments in HUVEC. Positive controls, insulin and bradykinin significantly induced phosphorylation of AKT and ERK1/2, respectively. SDF-1α induced phosphorylation of ERK1/2, but not AKT, whereas VUF11207 and TC14012 did not induce phosphorylation of AKT or ERK1/2 at any timepoint tested.

SDF-1α-induced phosphorylation of ERK1/2 was examined in both, VUF11207 and TC14012 experimental sets. In both cases, the same experimental conditions were used; however, the obtained results differ between the two sets. There was a notable SDF-1α-dependent ERK1/2 phosphorylation, when SDF-1α (250 nM) was administered 10 min before cell lysis, in the set of western blotting experiments using VUF11207 (Figure 5-2), but not in the experimental set using TC14012 (Figure 5-5). In both cases, there was a large standard error present in the SDF-1α data set, showing a large degree of variability in the cell response. Statistical power of the TC14012 experimental set was adequate (97.5%) and should enable statistical detection of ERK1/2 phosphorylation changes. Having an adequately powered experiment reduces the probability of Type II error, and since sample size was lower in the TC14012 vs VUF11207 data set (n=3 vs n=5), this could have hindered detection of statistical significance [322, 323].

Furthermore, since HUVEC are primary cells, the reproducibility of results can vary from donor to donor. Even though commercially available HUVEC from pooled donors were used in our western blotting experiments, the inherent variability of HUVEC cannot be excluded as a possible reason for observed differences in obtained results. For that reason we have pooled data from control, insulin and SDF-1α from experimental sets including both, TC14012 and VUF11207 (Figure 5-7). Pooled data revealed that administration of insulin significantly increased induction of ERK1/2 phosphorylation. Since administration of insulin in our individual experiments displayed a relatively small effect size, pooling the data provided us with more statistical power and; therefore, enabled us to observe this effect, which would have likely gone unnoticed. Insulin-induced ERK1/2 phosphorylation observed in our pooled data has been described before as part of the MAPK arm of insulin signalling response with broad physiological implications [324, 325]. While an interesting observation, the role of insulin in RISK signalling, and more broadly, cardioprotection, goes beyond the scope of this thesis, where the primary role of using insulin was as a positive control for induction of AKT phosphorylation.

Pooled data also revealed significantly increased induction of ERK1/2 phosphorylation after administration of SDF-1α. Individual values obtained for SDF-1α-induced phosphorylation of ERK1/2 exhibited a wide spread of data points. This was in part counteracted by increasing the sample size by pooling data from separate VUF11207 and TC14012 experiments, which allowed us to show that administration of SDF-1α (250 nM) does induce ERK1/2 phosphorylation, which was statistically significant.

Our results agree with work published by others, showing that SDF-1α induces ERK1/2 phosphorylation in various cell types. Chen *et al*. showed ERK1/2 phosphorylation in cardiac stem cells stimulated with SDF-1α (100 ng/mL ~ 12.5 nM), which peaked after a 30 min incubation period [219].

Similarly, Laakko *et al*. showed that Jurkat T cells incubated with SDF-1α (20 ng/mL ~ 2.5 nM) for 5 min exhibit increased phosphorylation of ERK1/2 [326]. Additionally, a study by Zhuo *et al*. showed that SDF-1α (100 ng/mL ~ 12.5 nM) induces phosphorylation of ERK1/2 in lymphatic endothelial cells, which peaks 30 min after administration. This supports our findings that SDF-1α induces ERK1/2 phosphorylation, although altering the time of incubation might be crucial in achieving a maximum phosphorylation response, since both Chen's and Zhuo's group found peak phosphorylation response to occur 30 min after beginning of the incubation period. In our experiment, SDF-1α was administered in the absence of CXCR7 or CXCR4 inhibitors and activate RISK pathway signalling in endothelial cells. Therefore, ERK1/2 phosphorylation could have occurred as a consequence of either CXCR4 or CXCR7 activation. We have shown that SDF-1α is capable of eliciting a response through ERK1/2, but not AKT on endothelial cells, both important players in many signalling pathways. However, they also form a crucial part of the RISK cardioprotection signalling pathway, shared by many cardioprotective interventions.

In contrast, administration of SDF-1α (250 nM) did not induce phosphorylation of AKT in the experimental set using neither VUF11207 nor TC14012. Pooling the data from both experimental sets allowed us to increase the sample size, although it was clear that administration of SDF-1α did not induce phosphorylation of AKT. On the other hand, positive control insulin (100 nM) performed as expected and induced a significant AKT phosphorylation response showing that HUVEC have respond to stimuli as expected.

Our results do not agree with previously published work, where SDF-1α has been shown to induce phosphorylation of AKT in various cell types. Possible reasons for the discrepancies in obtained results are discussed below.

There are two key phosphorylation sites on AKT, namely Thr308 (Threonine 308) and Ser473 (Serine 473) with our research focused on Ser473, which can be found on the C-terminal hydrophobic motif of the AKT kinase [197, 327]. Chen *et al*. also examined phosphorylation of Ser473 on AKT kinase and found that SDF-1α (100 ng/mL ~ 12.5 nM) administration induced phosphorylation of AKT on cardiac stem cells, which peaked after 30 min of incubation [219]. Similarly, Shao *et al*. showed that administration of SDF-1α (100 ng/mL ~ 12.5 nM) for 5 min before cell lysis on bone marrow-derived cells induced phosphorylation of AKT; however the exact phosphorylation site investigated was not reported [328]. The investigated site of AKT phosphorylation, which is not always reported, could contribute to different results observed in AKT phosphorylation studies. Importantly, neither of the above studies used endothelial cells. The choice of cell type might be especially relevant in the case of cardiac stem cells, which are not terminally differentiated and display hugely different characteristics to differentiated cells, including a different transcriptomic profile and signalling ability [329]. The same is true for differences between our obtained results and those obtained by other in regards to ERK1/2 phosphorylation, with the exception of the site of phosphorylation. Site of phosphorylation is not an issue with ERK1/2 as the antibodies for phospho-ERK1/2 target the same two phosphorylation sites at Tyr204/187 (Tyrosine 204/187) and Thr202/185 (Threonine 202/185) [330]

When examining the activation of phospho-AKT in endothelial cells, Zhang *et al*. previously reported that SDF-1α (100 ng/mL ~ 12.5 nM) induced phosphorylation of AKT specifically in HUVEC cells [222]. However, they do not report the time of incubation or the phosphorylation site examined, which hinders any direct comparison with our study. Meanwhile, Zhuo *et al.* showed that SDF-1α (100 ng/mL ~ 12.5 nM) induced AKT phosphorylation in lymphatic endothelial cells with peak phosphorylation response present between 10 and 30 min post-administration [331]. They also do not report exactly which phosphorylation site they examined; however, their use of cells of endothelial origin seems to suggest that cell type is not the reason for the different results obtained by other groups and

ours. However, endothelial cells exhibit different phenotypes depending on their site of origin. While HUVEC are venous endothelial cells, it is arterial and capillary endothelial cells that might represent a more relevant cell type in the myocardium [332, 333]. There are not many commercially available cardiac endothelial cell lines and a specific subtype (e.g. arterial) of endothelial cells can be difficult to isolate. That is why HUVEC are a popular endothelial cell model; however, it is important to remember that their venous origins might not accurately reflect the *in vivo* state.

Additional reasons for varying results obtained by us and others, could also include the duration of cell starvation without serum, which is intended to reduce the basal signalling activity but is often not well reported in published literature [334]. In our study, the cells were starved for 3 h, whereas most other groups do not report whether the cells were starved or not [222, 331]. This could mean that the basal level of phosphorylation was different between various studies, making increases in phosphorylation response more or less difficult to identify.

Since our interests lay primarily in the CXCR7-dependent activation of RISK pathway, CXCR7 agonists VUF11207 and TC14012 were utilized to induce CXCR7 signalling in HUVEC. Administration of neither VUF11207 (100 nM and 250 nM) or TC14012 (30 µM) was able to induce phosphorylation of ERK1/2 or AKT in HUVEC. This disagrees with some of the already published data, previously discussed in section 1.4.2 and briefly outlined below.

SDF-1α incubation in the presence of CXCR4-blocking antibody has been shown to elicit maximal phosphorylation of ERK1/2 10 min post-administration on Jurkat T cells [220]. Additionally, Rajagopal *et al.* showed that HEK293 cells transfected with CXCR7 and stimulated with SDF-1α exhibited sustained ERK1/2 activation 30 min post administration[123]. This is in contrast with our results, where direct stimulation of CXCR7 via either VUF11207 or TC14012 did not induce phosphorylation of ERK1/2, despite the use of similar incubation time points.

Similarly, Kumar *et al.* showed that administration of SDF-1α on Jurkat T cells pre-treated with CXCR4-blocking antibody induced maximal phosphorylation of AKT 15 min after administration [220]. Additionally, Zhang *et al.* showed that activation of CXCR7 via administration of TC14012 (30 μM) in HUVEC induces phosphorylation of PI3K, but no time of incubation was discussed [222]. We did not observe an increase in AKT phosphorylation as a result of CXCR7 stimulation (via VUF11207 and TC141012). However, we have found that administration of SDF-1α alone was already incapable of eliciting an induction of AKT phosphorylation, which means that perhaps HUVEC used in this experimental setting are not capable of a response in the form of AKT phosphorylation. Due to that fact, it was not surprising that the two utilized CXCR7 agonists also did not elicit an induction of AKT phosphorylation.

Hao *et al*. decided on a slightly different approach to investigating the involvement of CXCR7 in signalling through PI3K/AKT and ERK1/2. They did not induce CXCR7 signalling directly, but instead they pre-incubated aortic endothelial cells with IL-1β, which increased CXCR7 mRNA levels. Incubation with IL-1β also mimics what happens after myocardial infarction *in vivo*, when IL-1β signalling is known to be active [335]. After, they used CXCR7-specific inhibitors to show that lack of CXCR7 signalling reduces phosphorylation of ERK1/2 and AKT. Since their study differs greatly from the one we performed, we cannot directly compare to our results; however, they show that CXCR7-dependent signalling through RISK pathway in endothelial cells does occur, at least in the presence of IL-1β.

The length of incubation with CXCR7 agonists, might also be important, since it is possible that a longer duration of receptor stimulation is needed to achieve β-arrestin-dependent signalling through CXCR7. Such intricacies of CXCR7 signalling are not well explored and based on available studies we cannot form a complete picture of what happens when a CXCR7 agonist binds to its receptor, or the exact impact that signal duration or concentration might exert on the CXCR4 and CXCR7 receptor signalling.

Recently, Gutkind and Kostenis, published an interesting short paper proposing that β-arrestins act as rheostats, modulating G protein-dependent signalling, but requiring G proteins for signalling through ERK1/2 [336]. In a classical model of G protein signalling, G proteins and β-arrestins compete for binding to the receptor, with G proteins initiating signalling and β-arrestins desensitizing the receptor by outcompeting the G proteins through steric hindrance. Gutkind and Kostenis present a plausible alternative hypothesis, which could help explain why CXCR7 stimulation is able to induce ERK1/2 signalling in some cases but not others [336]. They note that β-arrestins can be recruited to receptors without any detectable G protein activity, although this does not lead to successful ERK1/2 phosphorylation [336]. Perhaps something similar occurs with CXCR7-specific agonists, which are only able to signal through β-arrestin-biased CXCR7 receptor but fail to activate the G protein coupled CXCR4 receptors. To date, no studies explored the possibility of a similar connection between G proteins and arrestin-biased ligands in PI3K/AKT signalling; therefore, we cannot comment on the possibility of similar action occurring during AKT phosphorylation.

There is not a lot of published research investigating SDF-1α-dependent RISK pathway activation specifically in endothelial cells. However, RISK pathway, which includes activation of ERK1/2 MAPK kinase or PI3K/AKT pathway underpins many known acute cardioprotective interventions. Therefore, identifying whether CXCR7 agonists can elicit signalling through the RISK pathway can provide the first step towards identifying any acute cardioprotective effects the agonists might exhibit. We confirmed that SDF-1α is capable of inducing ERK1/2 phosphorylation response in endothelial cells; however, it was not able to elicit the same response in terms of AKT phosphorylation. Most importantly, neither CXCR7 agonist was able to induce phosphorylation of either ERK1/2 or AKT. This means that the ERK1/2 phosphorylation response seen with SDF-1α administration is more likely to come from interaction of SDF-1α and CXCR4, rather than SDF-1α and CXCR7 receptor. Based on work done by Hao et al. it seems that an initial stimuli, such as pro-inflammatory IL-1β, might need

to preclude CXCR7 signalling in order to initiate ERK1/2 and/or AKT phosphorylation. This might mean that basal state HUVEC, or indeed other endothelial cells, are not capable of RISK signalling response, which would need to be considered in further experimental approaches. Further work could therefore examine RISK signalling in endothelial cells that have undergone I/R injury, such as those, which could potentially be harvested from hearts undergoing a murine *ex vivo* heart perfusion experiment.

5.5.1 *Summary*

Positive controls insulin and bradykinin were able to successfully induce phosphorylation of AKT and ERK1/2 in HUVEC, respectively. While the increase in ERK1/2 phosphorylation in response to SDF-1α treatment was significant only in one of two experimental sets, it was again confirmed in the experimental set using pooled data from both sets of experiments. SDF-1α did not induce phosphorylation of AKT in either VUF11207 or TC14012 experimental set, nor when both data sets were pooled. Administration of CXCR7 agonists VUF11207 and TC14012 for various lengths of time also did not affect the phosphorylation status of either AKT or ERK1/2. All in all, VUF11207 and TC14012 were not able to initiate CXCR7-dependent RISK pathway signalling in HUVEC, under chosen experimental conditions. Further investigation is needed to confirm whether this occurred because CXCR7 does not signal through the RISK signalling pathway, or whether an adjustment of experimental conditions is needed to confirm CXCR7-dependent RISK pathway activation.

6 Unsuccessful endothelial-specific inducible Cxcr7 gene deletion with Pdgfb-CreER^{T2} in adult mice

6.1 Background

The ability to manipulate DNA sequence of an organism is an extremely valuable investigative tool in the arsenal of a scientist. Arguably the most famous mechanism for precision gene manipulation is the Cre-lox system, using a topoisomerase enzyme, Cre recombinase, which enables assessment of the importance of a specific gene by using *in vivo* genetic manipulation [337]. The Fruttiger group generated a Pdgfb-Cre construct, which is widely used by researchers and reportedly exhibits activity in aortic and capillary endothelial cells, with some non-endothelial cell activity recorded in keratinocytes and megakaryocytes [243, 338]. Platelet-derived growth factor beta (Pdgfb) plays an essential role in migration and proliferation of vascular smooth muscle cells, promotes differentiation of endothelial cells and participates in wound healing through recruitment of various cell types to the site of injury [339-341].

Fruttiger's group utilized the Pdgfb promoter in tandem with iCreER^{T2}, which is the improved, second generation CreER, efficient in initiating Cre recombination, and is currently the most successful version of Cre available [342]. Pdgfb-Cre line provided by the Fruttiger group has been previously successfully utilized to generate adult transgenic mice with endothelial-specific labelling of enhanced yellow fluorescent protein (EYFP), and was therefore deemed an appropriate line to use for our experiments [343].

In order to generate endothelial-specific transgenic mice we used Pdgfb-CreER^{T2} construct obtained from the Fruttiger group and Ackr3$^{tm1Twb\ flox/+}$ obtained from the MMRRC repository as described in section 2.2. [114, 243].

6.2 Research aims and objectives

Generate mice with inducible, endothelial-specific CXCR7 deletion:

- Characterize the mouse model by investigating endothelial CXCR7 RNA and protein content.

- Examine whether the mice exhibit the loss of endothelial CXCR7 protein.

6.3 Methods

In addition to the general methods described in Chapter 2, the following specific methods were used in the experiments described in this chapter.

6.3.1 *Transgenic animals*

$Cxcr7^{i\Delta EC}$ = $Cxcr7^{flox/flox}$ $Cre^{+/-}$ injected with Tamoxifen
$Cxcr7^{WT}$ = $Cxcr7^{flox/flox}$ $Cre^{+/+}$

Transgenic mice were generated as described in section 2.2. Experiments with $Cxcr7^{i\Delta EC}$ mice, were performed 3 weeks after the last tamoxifen injection. $Cxcr7^{WT}$ mice did not receive any injections.

6.3.2 *Western blotting*

The expression of CXCR7 was investigated in HUVEC, using western blotting methods described in section 2.5. Membranes were incubated with anti-CXCR7 rabbit monoclonal antibody (1:1000, ab138509, Abcam). Anti-GAPDH mouse monoclonal antibody (1:2000, ab8245, Abcam) was used as a loading control.

IRDye® 800CW goat anti-rabbit IgG (1:10,000, Li-COR), or IRDye® 680RD Goat anti-mouse IgG (1:10,000, LI-COR) secondary fluorescent antibodies were used for detection.

6.3.3 *WES western blotting*

The expression of CXCR7 was investigated on isolated mouse cardiac endothelial cells using WES western blotting method as described in section 2.5.4. Anti-CXCR7 rabbit monoclonal primary antibody (1:20, ab138509, Abcam) and anti-VDAC1 rabbit monoclonal antibody (1:50, ab154856, Abcam) were used in conjunction with rabbit antibody detection kit (ProteinSimple).

6.3.4 *RNAscope in situ hybridization*

RNAscope in situ hybridization experiment on whole mouse heart slices was performed as described in section 2.8. $Cxcr7^{i\Delta EC}$ mice used for RNAscope in situ hybridization were injected with 100 µL of 15 mg/mL tamoxifen for 3 consecutive days as described in section 2.2.5. Images of background staining for this experiment can be seen in Figure 3-2.

6.3.5 *Quantitative real-time PCR*

RNA extraction and quantitative real-time PCR were performed on aortas from male and female mice aged 8-12 weeks, as described in section 2.12.

6.4 Results

To examine whether endothelial-specific deletion of CXCR7 in mice was successful, several different experimental procedures were utilized. Firstly, western blotting was used to compare CXCR7 protein levels in whole mouse hearts between $Cxcr7^{WT}$ mice and genetically modified, tamoxifen injected $Cxcr7^{i\Delta EC}$ mice.

Tamoxifen administration was performed over 2 consecutive days, starting with 100 µL of 15 mg/mL of tamoxifen (2 mg/animal total) for 2 consecutive days, which did not affect CXCR7 protein levels in whole mouse hearts (Figure 6-1). Since the initial dose of tamoxifen was relatively low, the dose was increased for the subsequent experiments and injection days increased to 3 consecutive days.

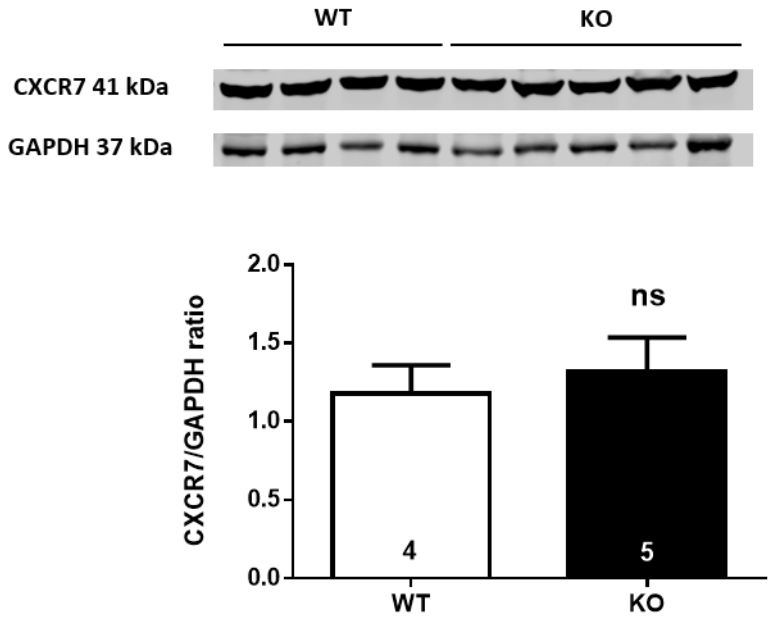

Figure 6-1: CXCR7 western blotting on Cxcr7^{WT} and Cxcr7$^{i\Delta EC}$ whole mouse hearts. Cxcr7$^{i\Delta EC}$ mice were injected with 100 µL of 15 mg/mL tamoxifen for 2 days (2 mg/animal total) to produce knockout mice. Wild type (Cxcr7^{WT}) mice received no injections. There was no significant difference between the CXCR7 protein levels of Cxcr7$^{i\Delta EC}$ and Cxcr7^{WT} mice. GAPDH was used as a loading control. Student's t-test, n = an individual mouse heart. KO = Cxcr7$^{i\Delta EC}$, WT = Cxcr7^{WT}, ns = non-significant.

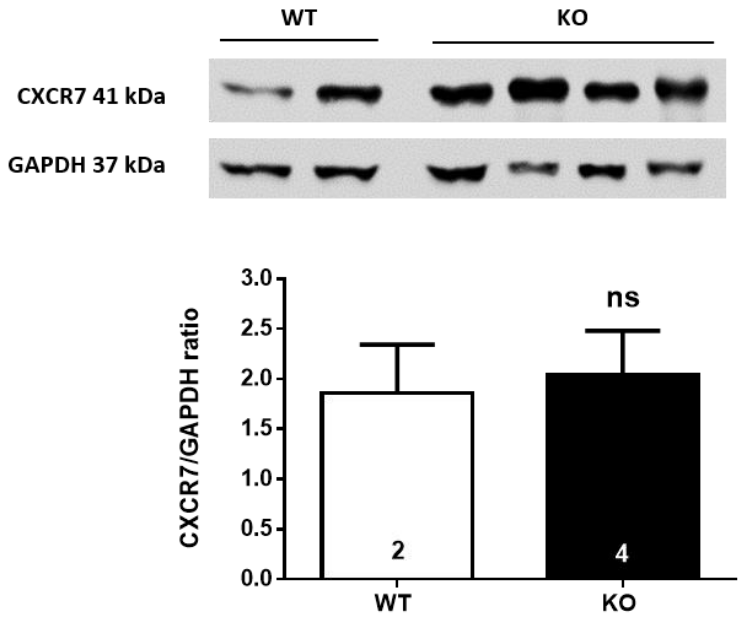

Figure 6-2: CXCR7 western blotting on Cxcr7^{WT} and Cxcr7$^{i\Delta EC}$ whole mouse hearts. Cxcr7$^{i\Delta EC}$ mice were injected with 100 µL of 15 mg/ml tamoxifen for 3 days (4.5 mg/animal total) to produce knockout mice. Wild type (Cxcr7^{WT}) mice received no injections. There was no significant difference between the CXCR7 protein levels of Cxcr7$^{i\Delta EC}$ and Cxcr7^{WT} mice. GAPDH was used as a loading control. Student's t-test, n = an individual mouse heart. KO = Cxcr7$^{i\Delta EC}$, WT = Cxcr7^{WT}, ns = non-significant.

Administration of 100 µL of 15 mg/mL tamoxifen (4.5 mg/animal total) for 3 consecutive days did not have a significant effect on CXCR7 protein levels in the whole mouse heart (Figure 6-2). The dose of tamoxifen was again increased to 100 µL of 20 mg/mL (6mg/animal total) and injected for 3 consecutive days. Following western blotting, CXCR7 levels in the whole mouse hearts were observed to be unchanged between the Cxcr7^{WT} and Cxcr7$^{i\Delta EC}$ mice (Figure 6-3). The bulk of the protein in whole mouse heart lysates comes from cardiomyocytes, which are large cells, in addition to vascular smooth muscle cells, fibroblasts and endothelial cells etc. It is possible that all of those cell types express CXCR7, making loss of CXCR7 expression in endothelial cells difficult to detect [43].

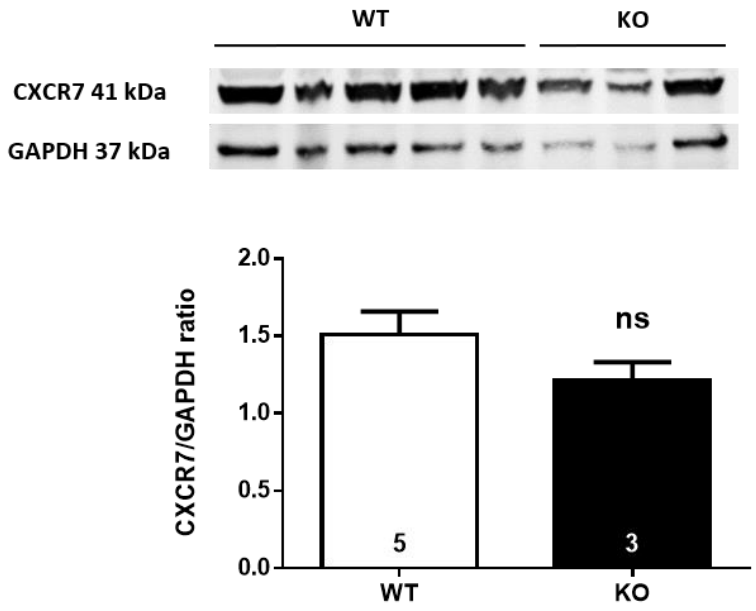

Figure 6-3: CXCR7 western blotting on Cxcr7^{WT} and Cxcr7$^{i\Delta EC}$ whole mouse hearts. Cxcr7$^{i\Delta EC}$ mice were injected with 100 µL of 20 mg/ml tamoxifen for 3 days (6 mg/animal total) to produce knockout mice. Wild type (Cxcr7^{WT}) mice received no injections. There was no significant difference between the CXCR7 protein levels of Cxcr7$^{i\Delta EC}$ and Cxcr7^{WT} mice. GAPDH was used as a loading control. Student's t-test, n = an individual mouse heart. KO = Cxcr7$^{i\Delta EC}$, WT = Cxcr7^{WT}, ns = non-significant.

Because it is challenging to isolate sufficient quantities of endothelial cells for standard western blotting, the WES automated western blotting system was used. In this system the samples are run and probed on small capillaries, allowing detection of bands using very small (~1 µg) quantities of protein. To determine whether CXCR7 protein was absent in mouse endothelial cells, WES automated blotting system was performed on isolated cardiac mouse endothelial cells, as previously described in section 2.5.4. This revealed no significant differences between the CXCR7 protein levels of Cxcr7^{WT} and Cxcr7$^{i\Delta EC}$ groups (Figure 6-4).

It was still challenging to obtain enough endothelial cells for robust analysis of CXCR7. CXCR7 should be deleted in all endothelial cells, not just in the heart; therefore, thoracic aortas were used to further examine whether endothelial CXCR7 deletion was successful.

Aortic tissue contains a higher ratio of endothelial cells to other cell types present in the tissue and should therefore provide a clearer picture of CXCR7 presence in endothelial cells [344]. Since investigation of CXCR7 protein levels revealed no differences between $Cxcr7^{WT}$ and $Cxcr7^{i\Delta EC}$ animals, CXCR7 RNA levels were also examined.

RT-qPCR for CXCR7 on $Cxcr7^{WT}$ and $Cxcr7^{i\Delta EC}$ mouse thoracic aortas did not reveal significant differences between the two groups based on their ΔCt values, where the smaller ΔCt denotes a higher CXCR7 RNA content (Figure 6-5). This translated into the 0.77-fold difference, which was not significant.

Aortas contain cells other than those of endothelial origin, which can impede the investigation of endothelial-specific CXCR7 gene deletion [344]. Therefore, RNAscope in situ hybridization was used to specifically and directly investigate endothelial-specific expression of CXCR7 RNA in whole mouse heart slices. $Cxcr7^{WT}$ tissues stained with CXCR7 RNA probe revealed CXCR7 RNA dots (white arrows) in IB4-delinated endothelial cells (Figure 6-6, upper panel). Interestingly, CXCR7 expression was mainly observed in endothelial cells, with lower levels of expression also present in other cell types (e.g. cardiomyocytes). Unfortunately, $Cxcr7^{i\Delta EC}$ tissues also revealed the presence of CXCR7 RNA dots in endothelial cells (yellow arrows), pointing to incomplete or unsuccessful endothelial-specific CXCR7 deletion (Figure 6-6, lower panel).

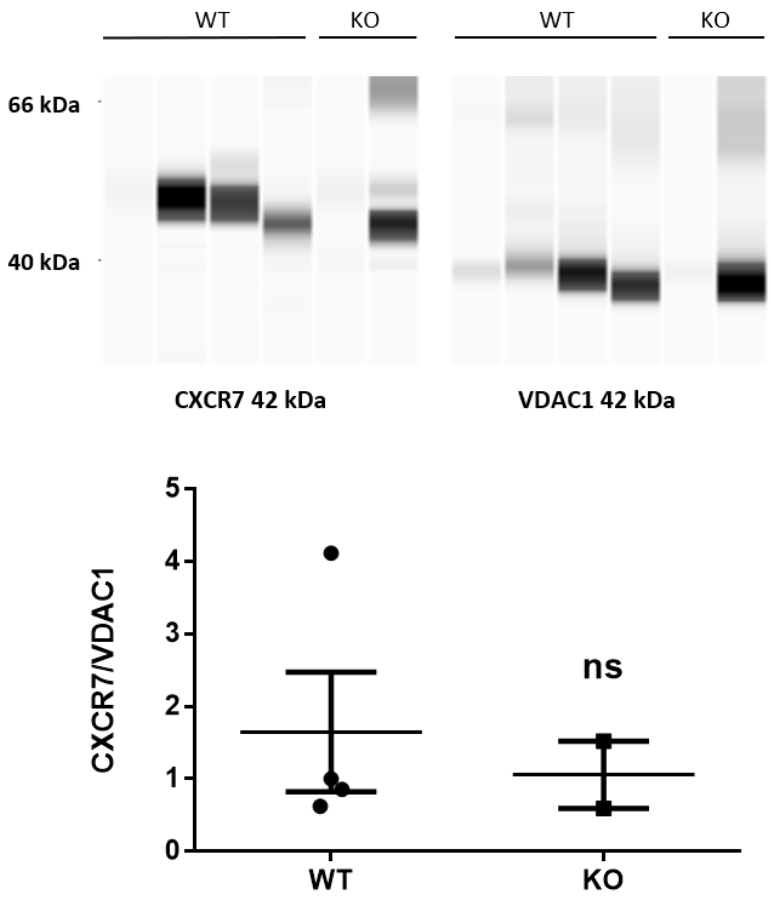

Figure 6-4: WES western blotting for CXCR7 on isolated mouse cardiac endothelial cells. $Cxcr7^{i\Delta EC}$ animals were injected with 100 µL of 15 mg/mL tamoxifen (4.5 mg/animal total) for 3 consecutive days to produce knockout animals. Despite some variability, there was no significant difference between the CXCR7 protein levels of $Cxcr7^{i\Delta EC}$ and $Cxcr7^{WT}$ mice. VDAC1 was used as a loading control. Note that in the WES automated blotting system, the protein samples run on individual capillaries, thus the position of the band can vary between "lanes". Student's t-test, n = a single cell isolation containing 2 - 4 mouse hearts. KO = $Cxcr7^{i\Delta EC}$, WT = $Cxcr7^{WT}$, ns = non-significant.

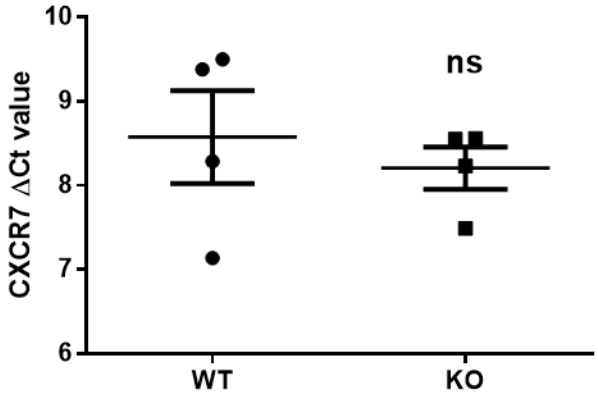

Figure 6-5: Quantitative real-time PCR for CXCR7 in mouse aortic tissue. Cxcr7$^{i\Delta EC}$ animals were injected with 100 µL of 15 mg/mL of tamoxifen for 3 consecutive days (4.5 mg total) to produce knockout animals. There was no significant difference detected in CXCR7 RNA content between the Cxcr7^{WT} and Cxcr7$^{i\Delta EC}$ mice. Gapdh and Hprt were used as housekeeping controls. Student's t-test, n = an individual mouse aorta. KO = Cxcr7$^{i\Delta EC}$, WT = Cxcr7^{WT}, ns = non-significant.

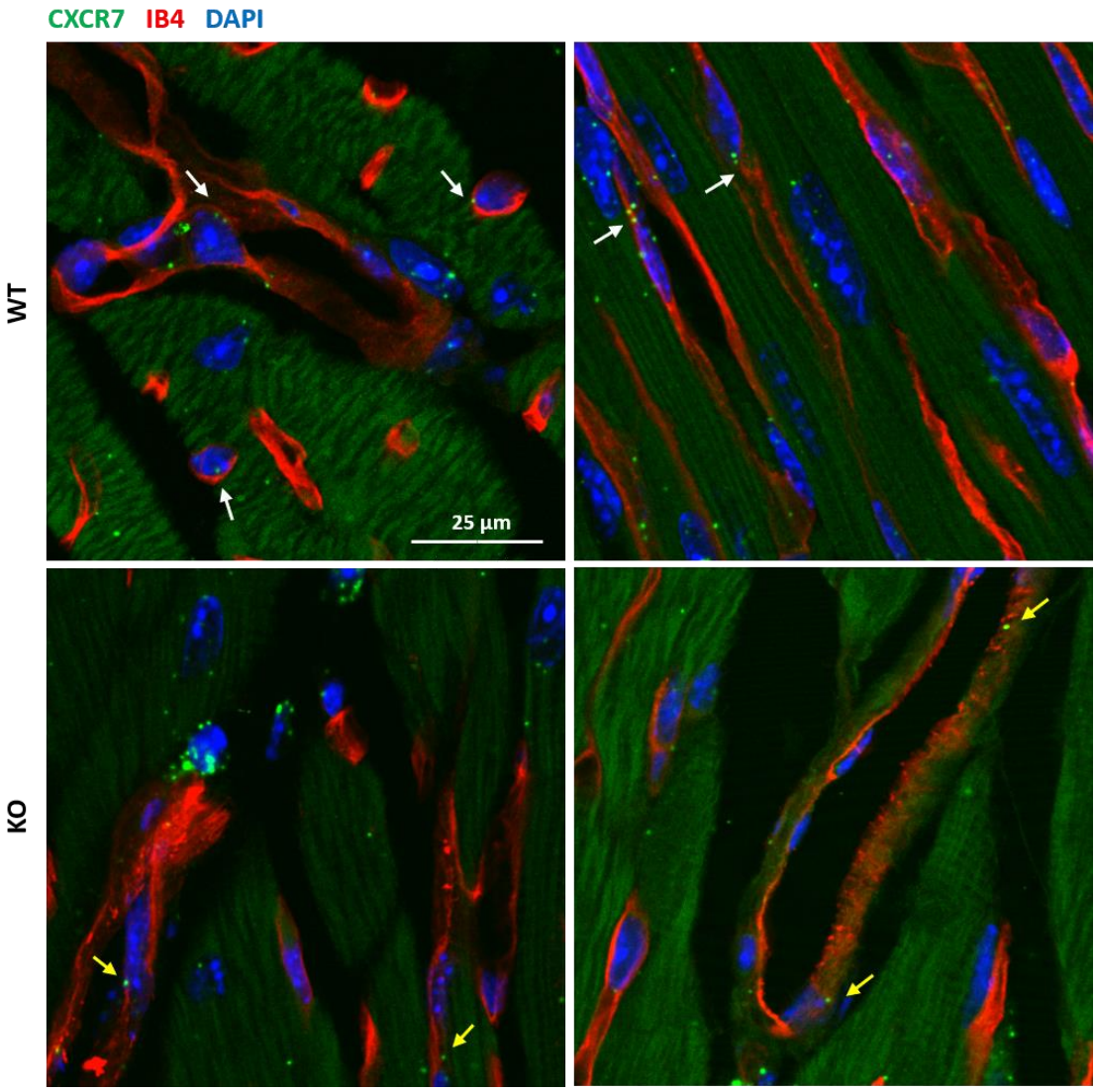

Figure 6-6: CXCR7 mRNA expression in Cxcr7^{WT} and Cxcr7$^{i\Delta EC}$ mouse whole heart slices. Cxcr7$^{i\Delta EC}$ animals were injected with 100 µL of 15 mg/mL tamoxifen (4.5 mg/animal total) for 3 consecutive days to produce knockout mice (Cxcr7$^{i\Delta EC}$). CXCR7 mRNA (green dots) is present in endothelial cells in wildtype (Cxcr7^{WT}, white arrows) and knockout (yellow arrows) adult mouse hearts as detected by RNAscope in situ hybridization. IB4 (red) was used to label endothelial cells and DAPI (blue) depicts cellular nuclei. Left and right panels show alternative regions of the same tissue slice. KO = Cxcr7$^{i\Delta EC}$, WT = Cxcr7^{WT}.

6.5 Discussion

The overall strategy behind the Cre-lox system is to employ site-specific recombination, which allows for genetic deletion of the target gene or sequence. It is a robust system, and successful recombination depends on both the Cre recombinase and the loxP sites performing their intended function. However, if the function of either element is impaired, it will result in incomplete or unsuccessful manipulation of the target gene.

After breeding several generations of $CXCR7^{i\Delta EC}$ mice, we did not observe endothelial-specific CXCR7 deletion using several different techniques. Western blotting examination revealed unchanged levels of CXCR7 protein when comparing $Cxcr7^{WT}$ and $Cxcr7^{i\Delta EC}$ animals. Similarly, RT-qPCR and RNAscope in situ hybridization showed that CXCR7 mRNA was still present in endothelial cells of $Cxcr7^{i\Delta EC}$ animals.

Western blotting of whole mouse heart tissue showed no changes between CXCR7 protein expression in $Cxcr7^{WT}$ and $Cxcr7^{i\Delta EC}$ mice. The initial dose of tamoxifen was set at 2 mg per animal total, as it is desirable to use the lowest dose of tamoxifen possible, due to its potential toxic side effects at higher doses [345]. Since this comparatively low dose of tamoxifen could have been the reason why CXCR7 protein levels persisted unchanged, tamoxifen dose was subsequently increased to 4.5 mg per animal total. Since this dose of tamoxifen also had no effect on the CXCR7 protein levels it was again raised to 6 mg of tamoxifen total. However, this also had no effect on the CXCR7 protein levels, which were not significantly different between $Cxcr7^{WT}$ and $Cxcr7^{i\Delta EC}$ animals. The dose of tamoxifen required for a successful initiation of Cre-mediated gene deletion via i.p. injection was derived from previously conducted experiments in our own lab and from published literature using the same strain of Pdgfb-$CreER^{T2}$ mice in which the target gene had been successfully deleted [343, 346].

Therefore, it is unlikely that a low concentration of tamoxifen is the reason for unsuccessful Cre recombination, and subsequently reduction of endothelial CXCR7 protein levels. Additionally, the i.p. route of tamoxifen dosing is a well-established and commonly used route and is unlikely that choosing this particular method over a different administration technique (e.g. oral gavage) played a part in the failure to achieve endothelial CXCR7 protein deletion.

Despite being a great tool to initiate Cre recombination, tamoxifen can be toxic, especially with repeat administration or in high doses. The toxicity exhibited by tamoxifen is seen in both sexes, and with both, oral and i.p. administration. We observed an approx. 10% mortality rate, which was not affected by the number of days of tamoxifen injections, although the highest tamoxifen dose of 20 mg/mL (6 mg per animal total) did exhibit a larger mortality rate of approx. 15% and was therefore not utilized beyond the initial experiments.

Huh *et al*. showed that tamoxifen toxicity (5 mg tamoxifen/ 20 mg body weight, 3 consecutive days) can be abolished by proton pump inhibition with omeprazole, which points at modulated acid secretion as the likely contributor to tamoxifen-associated toxicity [347]. Jahn *et al*. reports tamoxifen-associated mortality as 3.7% for 3 consecutive days of injection; however, the skill of the handler is also known to affect the mortality rate [345]. Furthermore, mortality rate of tamoxifen, although known, is often not reported which precludes us from making a more informed observation on whether our mortality rate was abnormal compared to that seen by others. There is a small possibility that tamoxifen at sufficiently high dose to activate Cre recombinase (6 mg/animal total) killed the mice, while in surviving mice and those with lower level of injected tamoxifen Cre was not induced and therefore CXCR7 loss could not be detected. Similarly, if endothelial CXCR7 deletion in adults is lethal, then the surviving mice would not exhibit detectable CXCR7 loss. However, both of these possibilities are unlikely to have occurred in our transgenic model.

It is also important to note that whole mouse heart tissue contains cells of non-endothelial origin that express CXCR7, which could hinder detection of CXCR7 protein changes on the endothelial level. For example, CXCR7 mRNA was found to be expressed in human fibroblasts, and CXCR7 protein and mRNA were detected in rat vascular smooth muscle cells [123, 267]. Further, CXCR7 mRNA was also shown to be expressed in mouse cardiomyocytes, as previously shown by us in section 3.4. and elsewhere [148]. The cumulative CXCR7 protein content of these non-endothelial cells could have obstructed detection of endothelial-specific CXCR7 changes, which means that it might be difficult to detect deletion of endothelial CXCR7 on the level of whole mouse heart.

For that reason, CXCR7 protein content was also assessed in isolated endothelial cells via WES western blotting method, which enables detection of protein level changes even in small protein samples. WES did not reveal any significant differences between the CXCR7 protein levels of $Cxcr7^{WT}$ and $Cxcr7^{i\Delta EC}$ mice. Despite a low sample size of $Cxcr7^{i\Delta EC}$ cells (n=2) , the observed standard error in both, $Cxcr7^{WT}$ and $Cxcr7^{i\Delta EC}$ mice, were such that altering the n number would perhaps have an effect on the statistical outcome of the experiment; however, we chose to examine endothelial CXCR7 expression with other methods (e.g. qPCR). Combined, western blotting experiments in whole mouse heart tissue and isolated endothelial cells point to unsuccessful deletion of endothelial CXCR7 gene.

Since protein content in endothelial cells persisted unchanged despite increasing the concentrations of tamoxifen, I examined more directly if CXCR7 mRNA was still present after tamoxifen administration. Ideally, isolated endothelial cells would have been used for this experiment; however, obtaining samples of isolated cells that were suitable for a successful qPCR experiment was challenging. Instead, thoracic aorta tissue was used to assess cellular mRNA levels.

Again, there was no difference observed between $Cxcr7^{WT}$ and $Cxcr7^{i\Delta EC}$ animals. However, like whole mouse heart tissue, aortic tissue also contains non-endothelial cell types, which could obstruct determination of endothelial-specific

CXCR7 deletion. For example, vascular smooth muscle cells that make up a large portion of aortic vessel wall, and fibroblasts, which can be found in the outer layer of the aortic vessel wall, both express CXCR7 [123, 267]. RNAscope in situ hybridization in combination with IB4 labelling was used to determine the presence of CXCR7 mRNA specifically in endothelial cells. Unsurprisingly, there was no difference between the $Cxcr7^{WT}$ and $Cxcr7^{i\Delta EC}$ mice, with both displaying CXCR7 mRNA dots in endothelial cells positively labelled with IB4. Interestingly, expression was mostly localized within EC suggesting that previous western blotting experiments should have been able to detect any reduction in CXCR7 expression if it had been decreased.

$Cxcr7^{WT}$ and $Cxcr7^{i\Delta EC}$ animals consistently displayed comparable levels of CXCR7 on protein and mRNA level, an indication of an unsuccessful CXCR7 gene excision/deletion. In summary, a combination of experiments investigating endothelial CXCR7 protein and mRNA changes showed that target gene deletion had not occurred, and endothelial cells continued to express CXCR7 protein. This could have occurred due to a variety of reasons. For example, the parent-of-origin effect, whereby the sex of the parent with a specific allele can have an effect on the expression of that gene, is known to occur in certain Cre driver lines [348, 349]. Additionally, Gallardo *et al*. and Hayashi *et al*. reported maternal Cre excision patterns that were different than those inherited paternally, for their respective Cre driver lines [350, 351]. Seeing as a functioning Cre recombinase is crucial for target gene deletion, any modification in expression of Cre recombinase could result in unsuccessful deletion of endothelial CXCR7 in our mouse model. This could have been verified by experiments to measure expression levels of Cre.

Other recombination anomalies, such as mosaic or inconsistent gene deletion and deletion in off-target tissues are also known to occur [352-354]. Additionally, Cre gene expression inconsistency between littermates is also possible, and variability in Cre expression has been shown in certain endothelial and haematopoietic Cre

driver lines [349, 355]. These gene expression anomalies can be difficult to detect, and such knowledge can become anecdotally known in specific labs, but it is rarely followed by a detailed characterization of a Cre driver line and is not commonly disseminated to a wider audience.

Cre protein is expressed and present in the cell cytoplasm until after the injection of tamoxifen, when it translocates into the nucleus and initiates Cre recombination at the loxP sites [342]. This attribute of Cre recombinase would enable us to check whether endothelial cells are the ones expressing Cre by using an anti-Cre antibody via a technique such as western blotting or immunohistochemistry. However, we know from personal correspondence with Kirsty Naylor and Prof. Christiana Ruhrberg (University College London, UK) that this particular Cre is indeed expressed in endothelial cells obtained from Cre transgenic mice. Furthermore, the Cre construct used in our experiments contains an EGFP element, which can also be used to assess the expression of Cre in target tissues. If EGFP can be detected in endothelial tissue of Cre-positive mice, then Cre recombinase is expressed in those tissues. Furthermore, to determine whether successful Cre recombination has taken place in target tissues, mice can be injected with tamoxifen and their target tissue genotyped for the presence of the recombined allele.

Experiments described above would inform us on whether Cre was successfully expressed in target tissues and the ability of said Cre recombinase to initiate loxP site recombination in those tissues. Additionally, we could have also utilized primers to distinguish a recombined (knockout) vs floxed allele, which would reveal directly whether Cxcr7 has been successfully excised in target tissues.

We would achieve that by designing primers that bind upstream and downstream of respective loxP sites surrounding exon 2 of the Cxcr7 gene. This would mean that when running a PCR, a floxed allele would produce a larger product and a recombined allele a shorter product, since the exon 2 of Cxcr7 would no longer be present in the target tissue of the mouse with a successfully recombined allele,

providing us with a clear-cut way to investigate whether our target sequence was successfully excised.

Mouse lines that were inbred for a significant number of generations over a long period of time can also accumulate mutations, leading to genetic drift [356]. Genetic drift refers to spontaneous changes occurring in genomic DNA, and can have an effect on the mouse phenotype [356]. The mice used in our experiments were not an inbred strain, which decreased the probability of genetic drift. Inbred mice are brother-sister mated for more than 20 generations and a small, spontaneous DNA mutation can have a significant impact on their genetic makeup, due to their genetic uniformity [356]. Mice that are not inbred or are regularly backcrossed to a relevant genetic background accumulate genetic changes at a slower rate and are not as susceptible to the occurrence of spontaneous DNA mutations [357]. Nevertheless, there is still a possibility that a critical mutation could have occurred in this time period. For example, in the event that the mutation was at or near a loxP site, the ability to excise the CXCR7 exon flanked by loxP sites could be lost. It could have been interesting to perform genomic sequencing on genetic material obtained from colony founders and later generations of mice to investigate if such mutations have indeed occurred.

Moreover, the distance between loxP sites can also have an impact on the success rate of Cre recombination, since the longer the distance the more difficult the DNA sequence can be to recombine [358]. However, the loxP sites in our mice were <1000 bp apart (as confirmed by PCR), which is far shorter than the >20,000 bp sequences that have previously been reported as challenging to recombine [359].

Most papers report favorable recombination efficiency with a comparable distance between loxP sites and it seems unlikely for this to be the reason why endothelial CXCR7 gene expression persisted in our transgenic mouse model [360].

Ultimately, the most likely reason for unsuccessful deletion of CXCR7 gene in endothelial cells rests with the actual Pdgfb-Cre driver line itself. Pdgfb is known to exhibit the highest level of expression in the endothelial tip cells, which lead sprouting vessels during development, while stalk cells, which form most of the trunk of the sprouting vessel, are known to express less [361]. Consequently, using the Pdgfb-Cre driver will result in different subpopulations of endothelial cells (e.g. stalk cells) exhibiting varying levels of Cre recombinase activity.

Furthermore, Claxton *et al*. report that in these mice certain large vessels such as the dorsal aorta do not exhibit Cre recombinase activity at P1 [243]. Since dorsal aorta later develops into parts of descending aorta, it is possible that this lack of Cre activity affects a large portion of mouse aorta (used in our characterization experiments), which would prevent CXCR7 gene deletion in the vessel from occurring [243]. It is also important to note that most of their model characterization was performed on pups with the majority of focused placed on endothelial cells found within developing vessels. Additionally, when Cre recombination was induced in the retinal plexus of an adult animal as opposed to a pup, recombination was seen to occur only in a small subpopulation of cells [243]. It is possible that this extends beyond the retina to other vascular beds, which would make Pdgfb unsuitable as an endothelial Cre driver line in adult mice and more suitable for investigating endothelial cells during blood vessel development. However, in my experiments, expression of Cre was not investigated, and therefore it is not known whether Cre was actively expressed in target tissues. The hypothesis that Pdgfb-Cre is more suitable to use in pups could have been tested by investigating CXCR7 endothelial-cell deletion in adults and pups injected with tamoxifen.

If pups injected with tamoxifen displayed successful deletion of CXCR7 in a large population of endothelial cells, but not adult mice, then it is likely that age of mouse at tamoxifen injection is important for successful deletion of CXCR7 in endothelial

cells. Further work is needed to validate these hypotheses, and asses the suitability of Pdgfb-Cre in adult inducible transgenic mouse models.

Therefore, for researchers hoping to use an endothelial-specific Cre driver line for generating adult transgenic mice, I would recommend one of the well-researched vascular cadherin 5 (Chd5) Cre driver lines, since Chd5 is expressed in all endothelial cells, and its Cre constructs exhibit good rates of recombination [338].

6.5.1 *Summary*

Western blotting, qPCR and RNAscope in situ hybridization revealed that CXCR7 protein and mRNA levels continued to be detected in endothelial cells of the heart and aorta of $Cxcr7^{i\Delta EC}$ animals. Expression of CXCR7 mRNA and protein in $Cxcr7^{i\Delta EC}$ cells was quite robust and comparable to the levels observed in $Cxcr7^{WT}$ mice. It is therefore possible that endothelial-specific CXCR7 gene deletion was unsuccessful. Based on the paper by Claxton *et al*., the Cre recombination activity of Pdgfb-Cre line is far superior in neonatal mice, while Cre recombination activity, when induced in adult mice is poor and limited to a small subpopulation of cells [243]. Therefore, an alternative Cre driver line (e.g. Chd5) should be considered for future transgenic models with endothelial-specific inducible CXCR7 deletion in adult mice.

7 Examining the effect of VUF11207 and TC14012 on endothelial cell migration

This chapter contains work that was carried out in collaboration with Kaloyan Takov, who provided two experimental repeats for Figure 7-4.

7.1 Background

Angiogenesis is a crucial physiological process, which enables formation of new vessels from pre-existing vasculature and is described in more detail in section 1.2.2 [362]. Along with its role in vascular development, angiogenesis is also involved in many pathological processes, such as diabetic retinopathy and wound healing [363, 364]. It consists of different stages of vessel formation, one of which is cell migration. However, angiogenesis as a whole, and specifically cell migration require a trigger, which can be either mechanical, chemical or in the form of an immobilized ligand [62-67].

SDF-1α has previously been shown as a pro-angiogenic factor capable of stimulating endothelial cell migration [62, 365]. However, there is limited data available regarding CXCR7-dependent cell migration since most studies either focused on the CXCR4 receptor or did not differentiate between the two [366, 367]. Therefore, we wanted to examine the role of CXCR7 in endothelial cell migration *in vitro*, for which CXCR7 agonist TC14012 and VUF11207 were used in a multiwell Boyden chamber assay. CXCR7 agonists used for cell migration experiments were previously described in detail in section 1.3.3.

7.2 Research aims and objectives

Investigate the effects of CXCR7 agonists on HUVEC migration:

- Examine the effects of CXCR7 agonists, VUF11207 and TC14012 on HUVEC migration via Boyden chemotaxis chamber.

7.3 Methods

In addition to the general methods described in Chapter 2, the following specific methods were used in the experiments described in this chapter.

7.3.1 *Cell culture*

HUVEC were cultured as previously described in section 2.3. Prior to the experiment, HUVEC were serum-starved for 3 h with DMEM medium (Gibco) supplemented with penicillin/streptomycin (Gibco). HUVEC were used in the experiment between passages 5-8.

7.3.2 *Cell treatments with VUF11207 and TC14012*

HUVEC were cultured as described in section 2.10. At the beginning of the experiment VUF11207 (100 nM, 1 µM, 30 µM), SDF-1α (100 nM), TC14012 (1 µM, 10 µM, 30 µM), TC14012 (1 µM) + SDF-1α (100 nM), PBS alone or 10% FBS diluted in PBS were added to the migration chamber for the duration of the experiment. For experimental sets containing TC14012, DMSO (<0.05% final conc.) was added to all treatments. All individual migration experiments were normalized to 10% FBS.

7.3.3 *Cell migration analysis*

After the conclusion of the experiment, blots were stained with 0.5% crystal violet as described in section 2.10 and visualized with LiDE 210 Canon scanner. Each sample was assayed in duplicate. Obtained images were analysed using ImageJ software.

7.4 Results

To investigate whether CXCR7 agonists, VUF11207 and TC14012 stimulate migration of HUVEC, a series of cell migration experiments were performed. As shown in Figure 7-1, administration of SDF-1α (100 nM) or VUF11207 at various concentrations did not significantly increase cell migration after a 6 h migration experiment in HUVEC.

Based on previously published data and observed lower variation in cell response, the duration of cell migration was shortened to 3 h and the above experiment repeated [368, 369]. As seen in Figure 7-2, SDF-1α (100 nM), but not VUF11207 (100 nM – 30 µM), significantly increased HUVEC cell migration compared to control (SDF-1α vs ctrl = 79.1 ± 13.3 % vs 45.6 ± 7.6 %, $p < 0.01$). However, no effects on migration were seen with VUF11207.

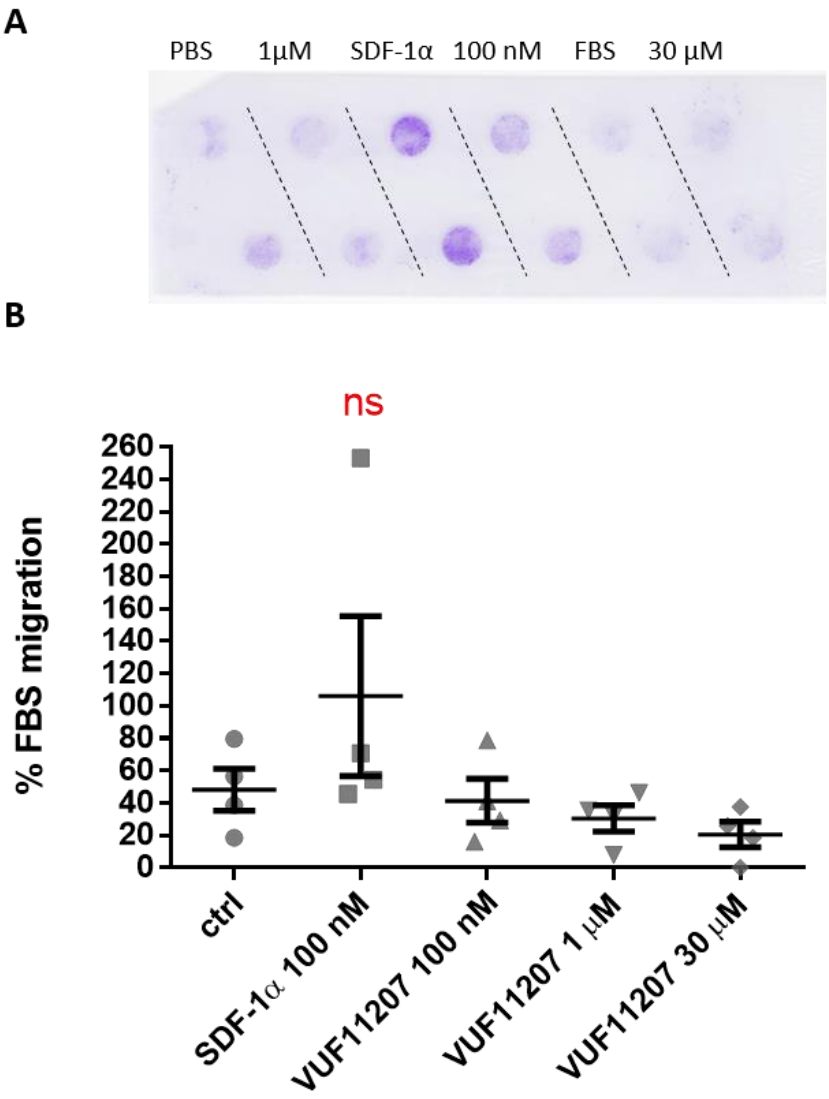

Figure 7-1: The effect of VUF11207 on 6 h cell migration in HUVEC. Cells were treated with SDF-1α or VUF11207 at the beginning of the experiment and allowed to undergo cell migration for 6 h**.** None of the treatments significantly increased cell migration compared to control. A.) Representative image of cell migration membrane stained with 0.5% crystal violet. VUF11207 is listed only as respective concentrations. B.) Quantification of cell migration. Results were normalized to 10% FBS. One-way ANOVA with Dunnet's post-hoc test with all groups compared to control, all comparisons were non-significant; n = 4 individual migration experiments. Ns = non-significant.

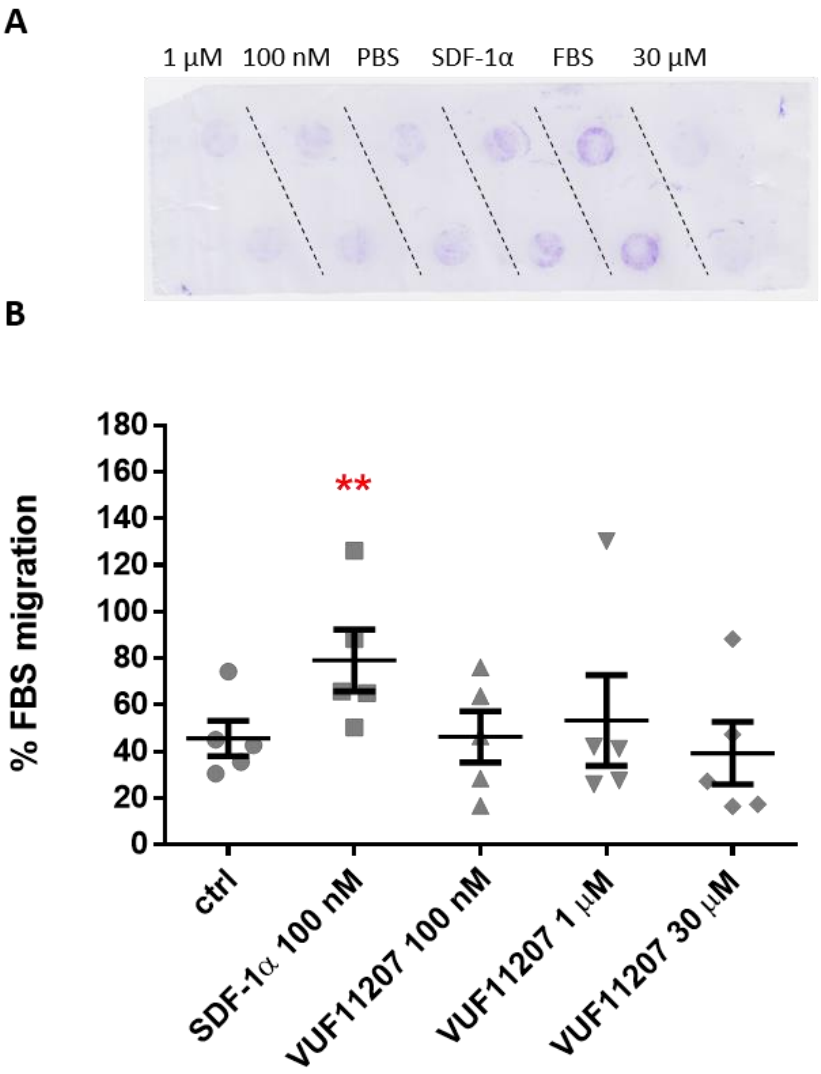

Figure 7-2: The effect of VUF11207 on 3 h cell migration in HUVEC. Cells were treated with SDF-1α or VUF11207 at the beginning of the experiment and allowed to undergo cell migration for 3 h**.** Administration of SDF-1α (100 nM) significantly increased cell migration compared to control. A.) Representative image of cell migration membrane stained with 0.5% crystal violet. VUF11207 is listed only as respective concentrations. B.) Quantification of cell migration. Results were normalized to 10% FBS. ** $p < 0.01$ SDF-1α 100 nM vs ctrl, One-way ANOVA with Dunnet's post-hoc test with all groups compared to control; n = 5 individual migration experiments.

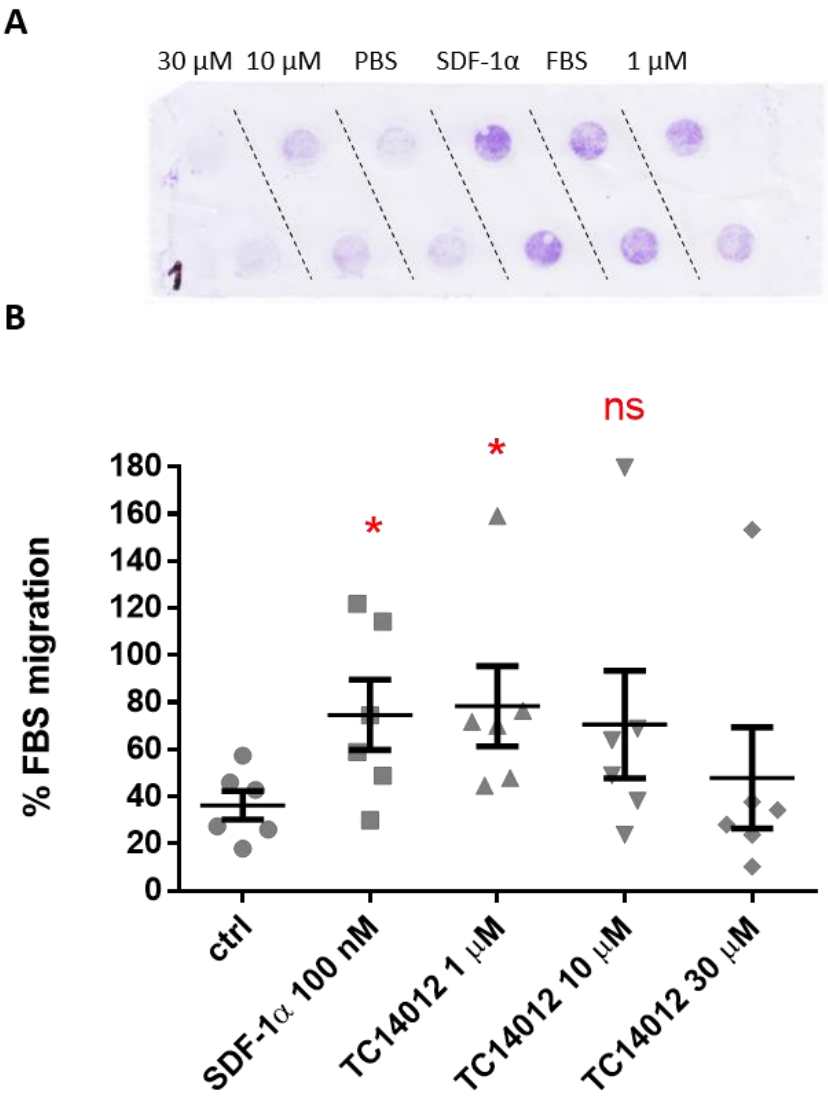

Figure 7-3: The effect of TC14012 on cell migration in HUVEC. Cells were treated with SDF-1α or TC14012 at the beginning of the experiment and allowed to undergo cell migration for 3 h**.** Administration of SDF-1α (100 nM) or TC141012 (1 µM) significantly increased cell migration compared to control. A.) Representative image of cell migration membrane stained with 0.5% crystal violet. TC14012 is listed only as respective concentrations. B.) Quantification of cell migration. Results were normalized to 10% FBS. * $p < 0.05$ SDF-1α 100 nM vs ctrl, TC14012 1 µM vs ctrl, One-way ANOVA with Dunnet's post-hoc test with all groups compared to control; n = 6 individual migration experiments. Ns = non-significant.

In order to confirm the above experiments, an alternative CXCR7 agonist, TC14012, was tested in a new set of experiments using 3 h cell migration. Here, SDF-1α (100 nM) significantly increased HUVEC migration (Figure 7-3) compared to control, as expected (SDF-1α vs ctrl = 74.7 ± 14.9 % vs 36.3 ± 6.1 %, $p < 0.05$). Similarly, administration of TC14012 (1 µM) resulted in a significant increase in HUVEC migration, compared to control (TC14012 vs ctrl = 78.4 ± 17.0 % vs 36.3 ± 6.1 $p < 0.05$). Higher concentrations of TC14012 (10 µM and 30 µM) had no effect on HUVEC migration.

Since both TC14012 and SDF-1α exhibited pro-migratory effects, we wanted to test whether a combination of both drugs would further increase HUVEC migration compared to each drug administered alone (Figure 7-4). Co-incubation of SDF-1α (100 nM) and TC14012 (1 µM) significantly increased HUVEC migration compared to control (SDF-1α + TC14012 vs ctrl = 109.5 ± 12.7 % vs 41.0 ± 5.8 %, $p < 0.01$). The additive cell migration effect was also significant when compared to TC14012 (1 µM) administered alone (SDF-1α + TC14012 vs TC14012 = 109.5 ± 12.7 % vs 69.5 ± 8.5 %, $p < 0.05$), but not when compared to SDF-1α (100 nM) administered alone. In contrast, incubation of either SDF-1α (100 nM) or TC14012 (1 µM) alone did not significantly increase HUVEC migration in this experiment.

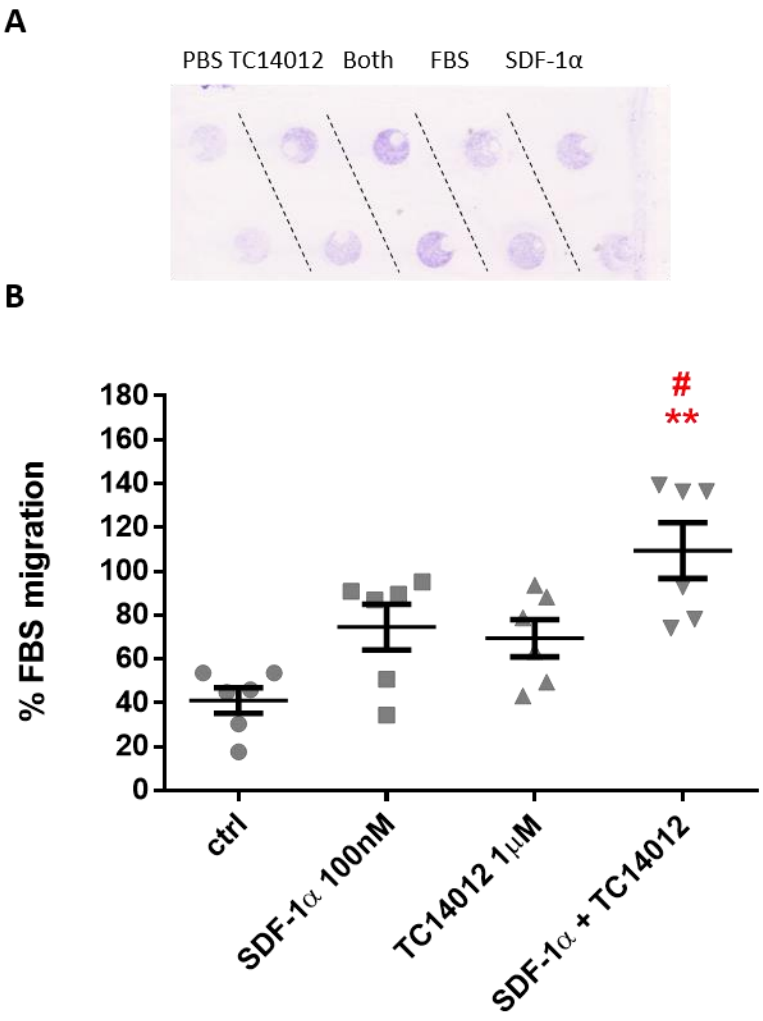

Figure 7-4: The effect of TC14012 + SDF-1α on cell migration in HUVEC. Cells were treated with SDF-1α, TC14012 or a combination of both at the beginning of the experiment and allowed to undergo cell migration for 3 h**.** Administration of SDF-1α (100 nM) + TC14012 (1 μM) significantly increased cell migration compared to control. SDF-1α (100 nM) or TC14012 (1 μM) administered on their own did not significantly increase HUVEC migration compared to control. A.) Representative image of cell migration membrane stained with 0.5 % crystal violet. B.) Quantification of cell migration. Results were normalized to 10% FBS. ** $p < 0.01$ SDF-1α + TC14012 vs ctrl, # $p < 0.05$ SDF-1α + TC14012 vs TC14012, One-way ANOVA with Tukey's post-hoc test comparing all groups to each other; n = 6 individual migration experiments.

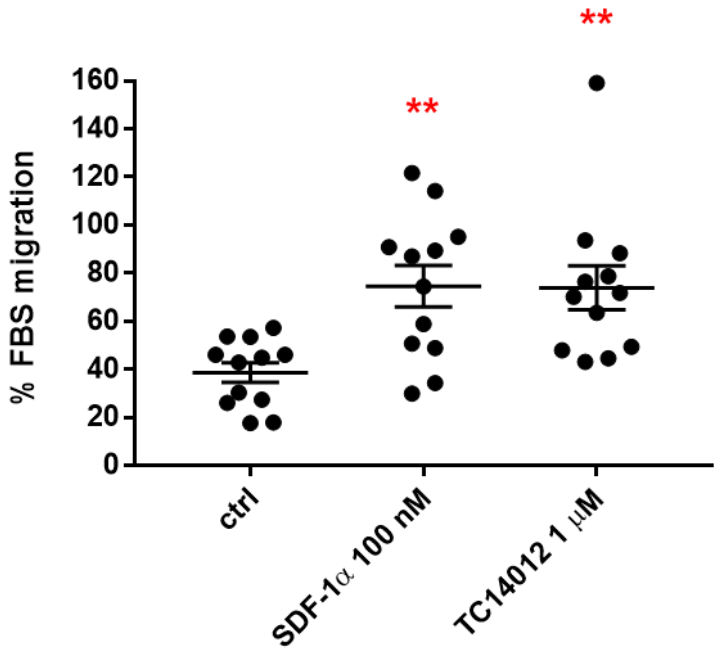

Figure 7-5: The effect of TC14012 and SDF-1α on cell migration in HUVEC - pooled data. Cells were either treated with SDF-1α (100 nM) or TC14012 (1 μM) at the beginning of the experiment and allowed to undergo cell migration for 3 h. Administration of either SDF-1α or TC14012 significantly increased cell migration compared to control. Data were pooled from experiments presented in Figure 7-3 and Figure 7-4. Results were normalized to 10% FBS. ** $p < 0.01$ SDF-1α vs ctrl and TC14012 vs ctrl, One-way ANOVA with Tukey's post-hoc test comparing all groups to each other; n = 12 individual migration experiments.

Administration of neither SDF-1α, nor TC14012 was able to consistently generate a significant increase in HUVEC cell migration in previous experiments. Therefore, we pooled data from two experiments utilizing comparable methodology (Figure 7-3 and 7-4), in order to increase the n numbers and show more definitively whether SDF-1α (100 nM) or TC14012 (1 μM) are capable of inducing cell migration. Separate administration of either SDF-1α or TC14012 significantly increased mean HUVEC cell migration when compared to control (SDF-1α vs ctrl = 74.6 ± 8.7 % vs 38.6 ± 4.7 %, $p < 0.01$; TC14012 vs ctrl = 73.9 ± 9.2 % vs 38.6 ± 4.7 %, $p < 0.01$). Based on the pooled data, both SDF-1α and TC14012, act in a pro-migratory fashion in our experimental model.

7.5 Discussion

Following the discovery of CXCR7 as an alternative receptor for SDF-1α, it was postulated that, like CXCR4, it plays an important role in a variety of physiological processes. Since SDF-1α is a known chemotactic factor, which participates in vessel regeneration, tumour cell migration, and homing of HSC and other stem cell types, a clear hypothesis was that CXCR7 is also involved in some, if not all of these processes [370-373]. With increased interest in the CXCR7 receptor, new agonists were developed, enabling investigation of the effects of CXCR7 separate from those of CXCR4 [151, 153]. Based on previous results indicating a role for CXCR7 in angiogenesis broadly, and cell migration specifically, we wanted to examine the role of CXCR7 in endothelial cell migration in an *in vitro* cell migration assay [366, 374].

SDF-1α (100 nM) increased HUVEC migration after 3 h, but not after 6 h of incubation. CXCR7 agonist VUF11207 did not increase HUVEC migration at any concentration tested, while TC14012 significantly increased HUVEC migration at 1 µM, but not at 10 or 30 µM. Pooling data from two separate experiments confirmed that both, SDF-1α and TC14012 increase HUVEC migration at 100 nM and 1 µM, respectively. As previously discussed in section 1.3.3.3 the concentration of both agonists used in the cell migration assay was based on their EC_{50} values and was expected to be sufficient to elicit a response.

CXCR7 has been shown to be involved in different aspects of angiogenesis of various types of endothelial cells and their progenitors [375]. Deletion of CXCR7 in cardiac microvessels has been shown to impair the expression of pro-angiogenic growth factor HB-EGF (Heparin-binding EGF-like growth factor) [119, 222, 375]. Furthermore, Melo *et al.* described an essential role for CXCR7 in HSC cell migration after stimulation with SDF-1α and Essencay *et al.* reported pro-migratory effects of SDF-1/CXCR7 axis in glioma cell migration [366, 367].

The majority of cell migration experiments were performed using a 3 h incubation protocol versus the 6 h migration protocol, due to the positive control (SDF-1α) exhibiting significantly increased cell migration only in the latter. One of the reasons for this might be unstable gradients in the cell migration chamber, created by fluid level imbalances [376]. Such imbalances can be introduced into the experiment during the pipetting phase or during the placement of a liquid-porous membrane over the bottom half of the migration chamber. It is challenging to account for such errors due to difficulties with quantifying and controlling said gradients in a migrations chamber [376]. Therefore, a 3 h incubation, which produced more reproducible and, therefore more reliable results was used for the remainder of cell migration experiments.

Not all researchers agree that CXCR7 exhibits pro-migratory effects, Mazzinghi *et al.* reported that while CXCR7 is involved in human renal EPC survival and adhesion to endothelium, it was CXCR4 that mediated cell migration [377]. Similarly, Dai *et al*. reported that the migration of bone marrow-derived EPC was not affected by the administration of either CXCR4-blocking antibody or CXCR7 inhibitor (CCX733) [374]. Interestingly, of the two agonists tested, only TC14012 significantly increased HUVEC migration in our study (Figure 7-3). This reflects the discrepancy observed in past studies, where there is little consensus over the existence of pro-migratory effects via CXCR7. The differences may also be related to the type of cell (EPC versus differentiated endothelial cell), and type of drug, (CXCR4 inhibitor vs CXCR7 agonist), that were seen to have an effect in the above experiments. After all, small molecules of different structures can have very different characteristics, including potential off-target effects.

Past research indicates that VUF11207 and TC14012 exhibit high affinity to CXCR7 and/or strong β-arrestin recruitment abilities. [151, 153, 308]. VUF11207 displayed high affinity (pKi = 8.1) in a CXCR7 radioligand binding assay using radiolabelled SDF-1α [153]. It also performed favourably in a β-arrestin2 recruitment assay, as discussed previously in section 1.3.3. [153].

TC14012, a CXCR4 inverse agonist, also exhibited good β-arrestin recruitment to CXCR7 using a BRET-based experimental system [151]. The investigation of β-arrestin recruitment to CXCR7 does not directly measure the specificity of VUF11207 and TC14012. Instead, it measures the ability of the agonist to initiate recruitment of β-arrestins, which is G-protein independent and limited to CXCR7. Additionally, measuring affinity does not directly measure specificity [378]. However, it is often argued that high-affinity can be equaled to high-specificity, since selecting for high-affinity compounds should ensure highly specific binding [378]. Therefore, selecting for high-affinity compounds based on functional binding assays coupled with sophisticated computer modelling experiments is considered a tried and tested approach of determining drug specificity [379]. Nevertheless, there are very few studies and consequently limited data available on the affinity, specificity and potency of both drugs, especially in the case of VUF11207, which was not commercially available until recently [153].

Levoye *et al*. reported that anti-CXCR7 antibody reduced SDF-1α-dependent migration at 30 nM, but not at 0.3 nM or 3 nM. They interpret these results as showing that CXCR7 acts as a modulator of migration by scavenging SDF-1α and thereby decreasing its activity on CXCR4 [120]. However, this interpretation does not agree with our results. If that were the case then TC14012 would not be able to increase cell migration when administered alone, since it does not bind to or activate CXCR4. Therefore, it could be that CXCR7 acts as a modulator of CXCR4-dependent cell migration when both receptors are active, while also being able to directly stimulate cell migration in the absence of CXCR4 activation [120].

We also wanted to examine the effect of both, SDF-1α and TC14012 combined on HUVEC migration. Co-administration of SDF-1α (100 nM) and TC14012 (1 μM) significantly increased cell migration of HUVEC, while in the same experiment either drug administered alone did not exhibit a significant increase in cell migration (Figure 7-4). Since SDF-1α and TC14012 were observed to significantly increase cell migration in previous experiments, increasing the number of repeats could increase the power of the experiment to detect a significant difference between the groups. Similarly, using an incubation time of more than 3 h might assist with analysis as the staining of migrated cell is clearer after a longer period of time; however, this can come at an expense of reproducibility/repeatability of results, as already discussed above. Interestingly, co-administration of SDF-1α and TC14012 also significantly increased cell migration, when compared to TC14012 (1 μM) alone.

To overcome the inconsistent results obtained with SDF-1α (100 nM) and TC14012 (1 μM) data was pooled from two separate experiments with comparable experimental setup (Figure 7-5). Combining the two experiments provided a higher n number and therefore more statistical power. In turn, both compounds produced statistically significant increases in HUVEC migration when compared to control. Therefore, we confirmed that SDF-1α acts as a pro-migratory molecule, as previously shown by others [222, 380, 381]. Since we did not differentiate between the CXCR4 and CXCR7 receptor involvement we cannot comment on whether pro-migratory signalling in this instance proceeds through either one single receptor or perhaps through both. On the other hand, administration of CXCR7 agonist TC14012 also resulted in HUVEC migration increase in our pooled data. Since TC14012 is not reported to show any signalling through CXCR4 it can be presumed that this pro-migratory effect proceeds entirely via the CXCR7 receptor. This is particularly interesting since CXCR7 has not been shown previously as actively involved in cell migration in HUVEC.

Instead it has been presented as capable only of aiding in cell migration by scavenging excess SDF-1α entering the pro-migratory SDF-1α/CXCR4 signalling axis [141]. However, our results show that TC14012 is capable of increasing endothelial cell migration through CXCR7, adding to the number of other pro-angiogenic processes that the CXCR7 receptor has been shown to participate in [112].

Interestingly, co-administration of SDF-1α and TC14012 did not significantly increase cell migration when compared to SDF-1α alone. As described earlier, increasing the number of repeats and using a slightly longer incubation period could help solve this problem. Alternatively, the SDF-1α concentration used in HUVEC cell migration experiments might not elicit a maximal chemotactic response, which could help explain the low effect size observed. Nevertheless, the obtained results suggest that CXCR7 plays an active role in cell migration and there are two possible reasons how this occurs.

In the event that SDF-1α at 100 nM does not elicit a maximal chemotactic response, be it through CXCR4 and/or CXCR7, addition of TC14012 further stimulates chemotactic signalling and consequently further increases the cell migration response. As previously stated, Jinquan *et al*. report that on CD4+ T lymphocytes they observed a bell-shaped SDF-1α dose response curve with the greatest chemotactic response observed at 100 ng/mL, which is equivalent to approx. 12.5 nM [382]. Since we used 100 nM SDF-1α in our experiments, this concentration could have already surpassed the dose needed for a maximal response. The experiments by Jinquan *et al.* were performed on CD4+ T lymphocytes and the question remains whether their findings can be directly extrapolated to endothelial cells [382]. This could be investigated by performing a dose-response curve for SDF-1α and TC14012 on HUVEC to determine which concentration elicits a maximal response in a cell migration experiment.

On the other hand, if 100 nM SDF-1α did already elicit a maximal response it could be that addition of TC14012 activates signalling through an alternative pathway to that utilized by SDF-1α. Past research suggests that SDF-1α/CXCR4-dependent cell migration signals through PI3K/Akt [230, 383]. We did not observe phosphorylation of Akt with TC14012 in our western blotting experiments (section 5.4), which would suggest CXCR7 chemotactic signalling proceeds through a different signalling pathway. Again, this could be examined by combining SDF-1α at a concentration that elicits a maximal chemotactic response with TC14012 to observe whether incubation of both drugs together results in further increase in cell migration compared to incubation of these drugs alone.

Additionally, TC14012 significantly increased cell migration only at 1 µM, but not at 10 or 30 µM. This might suggest a bell-shaped concentration-response curve, rather than a sigmoidal curve for involvement of TC14012 in cell migration. Bell-shaped concentration response curves are often indicative of a complex biological relationship between the ligand and its target [217]. Levoye *et al.* also suggest that the chemotactic curve of SDF-1α/CXCR7 interaction is bell-shaped, which translates into increased cell migration at lower concentrations. The existence of a bell-shaped chemotactic curve for SDF-1α is also shown by Jinquan *et al.* on CD4+ T lymphocytes and considering the intricate signalling interplay exhibited between CXCR4 and CXCR7 in other physiological and pathological processes lends this theory/hypothesis further credence [382, 384, 385].

Overall, we have shown that along with SDF-1α, TC14012 is also able to induce endothelial cell migration. This is important since pro-migratory effects of SDF-1α have been previously contributed solely to the SDF-1α/CXCR4 signalling axis, while we have shown that CXCR7 exhibits pro-migratory effects in its own right, along with its other pro-angiogenic actions described previously (e.g. tubule formation) [386]. In a broader setting this means that due to its various pro-angiogenic effects CXCR7 might play an important role in long-term regeneration of heart muscle after MI.

We know that angiogenesis plays a crucial role in the myocardium post-MI, as rebuilding the vascular network and establishing sufficient collateral circulation helps to reperfuse the heart after MI. Therefore, there is potential for developing of pro-regenerative therapies based on the CXCR7 receptor that would aid in myocardial salvage and recovery after MI. Despite the existence of many pro-angiogenic therapies, few have shown promise when taken into from bench to bedside. Therefore, any novel pro-angiogenic therapy represents an exciting target that could provide beneficial effects to patients who have suffered from a myocardial infarction and also prevent the occurrence of heart failure in these patients later in life.

7.5.1 *Summary*

Administration of SDF-1α (100 nM) exhibited pro-migratory effects on HUVEC after 3 h, but not after 6 h. CXCR7 agonist VUF11207 did not increase HUVEC migration at any concentration tested, while TC14012 elicited a cell migration response at 1 µM; demonstrating a possible pro-migratory role of CXCR7. Combined treatment of SDF-1α and TC14012 significantly increased cell migration, although in the same experiment SDF-1α and TC14012 administered alone did not significantly increase cell migration. Pooling data from multiple experiments revealed that both, SDF-1α (100 nM) and TC14012 (1 µM) exhibit pro-migratory effects. In conclusion, not only CXCR4 but also CXCR7 looks to be involved in endothelial cell migration downstream of SDF-1α binding. However, each receptor might stimulate endothelial cell migration through different intracellular pathways and further research is needed to elucidate their respective roles during this process.

8 General conclusions

CXCR7 has only recently been discovered as an atypical chemokine receptor for the ligand SDF-1α, in addition to the already established CXCR4 receptor. Since the role of CXCR4 in cardioprotection and angiogenesis has been well documented, focus was expanded to CXCR7 and its role in these processes, which was aided by emergence of novel CXCR7 receptor modulators.

To date, CXCR7 has been shown to be involved in anti-fibrotic and pro-regenerative effects in various endothelial cell types and shown to exert cardioprotective effects in murine tissues. Past research also revealed the presence of CXCR7 receptor in non-endothelial cell types; however, it is the endothelial CXCR7 which has shown most therapeutic potential. The main aim of this thesis was to investigate the effects of CXCR7 agonist administration on acute MI, as well as determining the mechanism behind CXCR7 receptor activation on endothelial cells. Furthermore, we also wanted to examine the pro-regenerative potential of endothelial CXCR7, by probing its participation in endothelial cell migration, a crucial step in the process of angiogenesis. Each of these factors has been discussed in detail in previous chapters.

After confirming the presence of CXCR7 on isolated endothelial cells and commercially available endothelial cell lines, our focus was shifted on to determining the cardioprotective potential of CXCR7 via the CXCR7 agonist VUF11207.

Described as CXCR7-biased with no purported action on CXCR4, it represented a fine investigative tool to be used on rat isolated perfusion model *ex vivo*. Interestingly, administration of VUF11207 immediately prior to reperfusion afforded no measurable cardioprotection in our model.

However, as previously discussed in section 4.5., there are numerous reasons why this could have occurred and what the implications are. Based on the cell-migration results presented in this thesis the culprit might be the agonist, VUF11207, which also failed to initiate endothelial cell migration, further described below. Therefore, this lack of observed cardioprotection does not necessarily signify the lack of CXCR7 cardioprotective potential immediately after MI. Further research would be needed to fully comprehend the role of CXCR7 in this setting by making use of reliable CXCR7 agonists to ensure the validity of obtained results.

This thesis also examined the role of the RISK signalling pathway in endothelial CXCR7 receptor activation. Since RISK pathway, which includes signalling through PI3K/AKT and MAPK pathways, is known as the main effector of cardioprotection, which is initiated by binding of SDF-1α to CXCR4, it was expected that CXCR7 would exhibit similar signalling properties. Surprisingly, this was not the case for CXCR7. Administration of CXCR7 agonists VUF11207 or TC14012 failed to activate either PI3K/AKT or MEK/ERK arm of the RISK signalling pathway. Again, this does not eliminate a possible role for CXCR7 in cardioprotection, although it suggests that a different signalling axis is behind any cardioprotective effects exhibited by CXCR7. There is still a lot of uncertainty and contrasting results regarding the signalling abilities of the CXCR7 receptor, compounded by the fact that it does not signal via classical G protein signalling, but instead utilizes less well understood β-arrestin-biased signalling. Further work is needed to decode the exact signalling pathway downstream of CXCR7 receptor activation and investigate whether its activation is capable of affording cardioprotection.

The aim of this thesis was also to generate an inducible transgenic mouse model of endothelial CXCR7 deletion, which could help shed light on the acute cardioprotective potential of endothelial CXCR7 receptor.

However, the desired transgenic model was not generated successfully, which somewhat hindered the plans for this thesis to be focused mainly on cardioprotection. In the light of the issues we faced with the transgenic mice, the focus was switched to another aspect of CXCR7 receptor function. As with CXCR4, there is evidence of CXCR7 involvement in various aspects of angiogenesis, including cell migration. In the scope of MI, angiogenesis is particularly important, since it has the ability to salvage ischaemic myocardium, impact ventricular remodelling and consequently prevent the transition to heart failure. Angiogenesis is also involved in tissue regeneration in the long term as opposed to acute cardioprotection, which affords beneficial effects immediately after MI. Therefore, CXCR7 participation in cell migration, and consequently angiogenesis, could present a potential pro-regenerative role of CXCR7.

Interestingly, multiwell Boyden chemotaxis assay suggested a pro-angiogenic role for CXCR7 agonist TC14012, but not VUF11207, using a commercially available endothelial cell line. Any pro-angiogenic effects observed with administration of SDF-1α have previously been attributed to its signalling via the CXCR4 receptor, with CXCR7 portrayed mainly in a scavenging role, regulating circulating SDF-1α. However, the data presented in this thesis suggest a pro-migratory role for CXCR7 in HUVEC, independent of the CXCR4 receptor, which represents a novel finding of this thesis. As discussed in Chapter 7 and elsewhere, the downstream effectors responsible for initiating cell migration might differ between the CXCR4 and CXCR7 receptors. This highlights a need for further research into the cell migration role of endothelial CXCR7, to elucidate the exact mechanism responsible for the observed effects and explain the difference in pro-angiogenic potential of both CXCR7 agonists, which have been discussed in detail in section 7.5.

In conclusion, I believe there was merit in querying the involvement of CXCR7 in cardioprotection and angiogenesis, specifically cell migration. For clarification, my original aims focused more on the role of immediate vs longer-term cardioprotection examined through generation of CXCR7 transgenic animals and utilization of commercially-available CXCR7 agonists. However, half way through my PhD a study was published by Hao *et al*., which already explored many of the same ideas that I was also interested in, which meant that the scope for undertaking novel research in this area shrunk significantly. To retain an aspect of novelty in my thesis I then turned to less-explored immediate cardioprotection (observed <day after initial MI), as well as the cell-migration role of endothelial CXCR7 as the central theme of this thesis. As discussed throughout this thesis, investigation of acute cardioprotective effects of CXCR7 mere hours post-MI did not yield positive results. This is perhaps not surprising as most beneficial effects that CXCR7 has been shown to exert, occurred throughout a longer period of time (weeks) post-MI. Since angiogenesis in the heart post-MI also does not occur immediately, but represents a long-term process it is more likely that CXCR7 exhibits its beneficial effects by affecting re-vascularization of the damaged myocardium. This would agree with the lack of acute cardioprotection seen in Chapter 4, as well as the lack of RISK pathway involvement seen in Chapter 5. Consequently, CXCR7 might represent an exciting target for pro-regenerative treatments, but its future as an acute cardioprotective effector seems uncertain. Hence, future work on this topic will be better suited to a research group that utilizes techniques, which are capable of successfully identifying and characterizing novel pro-regenerative targets.

9 References

1. Asri A, Sabour J, Atashi A, Soleimani M. Homing in hematopoietic stem cells: focus on regulatory role of CXCR7 on SDF1-α/CXCR4 axis. *Excli Journal* 2016;**15**:134-143.

2. Stoll G, Bendszus M. Inflammation and atherosclerosis - Novel insights into plaque formation and destabilization. *Stroke* 2006;**37**:1923-1932.

3. Lee RT, Libby P. The unstable atheroma. *Arteriosclerosis Thrombosis and Vascular Biology* 1997;**17**:1859-1867.

4. Swirski FK, Nahrendorf M. Leukocyte Behavior in Atherosclerosis, Myocardial Infarction, and Heart Failure. *Science* 2013;**339**:161-166.

5. Bentzon JF, Otsuka F, Virmani R, Falk E. Mechanisms of Plaque Formation and Rupture. *Circulation Research* 2014;**114**:1852-1866.

6. Cohn PF, Fox KM, Daly C. Silent myocardial ischemia. *Circulation* 2003;**108**:1263-1277.

7. Turner RC, Millns H, Neil HAW, Stratton IM, Manley SE, Matthews DR, Holman RR, United Kingdom Prospective Diabet Study G. Risk factors for coronary artery disease in non-insulin dependent diabetes mellitus: United kingdom prospective diabetes study (UKPDS : 23). *British Medical Journal* 1998;**316**:823-828.

8. Austin MA. Plasma triglyceride as a risk factor for cardiovascular disease. *Canadian Journal of Cardiology* 1998;**14**:14B-17B.

9. Bennett M, Wang J, Yu E, Gray K, Gorenne I. Atherosclerosis and aging. *Cardiology* 2013;**126**:221-221.

10. North BJ, Sinclair DA. The Intersection Between Aging and Cardiovascular Disease. *Circulation Research* 2012;**110**:1097-1108.

11. Gerczuk PZ, Kloner RA. An Update on Cardioprotection A Review of the Latest Adjunctive Therapies to Limit Myocardial Infarction Size in Clinical Trials. *Journal of the American College of Cardiology* 2012;**59**:969-978.

12. Frangogiannis NG. Pathophysiology of Myocardial Infarction. *Comprehensive Physiology* 2015;**5**:1841-1875.

13. Lewandrowski K, Chen A, Januzzi J. Cardiac markers for myocardial infarction. A brief review. *American journal of clinical pathology* 2002;**118 Suppl**:S93-99.

14. Hausenloy DJ, Yellon DM. Myocardial ischemia-reperfusion injury: a neglected therapeutic target. *Journal of Clinical Investigation* 2013;**123**:92-100.

15. Kubler W, Haass M. Cardioprotection: Definition, classification, and fundamental principles. *Heart* 1996;**75**:330-333.

16. Lonborg J, Kelbaek H, Vejlstrup N, Botker HE, Kim WY, Holmvang L, Jorgensen E, Helqvist S, Saunamaki K, Terkelsen CJ, Schoos MM, Kober L, Clemmensen P, Treiman M, Engstrom T. Exenatide Reduces Final Infarct Size in Patients With ST-Segment-Elevation Myocardial Infarction and Short-Duration of Ischemia. *Circulation-Cardiovascular Interventions* 2012;**5**:288-295.

17. Woo JS, Kim W, Ha SJ, Kim JB, Kim SJ, Kim WS, Seon HJ, Kim KS. Cardioprotective Effects of Exenatide in Patients With ST-Segment-Elevation Myocardial Infarction Undergoing Primary Percutaneous Coronary Intervention Results of Exenatide Myocardial Protection in Revascularization Study. *Arteriosclerosis Thrombosis and Vascular Biology* 2013;**33**:2252-2260.

18. Ibanez B, Macaya C, Sanchez-Brunete V, Pizarro G, Fernandez-Friera L, Mateos A, Fernandez-Ortiz A, Garcia-Ruiz JM, Garcia-Alvarez A, Iniguez A, Jimenez-Borreguero J, Lopez-Romero P, Fernandez-Jimenez R, Goicolea J, Ruiz-Mateos B, Bastante T, Arias M, Iglesias-Vazquez JA, Rodriguez MD, Escalera N, Acebal C, Cabrera JA, Valenciano J, de Prado AP, Fernandez-Campos MJ, Casado I, Garcia-Rubira JC, Garcia-Prieto J, Sanz-Rosa D, Cuellas C, Hernandez-Antolin R, Albarran A, Fernandez-Vazquez F, de la Torre-Hernandez JM, Pocock S, Sanz G, Fuster V. Effect of Early Metoprolol on Infarct Size in ST-Segment-Elevation Myocardial Infarction Patients Undergoing Primary Percutaneous Coronary Intervention The Effect of Metoprolol in Cardioprotection During an Acute Myocardial Infarction (METOCARD-CNIC) Trial. *Circulation* 2013;**128**:1495-1503.

19. Buja LM. Myocardial ischemia and reperfusion injury. *Cardiovascular Pathology* 2005;**14**:170-175.

20. Kalogeris T, Baines CP, Krenz M, Korthuis RJ. Cell biology of ischaemia/reperfusion injury. *International Review of Cell and Molecular Biology, Vol 298* 2012;**298**:229-317.

21. Bing RJ. Some aspects of biochemistry of myocardial infarction. *Cellular and Molecular Life Sciences* 2001;**58**:351-355.

22. Verma S, Fedak PWM, Weisel RD, Butany J, Rao V, Maitlund A, Li RK, Dhillon B, Yau TM. Fundamentals of reperfusion injury for the clinical cardiologist. *Circulation* 2002;**105**:2332-2336.

23. White HD, Chew DP. Acute myocardial infarction. *Lancet* 2008;**372**:570-584.

24. Burke AP, Virmani R. Pathophysiology of acute myocardial infarction. *Medical Clinics of North America* 2007;**91**:553-+.

25. Hori M, Nishida K. Oxidative stress and left ventricular remodelling after myocardial infarction. *Cardiovascular Research* 2009;**81**:457-464.

26. Sanada S, Komuro I, Kitakaze M. Pathophysiology of myocardial reperfusion injury: preconditioning, postconditioning, and translational aspects of protective measures. *American Journal of Physiology-Heart and Circulatory Physiology* 2011;**301**:H1723-H1741.

27. Marban E, Kitakaze M, Kusuoka H, Porterfield JK, Yue DT, Chacko VP. Intracellular free calcium-concentration measured with F-19 NMR-spectroscopy in intact ferret hearts. *Proceedings of the National Academy of Sciences of the United States of America* 1987;**84**:6005-6009.

28. Inserte J, Barba I, Poncelas-Nozal M, Hernando V, Agullo L, Ruiz-Meana M, Garcia-Dorado D. cGMP/PKG pathway mediates myocardial postconditioning protection in rat hearts by delaying normalization of intracellular acidosis during reperfusion. *Journal of Molecular and Cellular Cardiology* 2011;**50**:903-909.

29. Zahger D, Yano J, Chaux A, Fishbein MC, Ganz W. Absence of lethal reperfusion injury after 3 hours of reperfusion - a study in single-canine-heart model of ischaemia-reperfusion. *Circulation* 1995;**91**:2989-2994.

30. Kloner RA. Does reperfusion injury exist in humans. *Journal of the American College of Cardiology* 1993;**21**:537-545.

31. Opie LH. Reperfusion injury and its pharmacologic modification. *Circulation* 1989;**80**:1049-1062.

32. Agati L. Microvascular integrity after reperfusion therapy. *American Heart Journal* 1999;**138**:S76-S78.

33. Turer AT, Hill JA. Pathogenesis of Myocardial Ischemia-Reperfusion Injury and Rationale for Therapy. *American Journal of Cardiology* 2010;**106**:360-368.

34. Niccoli G, Burzotta F, Galiuto L, Crea F. Myocardial No-Reflow in Humans. *Journal of the American College of Cardiology* 2009;**54**:281-292.

35. Brosh D, Assali AR, Mager A, Porter A, Hasdai D, Teplitsky I, Rechavia E, Fuchs S, Battler A, Kornowski R. Effect of no-reflow during primary percutaneous coronary intervention for acute myocardial infarction on six-month mortality. *American Journal of Cardiology* 2007;**99**:442-445.

36. Wong DTL, Puri R, Richardson JD, Worthley MI, Worthley SG. Myocardial 'no-reflow' - Diagnosis, pathophysiology and treatment. *International Journal of Cardiology* 2013;**167**:1798-1806.

37. Camici PG, Prasad SK, Rimoldi OE. Stunning, hibernation, and assessment of myocardial viability. *Circulation* 2008;**117**:103-114.

38. Buja LM. Modulation of the myocardial response to ischemia. *Laboratory Investigation* 1998;**78**:1345-1373.

39. Xiong JW. Molecular and developmental biology of the hemangioblast. *Developmental Dynamics* 2008;**237**:1218-1231.

40. Kubo H, Alitalo K. The bloody fate of endothelial stem cells. *Genes & Development* 2003;**17**:322-329.

41. Choi K. The hemangioblast: A common progenitor of hematopoietic and endothelial cells. *Journal of Hematotherapy & Stem Cell Research* 2002;**11**:91-101.

42. Marcelo KL, Goldie LC, Hirschi KK. Regulation of Endothelial Cell Differentiation and Specification. *Circulation Research* 2013;**112**:1272-1287.

43. Pinto AR, Ilinykh A, Ivey MJ, Kuwabara JT, D'Antoni ML, Debuque R, Chandran A, Wang LN, Arora K, Rosenthal NA, Tallquist MD. Revisiting Cardiac Cellular Composition. *Circulation Research* 2016;**118**:400-409.

44. Anversa P, Olivetti G, Melissari M, Loud AV. STEREOLOGICAL MEASUREMENT OF CELLULAR AND SUBCELLULAR HYPERTROPHY AND HYPERPLASIA IN THE PAPILLARY-MUSCLE OF ADULT-RAT. *Journal of Molecular and Cellular Cardiology* 1980;**12**:781-795.

45. Zhou PZ, Pu WT. Recounting Cardiac Cellular Composition. *Circulation Research* 2016;**118**:368-370.

46. Banerjee I, Fuseler JW, Price RL, Borg TK, Baudino TA. Determination of cell types and numbers during cardiac development in the neonatal and adult rat and mouse. *American Journal of Physiology-Heart and Circulatory Physiology* 2007;**293**:H1883-H1891.

47. Brutsaert DL. Cardiac endothelial-myocardial signaling: Its role in cardiac growth, contractile performance, and rhythmicity. *Physiological Reviews* 2003;**83**:59-115.

48. Bauersachs J, Widder JD. Endothelial dysfunction in heart failure. *Pharmacological Reports* 2008;**60**:119-126.

49. Asahara T, Murohara T, Sullivan A, Silver M, vanderZee R, Li T, Witzenbichler B, Schatteman G, Isner JM. Isolation of putative progenitor endothelial cells for angiogenesis. *Science* 1997;**275**:964-967.

50. Urbich C, Dimmeler S. Endothelial progenitor cells - Functional characterization. *Trends in Cardiovascular Medicine* 2004;**14**:318-322.

51. Yoder MI, Ingram DA. Endothelial progenitor cell: ongoing controversy for defining these cells and their role in neoangiogenesis in the murine system. *Current Opinion in Hematology* 2009;**16**:269-273.

52. Yoder MC. Endothelial stem and progenitor cells (stem cells): (2017 Grover Conference Series). *Pulmonary Circulation* 2017;**8**.

53. Hur J, Yoon CH, Kim HS, Choi JH, Kang HJ, Hwang KK, Oh BH, Lee MM, Park YB. Characterization of two types of endothelial progenitor cells and their different contributions to neovasculogenesis. *Arteriosclerosis Thrombosis and Vascular Biology* 2004;**24**:288-293.

54. Hagensen MK, Shim J, Thim T, Falk E, Bentzon JF. Circulating Endothelial Progenitor Cells Do Not Contribute to Endothelial Regeneration in Atherosclerosis in ApoE(-/-) Mice. *Arteriosclerosis Thrombosis and Vascular Biology* 2009;**29**:E124-E124.

55. Rinkevich Y, Lindau P, Ueno H, Longaker MT, Weissman IL. Germ-layer and lineage-restricted stem/progenitors regenerate the mouse digit tip. *Nature* 2011;**476**:409-U453.

56. Medina RJ, Barber CL, Sabatier F, Dignat-George F, Melero-Martin JM, Khosrotehrani K, Ohneda O, Randi AM, Chan JKY, Yamaguchi T, Van Hinsbergh VWM, Yoder MC, Stitt AW. Endothelial Progenitors: A Consensus Statement on Nomenclature. *Stem Cells Translational Medicine* 2017;**6**:1316-1320.

57. Tahergorabi Z, Khazaei M. A Review on Angiogenesis and Its Assays. *Iranian Journal of Basic Medical Sciences* 2012;**15**:1110-1126.

58. Ferrara N, Kerbel RS. Angiogenesis as a therapeutic target. *Nature* 2005;**438**:967-974.

59. Baker M, Robinson SD, Lechertier T, Barber PR, Tavora B, D'Amico G, Jones DT, Vojnovic B, Hodivala-Dilke K. Use of the mouse aortic ring assay to study angiogenesis. *Nature Protocols* 2012;**7**:89-104.

60. Carmeliet P. Angiogenesis in life, disease and medicine. *Nature* 2005;**438**:932-936.

61. Ribatti D, Crivellato E. "Sprouting angiogenesis", a reappraisal. *Developmental Biology* 2012;**372**:157-165.

62. Mirshahi F, Pourtau J, Li H, Muraine M, Trochon V, Legrand E, Vannier JP, Soria J, Vasse M, Soria C. SDF-1 activity on microvascular endothelial cells: Consequences on angiogenesis in in vitro and in vivo models. *Thrombosis Research* 2000;**99**:587-594.

63. Oduk Y, Zhu W, Kannappan R, Zhao M, Borovjagin AV, Oparil S, Zhang J. VEGF nanoparticles repair the heart after myocardial infarction. *American Journal of Physiology-Heart and Circulatory Physiology* 2018;**314**:H278-H284.

64. Wang DY, Anderson JC, Gladson CL. The role of the extracellular matrix in angiogenesis in malignant glioma tumors. *Brain Pathology* 2005;**15**:318-326.

65. Li S, Huang NF, Hsu S. Mechanotransduction in endothelial cell migration. *Journal of Cellular Biochemistry* 2005;**96**:1110-1126.

66. Hsu S, Thakar R, Li S. Haptotaxis of endothelial cell migration under flow. *Methods in Molecular Medicine* 2007;**139**:237-250.

67. Lamalice L, Le Boeuf F, Huot J. Endothelial cell migration during angiogenesis. *Circulation Research* 2007;**100**:782-794.

68. De Luca G, van't Hof AWJ, de Boer MJ, Ottervanger JP, Hoorntje JCA, Gosselink ATM, Dambrink JHE, Zijlstra F, Suryapranata H. Time-to-treatment significantly affects the

extent of ST-segment resolution and myocardial blush in patients with acute myocardial infarction treated by primary angioplasty. *European Heart Journal* 2004;**25**:1009-1013.

69. Ware JA, Simons M. Angiogenesis in ischemic heart disease. *Nature Medicine* 1997;**3**:158-164.

70. Dery MAC, Michaud MD, Richard DE. Hypoxia-inducible factor 1: regulation by hypoxic and non-hypoxic activators. *International Journal of Biochemistry & Cell Biology* 2005;**37**:535-540.

71. Townley-Tilson WHD, Pi XC, Xie L. The Role of Oxygen Sensors, Hydroxylases, and HIF in Cardiac Function and Disease. *Oxidative Medicine and Cellular Longevity* 2015.

72. Rahimi N. The Ubiquitin-Proteasome System Meets Angiogenesis. *Molecular Cancer Therapeutics* 2012;**11**:538-548.

73. van der Laan AM, Piek JJ, van Royen N. Targeting angiogenesis to restore the microcirculation after reperfused MI. *Nature Reviews Cardiology* 2009;**6**:515-523.

74. Goncalves LM. Angiogenic growth factors: potential new treatment for acute myocardial infarction? *Cardiovascular Research* 2000;**45**:294-302.

75. Janowski M. Functional diversity of SDF-1 splicing variants. *Cell Adhesion & Migration* 2009;**3**:243-249.

76. Teicher BA, Fricker SP. CXCL12 (SDF-1)/CXCR4 Pathway in Cancer. *Clinical Cancer Research* 2010;**16**:2927-2931.

77. Lagerstrom MC, Schioth HB. Structural diversity of G protein-coupled receptors and significance for drug discovery. *Nature Reviews Drug Discovery* 2008;**7**:339-357.

78. Balabanian K, Lagane B, Infantino S, Chow KYC, Harriague J, Moepps B, Arenzana-Seisdedos F, Thelen M, Bachelerie F. The chemokine SDF-1/CXCL12 binds to and signals through the orphan receptor RDC1 in T lymphocytes. *Journal of Biological Chemistry* 2005;**280**:35760-35766.

79. Sierra MD, Yang FQ, Narazaki M, Salvucci O, Davis D, Yarchoan R, Zhang HWH, Fales H, Tosato G. Differential processing of strornal-derived factor-1 alpha and strornal-derived factor-1 beta explains functional diversity. *Blood* 2004;**103**:2452-2459.

80. Davis DA, Singer KE, Sierra MD, Narazaki M, Yang FQ, Fales HM, Yarchoan R, Tosato G. Identification of carboxypeptidase N as an enzyme responsible for C-terminal cleavage of stromal cell-derived factor-1 alpha in the circulation. *Blood* 2005;**105**:4561-4568.

81. Gleichmann M, Gillen C, Czardybon M, Bosse F, Greiner-Petter R, Auer J, Muller HW. Cloning and characterization of SDF-1 gamma a novel SDF-1 chemokine transcript with developmentally regulated expression in the nervous system. *European Journal of Neuroscience* 2000;**12**:1857-1866.

82. Yu L, Cecil J, Peng SB, Schrementi J, Kovacevic S, Paul D, Su EW, Wang J. Identification and expression of novel isoforms of human stromal cell-derived factor 1. *Gene* 2006;**374**:174-179.

83. Pillarisetti K, Gupta SK. Cloning and relative expression analysis of rat stromal cell derived factor-1 (SDF-1)(1): SDF-1 alpha mRNA is selectively induced in rat model of myocardial infarction. *Inflammation* 2001;**25**:293-300.

84. Wuerth R, Bajetto A, Harrison JK, Barbieri F, Florio T. CXCL12 modulation of CXCR4 and CXCR7 activity in human glioblastoma stem-like cells and regulation of the tumor microenvironment. *Frontiers in Cellular Neuroscience* 2014;**8**.

85. Tang YL, Zhu WQ, Cheng M, Chen LJ, Zhang J, Sun T, Kishore R, Phillips MI, Losordo DW, Qin GJ. Hypoxic Preconditioning Enhances the Benefit of Cardiac Progenitor Cell Therapy for Treatment of Myocardial Infarction by Inducing CXCR4 Expression. *Circulation Research* 2009;**104**:1209-U1218.

86. Zlotnik A, Yoshie O. Chemokines: A new classification system and their role in immunity. *Immunity* 2000;**12**:121-127.

87. Murdoch C. CXCR4: chemokine receptor extraordinaire. *Immunological Reviews* 2000;**177**:175-184.

88. Zou YR, Kottmann AH, Kuroda M, Taniuchi I, Littman DR. Function of the chemokine receptor CXCR4 in haematopoiesis and in cerebellar development. *Nature* 1998;**393**:595-599.

89. Molino M, Woolkalis MJ, Prevost N, Pratico D, Barnathan ES, Taraboletti G, Haggarty BS, Hesselgesser J, Horuk R, Hoxie JA, Brass LF. CXCR4 on human endothelial cells can serve as both a mediator of biological responses and as a receptor for HIV-2. *Biochimica Et Biophysica Acta-Molecular Basis of Disease* 2000;**1500**:227-240.

90. Gupta SK, Lysko PG, Pillarisetti K, Ohlstein E, Stadel JM. Chemokine receptors in human endothelial cells - Functional expression of CXCR4 and its transcriptional regulation by inflammatory cytokines. *Journal of Biological Chemistry* 1998;**273**:4282-4287.

91. Hu X, Dai S, Wu W-J, Tan W, Zhu X, Mu J, Guo Y, Bolli R, Rokosh G. Stromal cell-derived factor-1 alpha confers protection against myocardial ischemia/reperfusion injury - Role of the cardiac stromal cell-derived factor-1 alpha-CXCR4 axis. *Circulation* 2007;**116**:654-663.

92. Rettig MP, Ansstas G, DiPersio JF. Mobilization of hematopoietic stem and progenitor cells using inhibitors of CXCR4 and VLA-4. *Leukemia* 2012;**26**:34-53.

93. Debnath B, Xu SL, Grande F, Garofalo A, Neamati N. Small Molecule Inhibitors of CXCR4. *Theranostics* 2013;**3**:47-75.

94. Domanska UM, Kruizinga RC, Nagengast WB, Timmer-Bosscha H, Huls G, de Vries EGE, Walenkamp AME. A review on CXCR4/CXCL12 axis in oncology: No place to hide. *European Journal of Cancer* 2013;**49**:219-230.

95. Doring Y, Pawig L, Weber C, Noels H. The CXCL12/CXCR4 chemokine ligand/receptor axis in cardiovascular disease. *Frontiers in Physiology* 2014;**5**.

96. Zaruba M-M, Franz W-M. Role of the SDF-1-CXCR4 axis in stem cell-based therapies for ischemic cardiomyopathy. *Expert Opinion on Biological Therapy* 2010;**10**:321-335.

97. Ceradini DJ, Kulkarni AR, Callaghan MJ, Tepper OM, Bastidas N, Kleinman ME, Capla JM, Galiano RD, Levine JP, Gurtner GC. Progenitor cell trafficking is regulated by hypoxic gradients through HIF-1 induction of SDF-1. *Nature Medicine* 2004;**10**:858-864.

98. Bromage DI, Davidson SM, Yellon DM. Stromal derived factor 1 alpha: A chemokine that delivers a two-pronged defence of the myocardium. *Pharmacology & Therapeutics* 2014;**143**:305-315.

99. Sasaki T, Fukazawa R, Ogawa S, Kanno S, Nitta T, Ochi M, Shimizu K. Stromal cell-derived factor-1 alpha improves infarcted heart function through angiogenesis in mice. *Pediatrics International* 2007;**49**:966-971.

100. Saxena A, Fish JE, White MD, Yu S, Smyth JWP, Shaw RM, DiMaio JM, Srivastava D. Stromal cell-derived factor-1 alpha is cardioprotective after myocardial infarction. *Circulation* 2008;**117**:2224-2231.

101. Burton PR, Clayton DG, Cardon LR, Craddock N, Deloukas P, Duncanson A, Kwiatkowski DP, McCarthy MI, Ouwehand WH, Samani NJ, Todd JA, Donnelly P, Barrett JC, Davison D, Easton D, Evans D, Leung HT, Marchini JL, Morris AP, Spencer CCA, Tobin MD, Attwood AP, Boorman JP, Cant B, Everson U, Hussey JM, Jolley JD, Knight AS, Koch K, Meech E, Nutland S, Prowse CV, Stevens HE, Taylor NC, Walters GR, Walker NM, Watkins NA, Winzer T, Jones RW, McArdle WL, Ring SM, Strachan DP, Pembrey M, Breen G, St Clair D, Caesar S, Gordon-Smith K, Jones L, Fraser C, Green EK, Grozeva D, Hamshere ML, Holmans PA, Jones IR, Kirov G, Moskvina V, Nikolov I, O'Donovan MC, Owen MJ, Collier DA, Elkin A, Farmer A, Williamson R, McGuffin P, Young AH, Ferrier IN, Ball SG, Balmforth AJ, Barrett JH, Bishop DT, Iles MM, Maqbool A, Yuldasheva N, Hall AS, Braund PS, Dixon RJ, Mangino M, Stevens S, Thompson JR, Bredin F, Tremelling M, Parkes M, Drummond H, Lees CW, Nimmo ER, Satsangi J, Fisher SA, Forbes A, Lewis CM, Onnie CM, Prescott NJ, Sanderson J, Mathew CG, Barbour J, Mohiuddin MK, Todhunter CE, Mansfield JC, Ahmad T, Cummings FR, Jewell DP, Webster J, Brown MJ, Lathrop GM, Connell J, Dominiczak A, Marcano CAB, Burke B, Dobson R, Gungadoo J, Lee KL, Munroe PB, Newhouse SJ, Onipinla A, Wallace C, Xue MZ, Caulfield M, Farrall M, Barton A, Bruce IN, Donovan H, Eyre S, Gilbert PD, Hider SL, Hinks AM, John SL, Potter C, Silman AJ, Symmons DPM, Thomson W, Worthington J, Dunger DB, Widmer B, Frayling TM, Freathy RM, Lango H, Perry JRB, Shields BM, Weedon MN, Hattersley AT, Hitman GA, Walker M, Elliott KS, Groves CJ, Lindgren CM, Rayner NW, Timpson NJ, Zeggini E, Newport M, Sirugo G, Lyons E, Vannberg F, Brown MA, Franklyn JA, Heward JM, Simmonds MJ, Hill AVS, Bradbury LA,

Farrar C, Pointon JJ, Wordsmith P, Gough SCL, Seal S, Stratton MR, Rahman N, Ban M, Goris A, Sawcer SJ, Compston A, Conway D, Jallow M, Bumpstead SJ, Chaney A, Downes K, Ghori MJR, Gwilliam R, Inouye M, Keniry A, King E, McGinnis R, Potter S, Ravindrarajah R, Whittaker P, Withers D, Pereira-Gale J, Hallgrimsdottir IB, Howie BN, Su Z, Teo YY, Vukcevic D, Bentley D, Wellcome Trust Case Control C, Biol RAG, Genom Study S, Breast Canc Susceptib C. Genome-wide association study of 14,000 cases of seven common diseases and 3,000 shared controls. *Nature* 2007;**447**:661-678.

102. Kathiresan S, Altschuler D, Anand S, Ardissino D, Asselta R, Ball SG, Balmforth AJ, Berger K, Berglund G, Bernardi F, Bernardinelli L, Berzuini C, Braund PS, Burnett MS, Burtt N, Cambien F, Casari G, Celli P, Chen Z, Corrocher R, Daly MJ, Deloukas P, Devaney J, Do R, Duga S, Elosua R, Engert JC, Epstein SE, Erdmann J, Ferrario M, Fetiveau R, Fischer M, Friedlander Y, Gabriel SB, Galli M, Gianniny L, Girelli D, Grosshennig A, Guiducci C, Hakonarson HH, Hall AS, Havulinna AS, Hengstenberg C, Hirschhorn JN, Holm H, Huge A, Kent KM, Konig IR, Korn JM, Li M, Lieb W, Lindsay JM, Linsel-Nitschke P, Lucas G, MacRae CA, Mannucci PM, Marrugat J, Martinelli N, Marziliano N, Matthai W, McCarroll SA, McKeown PP, Meigs JB, Melander O, Merlini PA, Mirel D, Morgan T, Musunuru K, Nathan DM, Nemesh J, O'Donnell CJ, Olivieri O, Ouwehand W, Parkin M, Patterson CC, Peltonen L, Peyvandi F, Piazza A, Pichard AD, Preuss M, Purcell S, Qasim A, Rader DJ, Ramos R, Reilly MP, Ribichini F, Rossi M, Sala J, Salomaa V, Samani NJ, Satler L, Scheffold T, Scholz M, Schreiber S, Schunkert H, Schwartz SM, Siscovick DS, Spertus JA, Spreafico M, Stark K, Stefansson K, Stoll M, Subirana I, Surti A, Thompson JR, Thorleifsson G, Thorsteinsdottir U, Tubaro M, Voight BF, Waksman R, Wichmann HE, Wilensky R, Williams G, Wright BJ, Xie C, Yee J, Ziegler A, Zonzin P, Myocardial Infarction Genetics C. Genome-wide association of early-onset myocardial infarction with single nucleotide polymorphisms and copy number variants. *Nature Genetics* 2009;**41**:334-341.

103. Mehta NN, Matthews GJ, Krishnamoorthy P, Shah R, McLaughlin C, Patel P, Budoff M, Chen J, Wolman M, Go A, He J, Kanetsky PA, Master SR, Rader DJ, Raj D, Gadegbeku CA, Schreiber M, Fischer MJ, Townsend RR, Kusek J, Feldman HI, Foulkes AS, Reilly MP, Chronic Renal Insufficiency C. Higher plasma CXCL12 levels predict incident myocardial infarction and death in chronic kidney disease: findings from the Chronic Renal Insufficiency Cohort study. *European Heart Journal* 2014;**35**:2115-+.

104. Crump MP, Gong JH, Loetscher P, Rajarathnam K, Amara A, Arenzana-Seisdedos F, Virelizier JL, Baggiolini M, Sykes BD, Clark-Lewis I. Solution structure and basis for functional activity of stromal cell-derived factor-1; dissociation of CXCR4 activation from binding and inhibition of HIV-1. *Embo Journal* 1997;**16**:6996-7007.

105. Libert F, Parmentier M, Lefort A, Dumont JE, Vassart G. Complete nucleotide-sequence of a putative-G protein coupled receptor - RDC1. *Nucleic Acids Research* 1990;**18**:1917-1917.

106. Cook JS, Wolsing DH, Lameh J, Olson CA, Correa PE, Sadee W, Blumenthal EM, Rosenbaum JS. Characterization of the RDC1 gene which encodes the canine homolog of a proposed human VIP receptor - expression does not correlate with an increase in VIP binding-sites. *Febs Letters* 1992;**300**:149-152.

107. Nagata S, Ishihara T, Robberecht P, Libert F, Parmentier M, Christophe J, Vassart G. RDC1 may not be VIP receptor. *Trends in Pharmacological Sciences* 1992;**13**:102-103.

108. McLatchie LM, Fraser NJ, Main MJ, Wise A, Brown J, Thompson N, Solari R, Lee MG, Foord SM. RAMPs regulate the transport and ligand specificity of the calcitonin-receptor-like receptor. *Nature* 1998;**393**:333-339.

109. Sanchez-Martin L, Sanchez-Mateos P, Cabanas C. CXCR7 impact on CXCL12 biology and disease. *Trends in Molecular Medicine* 2013;**19**:12-22.

110. Costello CM, McCullagh B, Howell K, Sands M, Belperio JA, Keane MP, Gaine S, McLoughlin P. A role for the CXCL12 receptor, CXCR7, in the pathogenesis of human pulmonary vascular disease. *European Respiratory Journal* 2012;**39**:1415-1424.

111. Neusser MA, Kraus AK, Regele H, Cohen CD, Fehr T, Kerjaschki D, Wuthrich RP, Penfold MET, Schall T, Segerer S. The chemokine receptor CXCR7 is expressed on lymphatic endothelial cells during renal allograft rejection. *Kidney International* 2010;**77**:801-808.

112. Yan X, Cai S, Xiong X, Sun W, Dai X, Chen S, Ye Q, Song Z, Jiang Q, Xu Z. Chemokine receptor CXCR7 mediates human endothelial progenitor cells survival, angiogenesis, but not proliferation. *Journal of Cellular Biochemistry* 2012;**113**:1437-1446.

113. Burns JM, Summers BC, Wang Y, Melikian A, Berahovich R, Miao Z, Penfold MET, Sunshine MJ, Littman DR, Kuo CJ, Wei K, McMaster BE, Wright K, Howard MC, Schall TJ. A novel chemokine receptor for SDF-1 and I-TAC involved in cell survival, cell adhesion, and tumor development. *Journal of Experimental Medicine* 2006;**203**:2201-2213.

114. Yu S, Crawford D, Tsuchihashi T, Behrens TW, Srivastava D. The Chemokine Receptor CXCR7 Functions to Regulate Cardiac Valve Remodeling. *Developmental Dynamics* 2011;**240**:384-393.

115. Hao HF, Hu S, Chen H, Bu DW, Zhu LY, Xu CS, Chu F, Huo XY, Tang Y, Sun XG, Ding BS, Liu DP, Hu SS, Wang M. Loss of Endothelial CXCR7 Impairs Vascular Homeostasis and Cardiac Remodeling After Myocardial Infarction Implications for Cardiovascular Drug Discovery. *Circulation* 2017;**135**:1253-+.

116. Nolan DJ, Ginsberg M, Israely E, Palikuqi B, Poulos MG, James D, Ding BS, Schachterle W, Liu Y, Rosenwaks Z, Butler JM, Xiang J, Rafii A, Shido K, Rabbany SY, Elemento O, Rafii S. Molecular Signatures of Tissue-Specific Microvascular Endothelial Cell Heterogeneity in Organ Maintenance and Regeneration. *Developmental Cell* 2013;**26**:204-219.

117. Wilson HK, Canfield SG, Shusta EV, Palecek SP. Concise Review: Tissue-Specific Microvascular Endothelial Cells Derived From Human Pluripotent Stem Cells. *Stem Cells* 2014;**32**:3037-3045.

118. Cencioni C, Capogrossi MC, Napolitano M. The SDF-1/CXCR4 axis in stem cell preconditioning. *Cardiovascular Research* 2012;**94**:400-407.

119. Sierro F, Biben C, Martinez-Munoz L, Mellado M, Ransohoff RM, Li M, Woehl B, Leung H, Groom J, Batten M, Harvey RP, Martinez-A C, Mackay CR, Mackay F. Disrupted cardiac development but normal hematopoiesis in mice deficient in the second CXCL12/SDF-1 receptor, CXCR7. *Proceedings of the National Academy of Sciences of the United States of America* 2007;**104**:14759-14764.

120. Levoye A, Balabanian K, Baleux F, Bachelerie F, Lagane B. CXCR7 heterodimerizes with CXCR4 and regulates CXCL12-mediated G protein signaling. *Blood* 2009;**113**:6085-6093.

121. Petrou T, Olsen HL, Thrasivoulou C, Masters JR, Ashmore JF, Ahmed A. Intracellular Calcium Mobilization in Response to Ion Channel Regulators via a Calcium-Induced Calcium Release Mechanisms. *Journal of Pharmacology and Experimental Therapeutics* 2017;**360**:378-387.

122. Agle KA, Vongsa RA, Dwinell MB. Calcium Mobilization Triggered by the Chemokine CXCL12 Regulates Migration in Wounded Intestinal Epithelial Monolayers. *Journal of Biological Chemistry* 2010;**285**:16066-16075.

123. Rajagopal S, Kim J, Ahn S, Craig S, Lam CM, Gerard NP, Gerard C, Lefkowitz RJ. beta-arrestin- but not G protein-mediated signaling by the "decoy" receptor CXCR7. *Proceedings of the National Academy of Sciences of the United States of America* 2010;**107**:628-632.

124. DeWire SM, Ahn S, Lefkowitz RJ, Shenoy SK. beta-arrestins and cell signaling. *Annual Review of Physiology* 2007;**69**:483-510.

125. Zabel BA, Wang Y, Lewen S, Berahovich RD, Penfold MET, Zhang PL, Powers J, Summers BC, Miao ZH, Zhao B, Jalili A, Janowska-Wieczorek A, Jaen JC, Schall TJ. Elucidation of CXCR7-Mediated Signaling Events and Inhibition of CXCR4-Mediated Tumor Cell Transendothelial Migration by CXCR7 Ligands. *Journal of Immunology* 2009;**183**:3204-3211.

126. Kalatskaya I, Berchiche YA, Gravel S, Limberg BJ, Rosenbaum JS, Heveker N. AMD3100 Is a CXCR7 Ligand with Allosteric Agonist Properties. *Molecular Pharmacology* 2009;**75**:1240-1247.

127. Oedemis V, Boosmann K, Heinen A, Kuery P, Engele J. CXCR7 is an active component of SDF-1 signalling in astrocytes and Schwann cells. *Journal of Cell Science* 2010;**123**:1081-1088.

128. Torossian F, Anginot A, Chabanon A, Clay D, Guerton B, Desterke C, Boutin L, Marullo S, Scott MGH, Lataillade JJ, Le Bousse-Kerdiles MC. CXCR7 participates in CXCL12-induced CD34(+) cell cycling through beta-arrestin-dependent Akt activation. *Blood* 2014;**123**:191-202.

129. Haraldsen G, Rot A. Commentary: Coy decoy with a new ploy: Interceptor controls the levels of homeostatic chemokines. *European Journal of Immunology* 2006;**36**:1659-1661.

130. Oedemis V, Lipfert J, Kraft R, Hajek P, Abraham G, Hattermann K, Mentlein R, Engele J. The presumed atypical chemokine receptor CXCR7 signals through Gi/o proteins in primary rodent astrocytes and human glioma cells. *Glia* 2012;**60**:372-381.

131. Singh AK, Arya RK, Trivedi AK, Sanyal S, Baral R, Dormond O, Briscoe DM, Datta D. Chemokine receptor trio: CXCR3, CXCR4 and CXCR7 crosstalk via CXCL11 and CXCL12. *Cytokine & Growth Factor Reviews* 2013;**24**:41-49.

132. Lipfert J, Odemis V, Engele J. Grk2 is an Essential Regulator of CXCR7 Signalling in Astrocytes. *Cellular and Molecular Neurobiology* 2013;**33**:111-118.

133. Naumann U, Cameroni E, Pruenster M, Mahabaleshwar H, Raz E, Zerwes H-G, Rot A, Thelen M. CXCR7 Functions as a Scavenger for CXCL12 and CXCL11. *Plos One* 2010;**5**.

134. Luker KE, Steele JM, Mihalko LA, Ray P, Luker GD. Constitutive and chemokine-dependent internalization and recycling of CXCR7 in breast cancer cells to degrade chemokine ligands. *Oncogene* 2010;**29**:4599-4610.

135. Decaillot FM, Kazmi MA, Lin Y, Ray-Saha S, Sakmar TP, Sachdev P. CXCR7/CXCR4 Heterodimer Constitutively Recruits beta-Arrestin to Enhance Cell Migration. *Journal of Biological Chemistry* 2011;**286**:32188-32197.

136. Luttrell LM, Lefkowitz RJ. The role of beta-arrestins in the termination and transduction of G-protein-coupled receptor signals. *Journal of Cell Science* 2002;**115**:455-465.

137. Molyneaux KA, Zinszner H, Kunwar PS, Schaible K, Stebler J, Sunshine MJ, O'Brien W, Raz E, Littman D, Wylie C, Lehmann R. The chemokine SDF1/CXCL12 and its receptor CXCR4 regulate mouse germ cell migration and survival. *Development* 2003;**130**:4279-4286.

138. Kavanagh DPJ, Kalia N. Hematopoietic Stem Cell Homing to Injured Tissues. *Stem Cell Reviews and Reports* 2011;**7**:672-682.

139. Drury LJ, Ziarek JJ, Gravel S, Veldkamp CT, Takekoshi T, Hwang ST, Heveker N, Volkman BF, Dwinell MB. Monomeric and dimeric CXCL12 inhibit metastasis through distinct CXCR4 interactions and signaling pathways. *Proceedings of the National Academy of Sciences of the United States of America* 2011;**108**:17655-17660.

140. Ray P, Lewin SA, Mihalko LA, Lesher-Perez S-C, Takayama S, Luker KE, Luker GD. Secreted CXCL12 (SDF-1) forms dimers under physiological conditions. *Biochemical Journal* 2012;**442**:433-442.

141. Boldajipour B, Mahabaleshwar H, Kardash E, Reichman-Fried M, Blaser H, Minina S, Wilson D, Xu Q, Raz E. Control of chemokine-guided cell migration by ligand sequestration. *Cell* 2008;**132**:463-473.

142. Song ZY, Wang F, Cui SX, Gao ZH, Qu XJ. CXCR7/CXCR4 heterodimer-induced histone demethylation: a new mechanism of colorectal tumorigenesis. *Oncogene* 2019;**38**:1560-1575.

143. Sanchez-Martin L, Estecha A, Samaniego R, Sanchez-Ramon S, Angel Vega M, Sanchez-Mateos P. The chemokine CXCL12 regulates monocyte-macrophage differentiation and RUNX3 expression. *Blood* 2011;**117**:88-97.

144. Hartmann TN, Grabovsky V, Pasvolsky R, Shulman Z, Buss EC, Spiegel A, Nagler A, Lapidot T, Thelen M, Alon R. A crosstalk between intracellular CXCR7 and CXCR4 involved in rapid CXCL12-triggered integrin activation but not in chemokine-triggered motility of human T lymphocytes and CD34(+) cells. *Journal of Leukocyte Biology* 2008;**84**:1130-1140.

145. Lavine KJ, Ornitz DM. Shared Circuitry Developmental Signaling Cascades Regulate Both Embryonic and Adult Coronary Vasculature. *Circulation Research* 2009;**104**:159-169.

146. Ma Q, Jones D, Borghesani PR, Segal RA, Nagasawa T, Kishimoto T, Bronson RT, Springer TA. Impaired B-lymphopoiesis, myelopoiesis, and derailed cerebellar neuron migration in CXCR4- and SDF-1-deficient mice. *Proceedings of the National Academy of Sciences of the United States of America* 1998;**95**:9448-9453.

147. Nagasawa T, Hirota S, Tachibana K, Takakura N, Nishikawa S, Kitamura Y, Yoshida N, Kikutani H, Kishimoto T. Defects of B-cell lymphopoiesis and bone-marrow myelopoiesis in mice lacking the CXC chemokine PBSF/SDF-1. *Nature* 1996;**382**:635-638.

148. Gerrits H, Schenau DSvI, Bakker NEC, van Disseldorp AJM, Strik A, Hermens LS, Koenen TB, Krajnc-Franken MAM, Gossen JA. Early postnatal lethality and cardiovascular defects in CXCR7-deficient mice. *Genesis* 2008;**46**:235-245.

149. Puchert M, Engele J. The peculiarities of the SDF-1/CXCL12 system: in some cells, CXCR4 and CXCR7 sing solos, in others, they sing duets. *Cell and Tissue Research* 2014;**355**:239-253.

150. Tamamura H, Xu YO, Hattori T, Zhang XY, Arakaki R, Kanbara K, Omagari A, Otaka A, Ibuka T, Yamamoto N, Nakashima H, Fujii N. A low-molecular-weight inhibitor against the chemokine receptor CXCR4: A strong anti-HIV peptide T140. *Biochemical and Biophysical Research Communications* 1998;**253**:877-882.

151. Montpas N, Cabana J, St-Onge G, Gravel S, Morin G, Kuroyanagi T, Lavigne P, Fujii N, Oishi S, Heveker N. Mode of Binding of the Cyclic Agonist Peptide TC14012 to CXCR7: Identification of Receptor and Compound Determinants. *Biochemistry* 2015;**54**:1505-1515.

152. Tamamura H, Omagari A, Hiramatsu K, Gotoh K, Kanamoto T, Xu YN, Kodama E, Matsuoka M, Hattori T, Yamamoto N, Nakashima H, Otaka A, Fujii N. Development of specific CXCR4 inhibitors possessing high selectivity indexes as well as complete stability in serum based on an anti-HIV peptide T140. *Bioorganic & Medicinal Chemistry Letters* 2001;**11**:1897-1902.

153. Wijtmans M, Maussang D, Sirci F, Scholten DJ, Canals M, Mujic-Delic A, Chong M, Chatalic KLS, Custers H, Janssen E, de Graaf C, Smit MJ, de Esch IJP, Leurs R. Synthesis, modeling

and functional activity of substituted styrene-amides as small-molecule CXCR7 agonists. *European Journal of Medicinal Chemistry* 2012;**51**:184-192.

154. Messerli FH, Bangalore S, Yao SS, Steinberg JS. Cardioprotection with beta-blockers: myths, facts and Pascal's wager. *Journal of Internal Medicine* 2009;**266**:232-241.

155. Van de Werf F, Janssens L, Brzostek T, Mortelmans L, Wackers FJT, Willems GM, Heidbuchel H, Lesaffre E, Scheys I, Collen D, De Geest H. Short-Term Effects of Early Intravenous Treatment With a Beta-Adrenergic Blocking Agent or a Specific Bradycardiac Agent in Patients With Acute Myocardial Infarction Receiving Thrombolytic Therapy. *Journal of the American College of Cardiology* 1993;**22**:407-416.

156. Hjalmarson A, Armitage P, Chamberlain D, Lubsen J, Yusuf S. Metoprolol in acute myocardial-infarction (Miami) - a randomized placebo-controlled international trial. *European Heart Journal* 1985;**6**:199-226.

157. Roberts R, Rogers WJ, Mueller HS, Lambrew CT, Diver DJ, Smith HC, Willerson JT, Knatterud GL, Forman S, Passamani E, Zaret BL, Wackers FJT, Braunwald E. Immediate versus deferred beta-blockade following thrombolytic therapy in patients with acute myocardial-infarction -results of the Thrombolysis In Myocardial-Infarction (TIMI) II-B study. *Circulation* 1991;**83**:422-437.

158. Pfisterer M, Cox JL, Granger CB, Brener SJ, Naylor CD, Califf RM, van de Werf F, Stebbins AL, Lee KL, Topol EJ, Armstrong PW, Investigators G-I. Atenolol use and clinical outcomes after thrombolysis for acute myocardial infarction: The GUSTO-I experience. *Journal of the American College of Cardiology* 1998;**32**:634-640.

159. Schwartz BG, Kloner RA, Thomas JL, Bui Q, Mayeda GS, Burstein S, Hale SL, Economides C, French WJ. Therapeutic Hypothermia for Acute Myocardial Infarction and Cardiac Arrest. *American Journal of Cardiology* 2012;**110**:461-466.

160. Erlinge D, Gotberg M, Noc M, Lang I, Holzer M, Clemmensen P, Jensen U, Metzler B, James S, Botker HE, Omerovic E, Koul S, Engblom H, Carlsson M, Arheden H, Ostlund O, Wallentin L, Klos B, Harnek J, Olivecrona GK. Therapeutic Hypothermia for the Treatment of Acute Myocardial Infarction-Combined Analysis of the RAPID MI-ICE and the CHILL-MI Trials. *Therapeutic Hypothermia and Temperature Management* 2015;**5**:77-84.

161. Batista LM, Lima FO, Januzzi JL, Donahue V, Snydeman C, Greer DM. Feasibility and safety of combined percutaneous coronary intervention and therapeutic hypothermia following cardiac arrest. *Resuscitation* 2010;**81**:398-403.

162. Boyce SW, Bartels C, Bolli R, Chaitman B, Chen JC, Chi E, Jessel A, Kereiakes D, Knight J, Thulin L, Theroux P, Investigators GS. Impact of sodium-hydrogen exchange inhibition by cariporide on death or myocardial infarction in high-risk CABG surgery patients: Results of the CABG surgery cohort of the GUARDIAN study. *Journal of Thoracic and Cardiovascular Surgery* 2003;**126**:420-427.

163. Avkiran M, Marber MS. Na+/H+ exchange inhibitors for cardioprotective therapy: Progress, problems and prospects. *Journal of the American College of Cardiology* 2002;**39**:747-753.

164. Mentzer RM, Bartels C, Bolli R, Boyce S, Buckberg GD, Chaitman B, Haverich A, Knight J, Menasche P, Myers ML, Nicolau J, Simoons M, Thulin L, Weisel RD, Investigators ES. Sodium-hydrogen exchange inhibition by cariporide to reduce the risk of ischemic cardiac events in patients undergoing coronary artery bypass grafting: Results of the EXPEDITION study. *Annals of Thoracic Surgery* 2008;**85**:1261-1270.

165. Hausenloy DJ, Boston-Griffiths E, Yellon DM. Cardioprotection during cardiac surgery. *Cardiovascular Research* 2012;**94**:253-265.

166. Reddy K, Khaliq A, Henning RJ. Recent advances in the diagnosis and treatment of acute myocardial infarction. *World Journal of Cardiology* 2015;**7**:243-276.

167. Hiatt MD. Thrombolytic therapy with streptokinase and tissue plasminogen activator in a patient with suspected acute myocardial infarction: A decision analysis. *Cardiology* 1999;**91**:243-249.

168. White HD, Van de Werf FJJ. Thrombolysis for acute myocardial infarction. *Circulation* 1998;**97**:1632-1646.

169. Zhang Y, Huo Y. Early reperfusion strategy for acute myocardial infarction: a need for clinical implementation. *Journal of Zhejiang University-Science B* 2011;**12**:629-632.

170. Kato R, Foex P. Myocardial protection by anesthetic agents against ischemia-reperfusion injury: an update for anesthesiologists. *Canadian Journal of Anaesthesia-Journal Canadien D Anesthesie* 2002;**49**:777-791.

171. Symons JA, Myles PS. Myocardial protection with volatile anaesthetic agents during coronary artery bypass surgery: a meta-analysis. *British Journal of Anaesthesia* 2006;**97**:127-136.

172. Freedman BM, Hamm DP, Everson CT, Wechsler AS, Christian CM. Enflurane enhances postischemic functional recovery in the isolated rat-heart. *Anesthesiology* 1985;**62**:29-33.

173. Feng JH, Lucchinetti E, Ahuja P, Pasch T, Perriard JC, Zaugg M. Isoflurane postconditioning prevents opening of the mitochondrial permeability transition pore through inhibition of glycogen synthase kinase 3 beta. *Anesthesiology* 2005;**103**:987-995.

174. Bose AK, Mocanu MM, Carr RD, Brand CL, Yellon DM. Glucagon-like peptide 1 can directly protect the heart against ischemia/reperfusion injury. *Diabetes* 2005;**54**:146-151.

175. Timmers L, Henriques JPS, de Kleijn DPV, DeVries JH, Kemperman H, Steendijk P, Verlaan CWJ, Kerver M, Piek JJ, Doevendans PA, Pasterkamp G, Hoefer IE. Exenatide Reduces

Infarct Size and Improves Cardiac Function in a Porcine Model of Ischemia and Reperfusion Injury. *Journal of the American College of Cardiology* 2009;**53**:501-510.

176. Bulluck H, Yellon DM, Hausenloy DJ. Reducing myocardial infarct size: challenges and future opportunities. *Heart* 2016;**102**:341-348.

177. Ong SB, Samangouei P, Kalkhoran SB, Hausenloy DJ. The mitochondrial permeability transition pore and its role in myocardial ischemia reperfusion injury. *Journal of Molecular and Cellular Cardiology* 2015;**78**:23-34.

178. Cung TT, Morel O, Cayla G, Rioufol G, Garcia-Dorado D, Angoulvant D, Bonnefoy-Cudraz E, Guerin P, Elbaz M, Delarche N, Coste P, Vanzetto G, Metge M, Aupetit JF, Jouve B, Motreff P, Tron C, Labeque JN, Steg PG, Cottin Y, Range G, Clerc J, Claeys MJ, Coussement P, Prunier F, Moulin F, Roth O, Belle L, Dubois P, Barragan P, Gilard M, Piot C, Colin P, De Poli F, Morice MC, Ider O, Dubois-Rande JL, Unterseeh T, Le Breton H, Beard T, Blanchard D, Grollier G, Malquarti V, Staat P, Sudre A, Elmer E, Hansson MJ, Bergerot C, Boussaha I, Jossan C, Derumeaux G, Mewton N, Ovize M. Cyclosporine before PCI in Patients with Acute Myocardial Infarction. *New England Journal of Medicine* 2015;**373**:1021-1031.

179. Murry CE, Jennings RB, Reimer KA. Preconditioning with ischemia - a delay of lethal cell injury in ischemic myocardium. *Circulation* 1986;**74**:1124-1136.

180. Yellon DM, Baxter GF, Garcia-Dorado D, Heusch G, Sumeray MS. Ischaemic preconditioning: present position and future directions. *Cardiovascular Research* 1998;**37**:21-33.

181. Schott RJ, Rohmann S, Braun ER, Schaper W. Ischemic preconditioning reduces infarct size in swine myocardium. *Circulation Research* 1990;**66**:1133-1142.

182. Liu GS, Thornton J, Vanwinkle DM, Stanley AWH, Olsson RA, Downey JM. Protection against infarction afforded by preconditioning is mediated by A1 adenosine receptors in rabbit heart. *Circulation* 1991;**84**:350-356.

183. Liu YG, Downey JM. Ischemic preconditioning protects against infarction in rat-heart. *American Journal of Physiology* 1992;**263**:H1107-H1111.

184. Zhao ZQ, Corvera JS, Halkos ME, Kerendi F, Wang NP, Guyton RA, Vinter-Johansen J. Inhibition of myocardial injury by ischemic postconditioning during reperfusion: comparison with ischemic preconditioning. *American Journal of Physiology-Heart and Circulatory Physiology* 2003;**285**:H579-H588.

185. Zhao ZQ, Vinten-Johansen J. Postconditioning: Reduction of reperfusion-induced injury. *Cardiovascular Research* 2006;**70**:200-211.

186. Staat P, Rioufol G, Piot C, Cottin Y, Cung TT, L'Huillier I, Aupetit JF, Bonnefoy E, Finet G, Andre-Fouet X, Ovize M. Postconditioning the human heart. *Circulation* 2005;**112**:2143-2148.

187. Engstrom T, Kelbaek H, Helqvist S, Hofsten DE, Klovgaard L, Holmvang L, Jorgensen E, Pedersen F, Saunamaki K, Clemmensen P, De Backer O, Ravkilde J, Tilsted HH, Villadsen AB, Aaroe J, Jensen SE, Raungaard B, Kober L, Investigators D-P. Complete revascularisation versus treatment of the culprit lesion only in patients with ST-segment elevation myocardial infarction and multivessel disease (DANAMI-3-PRIMULTI): an open-label, randomised controlled trial. *Lancet* 2015;**386**:665-671.

188. Hahn JY, Song YB, Kim EK, Yu CW, Bae JW, Chung WY, Choi SH, Choi JH, Bae JH, An KJ, Park JS, Oh JH, Kim SW, Hwang JY, Ryu JK, Park HS, Lim DS, Gwon HC. Ischemic Postconditioning During Primary Percutaneous Coronary Intervention The Effects of Postconditioning on Myocardial Reperfusion in Patients With ST-Segment Elevation Myocardial Infarction (POST) Randomized Trial. *Circulation* 2013;**128**:1889-1896.

189. Schulman D, Latchman DS, Yellon DM. Urocortin protects the heart from reperfusion injury via upregulation of p42/p44 MAPK signaling pathway. *American Journal of Physiology-Heart and Circulatory Physiology* 2002;**283**:H1481-H1488.

190. Rossello X, Yellon DM. The RISK pathway and beyond. *Basic Research in Cardiology* 2018;**113**.

191. Hausenloy DJ, Tsang A, Mocanu MM, Yellon DM. Ischemic preconditioning protects by activating prosurvival kinases at reperfusion. *American Journal of Physiology-Heart and Circulatory Physiology* 2005;**288**:H971-H976.

192. Hausenloy DJ, Yellon DM. Reperfusion injury salvage kinase signalling: taking a RISK for cardioprotection. *Heart Failure Reviews* 2007;**12**:217-234.

193. Hausenloy DJ, Duchen MR, Yellon DM. Inhibiting mitochondrial permeability transition pore opening at reperfusion protects against ischaemia-reperfusion injury. *Cardiovascular Research* 2003;**60**:617-625.

194. Davidson SM, Hausenloy D, Duchen MR, Yellon DM. Signalling via the reperfusion injury signalling kinase (RISK) pathway links closure of the mitochondrial permeability transition pore to cardioprotection. *International Journal of Biochemistry & Cell Biology* 2006;**38**:414-419.

195. Headrick JP, Hoe LES, Du Toit EF, Peart JN. Opioid receptors and cardioprotection - 'opioidergic conditioning' of the heart. *British Journal of Pharmacology* 2015;**172**:2026-2050.

196. Salie R, Moolman JA, Lochner A. The mechanism of beta-adrenergic preconditioning: roles for adenosine and ROS during triggering and mediation. *Basic Research in Cardiology* 2012;**107**.

197. Manning BD, Toker A. AKT/PKB Signaling: Navigating the Network. *Cell* 2017;**169**:381-405.

198. Wortzel I, Seger R. The ERK Cascade: Distinct Functions within Various Subcellular Organelles. *Genes & cancer* 2011;**2**:195-209.

199. Lacerda L, Somers S, Opie LH, Lecour S. Ischaemic postconditioning protects against reperfusion injury via the SAFE pathway. *Cardiovascular Research* 2009;**84**:201-208.

200. Kalakech H, Hibert P, Prunier-Mirebeau D, Tamareille S, Letournel F, Macchi L, Pinet F, Furber A, Prunier F. RISK and SAFE Signaling Pathway Involvement in Apolipoprotein A-I-Induced Cardioprotection. *Plos One* 2014;**9**.

201. Heusch G. Molecular Basis of Cardioprotection Signal Transduction in Ischemic Pre-, Post-, and Remote Conditioning. *Circulation Research* 2015;**116**:674-699.

202. Ovize M, Baxter GF, Di Lisa F, Ferdinandy P, Garcia-Dorado D, Hausenloy DJ, Heusch G, Vinten-Johansen J, Yellon DM, Schulz R. Postconditioning and protection from reperfusion injury: where do we stand?Position Paper from the Working Group of Cellular Biology of the Heart of the European Society of Cardiology. *Cardiovascular Research* 2010;**87**:406-423.

203. Huang CY, Gu HM, Zhang WJ, Manukyan MC, Shou WNA, Wang MJ. SDF-1/CXCR4 mediates acute protection of cardiac function through myocardial STAT3 signaling following global ischemia/reperfusion injury. *American Journal of Physiology-Heart and Circulatory Physiology* 2011;**301**:H1496-H1505.

204. Huang CY, Gu HM, Yu Q, Manukyan MC, Poynter JA, Wang MJ. Sca-1+Cardiac Stem Cells Mediate Acute Cardioprotection via Paracrine Factor SDF-1 following Myocardial Ischemia/Reperfusion. *Plos One* 2011;**6**.

205. Dong F, Harvey J, Finan A, Weber K, Agarwal U, Penn MS. Myocardial CXCR4 Expression Is Required for Mesenchymal Stem Cell Mediated Repair Following Acute Myocardial Infarction. *Circulation* 2012;**126**:314-324.

206. Penn MS, Pastore J, Miller T, Aras R. SDF-1 in myocardial repair. *Gene Therapy* 2012;**19**:583-587.

207. MacArthur JW, Jr., Purcell BP, Shudo Y, Cohen JE, Fairman A, Trubelja A, Patel J, Hsiao P, Yang E, Lloyd K, Hiesinger W, Atluri P, Burdick JA, Woo YJ. Sustained Release of Engineered Stromal Cell-Derived Factor 1-alpha From Injectable Hydrogels Effectively Recruits Endothelial Progenitor Cells and Preserves Ventricular Function After Myocardial Infarction. *Circulation* 2013;**128**:S79-S86.

208. Elmadbouh I, Haider HK, Jiang SJ, Idris NM, Lu G, Ashraf M. Ex vivo delivered stromal cell-derived factor-1 alpha promotes stem cell homing and induces angiomyogenesis in the infarcted myocardium. *Journal of Molecular and Cellular Cardiology* 2007;**42**:792-803.

209. Deglurkar I, Mal N, Mills WR, Popovic ZB, McCarthy P, Blackstone EH, Laurita KR, Penn MS. Mechanical and electrical effects of cell-based gene therapy for ischemic cardiomyopathy are independent. *Human Gene Therapy* 2006;**17**:1144-1151.

210. Liehn EA, Tuchscheerer N, Kanzler I, Drechsler M, Fraemohs L, Schuh A, Koenen RR, Zander S, Soehnlein O, Hristov M, Grigorescu G, Urs AO, Leabu M, Bucur I, Merx MW, Zernecke A, Ehling J, Gremse F, Lammers T, Kiessling F, Bernhagen J, Schober A, Weber C. Double-Edged Role of the CXCL12/CXCR4 Axis in Experimental Myocardial Infarction. *Journal of the American College of Cardiology* 2011;**58**:2415-2423.

211. Chen JQ, Chemaly E, Liang LF, Kho C, Lee A, Park J, Altman P, Schecter AD, Hajjar RJ, Tarzami ST. Effects of CXCR4 Gene Transfer on Cardiac Function After Ischemia-Reperfusion Injury. *American Journal of Pathology* 2010;**176**:1705-1715.

212. Muhlstedt S, Ghadge SK, Duchene J, Qadri F, Jarve A, Vilianovich L, Popova E, Pohlmann A, Niendorf T, Boye P, Ozcelik C, Bader M. Cardiomyocyte-derived CXCL12 is not involved in cardiogenesis but plays a crucial role in myocardial infarction. *Journal of Molecular Medicine-Jmm* 2016;**94**:1005-1014.

213. Agarwal U, Ghalayini W, Dong F, Weber K, Zou YR, Rabbany SY, Rafii S, Penn MS. Role of Cardiac Myocyte CXCR4 Expression in Development and Left Ventricular Remodeling After Acute Myocardial Infarction. *Circulation Research* 2010;**107**:667-U236.

214. Lin L, Han MM, Wang F, Xu LL, Yu HX, Yang PY. CXCR7 stimulates MAPK signaling to regulate hepatocellular carcinoma progression. *Cell Death & Disease* 2014;**5**.

215. Lazennec G, Richmond A. Chemokines and chemokine receptors: new insights into cancer-related inflammation. *Trends in Molecular Medicine* 2010;**16**:133-144.

216. Kruizinga RC, Bestebroer J, Berghuis P, de Haas CJC, Links TP, de Vries EGE, Walenkamp AME. Role of Chemokines and Their Receptors in Cancer. *Current Pharmaceutical Design* 2009;**15**:3396-3416.

217. Sun XQ, Cheng GC, Hao MG, Zheng JH, Zhou XM, Zhang JA, Taichman RS, Pienta KJ, Wang JH. CXCL12/CXCR4/CXCR7 chemokine axis and cancer progression. *Cancer and Metastasis Reviews* 2010;**29**:709-722.

218. Barbieri F, Bajetto A, Thellung S, Wurth R, Florio T. Drug design strategies focusing on the CXCR4/CXCR7/CXCL12 pathway in leukemia and lymphoma. *Expert Opinion on Drug Discovery* 2016;**11**:1093-1109.

219. Chen D, Xia Y, Zuo K, Wang Y, Zhang S, Kuang D, Duan Y, Zhao X, Wang G. Crosstalk between SDF-1/CXCR4 and SDF-1/CXCR7 in cardiac stem cell migration. *Scientific Reports* 2015;**5**.

220. Kumar R, Tripathi V, Ahmad M, Nath N, Mir RA, Chauhan SS, Luthra K. CXCR7 mediated Gi alpha independent activation of ERK and Akt promotes cell survival and chemotaxis in T cells. *Cellular Immunology* 2012;**272**:230-241.

221. Zhao Y, Tan Y, Xi S, Li Y, Li C, Cui J, Yan X, Li X, Wang G, Li W, Cai L. A Novel Mechanism by Which SDF-1 beta Protects Cardiac Cells From Palmitate-Induced Endoplasmic Reticulum

Stress and Apoptosis via CXCR7 and AMPK/p38 MAPK-Mediated Interleukin-6 Generation. *Diabetes* 2013;**62**:2545-2558.

222. Zhang M, Qiu LS, Zhang YY, Xu DS, Zheng JLC, Jiang L. CXCL12 enhances angiogenesis through CXCR7 activation in human umbilical vein endothelial cells. *Scientific Reports* 2017;**7**.

223. Prasad A, Gersh BJ. Management of microvascular dysfunction and reperfusion injury. *Heart* 2005;**91**:1530-1532.

224. Wu GF, Du ZM, Hu CH, Zheng ZS, Zhan CY, Ma H, Fang DQ, Hui JCK, Lawson WE. Microvessel angiogenesis : a possible card ioprotective mechanism of external counterpulsation for canine myocardial infarction. *Chinese Medical Journal* 2005;**118**:1182-1189.

225. Cochain C, Channon KM, Silvestre JS. Angiogenesis in the Infarcted Myocardium. *Antioxidants & Redox Signaling* 2013;**18**:1100-1113.

226. Karam R, Healy BP, Wicker P. CORONARY RESERVE IS DEPRESSED IN POSTMYOCARDIAL INFARCTION REACTIVE CARDIAC-HYPERTROPHY. *Circulation* 1990;**81**:238-246.

227. Shafei AE-S, Ali MA, Ghanem HG, Shehata AI, Abdelgawad AA, Handal HR, Talaat KA, Ashaal AE, El-Shal AS. Mesenchymal stem cell therapy: A promising cell-based therapy for treatment of myocardial infarction. *Journal of Gene Medicine* 2017;**19**.

228. Korf-Klingebiel M, Reboll MR, Klede S, Brod T, Pich A, Polten F, Napp LC, Bauersachs J, Ganser A, Brinkmann E, Reimann I, Kempf T, Niessen HW, Mizrahi J, Schoenfeld H-J, Iglesias A, Bobadilla M, Wang Y, Wollert KC. Myeloid-derived growth factor (C19orf10) mediates cardiac repair following myocardial infarction. *Nature Medicine* 2015;**21**:52-61.

229. Deshane J, Chen SF, Caballero S, Grochot-Przeczek A, Was H, Calzi SL, Lach R, Hock TD, Chen B, Hill-Kapturczak N, Siegal GP, Dulak J, Jozkowicz A, Grant MB, Agarwal A. Stromal cell-derived factor 1 promotes angiogenesis via a heme oxygenase 1-dependent mechanism. *Journal of Experimental Medicine* 2007;**204**:605-618.

230. Zheng H, Fu G, Dai T, Huang H. Migration of endothelial progenitor cells mediated by stromal cell-derived Factor-1 alpha/CXCR4 via PI3K/Akt/eNOS signal transduction pathway. *Journal of Cardiovascular Pharmacology* 2007;**50**:274-280.

231. Orlic D, Kajstura J, Chimenti S, Jakoniuk I, Anderson SM, Li BS, Pickel J, McKay R, Nadal-Ginard B, Bodine DM, Leri A, Anversa P. Bone marrow cells regenerate infarcted myocardium. *Nature* 2001;**410**:701-705.

232. Turan RG, Bozdag-Turan I, Ortak J, Akin I, Kische S, Schneider H, Rehders TC, Turan CH, Rauchhaus M, Kleinfeldt T, Chatterjee T, Sahin K, Nienaber CA, Ince H. Improvement of Cardiac Function by Intracoronary Freshly Isolated Bone Marrow Cells Transplantation in Patients With Acute Myocardial Infarction. *Circulation Journal* 2011;**75**:683-691.

233. Gao LR, Chen Y, Zhang NK, Yang XL, Liu HL, Wang ZG, Yan XY, Wang Y, Zhu ZM, Li TC, Wang LH, Chen HY, Chen YD, Huang CL, Qu P, Yao C, Wang B, Chen GH, Wang ZM, Xu ZY, Bai J, Lu D, Shen YH, Guo F, Liu MY, Yang Y, Ding YC, Tian HT, Ding QA, Li LN, Yang XC, Hu X. Intracoronary infusion of Wharton's jelly-derived mesenchymal stem cells in acute myocardial infarction: double-blind, randomized controlled trial. *Bmc Medicine* 2015;**13**.

234. Ding B-S, Cao Z, Lis R, Nolan DJ, Guo P, Simons M, Penfold ME, Shido K, Rabbany SY, Rafii S. Divergent angiocrine signals from vascular niche balance liver regeneration and fibrosis. *Nature* 2014;**505**:97-+.

235. Rafii S, Cao ZW, Lis R, Siempos, II, Chavez D, Shido K, Rabbany SY, Ding BS. Platelet-derived SDF-1 primes the pulmonary capillary vascular niche to drive lung alveolar regeneration. *Nature Cell Biology* 2015;**17**:123-+.

236. Saha A, Ahn S, Blando J, Su F, Kolonin MG, DiGiovanni J. Proinflammatory CXCL12-CXCR4/CXCR7 Signaling Axis Drives Myc-Induced Prostate Cancer in Obese Mice. *Cancer Research* 2017;**77**:5158-5168.

237. Zhang HW, Yang L, Teng XY, Liu ZY, Liu CX, Zhang L, Liu Z. The chemokine receptor CXCR7 is a critical regulator for the tumorigenesis and development of papillary thyroid carcinoma by inducing angiogenesis in vitro and in vivo. *Tumor Biology* 2016;**37**:2415-2423.

238. Miao Z, Luker KE, Summers BC, Berahovich R, Bhojani MS, Rehemtulla A, Kleer CG, Essner JJ, Nasevicius A, Luker GD, Howard MC, Schall TJ. CXCR7 (RDC1) promotes breast and lung tumor growth in vivo and is expressed on tumor-associated vasculature. *Proceedings of the National Academy of Sciences of the United States of America* 2007;**104**:15735-15740.

239. Raggo C, Ruhl R, McAllister S, Koon H, Dezube BJ, Fruh K, Moses AV. Novel cellular genes essential for transformation of endothelial cells by Kaposi's sarcoma-associated herpesvirus. *Cancer Research* 2005;**65**:5084-5095.

240. Cao ZW, Lis R, Ginsberg M, Chayez D, Shido K, Rabbany SY, Fong GH, Sakmar TP, Rafii S, Ding BS. Targeting of the pulmonary capillary vascular niche promotes lung alveolar repair and ameliorates fibrosis. *Nature Medicine* 2016;**22**:154-162.

241. Feil R, Wagner J, Metzger D, Chambon P. Regulation of Cre recombinase activity by mutated estrogen receptor ligand-binding domains. *Biochemical and Biophysical Research Communications* 1997;**237**:752-757.

242. Jullien N, Goddard I, Selmi-Ruby S, Fina JL, Cremer H, Herman JP. Use of ERT2-iCre-ERT2 for conditional transgenesis. *Genesis* 2008;**46**:193-199.

243. Claxton S, Kostourou V, Jadeja S, Chambon P, Hodivala-Dilke K, Fruttiger M. Efficient, inducible Cre-recombinase activation in vascular endothelium. *Genesis* 2008;**46**:74-80.

244. Nie YC, Waite J, Brewer F, Sunshine MJ, Littman DR, Zou YR. The role of CXCR4 in maintaining peripheral B cell compartments and humoral immunity. *Journal of Experimental Medicine* 2004;**200**:1145-1156.

245. Zhang JF, Zhong W, Cui TX, Hu X, Xu KF, Xie CQ, Xue CY, Gibbons GH, Chen YQE, Yang MZ, Li L, Liu CY. Generation of an adult smooth muscle cell-targeted Cre recombinase mouse model. *Arteriosclerosis Thrombosis and Vascular Biology* 2006;**26**:E23-E24.

246. Bouabe H, Okkenhaug K. Gene Targeting in Mice: A Review. *Virus-Host Interactions: Methods and Protocols* 2013;**1064**:315-336.

247. Lexow J, Poggioli T, Sarathchandra P, Santini MP, Rosenthal N. Cardiac fibrosis in mice expressing an inducible myocardial-specific Cre driver. *Disease Models & Mechanisms* 2013;**6**:1470-1476.

248. Korbie DJ, Mattick JS. Touchdown PCR for increased specificity and sensitivity in PCR amplification. *Nature Protocols* 2008;**3**:1452-1456.

249. Champy MF, Selloum M, Zeitler V, Caradec C, Jung B, Rousseau S, Pouilly L, Sorg T, Auwerx J. Genetic background determines metabolic phenotypes in the mouse. *Mammalian Genome* 2008;**19**:318-331.

250. Voyta JC, Via DP, Butterfield CE, Zetter BR. Identification and isolation of endothelial-cells based on their increased uptake of acetylated-low density lipoprotein. *Journal of Cell Biology* 1984;**99**:2034-2040.

251. Yellon DM, Downey JM. Preconditioning the myocardium: From cellular physiology to clinical cardiology. *Physiological Reviews* 2003;**83**:1113-1151.

252. Botker HE, Hausenloy D, Andreadou I, Antonucci S, Boengler K, Davidson SM, Deshwal S, Devaux Y, Di Lisa F, Di Sante M, Efentakis P, Femmino S, Garcia-Dorado D, Giricz Z, Ibanez B, Iliodromitis E, Kaludercic N, Kleinbongard P, Neuhauser M, Ovize M, Pagliaro P, Rahbek-Schmidt M, Ruiz-Meana M, Schluter KD, Schulz R, Skyschally A, Wilder C, Yellon DM, Ferdinandy P, Heusch G. Practical guidelines for rigor and reproducibility in preclinical and clinical studies on cardioprotection. *Basic Research in Cardiology* 2018;**113**.

253. Fishbein MC, Meerbaum S, Rit J, Lando U, Kanmatsuse K, Mercier JC, Corday E, Ganz W. EARLY PHASE ACUTE MYOCARDIAL INFARCT SIZE QUANTIFICATION - VALIDATION OF THE TRIPHENYL TETRAZOLIUM CHLORIDE TISSUE ENZYME STAINING TECHNIQUE. *American Heart Journal* 1981;**101**:593-600.

254. Povlsen JA, Lofgren B, Dalgas C, Jespersen NR, Johnsen J, Botker HE. Frequent biomarker analysis in the isolated perfused heart reveals two distinct phases of reperfusion injury. *International Journal of Cardiology* 2014;**171**:9-14.

255. Rossello X, Hall AR, Bell RM, Yellon DM. Characterization of the Langendorff Perfused Isolated Mouse Heart Model of Global Ischemia-Reperfusion Injury: Impact of Ischemia

and Reperfusion Length on Infarct Size and LDH Release. *Journal of Cardiovascular Pharmacology and Therapeutics* 2016;**21**:286-295.

256. Latimer P. LIGHT-SCATTERING VS MICROSCOPY FOR MEASURING AVERAGE CELL-SIZE AND SHAPE. *Biophysical Journal* 1979;**27**:117-126.

257. Benson MC, McDougal DC, Coffey DS. THE APPLICATION OF PERPENDICULAR AND FORWARD LIGHT SCATTER TO ASSESS NUCLEAR AND CELLULAR MORPHOLOGY. *Cytometry* 1984;**5**:515-522.

258. Rieger AM, Barreda DR. Accurate Assessment of Cell Death by Imaging Flow Cytometry. *Imaging Flow Cytometry: Methods and Protocols* 2016:209-220.

259. Romashko DN, Marban E, O'Rourke B. Subcellular metabolic transients and mitochondrial redox waves in heart cells. *Proceedings of the National Academy of Sciences of the United States of America* 1998;**95**:1618-1623.

260. Obata Y, Yamamoto K, Miyazaki M, Shimotohno K, Kohno S, Matsuyama T. Role of cyclophilin B in activation of interferon regulatory factor-3. *Journal of Biological Chemistry* 2005;**280**:18355-18360.

261. Allain F, Vanpouille C, Carpentier M, Slomianny MC, Durieux S, Spik G. Interaction with glycosaminoglycans is required for cyclophilin B to trigger integrin-mediated adhesion of peripheral blood T lymphocytes to extracellular matrix. *Proceedings of the National Academy of Sciences of the United States of America* 2002;**99**:2714-2719.

262. Wang P, Heitman J. The cyclophilins. *Genome Biology* 2005;**6**.

263. Zhang H, Fan Q, Xie HY, Lu L, Tao R, Wang F, Xi R, Hu J, Chen QJ, Shen WF, Zhang RY, Yan XX. Elevated Serum Cyclophilin B Levels Are Associated with the Prevalence and Severity of Metabolic Syndrome. *Frontiers in Endocrinology* 2017;**8**.

264. Rodionov DA, Vitreschak AG, Mironov AA, Gelfand MS. Regulation of lysine biosynthesis and transport genes in bacteria: yet another RNA riboswitch? *Nucleic Acids Research* 2003;**31**:6748-6757.

265. Berahovich RD, Zabel BA, Lewen S, Walters MJ, Ebsworth K, Wang Y, Jaen JC, Schall TJ. Endothelial expression of CXCR7 and the regulation of systemic CXCL12 levels. *Immunology* 2014;**141**:111-122.

266. Berahovich RD, Penfold MET, Schall TJ. Nonspecific CXCR7 antibodies. *Immunology Letters* 2010;**133**:112-114.

267. Van Rechem C, Rood BR, Touka M, Pinte S, Jenal M, Guerardel C, Ramsey K, Monte D, Begue A, Tschan MP, Stephan DA, Leprince D. Scavenger Chemokine (CXC Motif) Receptor 7 (CXCR7) Is a Direct Target Gene of HIC1 (Hypermethylated in Cancer 1). *Journal of Biological Chemistry* 2009;**284**:20927-20935.

268. Hare D, Collins S, Cuddington B, Mossman K. The Importance of Physiologically Relevant Cell Lines for Studying Virus-Host Interactions. *Viruses-Basel* 2016;**8**.

269. Campisi J. The biology of replicative senescence. *European Journal of Cancer* 1997;**33**:703-709.

270. Bernadotte A, Mikhelson VM, Spivak IM. Markers of cellular senescence. Telomere shortening as a marker of cellular senescence. *Aging-Us* 2016;**8**:3-11.

271. Bartelt RR, Cruz-Orcutt N, Collins M, Houtman JCD. Comparison of T Cell Receptor-Induced Proximal Signaling and Downstream Functions in Immortalized and Primary T Cells. *Plos One* 2009;**4**.

272. Chang MWF, Grillari J, Mayrhofer C, Fortschegger K, Allmaier G, Marzban G, Katinger H, Voglauer R. Comparison of early passage, senescent and hTERT immortalized endothelial cells. *Experimental Cell Research* 2005;**309**:121-136.

273. Yang JW, Nagavarapu U, Relloma K, Sjaastad MD, Moss WC, Passaniti A, Herron GS. Telomerized human microvasculature is functional in vivo. *Nature Biotechnology* 2001;**19**:219-224.

274. Pelekanos RA, Ting MJ, Sardesai VS, Ryan JM, Lim YC, Chan JKY, Fisk NM. Intracellular trafficking and endocytosis of CXCR4 in fetal mesenchymal stem/stromal cells. *Bmc Cell Biology* 2014;**15**.

275. Salcedo R, Wasserman K, Young HA, Grimm MC, Howard OMZ, Anver MR, Kleinman HK, Murphy WJ, Oppenheim JJ. Vascular endothelial growth factor and basic fibroblast growth factor induce expression of CXCR4 on human endothelial cells - In vivo neovascularization induced by stromal-derived factor-1 alpha. *American Journal of Pathology* 1999;**154**:1125-1135.

276. Madden SL, Cook BP, Nacht M, Weber WD, Callahan MR, Jiang YD, Dufault MR, Zhang XM, Zhang W, Walter-Yohrling J, Rouleau C, Akmaev VR, Wang CJ, Cao XH, Martin TBS, Roberts BL, Teicher BA, Klinger KW, Stan RV, Lucey B, Carson-Walter EB, Laterra J, Walter KA. Vascular gene expression in nonneoplastic and malignant brain. *American Journal of Pathology* 2004;**165**:601-608.

277. Infantino S, Moepps B, Thelen M. Expression and regulation of the orphan receptor RDC1 and its putative ligand in human dendritic and B cells. *Journal of Immunology* 2006;**176**:2197-2207.

278. Noma T, Lemaire A, Prasad SVN, Barki-Harrington L, Tilley DG, Chen J, Le Corvoisier P, Violin JD, Wei H, Lefkowitz RJ, Rockman HA. b-arrestin-mediated beta(1)-adrenergic receptor transactivation of the EGFR confers cardioprotection. *Journal of Clinical Investigation* 2007;**117**:2445-2458.

279. Lymperopoulos A, Rengo G, Koch WJ. Adrenergic Nervous System in Heart Failure Pathophysiology and Therapy. *Circulation Research* 2013;**113**:739-753.

280. Pfeffer MA, Pfeffer JM, Fishbein MC, Fletcher PJ, Spadaro J, Kloner RA, Braunwald E. MYOCARDIAL INFARCT SIZE AND VENTRICULAR-FUNCTION IN RATS. *Circulation Research* 1979;**44**:503-512.

281. Fletcher PJ, Pfeffer JM, Pfeffer MA, Braunwald E. LEFT-VENTRICULAR DIASTOLIC PRESSURE-VOLUME RELATIONS IN RATS WITH HEALED MYOCARDIAL-INFARCTION - EFFECTS ON SYSTOLIC FUNCTION. *Circulation Research* 1981;**49**:618-626.

282. Westman PC, Lipinski MJ, Luger D, Waksman R, Bonow RO, Wu E, Epstein SE. Inflammation as a Driver of Adverse Left Ventricular Remodeling After Acute Myocardial Infarction. *Journal of the American College of Cardiology* 2016;**67**:2050-2060.

283. Griffiths EJ, Halestrap AP. MITOCHONDRIAL NONSPECIFIC PORES REMAIN CLOSED DURING CARDIAC ISCHEMIA, BUT OPEN UPON REPERFUSION. *Biochemical Journal* 1995;**307**:93-98.

284. Di Lisa F, Menabo R, Canton M, Barile M, Bernardi P. Opening of the mitochondrial permeability transition pore causes depletion of mitochondrial and cytosolic NAD(+) and is a causative event in the death of myocytes in postischemic reperfusion of the heart. *Journal of Biological Chemistry* 2001;**276**:2571-2575.

285. Bell RM, Mocanu MM, Yellon DM. Retrograde heart perfusion: The Langendorff technique of isolated heart perfusion. *Journal of Molecular and Cellular Cardiology* 2011;**50**:940-950.

286. Sutherland FJ, Hearse DJ. The isolated blood and perfusion fluid perfused heart. *Pharmacological Research* 2000;**41**:613-627.

287. Clements-Jewery H, Curtis MJ. The Langendorff preparation. *Manual of Research Techniques in Cardiovascular Medicine* 2014:187-196.

288. Feiring AJ, Johnson MR, Kioschos JM, Kirchner PT, Marcus ML, White CW. THE IMPORTANCE OF THE DETERMINATION OF THE MYOCARDIAL AREA AT RISK IN THE EVALUATION OF THE OUTCOME OF ACUTE MYOCARDIAL-INFARCTION IN PATIENTS. *Circulation* 1987;**75**:980-987.

289. Yang XL, Cohen MV, Downey JM. Mechanism of Cardioprotection by Early Ischemic Preconditioning. *Cardiovascular Drugs and Therapy* 2010;**24**:225-234.

290. Ytrehus K, Liu YG, Downey JM. PRECONDITIONING PROTECTS THE ISCHEMIC RABBIT HEART BY PROTEIN-KINASE-C ACTIVATION. *Faseb Journal* 1993;**7**:A418-A418.

291. Ping PP, Song CX, Zhang J, Guo YR, Cao XN, Li RCX, Wu WJ, Vondriska TM, Pass JM, Tang XL, Pierce WM, Bolli R. Formation of protein kinase C epsilon-Lck signalling modules confers cardioprotection. *Journal of Clinical Investigation* 2002;**109**:499-507.

292. Inagaki K, Hahn HS, Dorn GW, Mochly-Rosen D. Additive protection of the ischemic heart ex vivo by combined treatment with delta-protein kinase C inhibitor and epsilon-protein kinase C activator. *Circulation* 2003;**108**:869-875.

293. Kawamura S, Yoshida K, Miura T, Mizukami Y, Matsuzaki M. Ischemic preconditioning translocates PKC-delta and -epsilon, which mediate functional protection in isolated rat heart. *American Journal of Physiology-Heart and Circulatory Physiology* 1998;**275**:H2266-H2271.

294. Hausenloy DJ, Maddock HL, Baxter GF, Yellon DM. Inhibiting mitochondrial permeability transition pore opening: a new paradigm for myocardial preconditioning? *Cardiovascular Research* 2002;**55**:534-543.

295. Rossello X, He ZH, Yellon DM. Myocardial Infarct Size Reduction Provided by Local and Remote Ischaemic Preconditioning: References Values from the Hatter Cardiovascular Institute. *Cardiovascular Drugs and Therapy* 2018;**32**:127-133.

296. Yellon DM, Alkhulaifi AM, Browne EE, Pugsley WB. ISCHEMIC PRECONDITIONING LIMITS INFARCT SIZE IN THE RAT-HEART. *Cardiovascular Research* 1992;**26**:983-987.

297. Lindsey ML, Bolli R, Canty JM, Du XJ, Frangogiannis NG, Frantz S, Gourdie RG, Holmes JW, Jones SP, Kloner RA, Lefer DJ, Liao R, Murphy E, Ping PP, Przyklenk K, Recchia FA, Longacre LS, Ripplinger CM, Van Eyk JE, Heusch G. Guidelines for experimental models of myocardial ischemia and infarction. *American Journal of Physiology-Heart and Circulatory Physiology* 2018;**314**:H812-H838.

298. Sun Y, Weber KT. Infarct scar: a dynamic tissue. *Cardiovascular Research* 2000;**46**:250-256.

299. Maxwell MP, Hearse DJ, Yellon DM. Species variation in the coronary collateral circulation during regional myocardial ischaemia: a critical determinant of the rate of evolution and extent of myocardial infarction. *Cardiovascular Research* 2000;**45**:213-214.

300. Toyota E, Warltier DC, Brock T, Ritman E, Kolz C, O'Malley P, Rocic P, Focardi M, Chilian WM. Vascular endothelial growth factor is required for coronary collateral growth in the rat. *Circulation* 2005;**112**:2108-2113.

301. Zhang H, Faber JE. De-novo collateral formation following acute myocardial infarction: Dependence on CCR2(+) bone marrow cells. *Journal of Molecular and Cellular Cardiology* 2015;**87**:4-16.

302. Seiler C, Stoller M, Pitt B, Meier P. The human coronary collateral circulation: development and clinical importance. *European Heart Journal* 2013;**34**:2674-2682.

303. Zhang H, Prabhakar P, Sealock R, Faber JE. Wide genetic variation in the native pial collateral circulation is a major determinant of variation in severity of stroke. *Journal of Cerebral Blood Flow and Metabolism* 2010;**30**:923-934.

304. Sealock R, Zhang H, Lucitti JL, Moore SM, Faber JE. Congenic Fine-Mapping Identifies a Major Causal Locus for Variation in the Native Collateral Circulation and Ischemic Injury in Brain and Lower Extremity. *Circulation Research* 2014;**114**:660-671.

305. Wang SL, Zhang H, Wiltshire T, Sealock R, Faber JE. Genetic Dissection of the Canq1 Locus Governing Variation in Extent of the Collateral Circulation. *Plos One* 2012;**7**.

306. Chalothorn D, Faber JE. Strain-dependent variation in collateral circulatory function in mouse hindlimb. *Physiological Genomics* 2010;**42**:469-479.

307. Tamamura H, Hiramatsu K, Kusano S, Terakubo S, Yamamoto N, Trent JO, Wang ZX, Peiper SC, Nakashima H. Synthesis of potent CXCR4 inhibitors possessing low cytotoxicity and improved biostability based on T140 derivatives. *Organic & Biomolecular Chemistry* 2003;**1**:3656-3662.

308. Gravel S, Malouf C, Boulais PE, Berchiche YA, Oishi S, Fujii N, Leduc R, Sinnett D, Heveker N. The Peptidomimetic CXCR4 Antagonist TC14012 Recruits beta-Arrestin to CXCR7 ROLES OF RECEPTOR DOMAINS. *Journal of Biological Chemistry* 2010;**285**:37939-37943.

309. Del Molino Del Barrio I, Wilkins GC, Meeson A, Ali S, Kirby JA. Breast Cancer: An Examination of the Potential of ACKR3 to Modify the Response of CXCR4 to CXCL12. *International journal of molecular sciences* 2018;**19**.

310. Vagner J, Qu H, Hruby VJ. Peptidomimetics, a synthetic tool of drug discovery. *Current Opinion in Chemical Biology* 2008;**12**:292-296.

311. Introduction to Biological and Small Molecule Drug Research and Development: Theory and Case Studies. *Introduction to Biological and Small Molecule Drug Research and Development: Theory and Case Studies* 2013:1-425.

312. Lee TH, Goldman L. SERUM ENZYME ASSAYS IN THE DIAGNOSIS OF ACUTE MYOCARDIAL-INFARCTION - RECOMMENDATIONS BASED ON A QUANTITATIVE-ANALYSIS. *Annals of Internal Medicine* 1986;**105**:221-231.

313. Rapaport E. NOMENCLATURE AND CRITERIA FOR DIAGNOSIS OF ISCHEMIC HEART-DISEASE - REPORT OF THE JOINT-INTERNATIONAL-SOCIETY-AND-FEDERATION-OF-CARDIOLOGY-WORLD-HEALTH-OR GANIZATION TASK-FORCE ON STANDARDIZATION OF CLINICAL NOMENCLATURE. *Circulation* 1979;**59**:607-609.

314. Jaffe AS, Landt Y, Parvin CA, Abendschein DR, Geltman EM, Ladenson JH. Comparative sensitivity of cardiac troponin I and lactate dehydrogenase isoenzymes for diagnosing acute myocardial infarction. *Clinical Chemistry* 1996;**42**:1770-1776.

315. Ajmani P, Yadav HN, Singh M, Sharma PL. Possible involvement of caveolin in attenuation of cardioprotective effect of ischemic preconditioning in diabetic rat heart. *Bmc Cardiovascular Disorders* 2011;**11**.

316. Charan K, Goyal A, Gupta JK, Yadav HN. Role of atrial natriuretic peptide in ischemic preconditioning-induced cardioprotection in the diabetic rat heart. *Journal of Surgical Research* 2016;**201**:272-278.

317. Knight ZA, Gonzalez B, Feldman ME, Zunder ER, Goldenberg DD, Williams O, Loewith R, Stokoe D, Balla A, Toth B, Balla T, Weiss WA, Williams RL, Shokat KM. A pharmacological map of the PI3-K family defines a role for p110 alpha in insulin signaling. *Cell* 2006;**125**:733-747.

318. Kim YB, Nikoulina SE, Ciaraldi TP, Henry RR, Kahn BB. Normal insulin-dependent activation of Akt/protein kinase B, with diminished activation of phosphoinositide 3-kinase, in muscle in type 2 diabetes. *Journal of Clinical Investigation* 1999;**104**:733-741.

319. Neuhaus T, Stier S, Totzke G, Gruenewald E, Fronhoffs S, Sachinidis A, Vetter H, Ko YD. Stromal cell-derived factor 1 alpha (SDF-1 alpha) induces gene-expression of early growth response-1 (Egr-1) and VEGF in human arterial endothelial cells and enhances VEGF induced cell proliferation. *Cell Proliferation* 2003;**36**:75-86.

320. Friedrich EB, Werner C, Walenta K, Boehm M, Scheller B. Role of extracellular signal-regulated kinase for endothelial progenitor cell dysfunction in coronary artery disease. *Basic Research in Cardiology* 2009;**104**:613-620.

321. Bernier SG, Haldar S, Michel T. Bradykinin-regulated interactions of the mitogen-activated protein kinase pathway with the endothelial nitric-oxide synthase. *Journal of Biological Chemistry* 2000;**275**:30707-30715.

322. Das S, Mitra K, Mandal M. Sample size calculation: Basic principles. *Indian Journal of Anaesthesia* 2016;**60**:652-656.

323. Akobeng AK. Understanding type I and type II errors, statistical power and sample size. *Acta Paediatrica* 2016;**105**:605-609.

324. Symons JD, McMillin SL, Riehle C, Tanner J, Palionyte M, Hillas E, Jones D, Cooksey RC, Birnbaum MJ, McClain DA, Zhang QJ, Gale D, Wilson LJ, Abel ED. Contribution of Insulin and Akt1 Signaling to Endothelial Nitric Oxide Synthase in the Regulation of Endothelial Function and Blood Pressure. *Circulation Research* 2009;**104**:1085-U1153.

325. Ozaki K, Awazu M, Tamiya M, Iwasaki Y, Harada A, Kugisaki S, Tanimura S, Kohno M. Targeting the ERK signaling pathway as a potential treatment for insulin resistance and type 2 diabetes. *American Journal of Physiology-Endocrinology and Metabolism* 2016;**310**:E643-E651.

326. Laakko T, Juliano RL. Adhesion regulation of stromal cell-derived factor-1 activation of ERK in lymphocytes by phosphatases. *Journal of Biological Chemistry* 2003;**278**:31621-31628.

327. Alessi DR, Andjelkovic M, Caudwell B, Cron P, Morrice N, Cohen P, Hemmings BA. Mechanism of activation of protein kinase B by insulin and IGF-1. *Embo Journal* 1996;**15**:6541-6551.

328. Shao HW, Xu QY, Wu QL, Ma Q, Salgueiro L, Wang JA, Eton D, Webster KA, Yu H. Defective CXCR4 expression in aged bone marrow cells impairs vascular regeneration. *Journal of Cellular and Molecular Medicine* 2011;**15**:2046-2056.

329. Keller G. Embryonic stem cell differentiation: emergence of a new era in biology and medicine. *Genes & Development* 2005;**19**:1129-1155.

330. Roskoski R. ERK1/2 MAP kinases: Structure, function, and regulation. *Pharmacological Research* 2012;**66**:105-143.

331. Zhuo W, Jia L, Song N, Lu XA, Ding YP, Wang XF, Song XM, Fu Y, Luo YZ. The CXCL12-CXCR4 Chemokine Pathway: A Novel Axis Regulates Lymphangiogenesis. *Clinical Cancer Research* 2012;**18**:5387-5398.

332. dela Paz NG, D'Amore PA. Arterial versus venous endothelial cells. *Cell and Tissue Research* 2009;**335**:5-16.

333. Ishii Y, Langberg J, Rosborough K, Mikawa T. Endothelial cell lineages of the heart. *Cell and Tissue Research* 2009;**335**:67-73.

334. Pirkmajer S, Chibalin AV. Serum starvation: caveat emptor. *American Journal of Physiology-Cell Physiology* 2011;**301**:C272-C279.

335. Bujak M, Dobaczewski M, Chatila K, Mendoza LH, Li N, Reddy A, Frangogiannis NG. Interleukin-1 receptor type I signaling critically regulates infarct healing and cardiac remodeling. *American Journal of Pathology* 2008;**173**:57-67.

336. Gutkind JS, Kostenis E. Arrestins as rheostats of GPCR signalling. *Nature Reviews Molecular Cell Biology* 2018;**19**:615-616.

337. Abremski K, Wierzbicki A, Frommer B, Hoess RH. Bacteriophage p1 cre-loxp site-specific recombination -

site-specific dna topoisomerase activity of the cre recombination protein. *Journal of Biological Chemistry* 1986;**261**:391-396.

338. Payne S, De Val S, Neal A. Endothelial-Specific Cre Mouse Models: Is Your Cre CREdibile? *Arteriosclerosis Thrombosis and Vascular Biology* 2018;**38**:2550-2561.

339. Rolny C, Nilsson I, Magnusson P, Armulik A, Jakobsson L, Wentzel P, Lindblom P, Norlin J, Betsholtz C, Heuchel R, Welsh M, Claesson-Welsh L. Platelet-derived growth factor receptor-beta promotes early endothelial cell differentiation. *Blood* 2006;**108**:1877-1886.

340. Hellstrom M, Kalen M, Lindahl P, Abramsson A, Betsholtz C. Role of PDGF-B and PDGFR-beta in recruitment of vascular smooth muscle cells and pericytes during embryonic blood vessel formation in the mouse. *Development* 1999;**126**:3047-3055.

341. Rajkumar VS, Xu SW, Bostrom M, Leoni P, Muddle J, Ivarsson M, Gerdin B, Denton CP, Bou-Gharios G, Black CM, Abraham DJ. Platelet-derived growth factor-beta receptor activation is essential for fibroblast and pericyte recruitment during cutaneous wound healing. *American Journal of Pathology* 2006;**169**:2254-2265.

342. Indra AK, Warot X, Brocard J, Bornert JM, Xiao JH, Chambon P, Metzger D. Temporally-controlled site-specific mutagenesis in the basal layer of the epidermis: comparison of the recombinase activity of the tamoxifen-inducible Cre-ERT and Cre-ERT2 recombinases. *Nucleic Acids Research* 1999;**27**:4324-4327.

343. Dube KN, Thomas TM, Munshaw S, Rohling M, Riley PR, Smart N. Recapitulation of developmental mechanisms to revascularize the ischemic heart. *Jci Insight* 2017;**2**.

344. Jones JA, Beck C, Barbour JR, Zavadzkas JA, Mukherjee R, Spinale FG, Ikonomidis JS. Alterations in Aortic Cellular Constituents during Thoracic Aortic Aneurysm Development Myofibroblast-Mediated Vascular Remodeling. *American Journal of Pathology* 2009;**175**:1746-1756.

345. Jahn HM, Kasakow CV, Helfer A, Michely J, Verkhratsky A, Maurer HH, Scheller A, Kirchhoff F. Refined protocols of tamoxifen injection for inducible DNA recombination in mouse astroglia. *Scientific Reports* 2018;**8**.

346. Bolte C, Flood HM, Ren XM, Jagannathan S, Barski A, Kalin TV, Kalinichenko VV. FOXF1 transcription factor promotes lung regeneration after partial pneumonectomy. *Scientific Reports* 2017;**7**.

347. Huh WJ, Khurana SS, Geahlen JH, Kohli K, Waller RA, Mills JC. Tamoxifen Induces Rapid, Reversible Atrophy, and Metaplasia in Mouse Stomach. *Gastroenterology* 2012;**142**:21-U105.

348. Guilmatre A, Sharp AJ. Parent of origin effects. *Clinical Genetics* 2012;**81**:201-209.

349. Heffner CS, Pratt CH, Babiuk RP, Sharma Y, Rockwood SF, Donahue LR, Eppig JT, Murray SA. Supporting conditional mouse mutagenesis with a comprehensive cre characterization resource. *Nature Communications* 2012;**3**.

350. Gallardo T, Shirley L, John GB, Castrillon DH. Generation of a germ cell-specific mouse transgenic Cre line, Vasa-Cre. *Genesis* 2007;**45**:413-417.

351. Hayashi S, Tenzen T, McMahon AP. Maternal inheritance of Cre activity in a Sox2Cre deleter train. *Genesis* 2003;**37**:51-53.

352. Zhuo L, Theis M, Alvarez-Maya I, Brenner M, Willecke K, Messing A. hGFAP-cre transgenic mice for manipulation of glial and neuronal function in vivo. *Genesis* 2001;**31**:85-94.

353. Means AL, Chytil A, Moses HL, Coffey RJ, Wright CVE, Taketo MM, Grady WM. Keratin 19 gene drives Cre recombinase expression throughout the early postimplantation mouse embryo. *Genesis* 2005;**42**:23-27.

354. Balordi F, Fishell G. Mosaic removal of hedgehog signaling in the adult SVZ reveals that the residual wild-type stem cells have a limited capacity for self-renewal. *Journal of Neuroscience* 2007;**27**:14248-14259.

355. Ogilvy S, Elefanty AG, Visvader J, Bath ML, Harris AW, Adams JM. Transcriptional regulation of vav, a gene expressed throughout the hematopoietic compartment. *Blood* 1998;**91**:419-430.

356. Casellas J. Inbred mouse strains and genetic stability: a review. *Animal* 2011;**5**:1-7.

357. Zeldovich L. Genetic drift: the ghost in the genome. *Lab Animal* 2017;**46**:255-257.

358. Liu J, Willet SG, Bankaitis ED, Xu YW, Wright CVE, Gu GQ. Non-parallel recombination limits cre-loxP-based reporters as precise indicators of conditional genetic manipulation. *Genesis* 2013;**51**:436-442.

359. Turlo KA, Gallaher SD, Vora R, Laski FA, Iruela-Arispe ML. When Cre-Mediated Recombination in Mice Does Not Result in Protein Loss. *Genetics* 2010;**186**:959-U312.

360. Zheng BH, Sage M, Sheppeard EA, Jurecic V, Bradley A. Engineering mouse chromosomes with Cre-loxP: Range, efficiency, and somatic applications. *Molecular and Cellular Biology* 2000;**20**:648-655.

361. Gerhardt H, Golding M, Fruttiger M, Ruhrberg C, Lundkvist A, Abramsson A, Jeltsch M, Mitchell C, Alitalo K, Shima D, Betsholtz C. VEGF guides angiogenic sprouting utilizing endothelial tip cell filopodia. *Journal of Cell Biology* 2003;**161**:1163-1177.

362. Jung S, Kleinheinz J. Angiogenesis - The Key to Regeneration. *Regenerative Medicine and Tissue Engineering* 2013:453-473.

363. Nissen NN, Polverini PJ, Koch AE, Volin MV, Gamelli RL, DiPietro LA. Vascular endothelial growth factor mediates angiogenic activity during the proliferative phase of wound healing. *American Journal of Pathology* 1998;**152**:1445-1452.

364. Tremolada G, Del Turco C, Lattanzio R, Maestroni S, Maestroni A, Bandello F, Zerbini G. The Role of Angiogenesis in the Development of Proliferative Diabetic Retinopathy: Impact of Intravitreal Anti-VEGF Treatment. *Experimental Diabetes Research* 2012.

365. Rudiger C, Kuhlmann W, Schaefer CA, Reinhold L, Tillmanns H, Erdogan A. Signalling mechanisms of SDF-induced endothelial cell proliferation and migration. *Biochemical and Biophysical Research Communications* 2005;**335**:1107-1114.

366. Melo RDC, Ferro KPV, Duarte ADS, Saad STO. CXCR7 participates in CXCL12-mediated migration and homing of leukemic and normal hematopoietic cells. *Stem Cell Research & Therapy* 2018;**9**.

367. Esencay M, Sarfraz Y, Zagzag D. CXCR7 is induced by hypoxia and mediates glioma cell migration towards SDF-1 alpha. *Bmc Cancer* 2013;**13**.

368. Volin MV, Huynh N, Klosowska K, Reyes RD, Woods JM. Fractalkine-Induced Endothelial Cell Migration Requires MAP Kinase Signaling. *Pathobiology* 2010;**77**:7-16.

369. Sawano A, Iwai S, Sakurai Y, Ito M, Shitara K, Nakahata T, Shibuya M. Flt-1, vascular endothelial growth factor receptor 1, is a novel cell surface marker for the lineage of monocyte-macrophages in humans. *Blood* 2001;**97**:785-791.

370. Kuhlmann CRW, Schaefer CA, Reinhold L, Tillmanns H, Erdogan A. Signalling mechanisms of SDF-induced endothelial cell proliferation and migration. *Biochemical and biophysical research communications* 2005;**335**:1107-1114.

371. Kollmar O, Rupertus K, Scheuer C, Junker B, Tilton B, Schilling MK, Menger MD. Stromal cell-derived factor-1 promotes cell migration and tumor growth of colorectal metastasis. *Neoplasia* 2007;**9**:862-870.

372. Ratajczak MZ, Kim CH, Abdel-Latif A, Schneider G, Kucia M, Morris AJ, Laughlin MJ, Ratajczak J. A novel perspective on stem cell homing and mobilization: review on bioactive lipids as potent chemoattractants and cationic peptides as underappreciated modulators of responsiveness to SDF-1 gradients. *Leukemia* 2012;**26**:63-72.

373. Lapidot T, Dar A, Kollet O. How do stem cells find their way home? *Blood* 2005;**106**:1901-1910.

374. Dai X, Tan Y, Cai S, Xiong X, Wang L, Ye Q, Yan X, Ma K, Cai L. The role of CXCR7 on the adhesion, proliferation and angiogenesis of endothelial progenitor cells. *Journal of Cellular and Molecular Medicine* 2011;**15**:1299-1309.

375. Chen Q, Zhang M, Li YJ, Xu DS, Wang Y, Song AH, Zhu B, Huang YL, Zheng JLC. CXCR7 Mediates Neural Progenitor Cells Migration to CXCL12 Independent of CXCR4. *Stem Cells* 2015;**33**:2574-2585.

376. Keenan TM, Folch A. Biomolecular gradients in cell culture systems. *Lab on a Chip* 2008;**8**:34-57.

377. Mazzinghi B, Ronconi E, Lazzeri E, Sagrinati C, Ballerini L, Angelotti ML, Parente E, Mancina R, Netti GS, Becherucci F, Gacci M, Carini M, Gesualdo L, Rotondi M, Maggi E, Lasagni L, Serio M, Romagnani S, Romagnani P. Essential but differential role for CXCR4 and CXCR7 in the therapeutic homing of human renal progenitor cells. *Journal of Experimental Medicine* 2008;**205**:479-490.

378. Eaton BE, Gold L, Zichi DA. LETS GET SPECIFIC - THE RELATIONSHIP BETWEEN SPECIFICITY AND AFFINITY. *Chemistry & Biology* 1995;**2**:633-638.

379. Huggins DJ, Sherman W, Tidor B. Rational Approaches to Improving Selectivity in Drug Design. *Journal of Medicinal Chemistry* 2012;**55**:1424-1444.

380. Liu XL, Duan BY, Cheng ZK, Jia XH, Mao LN, Fu H, Che YZ, Ou LL, Liu L, Kong DL. SDF-1/CXCR4 axis modulates bone marrow mesenchymal stem cell apoptosis, migration and cytokine secretion. *Protein & Cell* 2011;**2**:845-854.

381. Koshiba T, Hosotani R, Miyamoto Y, Ida J, Tsuji S, Nakajima S, Kawaguchi M, Kobayashi H, Doi R, Hori T, Fujii N, Imamura M. Expression of stromal cell-derived factor 1 and CXCR4 ligand receptor system in pancreatic cancer: A possible role for tumor progression. *Clinical Cancer Research* 2000;**6**:3530-3535.

382. Jinquan T, Quan S, Jacobi HH, Madsen HO, Glue C, Skov PS, Malling HJ, Poulsen LK. CXC chemokine receptor 4 expression and stromal cell-derived factor-1 alpha-induced chemotaxis in CD4(+) T lymphocytes are regulated by interleukin-4 andinterleukin-10. *Immunology* 2000;**99**:402-410.

383. Peng SB, Peek V, Zhai Y, Paul DC, Lou QY, Xia XL, Eessalu T, Kohn W, Tang SQ. Akt activation, but not extracellular signal - Regulated kinase activation, is required for SDF-1 alpha/CXCR4-mediated migration of epitheloid carcinoma cells. *Molecular Cancer Research* 2005;**3**:227-236.

384. Owen SC, Doak AK, Ganesh AN, Nedyalkova L, McLaughlin CK, Shoichet BK, Shoichet MS. Colloidal Drug Formulations Can Explain "Bell-Shaped" Concentration-Response Curves. *Acs Chemical Biology* 2014;**9**:777-784.

385. Dieckow J, Brandt W, Hattermann K, Schob S, Schulze U, Mentlein R, Ackermann P, Sel S, Paulsen FP. CXCR4 and CXCR7 Mediate TFF3-Induced Cell Migration Independently From the ERK1/2 Signaling Pathway. *Investigative Ophthalmology & Visual Science* 2016;**57**:56-65.

386. Qian TT, Liu YC, Dong Y, Zhang L, Dong YN, Sun YH, Sun DM. CXCR7 regulates breast tumor metastasis and angiogenesis in vivo and in vitro. *Molecular Medicine Reports* 2018;**17**:3633-3639.